Charles University

Faculty of Science

Study programme: Plant Anatomy and Physiology

Mgr. Michal Daněk

Characterization of *Arabidopsis thaliana* FLOTILLINs and HYPERSENSITIVE INDUCED RESPONSE proteins – dynamics, interactions and functions

Charakterizace FLOTILLINů and HYPERSENSITIVE INDUCED RESPONSE proteinů u *Arabidopsis thaliana* – dynamika, interakce a funkce

Doctoral thesis

Supervisor: RNDr. Jan Martinec, CSc.

Prague, May 2019

DECLARATIONS

I hereby declare that this Ph.D. thesis documents my own work and I wrote it independently. This work or any substantial part of the text is not a subject of any other defending procedure. I declare that all used sources were cited and acknowledged properly.

Prague, June 2019

Michal Daněk

On behalf of other co-authors, I declare that Michal Daněk has substantially contributed to all selected publications and I agree with the fact that these articles are presented as an integral part of this Ph.D. thesis. The publications were created by collectives of authors and the participation of the author of this thesis is specified below.

Prague, June 2019

Jan Martinec

ACKNOWLEDGEMENTS

First I would like to thank my supervisor Jan Martinec for leading me for seven years through not always easy paths of the research, for his valuable advice and comments on my work and also for giving me the chance to visit several conferences and meet new people and see beautiful places there. Great thanks goes also to Jan Petrášek for introducing me into the world of microscopy and the supervision over the microscopic part of this thesis. I would like to thank all my current and former colleagues from the Laboratory of Signal Transduction of the Institute of Experimental Botany who were the source of inspiration and sometimes moral support for me. Special thanks are reserved for Enric Zelazny and Amanda Martin Barranco from the Institute for Integrative Biology of the Cell, France for creating welcoming and friendly environment where I could learn some methods during two stays. Last bud certainly not least I want to thank my friends and family who were standing by me for so long.

FUNDING

Majority of the results presented here were achieved at the Institute of Experimental Botany, Czech Academy of Sciences, Prague, Czech Republic. Some works were carried out within a close collaboration with the Department of Biochemistry and Microbiology, University of Chemistry and Technology, Prague, Czech Republic. Based on shared research interest a new collaboration was established with the group Cell Signalling and Ubiquitin at the Department of Cell Biology, Institute for Integrative Biology of the Cell (I2BC), CNRS/CEA/University Paris-Sud, Gif-sur-Yvette, France, thanks to which Michal Daněk realized two short-term internships in the laboratory abroad.

Following grants helped the realization of the research presented in this thesis

14-096855 – Czech Science Foundation

7AMB17FR005 – Programme Barrande for Czech-French collaboration – Ministry of Education, Youth and Sports of CR; French Ministry for Europe and Foreign Affairs, and French Ministry of Higher Education, Research and Innovation

209 CZ.02.1.01/0.0/0.0/16_019/0000738 – Ministry of Education, Youth and Sports of CR from European Regional Development Fund-Project "Centre for Experimental Plant Biology"

CZ.2.16/3.1.00/21519 – operational program Prague – competitiveness

LM2015062 (Czech-BioImaging) – Ministry of Education, Youth and Sport

Contents

List of Abbreviations

Only a protein family name is explained here if more than one isoform is mentioned in the text.

ABA - abscisic acid

ABCG36 - ABC TRANSPORTER G FAMILY MEMBER 36

ABI1 - PROTEIN PHOSPHATASE 2C 56

AHA1 - H(+)-ATPASE 1

AMT3;1 - AMMONIUM TRANSPORTER 3;1

AP2 - ADAPTOR PROTEIN 2

BIK1 - BOTRYTIS-INDUCED KINASE 1

BMM - Botrytis cinerea BMM

BRI1 - BRASSINOSTEROID INSENSITIVE 1

BSK1 - BRASSINOSTEROID-SIGNALING KINASE 1

CESA - cellulose synthase

CLC2 - CLATHRIN HEAVY CHAIN 2

CPK21 - CALCIUM DEPENDENT PROTEIN KINASE 21

CRAC - cholesterol recognition/interaction amino acid consensus sequence

CV - coefficient of variation

CW - cell wall

DCB - 2,6-dichlorobenzonitrile

DRM - detergent-resistant membranes

DRP - dynamin-like protein

EGCG - epigallocatechin gallate

elf18 - acetylated 18-amino acid fragment from N-terminal of elongation factor Tu

ERD4 - EARLY RESPONSE TO DEHYDRATION 4

flg22 - 22-amino acid peptide from N-terminal part of flagellin

FLOT - flotillin

FLS2 - FLAGELLIN-SENSITIVE 2

FRAP - fluorescence recovery after photobleaching

GFP - green fluorescent protein

GPI - glycophosphatidylinositol

HIR - hypersensitive induced reaction protein

IRT1 - IRON-REGULATED TRANSPORTER 1

ISX – isoxaben

KAT1 - POTASSIUM CHANNEL IN ARABIDOPSIS THALIANA 1

KOR1 - KORRIGAN 1

LTI6b - LOW TEMPERATURE-INDUCED PROTEIN 6B

LYK3 - LYSIN MOTIF RECEPTOR-LIKE KINASE 3

MT - microtubule

MyoB1 - MYOSIN-BINDING PROTEIN 1

NAA - 1-naphthalene acetic acid

NHL3 - NDR1/HIN1-LIKE PROTEIN 3

NOX - NADPH oxidase

PALM - photoactivated localization microscopy

PCC – Pearson's correlation coefficient

PHOT1 - PHOTOTROPIN 1

PI4P - phosphatidylinositol 4-phosphate

PIN - PIN-FORMED

PIP - plasma membrane intrinsic protein

PM - plasma membrane

POM2 - CELLULOSE SYNTHASE-INTERACTIVE PROTEIN 1

Pst - Pseudomonas syringae pv. tomato strain DC3000

RabG3F - RAB GTPASE HOMOLOG G3F

RbohD - RESPIRATORY BURST OXIDASE D

REM - remorin

ROP - Rho of Plants GTPase

SLAC1 - SLOW ANION CHANNEL-ASSOCIATED 1

SLAH3 - SLAC1 homologue 3

SPFH - stomatin/prohibitin/flotillin/HflK/C

STED - stimulated emission depletion

STORM - stochastic optical reconstruction microscopy

stp - single particle tracking

SUT1 - SUCROSE TRANSPORTER 1

SYP71 - SYNTAXIN 71

TIRF/VAEM - total internal reflection fluorescence/variable angle epifluorescence

TWD40-2 - TRANSDUCIN/WD40-2

VHA-a1 - V-TYPE PROTON ATPASE SUBUNIT A1

YFP - yellow fluorescent protein

Abstract

This work is a collection of three research articles and one review article focused on flotillins (FLOTs) and hypersensitive induced reaction proteins (HIRs) in *Arabidopsis thaliana*. FLOTs and HIRs are closely related membrane-associated proteins forming two subfamilies both belonging to SPFH domain superfamily. While FLOTs are present in organisms of all evolutionary lineages HIRs are plant specific proteins. The review article sums up the knowledge gained on FLOTs and HIRs from different organisms in terms of cellular localization, interaction with cellular membranes and with other proteins, and physiological functions. The research articles were targeted at three aspects of *At*FLOTs and *At*HIRs: involvement in response to exogenous stimuli; determination of protein interactors; and subcellular localization and dynamics. The first aspect was approached by transcription measurement of *AtFLOT*s and phenotypic screen of single loss-of-function mutants of *AtFLOT*s upon various treatments covering biotic and abiotic stress and phytohormone application. Although we observed changes in transcription none of the treatments provoked a phenotype manifestation in any of *AtFLOT* mutants. In the second article we focused on interactome of *At*FLOT2 and performed co-immunoprecipitation followed by mass spectrometry determination of co-precipitated proteins. Several proteins involved in cellular transport, water stress or plant pathogen interactions were revealed and direct interaction of *At*FLOT2 with some of them was verified using split-ubiquitin system. These interactors point to the possible physiological functions of *At*FLOT2. The manuscript of the third article covers the investigation of localization and dynamics patterns in all isoforms of *At*FLOTs and *At*HIRs. We present general plasma membrane localization for both subfamilies with one exception where the protein is associated exclusively with the tonoplast. However, the presence of a minor tonoplast pool accompanying the predominant plasma membrane localization is shared among some other isoforms as well. At the plasma membrane the signal of both *A*tHIRs and *At*FLOTs is clustered in membrane microdomains. These microdomains are very stable over time, especially in *At*FLOTs. Despite the overall immobility revealed by FRAP approach for both subfamilies, a slightly higher dynamics was measured for *At*HIRs. Proteins from the both groups are restricted from linear patterns within the plasma membrane, so called corrals. We found these corrals to align with microtubules, however the disruption of cytoskeleton did not induce any change of *At*FLOT or *At*HIR localization. Finally, we observed an increase in mobility in *At*HIR1 upon pharmacological inhibition of cellulose synthesis and the same effect was also observed under partial enzymatic cell wall digestion in *At*HIR1 and *At*FLOT2. Altogether our findings suggest that plasma membrane microdomain localized FLOTs and HIRs interact with the cell wall which decreases their mobility. This interaction may be important for the communication events at the interface between the cell and its environment. *At*FLOTs may be involved in these events, especially in process like plant-pathogen interaction or water stress, which is suggested by the physiological functions of protein interactors of *At*FLOT2 and transcription responses of *AtFLOT*s to such stimuli.

Abstrakt

Předkládaná práce zahrnuje tři původní články a jeden článek přehledový zaměřené na tematiku flotillinů (FLOT) a hypersensitive induced reaction proteinů (HIR) u *Arabidopsis thaliana*. FLOT a HIR jsou příbuzné rodiny proteinů asociovaných s membránami, které náležejí do nadrodiny proteinů s SPFH doménou. Zatímco FLOTy jsou přítomné u organismů všech evolučních linií, HIRy se specificky vyskytují jen u rostlin. Přehledový článek sumarizuje poznatky o FLOTech a HIRech z různých organismů, především s ohledem na jejich buněčnou lokalizaci, interakci s membránami, interakci s ostatními proteiny a na jejich možnou funkci. Prezentované původní články sledovaly tři směry zkoumání *At*FLOTu a *At*HIRů: zapojení do reakcí na exogenní podněty; nalezení proteinových interakčních partnerů; a vnitrobuněčnou lokalizaci a popis dynamiky těchto proteinů. První přístup spočíval v měření transkripce a sady fenotypovacích pokusů provedených na deletantech pro jednotlivé *AtFLOT* při ošetřeních biotickým a abiotickým stresem a fytohormony. Byly zjištěny změny v transkripci, nicméně jsme nepozorovali žádný měřitelný fenotypový projev u deletantů *AtFLOT*, který by se lišil od účinku ošetření na divoký typ. V druhém článku jsme se zaměřili na interaktom *At*FLOT2 a pomocí koimunoprecipitace a následné hmotnostně spektrometrické analýzy jsme nalezli možné interaktory *At*FLOT2. Mezi nimi byly zejména proteiny s transportní funkcí a dále proteiny zapojené v reakci rostliny na útok patogenů. U některých proteinů byla pomocí split-ubiquitin kvasinkového systému potvrzena přímá interakce s *At*FLOT2. Nalezené interaktory mohou být vodítkem pro odhalení funkce *At*FLOT2. Ve třetím článku (prezentovaném jako submitovaný rukopis) jsme pozorovali buněčnou lokalizaci a dynamiku všech isoforem *At*FLOTů a *At*HIRů. Všechny isoformy se až na jednu výjimku, která lokalizovala pouze do tonoplastu, vyskytovaly na plasmatické membráně. Minoritní pool na tonoplastu doprovázející převládající lokalizaci na plasmatické membráně se však vyskytoval i u jiných isoforem. Na plasmatické membráně se *At*FLOTy a *At*HIRy vyskytovaly agregovány v mikrodoménách. Tyto mikrodomény byly velmi stabilní v čase, zejména u *At*FLOTů, *At*HIRy byly mírně, avšak signifikantně mobilnější. Proteiny obou skupin chyběly v lineárních oblastech v rámci plasmatické membrány, tzv. korálech, které kolokalizovali s mikrotubuly. Destabilizace mikrotubulů i aktinového cytoskeletu však nevedla ke změně charakteru lokalizace *At*FLOTů ani *At*HIRů. Zvýšení mobility bylo pozorováno u *At*HIR1 při inhibici syntézy celulózy a stejný efekt měla i enzymatická degradace buněčné stěny, která vedle *At*HIR1 zvýšila i laterální mobilitu *At*FLOT2. V souhrnu naše výsledky ukazují, že *At*FLOTy a *At*HIRy lokalizované v mikrodoménách na plasmatické membráně interagují s buněčnou stěnou, která omezuje jejich mobilitu. Tento vztah může hrát roli v komunikaci odehrávající se na rozhraní plasmatické membrány a buněčné stěny. *At*FLOTy se mohou na takových dějích podílet, zejména na reakcích rostliny na vodní stres nebo setkání s patogenem, což naznačují změny transkripce *At*FLOTů v takovýchto podmínkách, stejně jako fyziologické působení proteinů interagujících s *At*FLOT2 nalezených v naší studii.

Introduction

The proposed work deals with *Arabidopsis thaliana* members of two closely related protein subfamilies – flotillins (FLOT) and hypersentitive induced response (sometimes referred also as hypersensitive induced reaction) proteins (HIR) belonging to stomatin/prohibitin/flotillin/ HflK/C (SPFH) domain superfamily (also known as Band 7 domain or PHB (prohibitin) superfamily). As stated in the thesis title, three directions were followed to describe the studied proteins. Three original research papers (one in the form of resubmitted manuscript) are thus presented within the frame of the thesis, focused on (i) phenotypic analysis of single isoform loss-of-function mutants of FLOTs under abiotic and biotic stresses, (ii) determination of interactors of FLOT2, and (iii) the description of FLOT and HIR behaviour at the plasma membrane (PM). The research articles are introduced by a review article which was composed at the beginning of the project in order to clarify and arrange current knowledge and findings already published in literature. After the review article at the end of the Introduction chapter a sum of information concerning the topic of PM and microdomains is presented to provide the context and background for the topic of the presented work and to describe some common features in proteins sharing with FLOTs and HIRs similar localization pattern.

SPFH proteins not only in plants

In plants, SPFH protein superfamily is represented by prohibitins, stomatins, flotillins, erlins and HIRs (Di et al., 2010). Conserved SPFH domain (ca 200 aa) is found also in protein subfamilies that do not occur in plants, such as metazoan podocin or bacterial HflK and HflC proteins (Rivera-Milla et al., 2006). On the contrary, HIRs are plant-specific SPFH proteins with homologs found also in *Haptophyta* (Rose et al., 2014, Shi et al., 2015). Three isoforms of FLOT and four isoforms of HIR among total seventeen SPFH proteins were discovered in *A. thaliana* genome (Figure 1, (Gehl and Sweetlove, 2014, Di et al., 2010)). *At*FLOT1 and *At*FLOT2 are of tandem duplication origin which is why they are in some papers referred as *At*FLOT1a and *At*FLOT1b (Jarsch et al., 2014, Yu et al., 2017), however within this thesis the *At*FLOT/*At*HIR nomenclature is applied as depicted in Figure 1.

Despite the vast range of processes in which mammalian FLOTs were described to take part, plant isoforms remain still rather poorly characterized. On the other hand, more extensive knowledge, mainly on PM localization, induction of expression or interaction with leucine-rich repeat proteins during pathogen attack, is available for HIRs of several species. In order to deduce

possible processes and function in which plant FLOTs might be implicated we compared plant and mammalian FLOT homologs as well as summarized the published findings on HIRs from various species in the following review article.

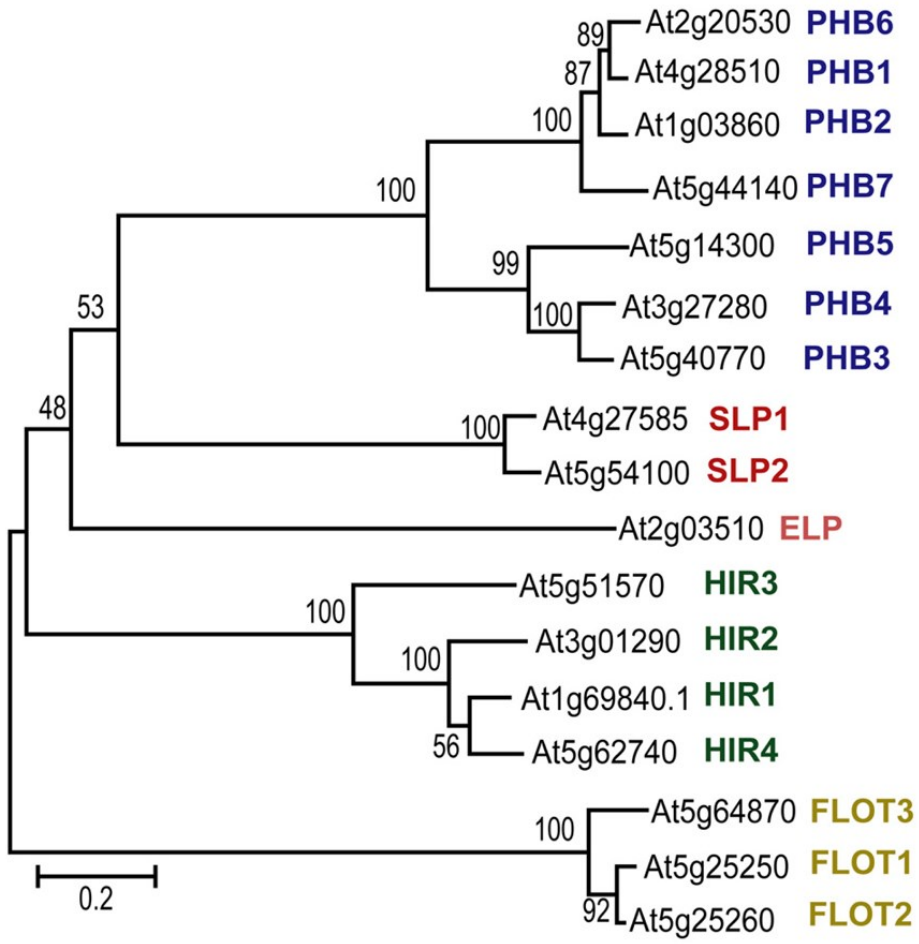

Figure 1: Cladogram of SPFH protein family of *Arabidopsis thaliana*. Flotillins are closely related to HIRs while proteins with mitochondrial localization – prohibitins and stomatins – form a distinct clade. PHB - prohibitin, SLP -stomatin, ELP – erlin, HIR - hypersensitive induced response protein, FLOT - flotillin. Adapted from Gehl and Sweetlove, 2014.

Since the time the review was published some new findings replenishing the information provided in the article have been gained. Importantly, *At*FLOT1 was found to bind *At*FLOT3 by its C-terminal domain, while N-terminal SPFH domain was not able to provide the interaction (Yu et al., 2017). This heterooligomerization of FLOT isoforms is known to be vital for stability, proper trafficking and functioning of the two mammalian FLOTs (Babuke et al., 2009, Solis et al., 2007) and was also reported for *At*HIRs where all four isoforms are able to form pairwise heterooligomers (Qi et al., 2011) as well as for apple *Md*HIR4 which binds other three *Md*HIR

isoforms (Chen et al., 2017). *At*HIR1 was also reported to form homo- mono- up to penta-mers (Lv et al., 2017b). Increasing number of evidence has been collected on the role of *At*FLOT1 in clathrin-independent endocytosis of PM-localized transporters or enzymes (Wang et al., 2013, Hao et al., 2014, Li et al., 2011) as well as receptor-like kinases which is promoted under their ligand recognition and that is further followed by FLOT-assisted endocytosis of the kinase (Wang et al., 2015, Cui et al., 2018). This is reminiscent of metazoan FLOT action where internalization of activated Epidermal Growth Factor Receptor is of the major flotillin functions (Solis et al., 2012). Similarly, in *Medicago truncatula Mt*FLOT4 colocalizes with activated coreceptor kinase *Mt*LYK3 (Haney et al., 2011), however, an additional membrane microdomain protein *Mt*SYMREM1interacting with *Mt*FLOT4 is involved in this process (Liang et al., 2018).

Paper # 1

Title: Flotillins, Erlins, and HIRs: From Animal Base Camp to Plant New Horizons

Authors: Michal Daněk, Olga Valentová, Jan Martinec

Summary: Plant stomatin/prohibitin/flotillin/HflK/C (SPFH) proteins are represented by prohibitins, flotillins, stomatins, erlins, and hypersensitive induced reaction proteins (HIRs). The purpose of this review is to summarize the current state of knowledge regarding plant flotillins and HIRs and to assign putative functions of plant flotillins and erlins based on the known functions of their mammalian homologs. Similar to human flotillins, plant flotillins are localized in membrane microdomains, and involved in endocytosis, and interact with receptor kinases. HIRs play an important role in plant immunity by promoting the hypersensitive response and binding to leucine-rich repeat proteins. In this way, they participate in resistance to bacterial or fungal pathogens. We further focused on flotillins, HIRs, and erlins in *Arabidopsis thaliana* and, using public databases, described them in terms of the following: 1) their transcription throughout plant ontogeny and under various environmental conditions; 2) the presence of conserved domains or characteristic motifs in their amino acid sequences; and 3) their potential interactions with other proteins. Based on these data, we hypothesize about their additional functions and properties.

DOI: 10.1080/07352689.2016.1249690

Citation: DANĚK, M., VALENTOVÁ, O. & MARTINEC, J. 2016. Flotillins, Erlins, and HIRs: From Animal Base Camp to Plant New Horizons. Critical Reviews in Plant Sciences.

My contribution: First and corresponding author. I performed the collection and research of literature, carried out prediction of domains and motifs in the protein sequences, realized search for protein interactors in databases, prepared figures and wrote the text.

CRITICAL REVIEWS IN PLANT SCIENCES
2016, VOL. 35, NO. 4, 191–214
http://dx.doi.org/10.1080/07352689.2016.1249690

Taylor & Francis
Taylor & Francis Group

Flotillins, Erlins, and HIRs: From Animal Base Camp to Plant New Horizons

Michal Daněk[a,b], Olga Valentová[c], and Jan Martinec[a]

[a]Institute of Experimental Botany, Czech Academy of Sciences, Prague, Czech Republic; [b]Department of Experimental Plant Biology, Charles University in Prague, Faculty of Science, Prague, Czech Republic; [c]Department of Biochemistry and Microbiology, University of Chemistry and Technology, Prague, Czech Republic

ABSTRACT
Plant stomatin/prohibitin/flotillin/HflK/C (SPFH) proteins are represented by prohibitins, flotillins, stomatins, erlins, and hypersensitive induced reaction proteins (HIRs). The purpose of this review is to summarize the current state of knowledge regarding plant flotillins and HIRs and to assign putative functions of plant flotillins and erlins based on the known functions of their mammalian homologs. Similar to human flotillins, plant flotillins are localized in membrane microdomains, and involved in endocytosis, and interact with receptor kinases. HIRs play an important role in plant immunity by promoting the hypersensitive response and binding to leucine-rich repeat proteins. In this way, they participate in resistance to bacterial or fungal pathogens. We further focused on flotillins, HIRs, and erlins in *Arabidopsis thaliana* and, using public databases, described them in terms of the following: 1) their transcription throughout plant ontogeny and under various environmental conditions; 2) the presence of conserved domains or characteristic motifs in their amino acid sequences; and 3) their potential interactions with other proteins. Based on these data, we hypothesize about their additional functions and properties.

KEYWORDS
Arabidopsis thaliana; erlin; flotillin; HIR; membrane microdomains; SPFH domain

I. Introduction

Cellular membranes provide many indispensable functions and serve as a crucial interface for communication, signaling, or transport. The membranes are functionally compartmentalized into distinguishable areas of various size—i.e., macro, micro, and nanodomains (Sekeres *et al.*, 2015; Zarsky *et al.*, 2009). The lateral discontinuum of the lipid composition of membranes was originally reported for sphingolipid-enriched areas preexisting within Golgi complex membranes that are sorted preferentially to the apical rather than basolateral plasma membrane in epithelial cells (Van Meer *et al.*, 1987). A subsequent association of sphingolipid-enriched membrane areas with glycophosphatidylinositol (GPI)-anchored proteins containing a sorting signal to the apical plasma membrane was observed (Brown and Rose, 1992). Finally, the term "lipid rafts" was proposed as the membrane trafficking principle resulting in different lipid-protein compositions of apical versus basolateral plasma membrane as well as signaling platform recruitment and clustering of proteins involved in membrane signaling (Simons and Ikonen, 1997). However, this has not yet been unambiguously confirmed (Kraft, 2013), and the term is inappropriate for plant membranes, for which the terms micro or nanodomains are to be used instead (Tapken and Murphy, 2015).

The stomatin/prohibitin/flotillin/HflK/C (SPFH) domain (also known as prohibitin homology (PHB) domain or Band_7 domain) protein superfamily comprises several types of proteins with different functions that are found in most evolutionary lineages (Rivera-Milla *et al.*, 2006). According to their cellular localization and biological function, the SPFH proteins are distinguished in several subfamilies. Metazoan SPFH proteins include flotillin/reggie (Schulte *et al.*, 1995), stomatin (Stewart *et al.*, 1993), prohibitin (Nuell *et al.*, 1991), erlin (Browman *et al.*, 2006), and podocin (Boute *et al.*, 2000). The bacterial membrane proteins HflK and HflC (Rivera-Milla *et al.*, 2006), and vacuolin of *Dictyostelium* (Rauchenberger *et al.*, 1997) are also SPFH protein superfamily members. Most of these proteins form microdomains in cell membranes. Besides, they are also enriched in detergent-resistant membrane (DRM) fraction (Browman *et al.*, 2007).

Plant SPFH proteins comprise prohibitins, flotillins, stomatins, erlins, and the plant-unique hypersensitive

CONTACT Michal Daněk danek@ueb.cas.cz Institute of Experimental Botany, Czech Academy of Sciences, Rozvojová 263, 165 02 Prague, Czech Republic.
Color versions of one or more of the figures in this article can be found online at www.tandfonline.com/bpts.

induced reaction proteins (HIRs) (Di *et al.*, 2010). SPFH protein homolog genes were identified in many plant species, including most common plant models such as *Arabidopsis thaliana, Chlamydomonas reinhardtii, Medicago truncatula, Oryza sativa, Physcomitrella patens, Populus tremula*, and *Sorghum bicolor* (Di *et al.*, 2010).

In this review, we attempt to summarize the knowledge acquired for HIRs, erlins, and flotillins. Because very little information is available for plant erlins and flotillins, we hypothesize about their putative functions based on current findings for their mammalian homologs, which play substantial roles in several essential processes—mainly signaling events. Plant stomatins and prohibitins, however, are not included in this review because they were recently reviewed by Gehl and Sweetlove (2014).

II. Flotillins—a wide range of functions

Flotillins were first discovered in goldfish (*Carassius auratus*) retinal ganglion cells (Schulte *et al.*, 1995) and originally named "reggie" because of their induced expression during optic nerve regeneration (Schulte *et al.*, 1997). Independent of the reggie discovery, a DRM protein found in caveolae membranes in mouse fibroblast tissue culture was denoted flotillin (Bickel *et al.*, 1997). The protein was homologous to a previously described human epidermal surface antigen (Bickel *et al.*, 1997; Schroeder *et al.*, 1994).

The *Arabidopsis thaliana* genome contains three coding regions for homologs of flotillin (At5g25250, At5g25260, and At5g64870). The first one was designated AtFlot1 (Borner *et al.*, 2005) or AtFLOT1A (Jarsch *et al.*, 2014), and the second was designated AtFLOT1B (Jarsch *et al.*, 2014). For the purpose of this review, we will refer them as follows: AtFlot1 (At5g25250), AtFlot2 (At5g25260), and AtFlot3 (At5g64870). *AtFlot1* and *AtFlot2* transcriptions predominate in leaves and shoots, whereas *AtFlot3* is mostly transcribed in flower parts and siliques (Figure 3).

A. The SPFH domain of flotillins is necessary for their proper membrane localization

The interaction of flotillins with membranes is provided through the SPFH domain in animal cells. The entire SPFH domain is pivotal for the localization of human Flotillin-2 to the plasma membrane and to endosomes in HeLa cells (Langhorst *et al.*, 2008). Similarly, the Flotillin-2 SPFH domain itself is sufficient for plasma membrane trafficking in Vero cells (Morrow *et al.*, 2002), whereas the truncated SPFH domain of Flotillin-2 lacking the N-terminal 1–40 aa (a hydrophobic stretch with acylation sites) does not localize to the plasma membrane in N2a cells (Solis *et al.*, 2007). Pronounced localization in Golgi cisternae has been observed for the truncated version of Flotillin-2 consisting of the N-terminal 1–30 aa stretch (containing palmitoylation and myristoylation sites) fused to the flotillin domain and lacking most of the SPFH domain (Langhorst *et al.*, 2008). Interestingly, whereas Flotillin-2 trafficking is impaired following treatment with Brefeldin A (BFA) and the protein was retained in accumulated Golgi vesicles (Langhorst *et al.*, 2008), Flotillin-1 localization is insensitive to BFA treatment. Thus, Flotillin-1 cellular trafficking is Golgi-independent (Morrow *et al.*, 2002).

The N-terminus of the SPFH domain is necessary for anchoring flotillins to membranes with palmitoyl and myristolyl residues in animal cells; truncated versions of both flotillins containing only the SPFH domain localize properly to the plasma membrane, whereas those lacking the SPFH domains accumulate in soluble fractions (Langhorst *et al.*, 2008; Morrow *et al.*, 2002; Neumann-Giesen *et al.*, 2004). Intriguingly, no palmitoylation or myristoylation sites were predicted in the N-terminus of any of the three *A. thaliana* flotillin homologs using public databases (Figure 1), and *A. thaliana* flotillins are thus considered to interact with membranes in a manner that differs from animal flotillins.

B. Flotillins are present in membrane microdomains and in detergent-resistant membranes

Flotillins are found in many animal cell types and lines (Volonté *et al.*, 1999; Zhao *et al.*, 2011). Regardless of rare findings in mitochondria in human (Ogura *et al.*, 2014) and murine cells (Zhang *et al.*, 2008), and in nuclei in human cell lines (Santamaria *et al.*, 2005), flotillins were most frequently associated with membrane microdomains (Baumann *et al.*, 2000; Dermine *et al.*, 2001; Frick *et al.*, 2007; Glebov *et al.*, 2006; Langhorst *et al.*, 2007, 2008; Neumann-Giesen *et al.*, 2007; Pust *et al.*, 2010; Riento *et al.*, 2009; Slaughter *et al.*, 2003; Solis *et al.*, 2007; Stuermer *et al.*, 2001). These are membrane areas that can be distinguished by physical properties and an enrichment of sterols, sphingolipids, saturated phospholipids, and GPI-anchored proteins from the surrounding membrane. DRM comprises a nonsolubilized membrane fraction that is extracted with mild, cold nonionic detergents (Brown and London, 1997; Brown and Rose, 1992); DRMs have traditionally been considered membrane microdomain counterparts. The association with DRMs is provided by hydrophobic stretches present at the N-termini of human flotillins (Liu *et al.*, 2005). Membrane microdomains, which have been reasonably classified by some authors as nanodomains with distinct lipid and protein composition, and DRMs have also been reported in plants

(Jarsch *et al.*, 2014; Mongrand *et al.*, 2004; Tapken and Murphy, 2015). The idea of microdomains being directly defined by areas of DRM has recently been overcome (Heerklotz, 2002; Lichtenberg *et al.*, 2005; Tanner *et al.*, 2011; Tapken and Murphy, 2015), but some authors still do not clearly distinguish between membrane microdomains and DRMs (Cacas *et al.*, 2016; Ishikawa *et al.*, 2015). This interconnection may seem intuitive because many proteins are present in both the DRM fractions (usually detected *in vitro*, e.g., on Western blots), and the membrane microdomains (observed as clusters or dots of tagged proteins using microscopic techniques), although neither of the two implies the existence of the other.

The plant flotillins AtFlot1, *Picea meyeri* PmFlot1, and rice OsFlot were enriched in the plasma membrane DRM fraction prepared from *A. thaliana* calli, spruce pollen tubes, and rice cells. Concomitant alteration of the sphingolipid composition of the DRM fraction and OsFlot contents in this DRM fraction was observed in rice overexpressing BI-1 (Ishikawa *et al.*, 2015). AtFlot1 and AtFlot2 fused to green fluorescent protein (GFP) or yellow fluorescent protein (YFP) were observed in plasma membrane clustered in dynamic punctate structures corresponding to membrane microdomains in leaf (Jarsch *et al.*, 2014) and root (Hao *et al.*, 2014; Li *et al.*, 2011, 2012) epidermal cells. Similar localization and punctate structure formation within plasma membrane in root epidermal cells were also observed for flotillin homologs of *M. truncatula* MtFLOT2 and MtFLOT4 (Haney and Long, 2010; Haney *et al.*, 2011).

Plant membrane microdomains can be distinguished according to their localization pattern, e.g., polar, equatorial, and punctate domains. Fluorescent-labeled flotillins, similar to, e.g., remorins, cellulose synthase, or plasma membrane intrinsic proteins, form discrete foci or punctate microdomains in the plasma membrane (Konrad and Ott, 2015).

C. Flotillin microdomains provide specific types of endocytosis

In addition to their plasma membrane localization, flotillins have been observed extensively in endosomes and

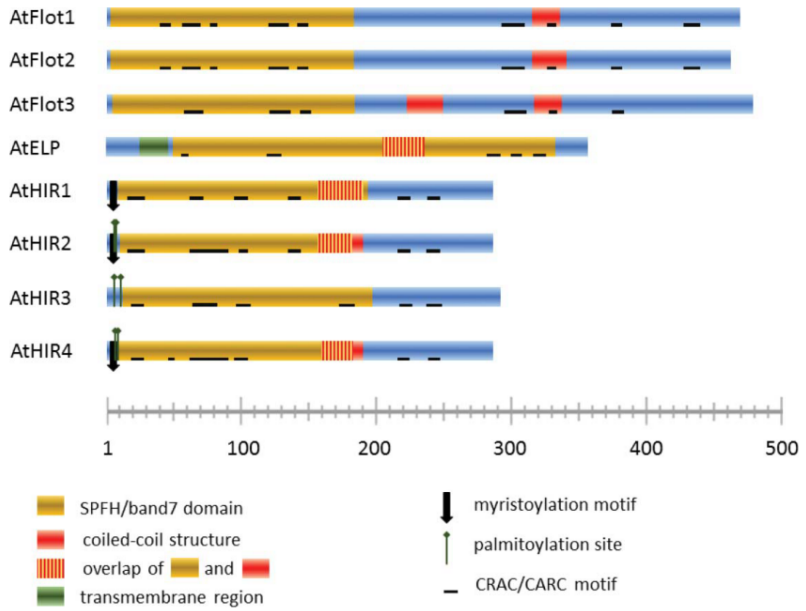

Figure 1. Structure of *Arabidopsis thaliana* SPFH proteins. Putative conserved SPFH (= band 7) domains (yellow), coiled-coil stretches (red), transmembrane stretches (green), N-myristoylation motifs (black downward arrows), and palmitoylation sites (green upward arrows) were identified using the NCBI conserved domain searching tool (http://www.ncbi.nlm.nih.gov/Structure/cdd/wrpsb.cgi), Max-Planck Institute for Developmental Biology Bioinformatics Toolkit (http://toolkit.tuebingen.mpg.de/pcoils, http://toolkit.tuebingen.mpg.de/marcoil), prediction of transmembrane helices in proteins using the TMHMM Server v. 2.0 (http://www.cbs.dtu.dk/services/TMHMM/), NBA-Palm—prediction of palmitoylation site (http://nbapalm.biocuckoo.org), CSS-Palm—prediction of palmitoylation site (http://csspalm.biocuckoo.org), PlantsP—plant-specific myristoylation predictor (http://plantsp.genomics.purdue.edu/myrist.html), NTM—the MYR predictor (http://mendel.imp.ac.at/myristate/SUPLpredictor.htm), and Myristoylator (http://web.expasy.org/myristoylator/). CRAC, CARC, and CRAC/CARC-like motifs (black horizontal segments) were searched manually using the ScanProsite tool (http://prosite.expasy.org/scanprosite/). The ruler indicates the protein length as the number of amino acids.

other vesicular compartments. The plasma membrane/endosome distribution ratio is different in various cell types or at different developmental stages (Dermine *et al.*, 2001; Liu *et al.*, 2005). Human flotillins are strongly endocytosed upon stimulation with epidermal growth factor (Babuke and Tikkanen, 2007; Neumann-Giesen *et al.*, 2007; Riento *et al.*, 2009), shiga toxin (Pust *et al.*, 2010), ricin (Pust *et al.*, 2010), or cholera toxin (Ait-Slimane *et al.*, 2009; Glebov *et al.*, 2006; Stuermer *et al.*, 2001).

Human Flotillin-1 is found in plasma membrane curvatures and invaginations, as well as endosomes that are distinct from clathrin-coated vesicles, with no overlap between fluorescentl-labeled flotillin and transferrin, a marker of clathrin-mediated endocytosis (Glebov *et al.*, 2006; Langhorst *et al.*, 2008). Moreover, the rate of transferrin endocytosis was not affected in Flotillin-2-knockdown cells (Ait-Slimane *et al.*, 2009), and Flotillin-1-positive vesicles displayed different dynamics from clathrin-coated vesicles (Glebov *et al.*, 2006). Unlike clathrin-coated vesicles, flotillin microdomain endosome budding is not dependent on dynamin in HeLa cells (Glebov *et al.*, 2006). However, endocytosis of sphingolipid-binding domain peptide, a sphingolipid tracer, GPI-GFP and CD59, a GPI protein, was mediated by Flotillin-2 and dependent on dynamin (Ait-Slimane *et al.*, 2009; Zhang *et al.*, 2009a). Thus, flotillins are crucial for the endocytosis of GPI-anchored proteins.

AtFlot1 was predominantly observed on the plasma membrane from which vesicles budded and co-localized with FM4-64-labeled endosomes in *A. thaliana*. AtFlot1-labeled endosomes differed from clathrin-coated endosomes in terms of size and mobility. The diffusion coefficient of AtFlot1 endosomes was not affected by tyrphostin A23, an inhibitor of clathrin-mediated endocytosis, but was decreased by the application of latrunculin B, an inhibitor of actin polymerization; oryzalin, an inhibitor of tubulin polymerization; and methyl-β-cyclodextrin, a sterol-depleting agent (Li *et al.*, 2012). Flotillin microdomains thus define a clathrin-independent endocytic pathway in both mammalian and *A. thaliana* cells. However, the extent to which one or the other pathway is utilized for the endocytosis of a specific cargo depends on external conditions in *A. thaliana* root cells. In the case of the plasma membrane aquaporin PIP2;1 and NADPH oxidase RbohD, both were predominantly endocytosed via a clathrin-dependent pathway under control conditions, with only a minor contribution of AtFlot1-positive endosomes. This proportion was dramatically increased under salt stress (Hao *et al.*, 2014; Li *et al.*, 2011). Similarly, the brassinosteroid receptor BRI1 is endocytosed in a mostly clathrin-dependent manner when only endogenous brassinosteroids are available. External application of epibrassinolide substantially increases AtFlot1-dependent endocytosis of BRI1 (Wang *et al.*, 2015). Based on these findings, for the same cargo proteins, the clathrin pathway may function as a constitutive endocytic mechanism, whereas flotillin microdomain-based endocytosis is induced by stress or in response to signaling events. This pathway may either serve as a simple contributor to the overall endocytic capacity, or it may direct the endocytosed cargo via an alternative trajectory (e.g., vacuolar degradation versus recycling).

Flotillin pits resemble another type of endocytic structure—caveolae, which are membrane invaginations characterized by the presence of proteins called caveolins (Glenney and Soppet, 1992). The caveolin structure and interaction with the membrane is very similar to those of flotillin, although the domain that interacts with the plasma membrane is located in the N-terminus of flotillins but in the C-terminus of caveolins (Bender *et al.*, 2002; Stuermer, 2010). An interaction of flotillins and caveolins in the formation of endocytic structures was observed in A498 cells (Volonté *et al.*, 1999) and adipocytes (Baumann *et al.*, 2000), and downregulated expression of Flotillin-1 caused a decrease in the concentration of Caveolin-1 in intestinal epithelial cells (Vassilieva *et al.*, 2009). A functional link was found in skeletal muscle cells during insulin-induced glucose transporter type 4 (GLUT-4) trafficking to the plasma membrane. In this process, the stimulated insulin receptor is first endocytosed through caveolae and caveolin-3, and then, is re-localized to GLUT-4-containing Flotillin-1 vesicles, where it provokes Flotillin-1/GLUT-4 vesicle recruitment to the plasma membrane (Fecchi *et al.*, 2006). By contrast, there is no co-localization between caveolins and flotillins in HeLa cells (Frick *et al.*, 2007; Glebov *et al.*, 2006), in which different caveolin and flotillin microdomain dynamics were observed (Frick *et al.*, 2007). Similarly, in human kidney epithelial cells, Flotillin-2 and Caveolin-1 define distinct non-co-localizing microdomains (Roitbak *et al.*, 2005). In DRM prepared from HEK293 cells, Flotillin-1 and Caveolin-1 are found in distinct sub-fractions (Mellgren, 2008). No co-localization was found between endocytosed CD59, a GPI-anchored protein, and caveolin (Ait-Slimane *et al.*, 2009).

Taken together, these findings suggest that there are several populations of flotillin endocytic structures, some of which mediate GPI-anchored protein endocytosis whereas others may contribute to the endocytosis of different cargos delivered by complexes of flotillins and caveolins.

However, the genes for caveolins have not been discovered in plants (Echarri and Del Pozo, 2012; Samaj *et al.*, 2004). Thus, it is tempting to hypothesize that based on structural and functional similarities, plant flotillins could potentially adopt or encompass some

processes that are mediated by caveolins in animal cells. The significance of plant flotillins in membrane transport is supported by the interaction of AtFlot2 and AtFlot3 with several proteins involved in vesicular trafficking and endocytosis, including ESCRT proteins, exocyst and SNARE subunits, and Rab-GTPase (Table 1).

D. Flotillins and sterols

Because sterols are important for the proper membrane microdomain constitution of some plant and yeast proteins (Grossmann *et al.*, 2007; Malínská *et al.*, 2003; Raffaele *et al.*, 2009), it has been questioned whether or not the amount of sterols present within membranes can affect flotillin microdomain properties. The most abundant sterol in animal cells, cholesterol (Espenshade and Hughes, 2007), is recognized by proteins through their cholesterol recognition/interaction amino acid consensus motifs, i.e., CRAC, with the following amino acid sequence: L/V-X_{1-5}-Y-X_{1-5}-K/R, where X = any amino acid (Li and Papadopoulos, 1998). The inverted motifs, K/R-X_{1-5}-Y -X_{1-5}-L/V or CARC, and the modified K/R-X_{1-5}-F-X_{1-5}-L/V or CARC-like were also found to bind cholesterol (Baier *et al.*, 2011). Mammalian Flotillin-2 was predicted to contain two putative CRAC motifs in its amino acid sequence, both of which reside in the SPFH domain (Roitbak *et al.*, 2005). Both murine flotillins were found to interact directly with Niemann-Pick 1-like 1 (NPC1L1) protein, which cycles between the plasma membrane and the endocytic recycling compartment to mediate cholesterol uptake. The complex of flotillins and NPC1L1 forms microdomains at plasma membrane co-localizing with cholesterol-rich foci stained with filipin. Moreover, the complex dissociates in the absence of cholesterol (Ge *et al.*, 2011). In Flotillin-knockdown cells, NPC1L1 and cholesterol are also predominantly present at the plasma membrane, and overall cholesterol uptake is decreased in comparison to cells expressing flotillins at normal levels (Ge *et al.*, 2011). Similarly, in *Aspergillus nidulans* strains with flotillin ortholog depletion, the localization pattern of sterol-rich domains (stained with filipin) differs from that of wild-type strains, although sterol-rich domains do not co-localize with flotillin ortholog microdomains (Takeshita *et al.*, 2012). Flotillin may thus affect sterol uptake/trafficking/localization both directly and indirectly in different cell types or evolutionary lineages.

Proper sterol composition and trafficking to membranes is also important for endocytic processes in plant (Sekeres *et al.*, 2015). The sterol content of DRMs is necessary for proper functioning of membrane microdomain-localized NADPH oxidase in *P. meyeri* (Liu *et al.*, 2009). Decreased sterol content in AtFlot1-knockdown lines (Li *et al.*, 2012) leads to a decrease in the structural order of the membrane (measured as generalized polarization) in these lines (Zhao *et al.*, 2015). Moreover, the depletion of sterol using methyl-β-cyclodextrin results in a decrease in the lateral mobility of AtFlot1 microdomains (Li *et al.*, 2012), which is consistent with the effect observed in N2a cells (Langhorst *et al.*, 2007). Although the effect of sterol depletion may be rather pleiotropic as a result of overall changes in membrane properties, flotillin microdomain dynamics appear to be particularly sensitive to the sterol content of the membrane. The most pronounced decrease in the diffusion coefficient was observed for AtFlot1 (80-fold decrease in the mode value) compared with some other plasma membrane microdomain or punctate-forming proteins such as clathrin (5-fold decrease), RbohD (28-fold decrease), or PIP2;1 (20-fold decrease) in response to the same methyl-β-cyclodextrin treatment (Hao *et al.*, 2014; Li *et al.*, 2011, 2012). The function of flotillins is thus affected by the presence or the amount of sterols, but flotillins also influence sterol uptake and its levels in the cell. *A. thaliana* possesses two sequence homologs of NPC1L1 (At1g42470 and At4g38350), but they do not appear to be involved in sterol metabolism or trafficking (Feldman *et al.*, 2015).

The sequestration of sterols from the plasma membrane leads to changes in the membrane order and fluidity following exposure to oomycetal elicitins such as cryptogein, cactorein, or parasiticein, which are produced by different species of *Phytophthora* (Mikes *et al.*, 1998; Vauthrin *et al.*, 1999). The transcription of all *A. thaliana* flotillin isoforms is highly induced in response to treatment with *Phytophthora* and *Hyaloperonospora* (Figure 2), which are common plant pathogens that encode numerous elicitins or elicitin-like proteins (Chen *et al.*, 2014). Given that *AtFlot1*-knockdown plants contain less sterols in plasma membranes (Li *et al.*, 2012), it is possible that AtFlots binds to sterols and thus prevents them from being trapped and removed from the plasma membrane by elicitins.

Because CRAC/CARC motifs have not yet been demonstrated to recognize sterols other than cholesterol, neither have they been investigated in plants. Thus, it is difficult to predict whether plant flotillin homologs can bind to sterols. In plant cells, phytosterols predominate over cholesterol, which is present in rather minute amounts. The CRAC/CARC motif recognizes the A or B ring of the sterane structure and iso-octyl chain of cholesterol (Fantini and Barrantes, 2013). The A and B cycles are common to cholesterol and the main phytosterols (i.e., β-sitosterol, campesterol, stigmasterol, and brassicasterol), whereas they differ from one another in terms of side chains (iso-octyl in cholesterol). However, phytosterols have been confirmed to bind with a relatively high efficiency to two cholesterol-binding proteins,

Table 1. Proteins that interact with flotillins or HIRs of *Arabidopsis thaliana*.

AGI	Name	Function/type	SPFH	Source
AT1G21240	WAK3	Signaling/receptor-like kinase	F1, F2, F3	a
AT2G42290	LRR protein kinase	Signaling/receptor-like kinase	F2, F3	a
AT2G20850	SRF1	Signaling/receptor-like kinase	F3	a
AT2G17290	CPK6	Signaling/calcium-dependent kinase	F3	a
AT3G48260	WNK3	Signaling/MAPKKK	F2	a
AT3G48040	ROP10	Rop GTPase	F1, F2, F3	a
AT5G42980	TRX3	Signaling/thioredoxin	F1, F2, F3	a
AT1G45145	TRX5	Signaling/thioredoxin	F2	a
AT2G26180	IQD6	Calcium binding	F1, F2, F3	a
AT4G37445	Unknown	Calcium binding	F2, F3	a
AT1G03950	VPS2.3	Protein sorting/ESCRT	F2	a
AT3G10640	VPS60.1	Protein sorting/ESCRT	F2, F3	a
AT1G54090	EXO70D2	Vesicular transport/exocyst subunit	F3	a
AT3G03800	SYP131	Vesicular transport/SNARE subunit	F3	a
AT4G35860	GB2	Rab GTPase	F3	a
AT1G17280	UBC34	Ubiquitination/conjugation enzyme	F2, F3	a
AT3G60820	PBF1	Proteasome subunit	F2, F3	a
AT4G38690	PLC-like	Phospholipid metabolism	F2, F3	a
AT3G08510	PLC2	Phospholipid metabolism	F3	a
AT4G21540	SPHK1	Sphingosine metabolism	F3	a
AT4G04850	CPA2	Monovalent cation:proton antiporter	F2	a
AT3G12180	Cornichon	Potassium/sodium transport	F1, F2, F3	a
AT5G22290	NAC089	Transcription factor	F2, F3	a
AT5G28290	NEK3	Cell-cycle regulator	F3	a
AT4G05370	BCS1	AAA ATPase	F2, F3	a
AT1G14700	PAP3	Purple acid phosphatase	F2	a
AT3G54260	TBL36	Trichome birefringence-like	F2, F3	a
AT3G01500	Carbonic anhydrase 1	Carbonic anhydrase	F2	a
AT1G34760	GRF11	14-3-3 protein	F3	a
AT1G19570	DHAR1	Dehydroascorbate reductase	F3	a
AT2G24940	MAPR2	Progesterone binding protein	F3	a
AT4G27610	Unknown	Unknown	F2	a
AT3G03210	Unknown	Unknown	F2	a
AT4G26090	RPS2	NB-Leucine-rich repeat protein	H1, H2	b, c
AT3G58140	Phe-tRNA synthetase	Phe-tRNA synthetase	H1, H2, H3, H4	b
AT5G35750	AHK2	Histidine kinase/cytokinin receptor	H1, H4	c
AT3G01670	SEOR2	Sieve element occlusion related	H3	c

Protein that interact with *Arabidopsis thaliana* SPFH proteins retrieved from protein-interaction databases. F1 = AtFlot1, F2 = AtFlot2, F3 = AtFlot3, H1 = AtHIR1, H2 = AtHIR2, H3 = AtHIR3, H4 = AtHIR4; a = Associomics (https://associomics.dpb.carnegiescience.edu/Associomics/Home.html), b = String (http://string-db.org/), c = Anap (http://gmdd.shgmo.org/Computational-Biology/ANAP/ANAP_V1.1/). Only interactions obtained experimentally (pull-down assay or Y2H screen) were considered. Concerning Associomics, only interactions of at least two positive screen results were assumed.

oxytocin receptor and cholecystokinin (type B) receptor (Gimpl *et al.*, 1997), of which the latter contains the CRAC motif essential for binding to cholesterol (Desai and Miller, 2012). In plants, only a limited number of proteins have been experimentally demonstrated to bind sterols. A sitosterol-binding protein, ORP3, contains an oxysterol-binding region (Saravanan *et al.*, 2009) with four putative CRAC/CARC/CARC-like motifs. Moreover, one of these motifs is contained within the conserved KPFNPLLGETF region that is shared among several oxysterol-binding proteins from *A. thaliana* and rice (Umate, 2011). Similarly, a stigmasterol- and phosphatidylethanolamine-binding protein, ROSY1, contains three putative CRAC/CARC/CARC-like motifs within its MD2 lipid-binding domain (Dalal *et al.*, 2016). Taken together, it is possible that CRAC/CARC motifs can recognize at least some phytosterols; therefore, we investigated the presence of putative CRAC/CARC motifs in *A. thaliana* flotillins, HIRs, and erlins (Figure 1). Several motifs were predicted for each protein within but also outside the SPFH domain.

E. Protein-protein interactions—flotillin mode of action

Because flotillins do not dispose of an activity like enzymes, transporters, and molecular motors, among others, their function likely consists of affecting other proteins via protein-protein interactions. First, mammalian flotillins interact with one another to form homotetramers (Neumann-Giesen *et al.*, 2004; Solis *et al.*, 2007) and heterotetramers (Solis *et al.*, 2007). Oligomerization is provided by coiled-coil structures outside of the SPFH domain within so-called flotillin domains in the C-terminal parts of the proteins (Solis *et al.*, 2007). The tetramers are quite resistant toward denaturation; they remain

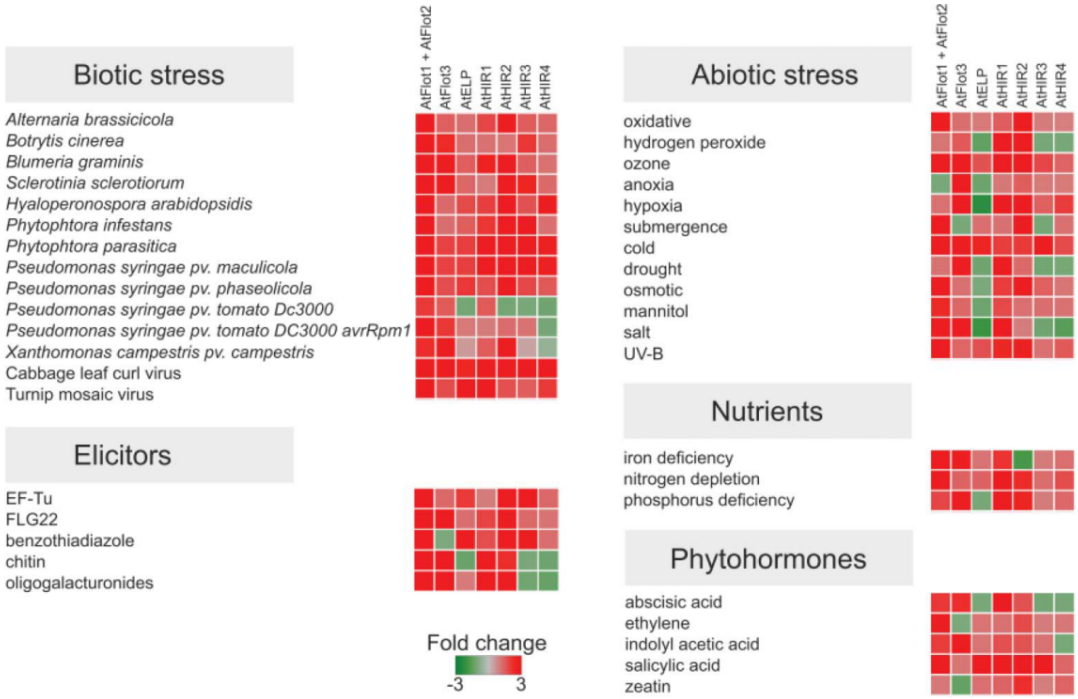

Figure 2. *Arabidopsis thaliana* SPFH gene transcription is affected by many factors. Affymetrix 22 K microarray data were retrieved from Genevestigator.

stable in 8 M urea (Solis *et al.*, 2007). The effects of mutual flotillin interactions on their localization within the plasma membrane have been established: when only one of the isoforms is overexpressed, it is evenly distributed throughout the plasma membrane, whereas under a similar expression level of both flotillins these two are predominantly concentrated and co-localize in plasma membrane microdomains (Frick *et al.*, 2007). Flotillin-2 affects Flotillin-1 stability by preventing its 26S proteasome degradation, while knockdown of Flotillin-1 had little or no effect on the Flotillin-2 concentration (Pust *et al.*, 2010; Solis *et al.*, 2007). However, endocytosis of the Flotillin-1/Flotillin-2 complex was impaired in Flotillin-1-knockout cells, demonstrating the importance of flotillin heterooligomerization for endocytosis (Babuke *et al.*, 2009). Given that there are three isoforms of flotillin homologs in the genome of *A. thaliana*, the situation in plant cells may be more complex.

Another relationship with 26S proteasome protein degradation was demonstrated via human Flotillin-1 binding to antisecretory factor (AF) protein, which displays antisecretory and anti-inflammatory features (Bjorck *et al.*, 2000; Davidson and Hickey, 2004) and has been shown to interact with the 26S proteasome (Lange *et al.*, 1999). AF is 42% identical to *A. thaliana* 26S proteasome non-ATPase regulatory subunit 4, which is also known as multiubiquitin chain binding protein 1 (At4g38630). Moreover, AtFlot2 and AtFlot3 were demonstrated to bind two proteins involved in ubiquitination and proteasome degradation (Table 1). Thus, plant flotillin activity may be controlled by ubiquitination or, moreover, flotillins themselves may be involved in regulating the degradation of other proteins.

F. Flotillins interact with kinases

One prominent group of proteins that interact with mammalian flotillins are tyrosine kinases such as epidermal growth factor receptor (EGFR) (Amaddii *et al.*, 2012), a transmembrane receptor kinase (Ullrich and Schlessinger, 1990), and Src family kinases (Neumann-Giesen *et al.*, 2007). Src proteins are nonreceptor kinases that are involved in many cellular processes, among which signal transduction is of the most substantial one (Parsons and Parsons, 2004; Sirvent *et al.*, 2015). The distribution of EGFR within the plasma membrane changes in response to stimulation with its ligand, EGF, forming clusters, and EGFR is enriched in the DRM (Roepstorff *et al.*, 2002). This clustering is impaired when Flotillin-1 is knocked down (Amaddii *et al.*, 2012). Upon stimulation with EGF, both flotillins co-precipitate with EGFR, even when EGFR kinase activity is inhibited (Amaddii *et al.*, 2012; Riento *et al.*, 2009), and are endocytosed together with EGFR from the plasma membrane

(Amaddii *et al.*, 2012; Neumann-Giesen *et al.*, 2007). This re-localization consists of the phosphorylation of Flotillin-2 (Neumann-Giesen *et al.*, 2007) but is independent of Flotillin-1 (Amaddii *et al.*, 2012). However, in Flotillin-1-knockout cells, the phosphorylation of EGFR itself is reduced (Amaddii *et al.*, 2012). Thus, flotillins mediate EGFR function and endocytosis, whereas EGFR does not affect flotillins by phosphorylating them.

Both human flotillins are phosphorylated on several Tyr residues within the SPFH domain by Fyn (Riento *et al.*, 2009) and Src (Neumann-Giesen *et al.*, 2007; Riento *et al.*, 2009) kinases belonging to Src family kinases. The phosphorylation of a specific Tyr of Flotillin-2 is necessary for endocytosis of the Flotillin-based complex (Neumann-Giesen *et al.*, 2007; Riento *et al.*, 2009). Src, Fyn, and Lyn kinases co-precipitate with flotillins (Kato *et al.*, 2006; Liu *et al.*, 2005; Neumann-Giesen *et al.*, 2007), and this interaction depends on the kinase activity of these Src family kinases (Neumann-Giesen *et al.*, 2007) and is mediated by Tyr residues of flotillins (Liu *et al.*, 2005).

Src-phosphorylated Flotillin-1 co-precipitates with the succinate dehydrogenase iron-sulfur subunit in mitochondria, and this interaction is impaired when Src kinase activity is inhibited (Ogura *et al.*, 2014). Thus, the phosphorylation of flotillins may be required for flotillins to bind to other proteins.

Although plants lack Tyr kinases, numerous dual specificity kinases have been described in *A. thaliana* that have structural similarities to animal Tyr kinases including Src, Lyn, and Fyn (Rudrabhatla *et al.*, 2006). Taken together with the observation that the proportion of phosphotyrosine among all phosphorylated amino acids in *A. thaliana* is similar to that in humans (Sugiyama *et al.*, 2008), it would be interesting to investigate whether the function of *A. thaliana* flotillins is also modulated by phosphorylation.

In plants, a pattern similar to the interaction of mammalian flotillin and EGFR induced by EGF stimulation has been described for *M. truncatula* MtFLOT4 and Lysin motif receptor-like kinase 3 (LYK3), a receptor of nodulation factor (NF) in root hairs. After stimulation of LYK3 and MtFLOT4 with NF, both proteins re-localize to the apex of the root hair and cluster and co-localize in the resulting microdomains, whereas without stimulation, they are both present in puncta that are evenly distributed throughout the plasma membrane without significant co-localization. The amount of MtFLOT4 in the plasma membrane of root hairs decreased in LYK3 kinase-inactive plants (Haney *et al.*, 2011). The LYK3 homolog in *A. thaliana* is Chitin elicitor receptor kinase 1 (At3g21630). Moreover, *AtFlot* transcription is upregulated by chitin (Figure 2). All AtFlot isoforms also bind to receptor-like kinases that can also play a role in signal transduction (Table 1).

An important type of plant kinase is wall-associated kinases (WAKs). The extracellular domain of WAK shares sequence similarity with EGFR (He *et al.*, 1996), and AtWAK3 binds to all the three isoforms of AtFlots (Table 1). Thus, it is possible that plant flotillins may be involved in cell responses to extracellular signals in a manner similar to mammalian flotillins. AtWAK1 and AtWAK2 have been reported to bind oligogalacturonides—products of cell-wall pectin cleavage caused by pathogens—and thus AtWAKs may mediate the defense response (Brutus *et al.*, 2010; Kohorn *et al.*, 2009). WAKs and WAK-likes have also been reported to be involved in mineral processing, especially heavy-metal uptake and responses (Hou *et al.*, 2005; Sivaguru *et al.*, 2003). Plant flotillin involvement in these WAK-mediated processes is supported by the upregulation of all *AtFlot* by oligogalacturonides and in response to iron and nitrogen deficiency (Figure 2).

G. Flotillin interactions with the cytoskeleton and extracellular matrix

In mammalian cells, flotillins co-localize with F-actin attached to the plasma membrane (Langhorst *et al.*, 2007; Liu *et al.*, 2005). This interaction is achieved via a multivalent adaptor protein, CAP/ponsin, which binds directly to both flotillins (Baumann *et al.*, 2000; Liu *et al.*, 2005) in their SPFH domain (Langhorst *et al.*, 2007) and actin (Liu *et al.*, 2005). Blocking actin polymerization with cytochalasin D does not affect the number or organization of flotillin domains (Langhorst *et al.*, 2007; Liu *et al.*, 2005), but their lateral mobility increases or decreases in response to disruption or enhanced polymerization of actin filaments, respectively. No such effect has been observed for microtubules in animal cells (Langhorst *et al.*, 2007).

The opposite situation is observed for the AtFlot1 diffusion coefficient, which decreases when both actin and tubulin polymerization are disrupted (Li *et al.*, 2012). Moreover, AtFlot1 vesicles co-localize with the myosin-binding protein MyoB1 (Peremyslov *et al.*, 2013). Given that movement along actin filaments is realized by myosin motor proteins (Vale, 2003), these findings suggest a possible functional linkage of plant flotillins and actin.

In animal cells, F-actin also interacts with flotillin associated with cadherin in adherens cell junctions (Guillaume *et al.*, 2013), and both flotillins directly interact with catenin, another protein in the cell junction complex (Kurrle *et al.*, 2013). Flotillins are vital for the stability and integrity of these junctions, and Flotillin-knockdown cells display aberrant junctions (Guillaume *et al.*, 2013; Kurrle *et al.*, 2013; Solis *et al.*, 2012).

Although cadherins are not present in plants (Hulpiau and van Roy, 2009), antibodies against animal cadherins and catenins display significant cross-immunoreactivity in corn, binding mainly to membrane structures (Baluska *et al.*, 1999). Catenins belong to a family of armadillo repeat (ARM)-containing proteins that are also found in plants (Coates, 2003). In *A. thaliana*, 108 ARM-containing proteins have been predicted, most of which are ubiquitin ligases (Mudgil *et al.*, 2004) associated with the plasma membrane (Vogelmann *et al.*, 2014).

As mentioned above, all three isoforms of AtFlots bind WAK3, which belongs to a family of plant kinases that mediate communication between the extracellular matrix and the cell (Wagner and Kohorn, 2001). Plant flotillins may—similarly to mammalian ones—participate in plasma membrane to cell wall communication with respect to structure formation and signaling.

H. The interactome and transcription profiles of Arabidopsis thaliana flotillins may indicate their additional function

Because the functions of animal flotillins consist mainly of interactions with other proteins, knowledge of plant Flotillin-interacting partners may indicate their possible roles. We analyzed the amino acid sequences of AtFlots (as well as other *A. thaliana* SPFH proteins) for coiled-coil motifs using web prediction tools. All three AtFlots contain putative coiled-coil motifs (Figure 1), suggesting a potential association with other proteins via these motifs. For three AtFlots, several interacting proteins are present in the Associomics Membrane-based Interactome Database (MIND) based on split-ubiquitin Y2H assays, thus assembling data on the interactions of membrane-bound proteins. As previously described, AtFlots interact with several receptor-like kinases. In addition, other proteins involved in cell signaling or regulation, such as Mitogen-activated protein kinase kinase kinase (MPKKK), calcium-binding proteins, or thioredoxins, have been found to bind AtFlots (Table 1).

Three proteins that interact with *A. thaliana* flotillins participate in phospholipid or sphingolipid metabolism. Because both sphingolipids and saturated phospholipids are necessary for membrane microdomain formation and composition, these interactions suggest possible roles of AtFlots in the actual microdomain establishment in terms of Flotillin-mediated modulation of proper membrane lipid composition.

As mentioned above, both animal and plant flotillins participate in clathrin-independent endocytosis. Therefore, it is not surprising that proteins involved in protein sorting (ESCRT) or vesicular transport (exocyst and SNARE subunits) interact with AtFlots.

The transcription of all *AtFlot* isoforms is highly induced under salt stress (Figure 2). AtFlot2 binds to CPA2, a monovalent cation transporter, and all three flotillin isoforms interact with cornichon, a protein of unknown function in the *A. thaliana*, an ortholog of which interacts with the potassium/sodium transporter in rice (Rosas-Santiago *et al.*, 2015). Thus, AtFlots may take part in monovalent cation uptake.

AtFlot1 co-localizes with PIP2;1 aquaporin within membrane microdomains. In response to NaCl treatment, PIP2;1 is endocytosed from the plasma membrane via a clathrin-independent pathway, i.e., a pathway that is likely mediated by AtFlot1 (Li *et al.*, 2011). Together with the considerable induction of *AtFlots* transcription by osmotic or water stress, this observation may indicate the potential involvement of AtFlot1 in the regulation of water uptake. A NADPH oxidase, RbohD, which is known to mediate plant responses to pathogens (Pogany *et al.*, 2009; Torres *et al.*, 2002) or salt stress (Xie *et al.*, 2011) through the production of reactive oxygen species (ROS), has also been found to co-localize with AtFlot1 (Hao *et al.*, 2014). In addition, in *P. meyeri*, pollen tube PmFlot1 was associated with the same DRM fraction as NADPH oxidase (Liu *et al.*, 2009). Because ROS signaling accompanies many plant stress reactions, including hypoxia or anoxia (Pucciariello *et al.*, 2012), and single *AtFlot* isoform transcription is upregulated by oxidative stress or hypoxia and anoxia, a contribution of flotillin to this cellular event may also be possible.

III. Erlins—important players in endoplasmic reticulum signaling

Erlins were discovered in human hematopoietic cell lines (Browman *et al.*, 2006). To date, they have been further characterized only in humans and *Caenorhabditis elegans* (Hoegg *et al.*, 2012). Only one sequence of an erlin homolog—erlin-like protein (AtELP, At2g03510)—was identified in *A. thaliana* (Di *et al.*, 2010; Gehl and Sweetlove, 2014). Its transcription throughout plant development and in organs is presented in Figure 3. It is generally expressed throughout all development stages and plant organs, with maximal expression potential in siliques and the lowest values in anthers, pollen, and vegetative parts of the inflorescence. *AtELP* transcription is upregulated in response to pathogens, namely *Phytophthora parasitica*, some strains of *Pseudomonas syringae*, and viruses. Among abiotic stresses and phytohormones, cold and salicylic acid (SA) have the most prominent effects.

A. Erlins form multimeric complexes in the endoplasmic reticulum membrane

Human erlins (Erlin-1 and Erlin-2) are localized to the endoplasmic reticulum (ER) and are highly enriched in

the DRM (Browman *et al.*, 2006). A transmembrane stretch is present in front of the SPFH domains of human erlins, and the N-terminus is localized in the cytoplasm whereas most of the molecule is inside the ER lumen (Pednekar *et al.*, 2011).

Two coiled-coil stretches are present at the C-terminus of human erlins. The coiled-coil motifs mediate the formation of erlin homo and heterooligomers (Hoegg *et al.*, 2009), among which heterotrimers are the most abundant (Pednekar *et al.*, 2011). Oligomers are further organized into an approximately 2-MDa complex consisting of ca 50 monomers with an Erlin-1/Erlin-2 ratio of 1:2 (Pearce *et al.*, 2009). This structure is assembled through an "association domain" that is present in erlin molecules beyond the coiled-coil motifs (Pednekar *et al.*, 2011). The 2-MDa complex is shaped like an open ring (Pednekar *et al.*, 2011), and is stable even during sterol depletion (Hoegg *et al.*, 2009).

AtELP also contains a putative transmembrane stretch as well as a coiled-coil motif (Figure 1). These predictions suggest possible AtELP membrane localization and an ability to bind to the same or other molecules, i.e., to form homooligomers or protein complexes.

B. Erlin supercomplexes are involved in inositol trisphosphate receptor degradation

Human erlins are involved in the ER-associated degradation (ERAD) pathway, a process during which some ER proteins (typically misfolded or undergoing rapid turnover) are polyubiquitinated and consequently degraded by the 26S proteasome (Vembar and Brodsky, 2008). Erlin-2 has been found to interact with several proteins involved in ERAD as well as with the inositol trisphosphate receptor (IP3R), and Erlin-2 knockdown cells display inhibition of the polyubiquitination of some ERAD substrates including IP3R (Pearce *et al.*, 2007). Mammalian IP3R is localized in the ER membrane and releases calcium ions into the cytoplasm following IP3 stimulation (Foskett *et al.*, 2007; Taylor *et al.*, 2004). The rapid increase in the calcium concentration is known to act as a second messenger in many signalization cascades. After stimulation and calcium release, IP3R is promptly degraded via ERAD (Bokkala and Joseph, 1997; Oberdorf *et al.*, 1999). Because the 2-MDa erlin complex binds to IP3R and the extent of this interaction increases after IP3 stimulation (Pearce *et al.*, 2007, 2009; Wang *et al.*, 2009), this complex plays a key role in the signal transduction induced by IP3. The interaction takes place before the beginning of IP3R ubiquitination (Pearce *et al.*, 2007). Monomeric erlins do not bind IP3R (Pearce *et al.*, 2009). Upon suppression of erlin expression, IP3R is ubiquitinated to a substantially lower extent (Pearce *et al.*, 2007; Sanchez-Quiles *et al.*, 2010), IP3 signaling is not attenuated, the ER is stressed and the cell can be damaged (Sanchez-Quiles *et al.*, 2010).

Regarding the shape of the 2-MDa erlin complex, it has been hypothesized that the complex acts as a retrotranslocon, a structure that can extrude stimulated IP3R or other proteins from the ER membrane after their interaction or that can draw an ubiquitin ligase that recognizes IP3R and thus mediates their association (Pearce *et al.*, 2009). Binding of the 2-MDa complex and RNF170, an activated IP3R-specific ubiquitin ligase, has been established (Lu *et al.*, 2011).

IP3-induced release of calcium ions into the cytoplasm is also an important signaling event in plant cells (Alexandre and Lassalles, 1992; Malho *et al.*, 1998). Vacuolar (Allen and Sanders, 1994; Brosnan and Sanders, 1993) and microsomal fraction compartments (Dasgupta *et al.*, 1997; Muir and Sanders, 1997; Scanlon *et al.*, 1996) were found to release Ca^{2+} in response to IP3 stimulation in several plant species, suggesting that a putative plant IP3R is present in these membrane compartments. Nevertheless, a plant protein homolog of metazoan IP3R has not been discovered to date (Krinke *et al.*, 2007; Taylor *et al.*, 2004). A binding site for IP3 (but not a specific protein) was found in ER membranes (Martinec *et al.*, 2000) in *Chenopodium rubrum*. Several tens of IP3-binding proteins have recently been identified in the ER membrane of *Oryza sativa* (Nie *et al.*, 2014).

IV. Hypersensitive induced reaction proteins—modulators of plant immunity

HIRs are plant-specific members of the SPFH protein superfamily. They were originally discovered in *Zea mays* (Nadimpalli *et al.*, 2000) and were found highly homologous to a tobacco NG1 cDNA product that causes a spontaneous hypersensitive response (HR) when overexpressed in tobacco leaves (Karrer *et al.*, 1998). HIR homologs have been further identified in barley (Rostoks *et al.*, 2003), rice (Chen *et al.*, 2007; Malakshah *et al.*, 2007), tomato (Jung and Hwang, 2007), pepper (Jung *et al.*, 2008), papaya (Porter *et al.*, 2008), wheat (Liu *et al.*, 2013; Yu *et al.*, 2008; Zhang *et al.*, 2009b, 2011), *A. thaliana* (Di *et al.*, 2010), apple (Zhou *et al.*, 2012), and soybean (Koellhoffer *et al.*, 2015; Xiang *et al.*, 2015). In the Haptophyte algae *Emiliania huxleyi* and *Tisochrysis lutea*, proteins related to *A. thaliana* HIRs in terms of sequence similarity and molecular mass have been identified (Rose *et al.*, 2014; Shi *et al.*, 2015). HIRs of *A. thaliana* are denoted herein according to Qi *et al.* (2011) as follows: AtHIR1 (At1g69840), AtHIR2 (At3g01290), AtHIR3 (At5g51570), and AtHIR4 (At5g62740). The expression of single isoforms differs during plant development and in various organs (Figure 3). *AtHIR1* is expressed

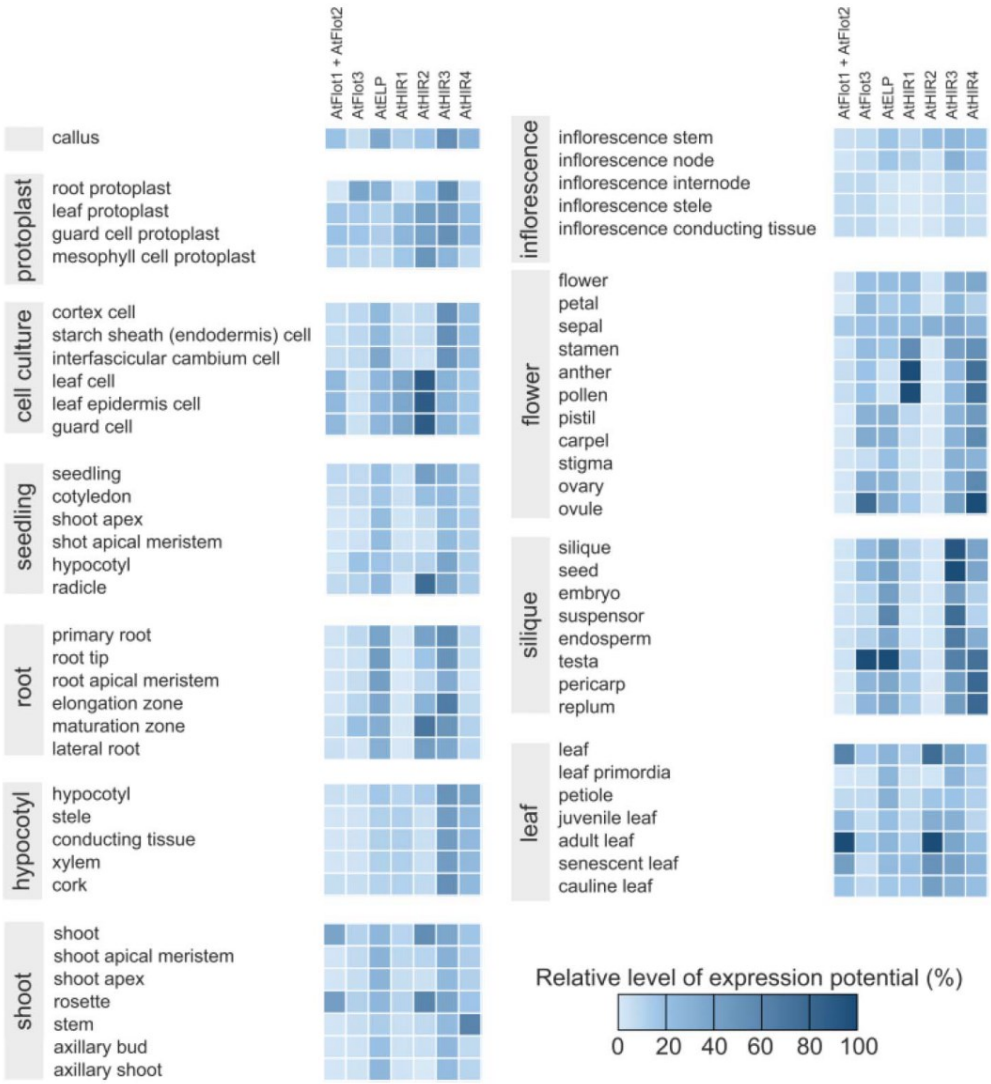

Figure 3. *Arabidopsis thaliana* SPFH genes are expressed differentially in various tissues throughout individual development. Affymetrix 22 K microarray data were retrieved from Genevestigator.

in leaves and some flower parts but is not expressed in root tissues. *AtHIR2* expression is highest in leaves and roots and almost absent in flowers and siliques. *AtHIR3* and *AtHIR4* are, to a certain extent, expressed during all developmental stages and in all organs, with the highest values exhibited in siliques and seeds or gametangia, gametophytes, and seed parts, respectively.

A. HIRs are localized on the plasma membrane

HIR proteins were found on the plasma membrane in rice (Chen *et al.*, 2007; Ishikawa *et al.*, 2015; Malakshah *et al.*, 2007), *A. thaliana* (Qi *et al.*, 2011), and pepper (Choi *et al.*, 2011), and on the tonoplast in rice (Zhou *et al.*, 2010) or the endosomes in pepper (Choi *et al.*, 2013). In wheat, TaHIR1 and TaHIR3 localize on the plasma membrane (Duan *et al.*, 2013), whereas TaHIR2 are present in the cell interior (Zhang *et al.*, 2011).

In pepper, the association of CaHIR1 with the plasma membrane is provided by the SPFH domain (Choi *et al.*, 2011). Zhou *et al.* (2010) and Xiang *et al.* (2015) predicted putative myristoylation sites and transmembrane stretches in the N-terminus for several isoforms of HIRs in soybean, rice, maize, wheat, and barley. However, our search using web prediction tools did not reveal any transmembrane stretches in the amino acid sequences of

any of the four HIR isoforms of *A. thaliana*, whereas N-terminal putative myristoylation and/or palmitoylation sites were identified for all of them (Figure 1). HIR-related protein was found to be a major membrane microdomain protein in *E. huxleyi* (Rose *et al.*, 2014). AtHIR1, AtHIR2, and AtHIR3, as well as OsHIR1, OsHIR3, and OsHIR5, were found in DRMs (Ishikawa *et al.*, 2015; Minami *et al.*, 2009). The association of AtHIRs with the DRM is not altered following sterol depletion induced by methyl-β-cyclodextrin (Kierszniowska *et al.*, 2009).

B. HIRs are upregulated in response to pathogen attack

Plant immunity consists mainly of two types of defense mechanisms corresponding to two types of molecules that are produced by pathogens. The so-called pathogen (or microbe)-associated molecular patterns (PAMPs or MAMPs) such as flagellin, elongation factor thermo unstable (EF-Tu), peptidoglycan, chitin, lipopolysaccharide, and glucan of pathogen cell walls, are generally conserved across pathogen taxa (Chisholm *et al.*, 2006) and play a role as elicitors. PAMPs are recognized by plant pathogen recognition receptors (PRRs) localized at cell surfaces (Jones and Dangl, 2006). The action initiated by PRRs results in the activation of innate immune response termed PAMP-triggered immunity (PTI) (Dangl and Jones, 2001).

To overcome PTI, pathogens have evolved another type of molecule that disrupts early steps in the PRR-induced response (He *et al.*, 2006). These so-called effectors or plant proteins damaged by these effectors are recognized by resistance proteins (R proteins) in plants (Chisholm *et al.*, 2006). Effectors are race or strain-specific, and their presence or absence in a pathogen determines its (a)virulence. An effector that is recognized by host R protein is called an avirulence protein because it provokes a supposed effector-triggered immunity (ETI) response in the host plant (Dangl and Jones, 2001). ETI comprises the production of ROS, reactive nitrogen oxide intermediates, and increased levels of the defense phytohormone jasmonic acid (JA) (Coll *et al.*, 2011), eventually leading to HR. SA signaling and the subsequent upregulation of pathogenesis-related proteins (Stintzi *et al.*, 1993) is involved in both the ETI and the PTI pathways (Janda and Ruelland, 2015).

HIR protein expression is generally increased during bacterial (Chen *et al.*, 2007; Jung and Hwang, 2007; Qi *et al.*, 2011; Zhou *et al.*, 2010) or fungal (or oomycetes) infection (Chen *et al.*, 2012; Liu *et al.*, 2013; Porter *et al.*, 2008; Xiang *et al.*, 2015; Yu *et al.*, 2008, 2013; Zhang *et al.*, 2009b, 2011; Zhou *et al.*, 2012). *HIR* upregulation is usually induced to a much greater extent by avirulent pathogens strains during incompatible interactions than by virulent strains during compatible interactions; however, both virulent and avirulent strains cause an increase in *HIR* expression (Chen *et al.*, 2007, 2012; Jung and Hwang, 2007; Liu *et al.*, 2013; Yu *et al.*, 2008, 2013; Zhang *et al.*, 2009b, 2011; Zhou *et al.*, 2010).

Genevestigator microarray transcription data (Figure 2) also show the upregulation of at least some HIR isoforms in response to several pathogen types including fungi (*Alternaria brassicae, Botrytis cinerea, Blumeria graminis*, and *Sclerotinia sclerotiorum*), oomycetes (*Hyaloperonospora arabidopsidis* and *Phytophthora infestans*), bacteria (*P. syringae* pv. *maculicola* and *phaseolicola, Xanthomonas campestris* pv. *campestris*), and several viruses. Interestingly, the effect of both virulent and avirulent strains of *P. syringae* pv. tomato on the transcription of AtHIR1, AtHIR2, and AtHIR3 (Qi *et al.*, 2011) is rather insignificant. In *E. huxleyi* viral infection causes changes in the size distribution of membrane microdomains defined by HIR-related protein (Rose *et al.*, 2014). Possible involvement of HIRs or HIR-related proteins in response to viral infection is consistent with highly upregulated AtHIR transcription in response to cabbage leaf curl virus or turnip mosaic virus infection (Figure 2).

HIR transcription is also induced by elicitors. *AtHIR1, AtHIR2*, and *AtHIR3* transcription is upregulated by flg22 peptide (Qi *et al.*, 2011), chitin, and EF-Tu (Figure 2). *CaHIR1* transcription is increased by infiltration of the purified Filamentous hemagglutinin-like protein (Fha1) of *Xanthomonas campestris* pv. *vesicatoria* into pepper leaves (Choi *et al.*, 2013). *CaHIR1* transcription is also increased in pepper leaves overexpressing INF1 elicitin of *Phytophthora capsici* (Feng *et al.*, 2014). Both Fha1 and INF1 elicit necrosis and HR in pepper leaves (Feng *et al.*, 2014; Choi *et al.*, 2013).

The effect of stressors and phytohormones on *HIR* expression seems to be specific for species and isoform. *OsHIR1* expression is induced by salt stress (100 mM NaCl) in rice (Malakshah *et al.*, 2007), whereas salt treatment (200 mM NaCl), cold stress (4°C), and osmotic stress (20% PEG6000) in wheat decrease the transcription of *TaHIR1* and *TaHIR3* (Duan *et al.*, 2013). *TaHIR1* and *TaHIR3* transcription are also reduced by ethylene (100 μM) and ABA (100 μM), with only a minor effect of MeJA (100 μM) or SA (2 mM) application (Duan *et al.*, 2013). This phenomenon is in contrast to the situation in pepper, in which SA (5 mM), MeJA (100 μM), ABA (100 μM), and ethylene (5 ppm) application increased *CaHIR1* transcription (Jung and Hwang, 2007). In soybean, hydrogen peroxide treatment (100 μM) repressed the transcription of *GmHIR1,*

GmHIR3, and *GmHIR4* (Xiang *et al.*, 2015). *AtHIR* transcription is upregulated by SA, a phytohormone that is involved in the plant response to pathogens, and zeatin. The effects of oxidative and osmotic stress, ozone, hypoxia UV-B, and cold seem to be similar for all *AtHIR* isoforms, whereas hydrogen peroxide, drought, salt, and ABA have opposite impacts on different isoforms, i.e., they increase or decrease the transcription of AtHIR1 and AtHIR2, or AtHIR3, and AtHIR4, respectively (Figure 2).

C. Overexpression of HIRs promotes the hypersensitive response

The HR regulates cell death at the site of infection, resulting in the restriction of pathogen growth and spreading. It typically occurs during incompatible interactions between plants and pathogens, and is manifested by plasma membrane depolarization and potassium ion efflux into the intercellular space (Atkinson *et al.*, 1990), an oxidative burst (Torres *et al.*, 2006), and callose deposition (Cuypers and Hahlbrock, 1988). These processes are mediated by SA, ABA, JA, and ethylene signaling (Fujita *et al.*, 2006). In pepper overexpressing *CaHIR1*, increased callose deposition and electrolyte leakage, and reduced SA content are observed in the absence of a pathogen (Choi *et al.*, 2011). Interestingly, when *CaHIR1* is expressed in *A. thaliana*, the plants exhibit elevated SA and hydrogen peroxide contents, a higher potassium ion concentration in the intercellular space, and constitutive upregulation of pathogenesis-related proteins (Jung and Hwang, 2007). *OsHIR1* expression in *A. thaliana* results in the spontaneous formation of lesions and a constitutive increase in *PR* expression (Zhou *et al.*, 2010). Barley lesion mimic mutants, i.e., mutant lines exhibiting constitutive necrosis formation, were found to constitutively overexpress *HvHIR1, HvHIR2, HvHIR3*, and *HvHIR4* (Rostoks *et al.*, 2003; Wright *et al.*, 2013). These lesion mimic mutants are more resistant to virulent biotrophic *Puccinia hordei*, but they have been reported to have an increased susceptibility to necrotrophic *Pyrenophora teres* f. sp. *teres* (Wright *et al.*, 2013). This observation suggests that HIR proteins may play a role in the crosstalk between SA and JA. SA is generally responsible for defense responses to biotrophs, whereas JA is involved in defense responses to necrotrophs (Glazebrook, 2005). Ectopic expression of *OsHIR1* and *CaHIR1* and overexpression of *AtHIR1* and *AtHIR2* lead to increased resistance to virulent *P. syringae* pv. tomato DC3000 (Jung and Hwang, 2007; Qi *et al.*, 2011; Zhou *et al.*, 2010). T-DNA-knockout lines of *AtHIR2* and *AtHIR3* consistently exhibit reduced resistance to avirulent *P. syringae* pv. tomato AvrRpt2 (Choi *et al.*, 2011). Similarly, virus-silenced (VIGS) *TaHIR1*- and *TaHIR3*-knockdown leaves have a less intense HR, better pathogen performance and an overall decrease in *PR* gene transcription compared with the control after infection with the avirulent strain of *Puccinia striiformis f. sp. tritici*. In contrast, infection of VIGS-*CaHIR1*-pepper leaves by both virulent and avirulent strains of *Xanthomonas campestris* pv. *vesicatoria* leads to reduced callose deposition and electrolyte leakage but an increased level of SA and the transcription of PR genes, which together result in improved pathogen resistance (Choi *et al.*, 2011).

In rice cells overexpressing BI-1, a cell death suppressor that increases plant tolerance to several stresses and signalization of which involves ROS formation, the association of OsHIR1, OsHIR3, and OsHIR5 as well as OsFlot with the DRM is markedly reduced, although their transcription level is not affected. Accordingly, knockdown or KO mutants of *OsHIR3* (or *OsFlot*) exposed to oxidative stress (induced by menadione or SA) exhibit reduced cell death (Ishikawa *et al.*, 2015). Oxidative stress generally increases *AtHIR* transcription (Figure 2), and because the oxidative burst is one of first steps in the HR, it is possible that the action of HIR occurs through ROS production and that proper functioning of HIRs may be dependent on their localization in the membrane microdomains.

D. HIRs physically and functionally interact with leucine-rich repeat proteins

Similar to mammalian flotillins and erlins, all isoforms of AtHIRs form homo and heterooligomers *in vitro*. All possible pairwise combinations of single isoforms have been detected (Qi *et al.*, 2011). Oligomerization may lead to the clustering of HIR molecules, giving rise to the protein scaffolds of microdomains. Binding of AtHIRs to other protein molecules may occur in coiled-coil regions within AtHIR molecules. Using web predictors, coiled-coil motifs were identified in amino acid sequences of all AtHIR isoforms with the exception of AtHIR3 (Figure 1)

HIRs have been reported to physically and functionally interact with leucine-rich repeat (LRR) superfamily proteins. In rice, an interaction of OsHIR1 with OsLRR1 was found in a Y2H screen. Furthermore, a Y2H screen showed that OsHIR1 can bind to AtLRR1 (At5g21090, an OsLRR1 homolog) and OsLRR1 can bind to AtHIR1 (Zhou *et al.*, 2009). Overexpression of *OsLRR1* upregulates *OsHIR1* expression and increases the localization of OsHIR1 on the plasma membrane (Zhou *et al.*, 2010). Similarly, CaLRR1 interacts with CaHIR1 in plasma membrane microdomains in pepper leaves and *CaLRR1* overexpression results in increased *CaHIR1* transcription (Choi *et al.*, 2011). Binding to CaHIR1 is provided by the

LRR domain of CaLRR1 (Jung and Hwang, 2007). Ectopic expression of *OsLRR1* in *A. thaliana* or overexpression of *CaLRR1* in pepper lead to the upregulation of PR genes and increase resistance of leaves to the pathogens *Xanthomonas campestris* pv. *vesicatoria* and *P. syringae* pv. tomato DC3000, respectively (Choi *et al.*, 2011; Zhou *et al.*, 2009, 2010). By contrast, *CaLRR1* is downregulated in response to *CaHIR1* overexpression. In VIGS-*CaHIR1* leaves, the level of *CaLRR1* transcription together with the SA content is increased to a much greater extent during incompatible interactions, which result in increased pathogen resistance (Choi *et al.*, 2011). Thus, LRR proteins stimulate the increased HIR protein level in rice and pepper, while HIR negatively regulates LRR expression in pepper. LRR seems to attenuate the function of HIR in the development of necrosis because the co-overexpression of *CaHIR1* and *CaLRR1* results in a less intense HR compared with *CaHIR1* overexpressing leaves during treatment with benzothiadiazole, an HR elicitor (Jung and Hwang, 2007).

AtHIR1 and AtHIR2 were found to bind RPS2 (At4g26090) (Qi *et al.*, 2011). RPS2 belongs to the nucleotide-binding-LRR subclass of LRR proteins (Bent *et al.*, 1994). It is a resistance protein that binds to RIN4 protein (At3g25070), a target of the bacterial effector AvrRpt2. When RIN4 is absent, RPS2 promotes HR (Axtell and Staskawicz, 2003; Mackey *et al.*, 2003). Thus, AtHIR1 and AtHIR2 play an important role in ETI.

E. HIRs are parts of protein complexes

As mentioned above, AtHIR1 and AtHIR2 were found to be components of a RPS2-based protein complex that also contained RIN4; a receptor-like kinase (At4g08850); aquaporin PIP1;2 (At2g45960); phototropin 1 and 2 (At3g45780 and At5g58140); patellin-1 (At1g72150)—a phosphoinositide-binding carrier protein; epithiospecifier modifier 1 (At3g14210), which mediates isothiocyanate production during glucosinolate hydrolysis; and heavy metal ATPase 3 (At4g30120) (Qi and Katagiri, 2009). Because these proteins were co-purified together with RPS2, it is possible that at least some of the proteins within this protein complex interact with AtHIR1 or AtHIR2. The transcription of both *AtHIR1* and *AtHIR2* increases during drought and salt stress, whereas the other two isoforms are slightly downregulated under these conditions (Figure 2). Together with the mentioned co-purification of both isoforms in a complex with PIP1;2, these findings suggest a possible effect of AtHIR1 and AtHIR2 on water uptake or transport. Similarly, within the HIR-related protein-based microdomains of *E. huxleyi*, several co-occurring proteins have been identified, including porin, the H^+-PPase pump, the mitochondrial import receptor subunit, heat shock protein, nitrate transporters, actin, histone, and many chloroplast proteins (Rose *et al.*, 2014).

Phospholipase D δ (PLDδ, At4g35790) has been reported to pull-down AtHIR1 together with clathrin heavy chain (At3g08530/At3g11130), heat shock protein 70 (At1g56410/At3g09440/At3g12580/At5g02490/At5g02500), ATP synthase subunits α (AtMg01190) and β (At5g08670/At5g08680/At5g08690), actin 7 (At5g09810), and β-tubulin (At4g20890/At5g23860/At5g44340/At5g62690/At5g62700) (Ho *et al.*, 2009). PLDδ is involved in several signaling processes, including drought, cold and frost, salt and water stress, oxidative and UV-B-induced damage, and biotic stress, particularly during the penetration of fungi into plants (Bargmann *et al.*, 2009; Katagiri *et al.*, 2001; Kawamura and Uemura, 2003; Li *et al.*, 2004; Pinosa *et al.*, 2013; Wang, 2005), and this interaction may suggest a broader-spectrum function of AtHIR1. This suggestion is supported by the altered *AtHIR* transcription in response to UV-B, cold, drought, salt, and oxidative stress (Figure 2). AtPLD participates in the maintenance of root elongation during phosphate deficiency (Li *et al.*, 2006a) by recycling phosphate via phospholipid cleavage, which is then replaced with galactolipids in membranes (Cruz-Ramirez *et al.*, 2006; Li *et al.*, 2006a, b). The transcription of all four AtHIR isoforms increases in response to phosphate deficiency (Figure 2), suggesting the involvement of AtHIR in this type of adaptation to low nutrient conditions.

The AtHIR4 content in DRM is reduced and its content in the detergent-soluble membrane fraction is increased after treatment with cytochalasin D, an actin polymerization inhibitor (Szymanski *et al.*, 2015). Because AtHIR1 was found in the AtPLDδ interactome together with actin 7 (Ho *et al.*, 2009), it is possible that AtPLDδ functions as a bonding bridge between AtHIRs and actin filaments. This interaction may determine the AtHIR microdomain pattern and its possible rearrangement during stress signaling. AtHIRs may be either directed to microdomains via oriented transport along actin filaments and/or retained at certain positions by actin bundles in cortical cytoplasm adjacent to the plasma membrane (Szymanski *et al.*, 2015). AtHIRs have been found to bind to AtAHK2, a cytokinin receptor, and Sieve element occlusion related protein 2 that participates in P-protein formation (Table 1). Considering that *AtHIR2* is upregulated by zeatin (Figure 2), these results suggest the potential involvement of AtHIR in cytokinin signaling.

V. Conclusions

Mammalian flotillins have recently been proven to play roles in many important processes, including membrane microdomain organization, endocytosis, signal transduction, cholesterol uptake, or intercellular communication.

Human erlins are involved in the modulation of IP3 signaling and ER-associated protein degradation. In plants, less is known about flotillins, and there is a complete lack of information for erlin.

However, plant flotillins exhibit features similar to human ones in terms of their occurrence in membrane microdomains, participation in clathrin-independent endocytosis or interactions with receptor kinases. Experimentally obtained data for the binding of *A. thaliana* proteins to flotillins and for the expression of AtFlot suggest the presence of additional functions such as cell signaling, pathogen responses, water and/or ion uptake control, vesicular transport, and protein trafficking. AtFlot1 has been shown to be involved in sterol uptake via the plasma membrane, and AtFlot2 and AtFlot3 have been observed to bind phospholipases and sphingosine kinase. AtFlots may thus affect three lipid components that are all established to increase membrane order and are pivotal for the membrane microdomain identity. Thus, flotillins may be crucial for determining these microdomains.

In most cases, HIR proteins present on the plasma membrane have been shown to promote the hypersensitive response after bacterial or fungal infection, thus playing an important role in plant resistance to pathogens. HIRs have been confirmed to interact with LRRs in pepper, rice, and *A. thaliana*. The ratio of HIR to LRR expression affects the plant response to infection. *A. thaliana* HIRs are part of protein complexes containing phospholipase D, cytoskeletal proteins, and ATPases, among others. The transcription data support the possible involvement of AtHIRs (apart from the response to pathogen attack) in some abiotic stress reactions, such as cold, UV-B, hyperosmotic stress, nutrient deficiency, and both oxidative stress and hypo/anoxia, as well as in hormone signaling. Moreover, two AtHIR isoforms bind to the cytokinin receptor.

VI. Future perspectives

To better understand the functions of plant flotillin, the first step would be experimental *in planta* verification of the putative protein interactions of AtFlots (Table 1) using fluorescence and confocal microscopy techniques such as Förster resonance energy transfer (FRET), fluorescence lifetime imaging (FLIM) or bimolecular fluorescence complementation (BiFC). Because these techniques are based on different principles, each is faced by specific limitations. FRET and FLIM allow the detection of direct interactions because they are sufficiently effective for identifying a distance between fluorophores that does not exceed 10 nm. To obtain relevant results, the concentration of fluorescent-labeled interaction partners must be high enough to permit clear detection. However, assuming that AtFlots are present at the plasma membrane in spatially limited microdomains, expression levels and molecule contents that are too high could lead to "crowding" of the molecules within these areas, resulting in false-positive FRET. False-positive as well as false-negative FRET results may also be obtained when the expression of the donor and acceptor-fused proteins is unbalanced. Thus, great care must be taken in terms of the gene expression of the protein partners (Xing *et al.*, 2016). Cloning both partners fused to fluorophores within one expression cassette or under one promoter in multicistronic vectors containing the sequence for 2A self-cleaving peptide may aid in preparing transformants with a suitable expression ratio.

BiFC is prone to exhibiting false-positive results because of irreversible self-assembly of the fluorophore employed, which is why it is vital to apply the appropriate negative controls and rather low expression levels by using, e.g., native promoters. However, BiFC may enable the detection of transient and weak interactions because they are stabilized through the re-assembled fluorophore. It can also be applied to visualize indirect interactions between proteins (Xing *et al.*, 2016). Ratiometric BiFC (rBiFC) involving internal control of the transformation and expression efficiency and thus allowing proportional quantification should be used preferentially (Grefen and Blatt, 2012). When applying BiFC to membrane-anchored proteins (i.e., flotillins and HIRs), steric constraints that impede split fluorophore reassembly may occur because the anchored proteins may not freely rotate and the split fluorophore fragments may not be able to assume the appropriate position for reassembly. This phenomenon can be, to a certain extent, overcome by using sufficiently long linkers.

Both FRET/FLIM- and BiFC-positive results should be verified by co-immunoprecipitation assays. In addition to the widely used western blot detection, single-molecule pull-down assays using protein bait immobilized on a microscopic slide and total internal reflection fluorescence imaging (TIRF) were also recently introduced in plant science, allowing the determination of not only the interaction itself but also its dynamics and the stoichiometry of the proteins that form the complexes (Husbands *et al.*, 2016).

The dynamics of these interactions (e.g., dissociation or formation of the protein complexes) under various conditions can be further addressed using particle analysis tools such as fluorescence cross-correlation spectroscopy (FCCS), which analyzes the fluctuation of fluorescent particles in a small defined confocal volume and thus provides information about the particle dynamics or concentration on a single-molecule level within microsecond-to-second

timescales. Its application is, however, limited to particles with a diffusion coefficient of no less than 0.1 $\mu m^2 s^{-1}$. Thus, it is biased toward faster moving molecules when used to measure lateral mobility due to photobleaching of the slow and methodological "invisibility" of immobile molecules lingering within the confocal volume. In fact, this phenomenon might concern at least some AtFlots because the AtFlot1 diffusion coefficient has been approximately hundredths of $\mu m^2 s^{-1}$ under different conditions, as determined by TIRF acquisition and subsequent tracking of fluorescent foci (Li *et al.*, 2012). In the case of stable molecules and complexes, raster image cross-correlation spectroscopy (RICCS) permits the analysis of particle diffusion coefficients as low as 0.001 $\mu m^2 s^{-1}$ (Digman *et al.*, 2005). The correlation spectroscopy methods require low (typically nanomolar) concentrations of fluorophores, supporting the use of the native promoters of the analyzed proteins, which would also avoid possible artifacts caused by overexpression. Both methods have been previously applied in analyses of plant membrane proteins (Lankova *et al.*, 2016; Li *et al.*, 2013).

Because many proteins are known to form membrane microdomains, the question is whether some of these microdomains overlap with SPFH protein-based ones. Electron microscopy and super-resolution imaging techniques could be a great asset to more precisely describe the organization of plant flotillin and HIR microdomains. For example, the stimulated emission depletion technique can reveal a substantially smaller size of potato remorin microdomains compared with the same microdomain size obtained using "standard" confocal microscopy (Demir *et al.*, 2013).

The previously reported involvement of AtFlot1 microdomains in endocytosis requires further exploration. One strategy is to focus on differences between flotillin and the well-described clathrin-mediated endocytosis in terms of their cargo specificity or their dependence on cytoskeleton or phosphorylation (which is known to be important for flotillin endocytosis in mammalian cells). The latter two may be addressed using specific inhibitors and cytoskeletal drugs.

Because membrane microdomains are characterized by their distinct lipid composition, it would be very interesting to assess the ability of plant SPHF proteins to bind these lipids. Because we revealed several CRAC/CARC motifs within each *A. thaliana* SPFH protein sequence, detection of phytosterol binding to these proteins should be explored. Another important group of membrane lipids that seems to be associated with plant flotillins are sphingolipids. AtFlot3 binds to sphingosine kinase, and concomitant alteration of glucosylceramide and rice flotillin and HIR content is detected in the DRM. Binding assays using lipid strips and purified proteins can be used to determine whether plant SPFH proteins really bind to these membrane lipids. Surface plasmon resonance would be the next step to better characterize the binding process. Moreover, in the case of cholesterol, it would be possible to explore whether the CRAC/CARC motifs serve to bind to phytosterols in plants because these motifs have, to date, only been reported to bind cholesterol in animal cells.

One of the properties in which defined membrane microdomains may differ is the lipid order. An interesting question emerges concerning whether this difference is a prerequisite for plant SPFH protein localization or *vice versa.* Using cells with different expression levels of plant SPFH proteins (i.e., loss-of-function mutants, ami-RNA lines, and (inducible) overexpressors, among others) and simultaneous monitoring of local fluctuations in the membrane lipid order using fluorescent dyes that exhibit different emission spectra when incorporated into a more ordered or disordered membrane environment (e.g., Laurdan, di-4-ANEPPDHQ) is an effective tool for ascertaining the relationship between flotillins and HIRs and the establishment of areas of different lipid orders in membranes.

Ubiquitination is a substantial pathway that controls specific protein activity. The prominent role of the mammalian erlin complex in ubiquitination and degradation of activated IP3R could be a clue for discovering the identity of plant IP3R, which has not yet been found, although its activity, which is similar to that in animals, has been well reported in plants. A thorough analysis of the ubiquitinated proteome and its differences in wild type compared with KO *AtELP* might identify the protein targets of AtELP-mediated ubiquitination activity, which might include a putative IP3R. However, this approach assumes the same activity of mammalian erlin and its plant homolog toward mammalian IP3R and its plant counterpart. This assumption may not reflect the real situation because plant IP3R is not likely to be a sequence homolog of mammalian IP3R. AtFlot2 and AtFlot3 also bind to proteins involved in ubiquitination and proteasome degradation. An investigation of protein targets (using the same approach applied for AtELP) and their function can also suggest the possible involvement of AtFlots in these functions. Moreover, ubiquitination also serves as a signal that results in protein internalization, as reported for the brassinosteroid receptor and the iron transporter (Barberon *et al.*, 2011; Martins *et al.*, 2015). An analysis of the ubiquitinated proteome obtained from immunopurified AtFlot-positive endosomes may thus be a possible way to identify cargo proteins that have been internalized via AtFlot-dependent endocytosis.

Abbreviations

ABA	abscisic acid
AF	antisecretory factor
AHK2	histidine kinase 2
ARM	armadillo repeat
AtELP	*Arabidopsis thaliana* erlin-like protein
BFA	brefeldin A
CARC	inverted CRAC
CRAC	cholesterol recognition/interaction amino acid consensus sequence
DRM	detergent-resistant membranes
EF-Tu	elongation factor thermo unstable
EGF	epidermal growth factor
EGFR	epidermal growth factor receptor
ER	endoplasmic reticulum
ERAD	endoplasmic-reticulum-associated degradation
ESCRT	endosomal sorting complexes required for transport
ETI	effector-triggered immunity
Fha1	filamentous hemagglutinin-like protein 1
FM4-64	N-(3-triethylammoniumpropyl)-4-(6-(4-(diethylamino) phenyl) hexatrienyl) pyridinium dibromide
GFP	green fluorescent protein
GLUT4	glucose transporter type 4
GPI	glycophosphatidylinositol
HR	hypersensitive response
HIR	hypersensitive induced reaction protein
IP3	inositol 1,4,5-trisphosphate
IP3R	inositol 1,4,5-trisphosphate receptor
JA	jasmonic acid
LRR	leucine-rich repeat
LYK3	lysin motif receptor-like kinase 3
MAMP	microbe-associated molecular pattern
MeJA	methyl jasmonate
MyoB1	myosin-binding protein 1
NPC1L1	Niemann-Pick C 1-like1
PAMP	pathogen-associated molecular pattern
PHB	prohibitin homology
PLDδ	phospholipase D δ
PIP2;1	plasma membrane intrinsic protein 2;1
PIP1;2	plasma membrane intrinsic protein 1;2
PRR	pathogen recognition receptor
PR	pathogenesis-related
PTI	PAMP-triggered immunity
RbohD	respiratory burst oxidase D
RIN4	resistance to *Pseudomonas syringae* pv. *maculicola* 1-interacting protein 4
ROS	reactive oxygen species
RPS2	resistance to *Pseudomonas syringae* protein 2
SA	salicylic acid
SNARE	soluble *N*-ethylmaleimide-sensitive fusion protein attachment protein receptor
SPFH	stomatin/prohibitin/flotillin/HflK/C
VIGS	virus-silenced gene silencing
WAK	wall-associated kinase
Y2H	yeast two-hybrid screening
YFP	yellow fluorescent protein

Acknowledgments

The authors would like to thank Dr. Jan Malínský (Institute of Experimental Medicine, Prague) for critical reading of and many inspiring comments on the manuscript.

Declaration of interest

The authors declare that there are no conflicts of interest.

Funding

The study was supported by the Czech Science Foundation grant no. 14-09685S.

ORCID

Jan Martinec http://orcid.org/0000-0002-5675-1706

References

Ait-Slimane, T., Galmes, R., Trugnan, G., and Maurice, M. 2009. Basolateral internalization of GPI-anchored proteins occurs via a clathrin-independent Flotillin-dependent pathway in polarized hepatic cells. *Mol. Biol. Cell* **20**: 3792–3800.

Alexandre, J., and Lassalles, J. P. 1992. Intracellular Ca^{2+} release by Insp(3) in plants and effect of buffers on Ca^{2+} diffusion. *Philos. Trans. R. Soc. Lond. Ser. B-Biol. Sci.* **338**: 53–61.

Allen, G. J., and Sanders, D. 1994. Osmotic-stress enhances the competence of *Beta vulgaris* vacuoles to respond to inositol 1,4,5-trisphosphate. *Plant J.* **6**: 687–695.

Amaddii, M., Meister, M., Banning, A., Tomasovic, A., Mooz, J., Rajalingam, K., and Tikkanen, R. 2012. Flotillin-1/Reggie-2 protein plays dual role in activation of receptor-tyrosine kinase/mitogen-activated protein kinase signaling. *J. Biol. Chem.* **287**: 7265–7278.

Atkinson, M. M., Keppler, L. D., Orlandi, E. W., Baker, C. J., and Mischke, C. F. 1990. Involvement of plasma-membrane calcium influx in bacterial induction of the K^+/H^+ and hypersensitive responses in tobacco. *Plant Physiol.* **92**: 215–221.

Axtell, M. J., and Staskawicz, B. J. 2003. Initiation of RPS2-specified disease resistance in *Arabidopsis* is coupled to the AvrRpt2-directed elimination of RIN4. *Cell* **112**: 369–377.

Babuke, T., Ruonala, M., Meister, M., Amaddii, M., Genzler, C., Esposito, A., and Tikkanen, R. 2009. Hetero-oligomerization of reggie-1/Flotillin-2 and reggie-2/Flotillin-1 is required for their endocytosis. *Cell. Signal.* **21**: 1287–1297.

Babuke, T., and Tikkanen, R. 2007. Dissecting the molecular function of reggie/flotillin proteins. *Eur. J. Cell Biol.* **86**: 525–532.

Baier, C. J., Fantini, J., and Barrantes, F. J. 2011. Disclosure of cholesterol recognition motifs in transmembrane domains of the human nicotinic acetylcholine receptor. *Sci. Rep.* **1**: 69.

Baluska, F., Samaj, J., and Volkmann, D. 1999. Proteins reacting with cadherin and catenin antibodies are present in maize showing tissue-, domain-, and development-specific associations with endoplasmic-reticulum membranes and actin microfilaments in root cells. *Protoplasma* **206**: 174–187.

Barberon, M., Zelazny, E., Robert, S., Conejero, G., Curie, C., Friml, J., and Vert, G. 2011. Monoubiquitin-dependent endocytosis of the IRON-REGULATED TRANSPORTER 1 (IRT1) transporter controls iron uptake in plants. *Proc. Natl. Acad. Sci. U. S. A.* **108**: E450–E458.

Bargmann, B. O. R., Laxalt, A. M., ter Riet, B., van Schooten, B., Merquiol, E., Testerink, C., Haring, M. A., Bartels, D., and Munnik, T. 2009. Multiple PLDs required for high salinity and water deficit tolerance in plants. *Plant Cell Physiol.* **50**: 78–89.

Baumann, C. A., Ribon, V., Kanzaki, M., Thurmond, D. C., Mora, S., Shigematsu, S., Bickel, P. E., Pessin, J. E., and Saltiel, A. R. 2000. CAP defines a second signalling pathway required for insulin-stimulated glucose transport. *Nature* **407**: 202–207.

Bender, F., Montoya, M., Monardes, V., Leyton, L., and Quest, A. F. G. 2002. Caveolae and caveolae-like membrane domains in cellular signaling and disease: identification of downstream targets for the tumor suppressor protein Caveolin-1. *Biol. Res.* **35**: 151–167.

Bent, A. F., Kunkel, B. N., Dahlbeck, D., Brown, K. L., Schmidt, R., Giraudat, J., Leung, J., and Staskawicz, B. J. 1994. RPS2 of *Arabidopsis thaliana*—a leucine-rich repeat class of plant-disease resistance genes. *Science* **265**: 1856–1860.

Bickel, P. E., Scherer, P. E., Schnitzer, J. E., Oh, P., Lisanti, M. P., and Lodish, H. F. 1997. Flotillin and epidermal surface antigen define a new family of caveolae-associated integral membrane proteins. *J. Biol. Chem.* **272**: 13793–13802.

Bjorck, S., Bosaeus, I., Ek, E., Jennische, E., Lonnroth, I., Johansson, E., and Lange, S. 2000. Food induced stimulation of the antisecretory factor can improve symptoms in human inflammatory bowel disease: a study of a concept. *Gut* **46**: 824–829.

Bokkala, S., and Joseph, S. K. 1997. Angiotensin II-induced down-regulation of inositol trisphosphate receptors in WB rat liver epithelial cells—evidence for involvement of the proteasome pathway. *J. Biol. Chem.* **272**: 12454–12461.

Borner, G. H. H., Sherrier, D. J., Weimar, T., Michaelson, L. V., Hawkins, N. D., MacAskill, A., Napier, J. A., Beale, M. H., Lilley, K. S., and Dupree, P. 2005. Analysis of detergent-resistant membranes in *Arabidopsis*. Evidence for plasma membrane lipid rafts. *Plant Physiol.* **137**: 104–116.

Boute, N., Gribouval, O., Roselli, S., Benessy, F., Lee, H., Fuchshuber, A., Dahan, K., Gubler, M. C., Niaudet, P., and Antignac, C. 2000. NPHS2, encoding the glomerular protein podocin, is mutated in autosomal recessive steroid-resistant nephrotic syndrome. *Nat. Genet.* **24**: 349–354.

Brosnan, J. M., and Sanders, D. 1993. Identification and characterization of high-affinity binding-sites for inositol trisphosphate in red beet. *Plant Cell* **5**: 931–940.

Browman, D. T., Hoegg, M. B., and Robbins, S. M. 2007. The SPFH domain-containing proteins: more than lipid raft markers. *Trends Cell Biol.* **17**: 394–402.

Browman, D. T., Resek, M. E., Zajchowski, L. D., and Robbins, S. M. 2006. Erlin-1 and erlin-2 are novel members of the prohibitin family of proteins that define lipid-raft-like domains of the ER. *J. Cell Sci.* **119**: 3149–3160.

Brown, D. A., and London, E. 1997. Structure of detergent-resistant membrane domains: does phase separation occur in biological membranes? *Biochem. Biophys. Res. Commun.* **240**: 1–7.

Brown, D. A., and Rose, J. K. 1992. Sorting of GPI-Anchored Proteins to Glycolipid-Enriched Membrane Subdomains during Transport to the Apical Cell-Surface. *Cell* **68**: 533–544.

Brutus, A., Sicilia, F., Macone, A., Cervone, F., and De Lorenzo, G. 2010. A domain swap approach reveals a role of the plant wall-associated kinase 1 (WAK1) as a receptor of oligogalacturonides. *Proc. Natl. Acad. Sci. U. S. A.* **107**: 9452–9457.

Cacas, J. L., Bure, C., Grosjean, K., Gerbeau-Pissot, P., Lherminier, J., Rombouts, Y., Maes, E., Bossard, C., Gronnier, J., Furt, F., and Fouillen, L. 2016. Revisiting plant plasma membrane lipids in tobacco: a focus on sphingolipids. *Plant Physiol.* **170**: 367–384.

Chen, J. P., Yu, X. M., Zhao, W. Q., Li, X., Meng, T., Liu, F., Yang, W. X., Zhang, T., and Liu, D. Q. 2012. Temporal and tissue-specific expression of wheat TaHIR2 gene and resistant role of recombinant protein during interactions between wheat and leaf rust pathogen. *Physiol. Mol. Plant Pathol.* **79**: 64–70.

Chen, F., Yuan, Y. X., Li, Q., and He, Z. H. 2007. Proteomic analysis of rice plasma membrane reveals proteins involved in early defense response to bacterial blight. *Proteomics* **7**: 1529–1539.

Chen, X. R., Zhang, B. Y., Xing, Y. P., Li, Q. Y., Li, Y. P., Tong, Y. H., and Xu, J. Y. 2014. Transcriptomic analysis of the phytopathogenic oomycete Phytophthora cactorum provides insights into infection-related effectors. *BMC Genomics* **15**: 1.

Chisholm, S. T., Coaker, G., Day, B., and Staskawicz, B. J. 2006. Host-microbe interactions: shaping the evolution of the plant immune response. *Cell* **124**: 803–814.

Choi, H. W., Kim, Y. J., and Hwang, B. K. 2011. The hypersensitive induced reaction and leucine-rich repeat proteins regulate plant cell death associated with disease and plant immunity. *Mol. Plant-Microbe Interact.* **24**: 68–78.

Choi, H. W., Kim, D. S., Kim, N. H., Jung, H. W., Ham, J. H., and Hwang, B. K. 2013. *Xanthomonas* filamentous hemagglutinin-like protein Fha1 interacts with pepper hypersensitive-induced reaction protein CaHIR1 and functions as a virulence factor in host plants. *Mol. Plant-Microbe Interact.* **26**: 1441–1454.

Coates, J. C. 2003. Armadillo repeat proteins: beyond the animal kingdom. *Trends Cell Biol.* **13**: 463–471.

Coll, N. S., Epple, P., and Dangl, J. L. 2011. Programmed cell death in the plant immune system. *Cell Death Differ.* **18**: 1247–1256.

Cruz-Ramirez, A., Oropeza-Aburto, A., Razo-Hernandez, F., Ramirez-Chavez, E., and Herrera-Estrella, L. 2006. Phospholipase DZ2 plays an important role in extraplastidic galactolipid biosynthesis and phosphate recycling in Arabidopsis roots. *Proc. Natl. Acad. Sci. U. S. A.* **103**: 6765–6770.

Cuypers, B., and Hahlbrock, K. 1988. Immunohistochemical studies of compatible and incompatible interactions of potato leaves with *Phytophthora infestans* and of the non-host response to *Phytophthora megasperma*. *Can. J. Bot.-Revue Can. Botan.* **66**: 700–705.

Dalal, J., Lewis, D. R., Tietz, O., Brown, E. M., Brown, C. S., Palme, K., Muday, G. K., and Sederoff, H. W. 2016. ROSY1, a novel regulator of gravitropic response is a stigmasterol binding protein. *J. Plant Physiol.* **196–197**: 28–40.

Dangl, J. L., and Jones, J. D. G. 2001. Plant pathogens and integrated defence responses to infection. *Nature* **411**: 826–833.

Dasgupta, S., Dasgupta, D., Chatterjee, A., Biswas, S., and Biswas, B. B. 1997. Conformational changes in plant Ins(1,4,5) P-3 receptor on interaction with different myo-inositol trisphosphates and its effect on Ca^{2+} release from microsomal fraction and liposomes. *Biochem. J.* **321**: 355–360.

Davidson, T. S., and Hickey, W. F. 2004. Distribution and immunoregulatory properties of antisecretory factor. *Lab. Investigat.* **84**: 307–319.

Demir, F., Horntrich, C., Blachutzik, J. O., Scherzer, S., Reinders, Y., Kierszniowska, S., Schulze, W. X., Harms, G. S., Hedrich, R., Geiger, D., and Kreuzer, I. 2013. Arabidopsis nanodomain-delimited ABA signaling pathway regulates the anion channel SLAH3. *Proc. Natl. Acad. Sci. U. S. A.* **110**: 8296–8301.

Dermine, J. F., Duclos, S., Garin, J., St-Louis, F., Rea, S., Parton, R. G., and Desjardins, M. 2001. Flotillin-1-enriched lipid raft domains accumulate on maturing phagosomes. *J. Biol. Chem.* **276**: 18507–18512.

Desai, A. J., and Miller, L. J. 2012. Sensitivity of cholecystokinin receptors to membrane cholesterol content. *Front. Endocrinol.* **3**: 123–123.

Di, C., Xu, W. Y., Su, Z., and Yuan, J. S. 2010. Comparative genome analysis of PHB gene family reveals deep evolutionary origins and diverse gene function. *BMC Bioinf.* **11**.

Digman, M. A., Brown, C. M., Sengupta, P., Wiseman, P. W., Horwitz, A. R., and Gratton, E. 2005. Measuring fast dynamics in solutions and cells with a laser scanning microscope. *Biophys. J.* **89**: 1317–1327.

Duan, Y. H., Guo, J., Shi, X. X., Guan, X. N., Liu, F. R., Bai, P. F., Huang, L. L., and Kang, Z. S. 2013. Wheat hypersensitive-induced reaction genes TaHIR1 and TaHIR3 are involved in response to stripe rust fungus infection and abiotic stresses. *Plant Cell Reports* **32**: 273–283.

Echarri, A., and Del Pozo, M. A. 2012. Caveolae. *Curr. Biol.* **22**: R114–R116.

Espenshade, P. J., and Hughes, A. L. 2007. Regulation of sterol synthesis in eukaryotes. *Annu. Rev. Genet.* **41**: 401–427.

Fantini, J., and Barrantes, F. J. 2013. How cholesterol interacts with membrane proteins: an exploration of cholesterol-binding sites including CRAC, CARC, and tilted domains. *Front. Physiol.* **4**: 31.

Fecchi, K., Volonte, D., Hezel, M. P., Schmeck, K., and Galbiati, F. 2006. Spatial and temporal regulation of GLUT4 translocation by Flotillin-1 and Caveolin-3 in skeletal muscle cells. *FASEB J.* **20**: 705–707.

Feldman, M., Poirier, B., and Lange, B. M. 2015. Misexpression of the Niemann-Pick disease type C1 (NPC1)-like protein in *Arabidopsis* causes sphingolipid accumulation and reproductive defects. *Planta* **242**: 921–933.

Feng, B. Z., Zhu, X. P., Fu, L., Lv, R. F., Storey, D., Tooley, P., and Zhang, X. G. 2014. Characterization of necrosis-inducing NLP proteins in *Phytophthora capsici*. *BMC Plant Biol.* **14**: 1.

Foskett, J. K., White, C., Cheung, K. H., and Mak, D. O. D. 2007. Inositol trisphosphate receptor Ca^{2+} release channels. *Physiol. Rev.* **87**: 593–658.

Frick, M., Bright, N. A., Riento, K., Bray, A., Merrified, C., and Nichols, B. J. 2007. Coassembly of flotillins induces formation of membrane microdomains, membrane curvature, and vesicle budding. *Curr. Biol.* **17**: 1151–1156.

Fujita, M., Fujita, Y., Noutoshi, Y., Takahashi, F., Narusaka, Y., Yamaguchi-Shinozaki, K., and Shinozaki, K. 2006. Crosstalk between abiotic and biotic stress responses: a current view from the points of convergence in the stress signaling networks. *Curr. Opin. Plant Biol.* **9**: 436–442.

Ge, L., Qi, W., Wang, L.-J., Miao, H.-H., Qu, Y.-X., Li, B.-L., and Song, B.-L. 2011. Flotillins play an essential role in Niemann-Pick C1-like 1-mediated cholesterol uptake. *Proc. Natl. Acad. Sci. U. S. A.* **108**: 551–556.

Gehl, B., and Sweetlove, L. J. 2014. Mitochondrial Band-7 family proteins: scaffolds for respiratory chain assembly? *Front. Plant Sci.* **5**: 141.

Gimpl, G., Burger, K., and Fahrenholz, F. 1997. Cholesterol as modulator of receptor function. *Biochemistry* **36**: 10959–10974.

Glazebrook, J. 2005. Contrasting mechanisms of defense against biotrophic and necrotrophic pathogens. *Annu. Rev. Phytopathol.* **43**: 205–227.

Glebov, O. O., Bright, N. A., and Nichols, B. J. 2006. Flotillin-1 defines a clathrin-independent endocytic pathway in mammalian cells. *Nat. Cell Biol.* **8**: 46–54.

Glenney, J. R., and Soppet, D. 1992. Sequence and expression of caveolin, a protein-component of caveolae plasma-membrane domains phosphorylated on tyrosine in rous-sarcoma virus-transformed fibroblasts. *Proc. Natl. Acad. Sci. U. S. A.* **89**: 10517–10521.

Grefen, C., and Blatt, M. R. 2012. A 2in1 cloning system enables ratiometric bimolecular fluorescence complementation (rBiFC). *Biotechniques* **53**: 311–314.

Grossmann, G., Opekarová, M., Malinsky, J., Weig-Meckl, I., and Tanner, W. 2007. Membrane potential governs lateral segregation of plasma membrane proteins and lipids in yeast. *EMBO J.* **26**: 1–8.

Guillaume, E., Comunale, F., Khoa, N. D., Planchon, D., Bodin, S., and Gauthier-Rouviere, C. 2013. Flotillin microdomains stabilize cadherins at cell-cell junctions. *J. Cell Sci.* **126**: 5293–5304.

Haney, C. H., and Long, S. R. 2010. Plant flotillins are required for infection by nitrogen-fixing bacteria. *Proc. Natl. Acad. Sci. U. S. A.* **107**: 478–483.

Haney, C. H., Riely, B. K., Tricoli, D. M., Cook, D. R., Ehrhardt, D. W., and Long, S. R. 2011. Symbiotic *Rhizobia* bacteria trigger a change in localization and dynamics of the *Medicago truncatula* receptor kinase LYK3. *Plant Cell* **23**: 2774–2787.

Hao, H. Q., Fan, L. S., Chen, T., Li, R. L., Li, X. J., He, Q. H., Botella, M. A., and Lin, J. X. 2014. Clathrin and membrane microdomains cooperatively regulate RbohD dynamics and activity in *Arabidopsis*. *Plant Cell* **26**: 1729–1745.

He, Z. H., Fujiki, M., and Kohorn, B. D. 1996. A cell wall-associated, receptor-like protein kinase. *J. Biol. Chem.* **271**: 19789–19793.

He, P., Shan, L., Lin, N. C., Martin, G. B., Kemmerling, B., Nurnberger, T., and Sheen, J. 2006. Specific bacterial suppressors of MAMP signaling upstream of MAPKKK in *Arabidopsis* innate immunity. *Cell* **125**: 563–575.

Heerklotz, H. 2002. Triton promotes domain formation in lipid raft mixtures. *Biophys. J.* **83**: 2693–2701.

Ho, A. Y. Y., Day, D. A., Brown, M. H., and Marc, J. 2009. *Arabidopsis* phospholipase D delta as an initiator of cytoskeleton-mediated signalling to fundamental cellular processes. *Funct. Plant Biol.* **36**: 190–198.

Hoegg, M. B., Browman, D. T., Resek, M. E., and Robbins, S. M. 2009. Distinct regions within the erlins are required for oligomerization and association with high molecular weight complexes. *J. Biol. Chem.* **284**: 7766–7776.

Hoegg, M. B., Robbins, S. M., and McGhee, J. D. 2012. Characterization of the *C. elegans* erlin homologue. *BMC Cell Biol.* **13**: 1.

Hou, X. W., Tong, H. Y., Selby, J., DeWitt, J., Peng, X. X., and He, Z. H. 2005. Involvement of a cell wall-associated kinase, WAKL4, in *Arabidopsis* mineral responses. *Plant Physiol.* **139**: 1704–1716.

Hulpiau, P., and van Roy, F. 2009. Molecular evolution of the cadherin superfamily. *Int. J. Biochem. Cell Biol.* **41**: 349–369.

Husbands, A., Aggarwal, V., Ha, T., and Timmermans, M. C. 2016. In planta single-molecule pull-down (SiMPull) reveals tetrameric stoichiometry of HD-ZIPIII:LITTLE ZIPPER complexes. *Plant Cell.* **28**: 1783–1794.

Ishikawa, T., Aki, T., Yanagisawa, S., Uchimiya, H., and Kawai-Yamada, M. 2015. Overexpression of BAX INHIBITOR-1 links plasma membrane microdomain proteins to stress. *Plant Physiol.* **169**: 1333–1343.

Janda, M., and Ruelland, E. 2015. Magical mystery tour: salicylic acid signalling. *Environ. Exp. Bot.* **114**: 117–128.

Jarsch, I. K., Konrad, S. S. A., Stratil, T. F., Urbanus, S. L., Szymanski, W., Braun, P., Braun, K. H., and Ott, T. 2014. Plasma membranes are subcompartmentalized into a plethora of coexisting and diverse microdomains in *Arabidopsis* and *Nicotiana benthamiana*. *Plant Cell* **26**: 1698–1711.

Jones, J. D. G., and Dangl, J. L. 2006. The plant immune system. *Nature* **444**: 323–329.

Jung, H. W., and Hwang, B. K. 2007. The leucine-rich repeat (LRR) protein, CaLRR1, interacts with the hypersensitive induced reaction (HIR) protein, CaHIR1, and suppresses cell death induced by the CaHIR1 protein. *Mol. Plant Pathol.* **8**: 503–514.

Jung, H. W., Lim, C. W., Lee, S. C., Choi, H. W., Hwang, C. H., and Hwang, B. K. 2008. Distinct roles of the pepper hypersensitive induced reaction protein gene CaHIR1 in disease and osmotic stress, as determined by comparative transcriptome and proteome analyses. *Planta* **227**: 409–425.

Karrer, E. E., Beachy, R. N., and Holt, C. A. 1998. Cloning of tobacco genes that elicit the hypersensitive response. *Plant Mol.Biol.* **36**: 681–690.

Katagiri, T., Takahashi, S., and Shinozaki, K. 2001. Involvement of a novel *Arabidopsis* phospholipase D, AtPLD delta, in dehydration-inducible accumulation of phosphatidic acid in stress signalling. *Plant J.* **26**: 595–605.

Kato, N., Nakanishi, M., and Hirashima, N. 2006. Flotillin-1 regulates IgE receptor-mediated signaling in rat basophilic leukemia (RBL-2H3) cells. *J. Immunol.* **177**: 147–154.

Kawamura, Y., and Uemura, M. 2003. Mass spectrometric approach for identifying putative plasma membrane proteins of *Arabidopsis* leaves associated with cold acclimation. *Plant J.* **36**: 141–154.

Kierszniowska, S., Seiwert, B., and Schulze, W. X. 2009. Definition of arabidopsis sterol-rich membrane microdomains by differential treatment with methyl-beta-cyclodextrin and quantitative proteomics. *Mol. Cell. Proteomics* **8**: 612–623.

Koellhoffer, J. P., Xing, A. Q., Moon, B. P., and Li, Z. S. 2015. Tissue-specific expression of a soybean hypersensitive-induced response (HIR) protein gene promoter. *Plant Mol. Biol.* **87**: 261–271.

Kohorn, B. D., Johansen, S., Shishido, A., Todorova, T., Martinez, R., Defeo, E., and Obregon, P. 2009. Pectin activation of MAP kinase and gene expression is WAK2 dependent. *Plant J.* **60**: 974–982.

Konrad, S. S. A., and Ott, T. 2015. Molecular principles of membrane microdomain targeting in plants. *Trends Plant Sci.* **20**: 351–361.

Kraft, M. L. 2013. Plasma membrane organization and function: moving past lipid rafts. *Mol. Biol. Cell* **24**: 2765–2768.

Krinke, O., Novotna, Z., Valentova, O., and Martinec, J. 2007. Inositol trisphosphate receptor in higher plants: is it real? *J. Exp. Bot.* **58**: 361–376.

Kurrle, N., Voellner, F., Eming, R., Hertl, M., Banning, A., and Tikkanen, R. 2013. Flotillins directly interact with gamma-catenin and regulate epithelial cell-cell adhesion. *PLoS One* **8**.

Lange, S., Jennische, E., Johansson, E., and Lonnroth, I. 1999. The antisecretory factor: synthesis and intracellular localisation in porcine tissues. *Cell Tissue Res.* **296**: 607–617.

Langhorst, M. F., Reuter, A., Jaeger, F. A., Wippich, F. M., Luxenhofer, G., Plattner, H., and Stuermer, C. A. O. 2008. Trafficking of the microdomain scaffolding protein reggie-1/Flotillin-2. *Eur. J. Cell Biol.* **87**: 211–226.

Langhorst, M. F., Solis, G. P., Hannbeck, S., Plattner, H., and Stuermer, C. A. O. 2007. Linking membrane microdomains to the cytoskeleton: regulation of the lateral mobility of reggie-1/Flotillin-2 by interaction with actin. *FEBS Lett.* **581**: 4697–4703.

Lankova, M., Humpolickova, J., Vosolsobe, S., Cit, Z., Lacek, J., Covan, M., Covanova, M., Hof, M., and Petrasek, J. 2016. Determination of dynamics of plant plasma membrane proteins with fluorescence recovery and raster image correlation spectroscopy. *Microsc. Microanal.* **22**: 290–299.

Li, W. Q., Li, M. Y., Zhang, W. H., Welti, R., and Wang, X. M. 2004. The plasma membrane-bound phospholipase D delta enhances freezing tolerance in *Arabidopsis thaliana*. *Nat. Biotechnol.* **22**: 427–433.

Li, R. L., Liu, P., Wan, Y. L., Chen, T., Wang, Q. L., Mettbach, U., Baluska, F., Samaj, J., Fang, X. H., Lucas, W. J., and Lin, J. 2012. A membrane microdomain-associated protein, *Arabidopsis* Flot1, is involved in a clathrin-independent endocytic pathway and is required for seedling development. *Plant Cell* **24**: 2105–2122.

Li, X. J., Luu, D. T., Maurel, C., and Lin, J. X. 2013. Probing plasma membrane dynamics at the single-molecule level. *Trends Plant Sci.* **18**: 617–624.

Li, H., and Papadopoulos, V. 1998. Peripheral-type benzodiazepine receptor function in cholesterol transport. Identification of a putative cholesterol recognition/interaction amino acid sequence and consensus patterns. *Endocrinology* **139**: 4991–4997.

Li, M., Qin, C., Welti, R., and Wang, X. 2006a. Double knockouts of phospholipases Dζ1 and Dζ2 in arabidopsis affect root elongation during phosphate-limited growth but do not affect root hair patterning. *Plant Physiol.* **140**: 761–770.

Li, X. J., Wang, X. H., Yang, Y., Li, R. L., He, Q. H., Fang, X. H., Luu, D. T., Maurel, C., and Lin, J. X. 2011. Single-molecule analysis of PIP2;1 dynamics and partitioning reveals multiple modes of *Arabidopsis* plasma membrane aquaporin regulation. *Plant Cell* **23**: 3780–3797.

Li, M., Welti, R., and Wang, X. 2006b. Quantitative profiling of arabidopsis polar glycerolipids in response to phosphorus starvation. roles of phospholipases Dζ1 and Dζ2 in phosphatidylcholine hydrolysis and digalactosyldiacylglycerol accumulation in phosphorus-starved plants. *Plant Physiol.* **142**: 750–761.

Lichtenberg, D., Goñi, F. M., and Heerklotz, H. 2005. Detergent-resistant membranes should not be identified with membrane rafts. *Trends Biochem. Sci.* **30**: 430–436.

Liu, J., DeYoung, S. M., Zhang, M., Dold, L. H., and Saltiel, A. R. 2005. The stomatin/prohibitin/flotillin/HflK/C domain of Flotillin-1 contains distinct sequences that direct plasma membrane localization and protein interactions in 3T3–L1 adipocytes. *J. Biol. Chem.* **280**: 16125–16134.

Liu, P., Li, R. L., Zhang, L., Wang, Q. L., Niehaus, K., Baluska, F., Samaj, J., and Lin, J. X. 2009. Lipid microdomain polarization is required for NADPH oxidase-dependent ROS signaling in Picea meyeri pollen tube tip growth. *Plant J.* **60**: 303–313.

Lu, J. P., Wang, Y., Sliter, D. A., Pearce, M. M. P., and Wojcikiewicz, R. J. H. 2011. RNF170 Protein, an endoplasmic reticulum membrane ubiquitin ligase, mediates inositol 1,4,5-trisphosphate receptor ubiquitination and degradation. *J. Biol. Chem.* **286**: 24426–24433.

Liu, F., Yu, X. M., Zhao, W. Q., Chen, J. P., Goyer, C., Yang, W. X., and Liu, D. Q. 2013. Effects of the leaf rust pathogen on expression of TaHIR4 at the gene and protein levels in wheat. *J. Plant Interact.* **8**: 304–311.

Mackey, D., Belkhadir, Y., Alonso, J. M., Ecker, J. R., and Dangl, J. L. 2003. *Arabidopsis* RIN4 is a target of the type III virulence effector AvrRpt2 and modulates RPS2-mediated resistance. *Cell* **112**: 379–389.

Malakshah, S. N., Rezaei, M. H., Heidari, M., and Salekdeh, G. H. 2007. Proteomics reveals new salt responsive proteins associated with rice plasma membrane. *Biosci. Biotechnol. Biochem.* **71**: 2144–2154.

Malho, R., Moutinho, A., van der Luit, A., and Trewavas, A. J. 1998. Spatial characteristics of calcium signalling: the calcium wave as a basic unit in plant cell calcium signalling. *Philos. Trans. R. Soc. Lond. Ser. B-Biol. Sci.* **353**: 1463–1473.

Malínská, K., Malínský, J., Opekarová, M., and Tanner, W. 2003. Visualization of protein compartmentation within the plasma membrane of living yeast cells. *Mol. Biol. Cell* **14**: 4427–4436.

Martinec, J., Feltl, T., Scanlon, C. H., Lumsden, P. J., and Machackova, I. 2000. Subcellular localization of a high affinity binding site for D-myo-inositol 1,4,5-trisphosphate from *Chenopodium rubrum*. *Plant Physiol.* **124**: 475–483.

Martins, S., Dohmann, E. M. N., Cayrel, A., Johnson, A., Fischer, W., Pojer, F., Satiat-Jeunemaitre, B., Jaillais, Y., Chory, J., Geldner, N., and Vert, G. 2015. Internalization and vacuolar targeting of the brassinosteroid hormone receptor BRI1 are regulated by ubiquitination. *Nat. Commun.* **6**: 6151.

Mellgren, R. L. 2008. Detergent-resistant membrane subfractions containing proteins of plasma membrane, mitochondrial, and internal membrane origins. *J. Biochem. Biophys. Methods* **70**: 1029–1036.

Mikes, V., Milat, M. L., Ponchet, M., Panabieres, F., Ricci, P., and Blein, J. P. 1998. Elicitins, proteinaceous elicitors of plant defense, are a new class of sterol carrier proteins. *Biochem. Biophys. Res. Commun.* **245**: 133–139.

Minami, A., Fujiwara, M., Furuto, A., Fukao, Y., Yamashita, T., Kamo, M., Kawamura, Y., and Uemura, M. 2009. Alterations in detergent-resistant plasma membrane microdomains in arabidopsis thaliana during cold acclimation. *Plant Cell Physiol.* **50**: 341–359.

Mongrand, S., Morel, J., Laroche, J., Claverol, S., Carde, J. P., Hartmann, M. A., Bonneu, M., Simon-Plas, F., Lessire, R., and Bessoule, J. J. 2004. Lipid rafts in higher plant cells—purification and characterization of triton X-100-insoluble microdomains from tobacco plasma membrane. *J. Biol. Chem.* **279**: 36277–36286.

Morrow, I. C., Rea, S., Martin, S., Prior, I. A., Prohaska, R., Hancock, J. F., James, D. E., and Parton, R. G. 2002. Flotillin-1/Reggie-2 traffics to surface raft domains via a novel Golgi-independent pathway—identification of a novel membrane targeting domain and a role for palmitoylation. *J. Biol. Chem.* **277**: 48834–48841.

Mudgil, Y., Shiu, S. H., Stone, S. L., Salt, J. N., and Goring, D. R. 2004. A large complement of the predicted *Arabidopsis* ARM repeat proteins are members of the U-box E3 ubiquitin ligase family. *Plant Physiol.* **134**: 59–66.

Muir, S. R., and Sanders, D. 1997. Inositol 1,4,5-trisphosphate-sensitive Ca^{2+} release across nonvacuolar membranes in cauliflower. *Plant Physiol.* **114**: 1511–1521.

Nadimpalli, R., Yalpani, N., Johal, G. S., and Simmons, C. R. 2000. Prohibitins, stomatins, and plant disease response genes compose a protein superfamily that controls cell proliferation, ion channel regulation, and death. *J. Biol. Chem.* **275**: 29579–29586.

Neumann-Giesen, C., Falkenbach, B., Beicht, P., Claasen, S., Luers, G., Stuermer, C. A. O., Herzog, V., and Tikkanen, R. 2004. Membrane and raft association of reggie-1/Flotillin-2: role of myristoylation, palmitoylation and oligomerization and induction of filopodia by overexpression. *Biochem. J.* **378**: 509–518.

Neumann-Giesen, C., Fernow, I., Amaddii, M., and Tikkanen, R. 2007. Role of EGF-induced tyrosine phosphorylation of reggie-1/Flotillin-2 in cell spreading and signaling to the actin cytoskeleton. *J. Cell Sci.* **120**: 395–406.

Nie, Y., Huang, F., Dong, S., Li, L., Gao, P., Zhao, H., Wang, Y., and Han, S. 2014. Identification of inositol 1,4,5-trisphosphate-binding proteins by heparin-agarose affinity purification and LTQ ORBITRAP MS in *Oryza sativa*. *Proteomics* **14**: 2335–2338.

Nuell, M. J., Stewart, D. A., Walker, L., Friedman, V., Wood, C. M., Owens, G. A., Smith, J. R., Schneider, E. L., Dellorco, R., and Lumpkin, C. K. 1991. Prohibitin, an evolutionarily conserved intracellular protein that blocks DNA-synthesis in normal fibroblasts and Hela-cells. *Mol. Cell. Biol.* **11**: 1372–1381.

Oberdorf, J., Webster, J. M., Zhu, C. C., Luo, S. G., and Wojcikiewicz, R. J. H. 1999. Down-regulation of types I, II and III inositol 1,4,5-trisphosphate receptors is mediated by the ubiquitin/proteasome pathway. *Biochem. J.* **339**: 453–461.

Ogura, M., Yamaki, J., Homma, M. K., and Homma, Y. 2014. Phosphorylation of Flotillin-1 by mitochondrial c-Src is required to prevent the production of reactive oxygen species. *FEBS Lett.* **588**: 2837–2843.

Parsons, S. J., and Parsons, J. T. 2004. Src family kinases, key regulators of signal transduction. *Oncogene* **23**: 7906–7909.

Pearce, M. M. P., Wang, Y., Kelley, G. G., and Wojcikiewicz, R. J. H. 2007. SPFH2 mediates the endoplasmic reticulum-associated degradation of inositol 1,4,5-trisphosphate receptors and other substrates in mammalian cells. *J. Biol. Chem.* **282**: 20104–20115.

Pearce, M. M. P., Wormer, D. B., Wilkens, S., and Wojcikiewicz, R. J. H. 2009. An endoplasmic reticulum (ER) membrane complex composed of SPFH1 and SPFH2 mediates the ER-associated degradation of inositol 1,4,5-trisphosphate receptors. *J. Biol. Chem.* **284**: 10433–10445.

Pednekar, D., Wang, Y., Fedotova, T. V., and Wojcikiewicz, R. J. H. 2011. Clustered hydrophobic amino acids in amphipathic helices mediate erlin1/2 complex assembly. *Biochem. Biophys. Res. Commun.* **415**: 135–140.

Peremyslov, V. V., Morgun, E. A., Kurth, E. G., Makarova, K. S., Koonin, E. V., and Dolja, V. V. 2013. Identification of myosin XI receptors in *Arabidopsis* defines a distinct class of transport vesicles. *Plant Cell* **25**: 3022–3038.

Pinosa, F., Buhot, N., Kwaaitaal, M., Fahlberg, P., Thordal-Christensen, H., Ellerstrom, M., and Andersson, M. X. 2013. *Arabidopsis* phospholipase D delta is involved in basal defense and nonhost resistance to powdery mildew fungi. *Plant Physiol.* **163**: 896–906.

Pogany, M., von Rad, U., Gruen, S., Dongo, A., Pintye, A., Simoneau, P., Bahnweg, G., Kiss, L., Barna, B., and Durner, J. 2009. Dual roles of reactive oxygen species and NADPH oxidase RBOHD in an *Arabidopsis-Alternaria* pathosystem. *Plant Physiol.* **151**: 1459–1475.

Porter, B. W., Aizawa, K. S., Zhu, Y. J., and Christopher, D. A. 2008. Differentially expressed and new non-protein-coding genes from a *Carica papaya* root transcriptome survey. *Plant Sci.* **174**: 38–50.

Pucciariello, C., Parlanti, S., Banti, V., Novi, G., and Perata, P. 2012. Reactive oxygen species-driven transcription in *Arabidopsis* under oxygen deprivation. *Plant Physiol.* **159**: 184–196.

Pust, S., Dyve, A. B., Torgersen, M. L., van Deurs, B., and Sandvig, K. 2010. Interplay between toxin transport and flotillin localization. *PLoS One* **5**: e8844.

Qi, Y. P., and Katagiri, F. 2009. Purification of low-abundance *Arabidopsis* plasma-membrane protein complexes and identification of candidate components. *Plant J.* **57**: 932–944.

Qi, Y. P., Tsuda, K., Nguyen, L. V., Wang, X., Lin, J. S., Murphy, A. S., Glazebrook, J., Thordal-Christensen, H., and Katagiri, F. 2011. Physical asssociation of *Arabidopsis* hypersensitive induced reaction proteins (HIRs) with the immune receptor RPS2. *J. Biol. Chem.* **286**: 31297–31307.

Raffaele, S., Bayer, E., Lafarge, D., Cluzet, S., German Retana, S., Boubekeur, T., Leborgne-Castel, N., Carde, J.-P., Lherminier, J., Noirot, E., and Satiat-Jeunemaître, B. 2009. Remorin, a solanaceae protein resident in membrane rafts and plasmodesmata, impairs potato virus X movement. *Plant Cell* **21**: 1541–1555.

Rauchenberger, R., Hacker, U., Murphy, J., Niewohner, J., and Maniak, M. 1997. Coronin and vacuolin identify consecutive stages of a late, actin-coated endocytic compartment in *Dictyostelium*. *Curr. Biol.* **7**: 215–218.

Riento, K., Frick, M., Schafer, I., and Nichols, B. J. 2009. Endocytosis of Flotillin-1 and Flotillin-2 is regulated by Fyn kinase. *J. Cell Sci.* **122**: 912–918.

Rivera-Milla, E., Stuermer, C. A. O., and Malaga-Trillo, E. 2006. Ancient origin of reggie (flotillin), reggie-like, and other lipid-raft proteins: convergent evolution of the SPFH domain. *Cell. Mol. Life Sci.* **63**: 343–357.

Roepstorff, K., Thomsen, P., Sandvig, K., and van Deurs, B. 2002. Sequestration of epidermal growth factor receptors in non-caveolar lipid rafts inhibits ligand binding. *J. Biol. Chem.* **277**: 18954–18960.

Roitbak, T., Surviladze, Z., Tikkanen, R., and Wandinger-Ness, A. 2005. A polycystin multiprotein complex constitutes a cholesterol-containing signalling microdomain in human kidney epithelia. *Biochem. J.* **392**: 29–38.

Rosas-Santiago, P., Lagunas-Gomez, D., Barkla, B. J., Vera-Estrella, R., Lalonde, S., Jones, A., Frommer, W. B., Zimmermannova, O., Sychrova, H., and Pantoja, O. 2015. Identification of rice cornichon as a possible cargo receptor for the Golgi-localized sodium transporter OsHKT1;3. *J. Exp. Bot.* **66**: 2733–2748.

Rose, S. L., Fulton, J. M., Brown, C. M., Natale, F., Van Mooy, B. A. S., and Bidle, K. D. 2014. Isolation and characterization of lipid rafts in *Emiliania huxleyi*: a role for membrane microdomains in host-virus interactions. *Environ. Microbiol.* **16**: 1150–1166.

Rostoks, N., Schmierer, D., Kudrna, D., and Kleinhofs, A. 2003. Barley putative hypersensitive induced reaction genes: genetic mapping, sequence analyses and differential expression in disease lesion mimic mutants. *Theor. Appl. Genet.* **107**: 1094–1101.

Rudrabhatla, P., Reddy, M. M., and Rajasekharan, R. 2006. Genome-wide analysis and experimentation of plant serine/threonine/tyrosine-specific protein kinases. *Plant Mol.Biol.* **60**: 293–319.

Samaj, J., Baluska, F., Voigt, B., Schlicht, M., Volkmann, D., and Menzel, D. 2004. Endocytosis, actin cytoskeleton, and signaling. *Plant Physiol.* **135**: 1150–1161.

Sanchez-Quiles, V., Santamaria, E., Segura, V., Sesma, L., Prieto, J., and Corrales, F. J. 2010. Prohibitin deficiency blocks proliferation and induces apoptosis in human hepatoma cells: molecular mechanisms and functional implications. *Proteomics* **10**: 1609–1620.

Santamaria, A., Castellanos, E., Gomez, V., Benedit, P., Renau-Piqueras, J., Morote, J., Reventos, J., Thomson, T. M., and Paciucci, R. 2005. PTOV1 enables the nuclear translocation and mitogenic activity of Flotillin-1, a major protein of lipid rafts. *Mol. Cell. Biol.* **25**: 1900–1911.

Saravanan, R. S., Slabaugh, E., Singh, V. R., Lapidus, L. J., Haas, T., and Brandizzi, F. 2009. The targeting of the oxysterol-binding protein ORP3a to the endoplasmic reticulum relies on the plant VAP33 homolog PVA12. *Plant J.* **58**: 817–830.

Scanlon, C. H., Martinec, J., Machackova, I., Rolph, C. E., and Lumsden, P. J. 1996. Identification and preliminary characterization of a Ca^{2+}-dependent high-affinity binding site for inositol-1,4,5-trisphosphate from *Chenopodium rubrum*. *Plant Physiol.* **110**: 867–874.

Schroeder, W. T., Stewartgaletka, S., Mandavilli, S., Parry, D. A. D., Goldsmith, L., and Duvic, M. 1994. Cloning and characterization of a novel epidermal-cell surface-antigen (ESA). *J. Biol. Chem.* **269**: 19983–19991.

Schulte, T., Lottspeich, F., and Stuermer, C. A. O. 1995. Characterization of Reggie-1 and isolation of Reggie-2, cell surface proteins of the goldfish CNS. *Soc. Neurosci. Abstr.* **21**: 795.

Schulte, T., Paschke, K. A., Laessing, U., Lottspeich, F., and Stuermer, C. A. O. 1997. Reggie-1 and reggie-2, two cell surface proteins expressed by retinal ganglion cells during axon regeneration. *Development* **124**: 577–587.

Sekeres, J., Pleskot, R., Pejchar, P., Zarsky, V., and Potocky, M. 2015. The song of lipids and proteins: dynamic lipid-protein interfaces in the regulation of plant cell polarity at different scales. *J. Exp. Bot.* **66**: 1587–1598.

Shi, Q., Araie, H., Bakku, R. K., Fukao, Y., Rakwal, R., Suzuki, I., and Shiraiwa, Y. 2015. Proteomic analysis of lipid body from the alkenone-producing marine haptophyte alga Tisochrysis lutea. *Proteomics* **15**: 4145–4158.

Simons, K., and Ikonen, E. 1997. Functional rafts in cell membranes. *Nature* **387**: 569–572.

Sirvent, A., Urbach, S., and Roche, S. 2015. Contribution of phosphoproteomics in understanding SRC signaling in normal and tumor cells. *Proteomics* **15**: 232–244.

Sivaguru, M., Ezaki, B., He, Z. H., Tong, H. Y., Osawa, H., Baluska, F., Volkmann, D., and Matsumoto, H. 2003. Aluminum-induced gene expression and protein localization of a cell wall-associated receptor kinase in *Arabidopsis*. *Plant Physiol.* **132**: 2256–2266.

Slaughter, N., Laux, I., Tu, X. L., Whitelegge, J., Zhu, X. M., Effros, R., Bickel, P., and Nel, A. 2003. The flotillins are integral membrane proteins in lipid rafts that contain TCR-associated signaling components: implications for T-cell activation. *Clin. Immunol.* **108**: 138–151.

Solis, G. P., Hoegg, M., Munderloh, C., Schrock, Y., Malaga-Trillo, E., Rivera-Milla, E., and Stuerivier, C. A. O. 2007. Reggie/flotillin proteins are organized into stable tetramers in membrane microdomains. *Biochem. J.* **403**: 313–322.

Solis, G. P., Schrock, Y., Hulsbusch, N., Wiechers, M., Plattner, H., and Stuermer, C. A. O. 2012. Reggies/flotillins regulate E-cadherin-mediated cell contact formation by affecting EGFR trafficking. *Mol. Biol. Cell* **23**: 1812–1825.

Stewart, G. W., Argent, A. C., and Dash, B. C. J. 1993. Stomatin—a putative cation-transport regulator in the red-cell membrane. *Biochim. Biophys. Acta* **1225**: 15–25.

Stintzi, A., Heitz, T., Prasad, V., Wiedemannmerdinoglu, S., Kauffmann, S., Geoffroy, P., Legrand, M., and Fritig, B. 1993. Plant pathogenesis-related proteins and their role in defense against pathogens. *Biochimie* **75**: 687–706.

Stuermer, C. A. O. 2010. The reggie/flotillin connection to growth. *Trends Cell Biol.* **20**: 6–13.

Stuermer, C. A. O., Lang, D. M., Kirsch, F., Wiechers, M., Deininger, S. O., and Plattner, H. 2001. Glycosylphosphatidyl inositol-anchored proteins and fyn kinase assemble in noncaveolar plasma membrane microdomains defined by reggie-1 and-2. *Mol. Biol. Cell* **12**: 3031–3045.

Sugiyama, N., Nakagami, H., Mochida, K., Daudi, A., Tomita, M., Shirasu, K., and Ishihama, Y. 2008. Large-scale phosphorylation mapping reveals the extent of tyrosine phosphorylation in *Arabidopsis*. *Mol. Syst. Biol.* **4**: 193.

Szymanski, W. G., Zauber, H., Erban, A., Gorka, M., Wu, X. N., and Schulze, W. X. 2015. Cytoskeletal components define protein location to membrane microdomains. *Mol. Cell. Proteomics* **14**: 2493–2509.

Takeshita, N., Diallinas, G., and Fischer, R. 2012. The role of flotillin FloA and stomatin StoA in the maintenance of apical sterol-rich membrane domains and polarity in the filamentous fungus *Aspergillus nidulans*. *Mol. Microbiol.* **83**: 1136–1152.

Tanner, W., Malinsky, J., and Opekarova, M. 2011. In plant and animal cells, detergent-resistant membranes do not define functional membrane rafts. *Plant Cell* **23**: 1191–1193.

Tapken, W., and Murphy, A. S. 2015. Membrane nanodomains in plants: capturing form, function, and movement. *J. Exp. Bot.* **66**: 1573–1586.

Taylor, C. W., da Fonseca, P. C. A., and Morris, E. P. 2004. IP3 receptors: the search for structure. *Trends Biochem. Sci.* **29**: 210–219.

Torres, M. A., Dangl, J. L., and Jones, J. D. G. 2002. *Arabidopsis* gp91(phox) homologues AtrbohD and AtrbohF are required for accumulation of reactive oxygen intermediates in the plant defense response. *Proc. Natl. Acad. Sci. U. S. A.* **99**: 517–522.

Torres, M. A., Jones, J. D. G., and Dangl, J. L. 2006. Reactive oxygen species signaling in response to pathogens. *Plant Physiol.* **141**: 373–378.

Ullrich, A., and Schlessinger, J. 1990. Signal transduction by receptors with tyrosine kinase-activity. *Cell* **61**: 203–212.

Umate, P. 2011. Oxysterol binding proteins (OSBPs) and their encoding genes in Arabidopsis and rice. *Steroids* **76**: 524–529.

Vale, R. D. 2003. The molecular motor toolbox for intracellular transport. *Cell* **112**: 467–480.

Van Meer, G., Stelzer, E. H. K., Wijnaendtsvanresandt, R. W., and Simons, K. 1987. Sorting of sphingolipids in epithelial (Madin-Darby canine kidney) cells. *J. Cell Biol.* **105**: 1623–1635.

Vassilieva, E. V., Ivanov, A. I., and Nusrat, A. 2009. Flotillin-1 stabilizes Caveolin-1 in intestinal epithelial cells. *Biochem. Biophys. Res. Commun.* **379**: 460–465.

Vauthrin, S., Mikes, V., Milat, M. L., Ponchet, M., Maume, B., Osman, H., and Blein, J. P. 1999. Elicitins trap and transfer sterols from micelles, liposomes and plant plasma membranes. *Biochim. Biophys. Acta-Biomembr.* **1419**: 335–342.

Vembar, S. S., and Brodsky, J. L. 2008. One step at a time: endoplasmic reticulum-associated degradation. *Nat. Rev. Mol. Cell Biol.* **9**: 944–957.

Vogelmann, K., Subert, C., Danzberger, N., Drechsel, G., Bergler, J., Kotur, T., Burmester, T., and Hoth, S. 2014. Plasma membrane-association of SAUL1-type plant U-box armadillo repeat proteins is conserved in land plants. *Front. Plant Sci.* **5**: 37.

Volonté, D., Galbiati, F., Li, S., Nishiyama, K., Okamoto, T., and Lisanti, M. P. 1999. Flotillins/Cavatellins are differentially expressed in cells and tissues and form a hetero-oligomeric complex with caveolins in vivo: characterization and epitope-mapping of a novel Flotillin-1 monoclonal antibody probe. *J. Biol. Chem.* **274**: 12702–12709.

Wagner, T. A., and Kohorn, B. D. 2001. Wall-associated kinases are expressed throughout plant development and are required for cell expansion. *Plant Cell* **13**: 303–318.

Wang, X. M. 2005. Regulatory functions of phospholipase D and phosphatidic acid in plant growth, development, and stress responses. *Plant Physiol.* **139**: 566–573.

Wang, L., Li, H., Lv, X. Q., Chen, T., Li, R. L., Xue, Y. Q., Jiang, J. J., Jin, B., Baluska, F., Samaj, J., and Wang, X. 2015. Spatiotemporal dynamics of the BRI1 receptor and its regulation by membrane microdomains in living arabidopsis cells. *Mol. Plant* **8**: 1334–1349.

Wang, Y., Pearce, M. M. P., Sliter, D. A., Olzmann, J. A., Christianson, J. C., Kopito, R. R., Boeckmann, S., Gagen, C., Leichner, G. S., Roitelman, J., and Wojcikiewicz, R. J. 2009. SPFH1 and SPFH2 mediate the ubiquitination and

degradation of inositol 1,4,5-trisphosphate receptors in muscarinic receptor-expressing HeLa cells. *Biochim. Biophys. Acta-Mol. Cell Res.* **1793**: 1710–1718.

Wright, S. A. I., Azarang, M., and Falk, A. B. 2013. Barley lesion mimics, supersusceptible or highly resistant to leaf rust and net blotch. *Plant Pathol.* **62**: 982–992.

Xiang, Y., Song, M., Zhang, M. Q., Cao, S. F., and Han, H. S. 2015. Molecular characterization of three hypersensitive-induced reaction genes that respond to *Phytophthora sojae* infection in Glycine max L. Merr. *Legume Res.* **38**: 313–320.

Xie, Y.-J., Xu, S., Han, B., Wu, M.-Z., Yuan, X.-X., Han, Y., Gu, Q., Xu, D.-K., Yang, Q., and Shen, W.-B. 2011. Evidence of *Arabidopsis* salt acclimation induced by up-regulation of HY1 and the regulatory role of RbohD-derived reactive oxygen species synthesis. *Plant J.* **66**: 280–292.

Xing, S., Wallmeroth, N., Berendzen, K. W., and Grefen, C. 2016. Techniques for the analysis of protein-protein interactions in vivo. *Plant Physiol.* **171**: 727–758.

Yu, X. M., Yu, X. D., Qu, Z. P., Huang, X. J., Guo, J., Han, Q. M., Zhao, J., Huang, L. L., and Kang, Z. S. 2008. Cloning of a putative hypersensitive induced reaction gene from wheat infected by stripe rust fungus. *Gene* **407**: 193–198.

Yu, X. M., Zhao, W. Q., Yang, W. X., Liu, F., Chen, J. P., Goyer, C., and Liu, D. Q. 2013. Characterization of a hypersensitive response-induced gene TaHIR3 from wheat leaves infected with leaf rust. *Plant Mol. Biol. Rep.* **31**: 314–322.

Zarsky, V., Cvrckova, F., Potocky, M., and Hala, M. 2009. Exocytosis and cell polarity in plants—exocyst and recycling domains. *New Phytol.* **183**: 255–272.

Zhang, G., Dong, Y. L., Zhang, Y., Li, Y. M., Wang, X. J., Han, Q. M., Guo, J., Huang, L. L., and Kang, Z. S. 2009b. Cloning and characterization of a novel hypersensitive-induced reaction gene from wheat infected by stripe rust pathogen. *J. Phytopathol.* **157**: 722–728.

Zhang, G., Li, Y. M., Sun, Y. F., Wang, J. M., Liu, B., Zhao, J., Guo, J., Huang, L. L., Chen, X. M., and Kang, Z. S. 2011. Molecular characterization of a gene induced during wheat hypersensitive reaction to stripe rust. *Biol. Plant.* **55**: 696–702.

Zhang, J., Liem, D. A., Mueller, M., Wang, Y., Zong, C., Deng, N., Vondriska, T. M., Korge, P., Drews, O., MacLellan, W. R., and Honda, H. 2008. Altered proteome biology of cardiac mitochondria under stress conditions. *J. Proteome Res.* **7**: 2204–2214.

Zhang, D. W., Manna, M., Wohland, T., and Kraut, R. 2009a. Alternate raft pathways cooperate to mediate slow diffusion and efficient uptake of a sphingolipid tracer to degradative and recycling compartments. *J. Cell Sci.* **122**: 3715–3728.

Zhao, X. Y., Li, R. L., Lu, C. F., Baluska, F., and Wan, Y. L. 2015. Di-4-ANEPPDHQ, a fluorescent probe for the visualisation of membrane microdomains in living Arabidopsis thaliana cells. *Plant Physiol. Biochem.* **87**: 53–60.

Zhao, F., Zhang, J., Liu, Y. S., Li, L., and He, Y. L. 2011. Research advances on flotillins. *Virol. J.* **8**: 1.

Zhou, L. A., Cheung, M. Y., Li, M. W., Fu, Y. P., Sun, Z. X., Sun, S. M., and Lam, H. M. 2010. Rice hypersensitive induced reaction protein 1 (OsHIR1) associates with plasma membrane and triggers hypersensitive cell death. *BMC Plant Biol.* **10**: 290.

Zhou, L., Cheung, M. Y., Zhang, Q., Lei, C. L., Zhang, S. H., Sun, S. S., and Lam, H. M. 2009. A novel simple extracellular leucine-rich repeat (eLRR) domain protein from rice (OsLRR1) enters the endosomal pathway and interacts with the hypersensitive-induced reaction protein 1 (OsHIR1). *Plant Cell Environ* **32**: 1804–1820.

Zhou, Q., Gao, H., Wang, M., Xu, Y., Guo, Y. Z., Wan, Y. Z., and Zhao, Z. Y. 2012. Characterization of defense-related genes in the 'Qinguan' apple in response to *Marssonina coronaria*. *S. Afr. J. Bot.* **80**: 36–43.

Plasma membrane structure and dynamics mainly in plants

In the original proposition, the fluid mosaic model of cellular membranes considered lipid bilayer a liquid environment in which membrane proteins are embedded and their behaviour is from a major part affected by the interaction with lipids of the bilayer with additional minor contribution of oligosaccharides bound to the proteins. Clustering of proteins within the membrane was already observed in the original paper even though monomolecular distribution in the fluid bilayer was supposed to occur under normal conditions while redistribution into clusters was proposed to happen upon protein modification (Singer and Nicolson, 1972).

Over the following decades the model has been revised and additional cell compartments have been taken into account to take part in the membrane organization. Effect of cytoskeleton components on membrane protein mobility by binding or steric confinement (Kusumi and Sako, 1996) as well as the restriction of mobility of phospholipids by F-actin (Fujiwara et al., 2002) are summarized in the picket and fence model of PM. Membrane component is there limited in its free movement in a restricted area delimited with cytoskeleton network (fences) underlying PM which is attached to PM by interaction with transmembrane proteins (pickets). The fences can be overcome by so called hop diffusion, however such an event is far less probable for objects of a higher size such as oligomers or protein complexes which can thus be immobilized (Ritchie et al., 2003). The model is supported by the fact that pharmacological alteration of cytoskeleton was reported to affect performance of several PM localized proteins also in plants. Microtubule (MT) depolymerisation decreased the density of microdomains defined by remorins without abolishing the microdomain identity (Szymanski et al., 2015, Liang et al., 2018), whereas actin depolymerisation induced the loss of microdomain localisation pattern which became homogeneous (Szymanski et al., 2015). Both tubulin and actin depolymerisation led to decrease of mobility of *At*FLOT1 and *At*HIR1 (Li et al., 2012, Lv et al., 2017b) and also to an increase of microdomain density in *At*HIR1 (Lv et al., 2017b). Moreover, the movement of *At*HIR1 fluorescence spots was confined within the areas delimited by cortical MTs (Lv et al., 2017b). On the other hand, cytoskeleton disruption increased single particle mobility of *At*FLS2 while there was no effect on mobility of *At*LTi6b or *At*PIN3 (McKenna et al., 2019) which suggests that there is no general impact of cytoskeleton on PM protein dynamics.

In plant cells, an additional confinement mechanism for PM protein mobility was observed – the cell wall (CW). CW structure disruption induced by pharmacological approach increase mobility and microdomain size of *At*PIN3 and *At*FLS2 (McKenna et al., 2019). Cellulose synthesis inhibition or digestion of CW polysaccharides as well as by plasmolysis which leads to separation of PM from CW was reported to increase the mobility of *At*PIN1 (Feraru et al., 2011), GPI-anchored GFP or GFP fused to extracellular terminus of a transmembrane domain

(Martiniere et al., 2012). Similarly, water transporter *At*PIP2;1 mobility was increased under osmotic challenging and mild plasmolysis (Hosy et al., 2014). Interestingly, plasmolysis had no effect on mobility of common PM marker protein *At*LTi6b (Hosy et al., 2014) while cellulose synthesis inhibition even decreased the mobility of the protein (Martiniere et al., 2012). The effect of PM and CW separation on the individual protein mobility may be also indirect as plasmolysis induces depolymerisation of actin filaments (Tolmie et al., 2017, Yu et al., 2018) which can also influence the PM-associated protein behaviour (see above).

Differential lipid and protein composition in different areas of PM was observed resulting in the concept of lipid rafts, membrane platforms of higher order enriched in sphingolipids and sterols which can recruit and cluster signalling proteins (Simons and Ikonen, 1997). The local sequestration of phosphatidylserine visualized using genetically encoded sensor into nanoclusters within PM has been recently observed by sptPALM approach (Platre et al., 2019). Relatively few reports have been made so far on the effect of lipid alteration on PM microdomain proteins by *in vivo* approaches. Among these, pharmacological sterol sequestration from PM or alteration of sterol, phosphoinositide or sphingolipid synthesis inhibited clustering of a *St*REM1.3 at PM (Gronnier et al., 2017) but promoted relocalization into larger clusters followed by overall decrease in foci density in *At*PIP2;1 (Li et al., 2011) and *At*RbohD (Hao et al., 2014). Alteration of phosphatidylserine levels changed the clustering of *At*ROP6 (Platre et al., 2019). In *At*FLS2, *At*FLOT1 and *At*HIR1 sterol sequestration decreased the mobility of the proteins when determined by sptTIRF/VAEM (Li et al., 2012, Lv et al., 2017b, Cui et al., 2018).

The proteins observed in microdomains are also often present in so called detergent-resistant membranes – DRM (also termed detergent-insoluble membranes – DIM), i.e. membrane fraction resistant to solubilisation with mild detergents such as Triton X-100 (Borner et al., 2005) or Brij-98 (Demir, 2010). This often leads to erroneous impression that membrane micro/nanodomains and DRM are interchangeable counterparts (e.g. (Mongrand et al., 2004). Besides protein accumulation DRM are also enriched in specific lipid classes such as sterols, polyphosphoinositides and glucosylceramides (Furt et al., 2010) however it is important to keep in mind that the concomitant separation of lipids and proteins into DRM is heavily impacted by the extraction conditions (Guillier et al., 2014) and DRM should be rather considered as a systematic artefact (yet valuable) since colocalization or simultaneous enrichment of such lipids and proteins was hardly ever observed *in vivo*. However, reduced DRM-associated proteome was observed in plants deficient in synthesis of sphingolipids (Nagano et al., 2016) or under sterol depletion (Demir et al., 2013). The association of a given protein with DRM may be affected by lipidation (Sorek et al., 2017) or phosphorylation (Demir et al., 2013). *At*FLOT1, *At*HIR1, *At*HIR2 and *At*HIR4 were identified enriched in DRM (Borner et al., 2005). *Os*FLOT was depleted from DRM in lines with lowered synthesis of sphingolipid while it was enriched in DRM in wild type rice (Nagano et al., 2016).

In artificial unilamellar vesicles prepared from lipid mixtures lipids can separate in distinct regions different in so called membrane or lipid order. Liquid-ordered phase (L_o) is enriched in rather saturated, long acyl chain lipid species which are more tightly and regularly organized while liquid-disordered phase (L_d) is more fluid and contains higher portion of unsaturated lipids (Veatch and Keller, 2003, Kaiser et al., 2009). Membrane order can be *in vivo* measured using fluorescence dyes which change their emission based on the order of membranes in which they are incorporated such as Laurdan or Di-4-ANEPPDHQ (Amaro et al., 2017). Sub-micrometer regions of higher membrane order were observed *in vivo* in spruce pollen tube (Liu et al., 2009) and epidermal leaf cells of tobacco (Gronnier et al., 2017). The main lipid species contributing to the change of order in artificial vesicles constituted from the mixture of phospholipids are in plants phytosterols while the sphingolipids do not induce significant alteration unless they are combined with phytosterols (Grosjean et al., 2015, Cacas et al., 2016). The effect of sterols was also observed in vivo in actual PM where sterol complexation induced by filipin increased the membrane order (Bonneau et al., 2010) while depletion of sterols promoted a decrease in order (Gerbeau-Pissot et al., 2014). Membrane order is also decreased by the presence of proteins in PM whereas CW or cytoskeleton disruption or overall inhibition of phosphorylation did not affect the order (Grosjean et al., 2018). Membrane microdomains formed by *St*REM1.3 or *Pm*NOX preferentially colocalized with PM areas of higher order (Liu et al., 2009, Gronnier et al., 2017). The lipid species are asymmetrically distributed between the inner and outer leaflet of PM (Tjellstrom et al., 2010) and sterols and sphingolipids were proposed to form subregions of higher order within PM spanning from outer to inner leaflet by so called interdigitation of long acyl chains of the lipids in these regions (Raghupathy et al., 2015, Cacas et al., 2016). Effect of phospholipids on membrane identity or mobility was described in *At*ROP6 (Platre et al., 2019) and *St*REM1.3 (Gronnier et al., 2017).

Human flotillins interact with cholesterol by recognition/interaction amino acid consensus (CRAC) motifs (Roitbak et al., 2005). We found several putative CRAC motifs also in the sequences of *At*FLOTs and *At*HIRs (Daněk et al., 2016), however experimental confirmation of such interaction still remains to be carried out. However, CRAC motif was proven to be crucial for PM microdomain localization in *Mx*IRT1 as well as for its enrichment in DRM (Tan et al., 2018) which suggests that CRAC motif may apply in phytosterol binding in plants too. Interestingly Arabidopsis lines with decreased expression of *At*FLOT1 showed lower amounts of sterols present in PM (Li et al., 2012) together with decrease of PM order (Zhao et al., 2015). Moreover, murine FLOT1 is important for trafficking of sphingosine, a sphingolipid precursor, to PM and enrichment of sphingolipids in DRM (Riento et al., 2018). These findings indicate that the relation between FLOTs and lipids may be double-sided, i.e. that proteins can also affect lipid fate in addition to the directions from lipids to proteins which seems to be prevailing research approach.

Plasma membrane micro/nanodomains in plants

With the ongoing progress in live imaging techniques many membrane-associated proteins are revealed to be unevenly localized throughout PM while they are found to form clusters or distinct fluorescent foci termed membrane microdomains or nanodomains. The latter term reflects the fact that the actual dimensions of the observed clusters is usually below one micrometre. Although the both terms are often used interchangeably in the literature my opinion is that the terms should be used not only based on the determined size (that can be *ex post* measured at the obtained images) but also the technique by which they were detected or analysed. In other words, approaches allowing the distinction at nanometre scale (reasonably called "nanoscopy": STED, STORM, PALM, MINFLUX, or the ones enabling single particle tracking such as TIRF/VAEM really provide the information about the domain at nanoscale while confocal techniques (which we used) with resolution in hundreds of nanometres provide the information on micrometre scale and the observed structures should be referred as "microdomains", which is the term I will use describing the achievement of the presented work.

Besides FLOTs and HIRs, plant proteins observed to form PM microdomain are involved in variety of functions such as transport: *At*SLAC1, *At*SLAH3, *At*PIP2;1, *At*KAT1, *At*SUT1, *At*PIN2, *At*AMT1;3 (Demir et al., 2013, Retzer et al., 2017, Jarsch et al., 2014, Krügel et al., 2008, Wang et al., 2013); cellulose synthesis: *At*CESA3, *At*CESA6, *At*KOR1, *At*POM2 (Bashline et al., 2015, Worden et al., 2015); clathrin-mediated endocytosis: *At*CLC2, *At*AP2, *At*TWD40-2, A*t*DRP1A, A*t*DRP1C (Konopka et al., 2008, Konopka and Bednarek, 2008, Li et al., 2011, Bashline et al., 2015); (de)phosphorylation: *At*ABI1, *At*CPK21, *At*ROP6 (Demir et al., 2013, Platre et al., 2019); ROS productions: *At*RbohD, *Pm*NOX (Liu et al., 2009, Hao et al., 2014); light sensing: *At*PHOT1 (Xue et al., 2018) or receptor recognition and subsequent signalling: *At*FLS2, *At*BRI1, *At*BIK1, *At*BSK1, *Mt*LYK3 (Haney et al., 2011, Wang et al., 2015, Bücherl et al., 2017). Prominent plant-unique protein family with many isoforms described as microdomain-associated are remorins (Raffaele et al., 2009, Jarsch et al., 2014, Gronnier et al., 2017, Bücherl et al., 2017). *At*REM1.3 was found to interact with *At*HIR1 (Lv et al., 2017b).

*At*FLOT1 microdomains partially colocalized with the ones of *At*RbohD (Hao et al., 2014), *At*PIP2;1 (Li et al., 2011), *At*AMT1;3 (Wang et al., 2013), *At*BRI1 (Wang et al., 2015) and *At*FLS2 (Cui et al., 2018). In the last two mentioned cases, the colocalization was increased after the treatment with epibrassinolide or flg22, respectively, i.e. by the ligands recognized by the receptor proteins. Together with the findings that upon flg22 treatment *At*FLOT1 microdomains were more mobile, the protein was to a greater extend endocytosed and degraded or callose deposition was lowered in *AtFLOT1* knock-down lines (Yu et al., 2017) it is possible that *At*FLOT roles comprise functional association with receptor like kinases.

Aims and Questions

The overall goal of the project was originally to find and describe physiological functions of *At*FLOTs and *At*HIRs in *A. thaliana*. As HIR roles in plant-pathogen interactions are well documented not only in Arabidopsis, we later focused mainly on *At*FLOTs. For that purpose, we chose three experimental approaches corresponding with three major questions:

(i) **What are the physiological cues in which *At*FLOTs and *At*HIRs are involved?**

To address this questions we performed a battery of phenotyping assays using the loss-of-function T-DNA insertion mutant. Treatments were selected in line with the data obtained from Genevestigator where an increase was indicated for *AtFLOT*s and *AtHIR*s expression.

(Paper # 2)

(ii) **What are the protein interacting with *At*FLOTs?**

We supposed that the interactome of a protein could suggest its functions based on the known roles of the interactors. We decided to assess the interactome of *At*FLOT2 as only little was published about this protein.

(Paper # 3)

(iii) **Which are the localization characteristics of *At*FLOT and *At*HIR single isoforms? Are there differences between individual isoforms? Which factors determine the protein localization or dynamics?**

We observed stable lines expressing fluorescently tagged isoforms of *At*FLOTs and *At*HIRs. We assume that the cues that would provoke changes in a given protein mobility or localization pattern could point us to the direction of its function.

(Paper – manuscript # 4)

Results

The obtained results are presented in form of two published papers and one submitted manuscript. The order and topic of the papers corresponds with the three areas of the study mentioned in Aims and Questions. In the Paper # 2 we report our results gained in the transcription analysis of *AtFLOT*s under different stimuli and in phenotypic screen of single loss-of-function mutants of *AtFLOT*s under several treatments. In the Paper # 3 we attempted to determine protein interactors of *At*FLOT2 by co-immunoprecipitation followed by mass-spectrometry analysis and verification of the direct interactions using split-ubiquitin system. We hoped that the revealed putative protein partners could help us find *At*FLOT2 function. Finally, in the manuscript of Paper # 3 we focused on the whole group of *At*FLOTs and *At*HIRs from the point of their behaviour in the cell. For that we used several approached of confocal observation of single isoforms tagged with fluorescent proteins.

Paper # 2

Title: Characterisation of *Arabidopsis* flotillins in response to stresses

Authors: Kristýna Kroumanová, Daniela Kocourková, Michal Daněk, Lucie Lamparová, Romana Pospíchalová, Kateřina Malínská, Zuzana Krčková, Lenka Burketová, Olga Valentová, Jan Martinec, Martin Janda

Summary: Plant flotillins, a subgroup of the SPFH domain protein superfamily, consist of three proteins, *At*FLOT1, *At*FLOT2, and *At*FLOT3 in *Arabidopsis thaliana*. The exact functions of flotillins in plant cell has not been established yet. In this study we focused on the role of flotillins in response to both abiotic and biotic stresses and on the response to phytohormones abscisic acid and 1-naphthalene acetic acid (NAA) in *A. thaliana*. We observed transcriptomic changes of *AtFLOT* genes in response to high salinity and cold, treatment with 22-amino acid peptide from N-terminal part of flagellin (flg22), and after infection with Botrytis cinerea. Transcription of *AtFLOT2* increased up to 60 times after flg22 treatment. Also, treatment with *B. cinerea* increased transcription of *AtFLOT1* 10 times and of *AtFLOT3* 14 times. Furthermore, we used T-DNA knock-out single mutants for all three *A. thaliana* flotillins and we measured root growth in response to high salinity, cold, phosphate starvation, nitrogen starvation, and abscisic acid and NAA treatments. Subsequently, we measured the reactive oxygen species production and callose accumulation after the treatment with flg22. Next, we performed resistance assays to *Pseudomonas syringae* pv. tomato DC3000 and *B. cinerea*. In contrast to transcriptomic changes, knocking-out of only single FLOT gene did not lead to significant changes in response to all tested stresses.

DOI: 10.32615/bp.2019.017

Citation: KROUMANOVÁ, K., KOCOURKOVÁ, D., DANĚK, M., LAMPAROVÁ, L., POSPÍCHALOVÁ, R., MALÍNSKÁ, K., KRČKOVÁ, Z., BURKETOVÁ, L., VALENTOVÁ, O., MARTINEC, J. & JANDA, M. 2019. Characterisation of Arabidopsis flotillins in response to stresses. Biologia plantarum, 63, 144-152.

My contribution: I collected the T-DNA insertion lines and isolated homozygotes. I performed the selection of treatments based on the analysis of expression of the single isoforms in Genevestigator. I carried out the initial set of experiments which were further developed and continued by the co-authors. I took part in writing the manuscript.

DOI: 10.32615/bp.2019.017 BIOLOGIA PLANTARUM 63: 144-152, 2019

Characterisation of *Arabidopsis* flotillins in response to stresses

K. KROUMANOVÁ[1], D. KOCOURKOVÁ[1], M. DANĚK[1,2], L. LAMPAROVÁ[1,3], R. POSPÍCHALOVÁ[1], K. MALÍNSKÁ[1], Z. KRČKOVÁ[1], L. BURKETOVÁ[1], O. VALENTOVÁ[3], J. MARTINEC[1], and M. JANDA[1,3]*

Institute of Experimental Botany of the Czech Academy of Sciences, CZ-16502, Prague, Czech Republic[1]
Department of Experimental Plant Biology, Faculty of Science, Charles University, CZ-12844 Prague, Czech Republic[2]
Department of Biochemistry and Microbiology, University of Chemistry and Technology, Prague, CZ-16628 Prague, Czech Republic[3]

Abstract

Plant flotillins, a subgroup of the SPFH domain protein superfamily, consist of three proteins, *At*FLOT1, *At*FLOT2, and *At*FLOT3 in *Arabidopsis thaliana*. The exact functions of flotillins in plant cell has not been established yet. In this study we focused on the role of flotillins in response to both abiotic and biotic stresses and on the response to phytohormones abscisic acid and 1-naphthalene acetic acid (NAA) in *A. thaliana*. We observed transcriptomic changes of *AtFLOT* genes in response to high salinity and cold, treatment with 22-amino acid peptide from N-terminal part of flagellin (flg22), and after infection with *Botrytis cinerea*. Transcription of *AtFLOT2* increased up to 60 times after flg22 treatment. Also, treatment with *B. cinerea* increased transcription of *AtFLOT1* 10 times and of *AtFLOT3* 14 times. Furthermore, we used T-DNA knock-out single mutants for all three *A. thaliana* flotillins and we measured root growth in response to high salinity, cold, phosphate starvation, nitrogen starvation, and abscisic acid and NAA treatments. Subsequently, we measured the reactive oxygen species production and callose accumulation after the treatment with flg22. Next, we performed resistance assays to *Pseudomonas syringae* pv. *tomato* DC3000 and *B. cinerea*. In contrast to transcriptomic changes, knocking-out of only single *FLOT* gene did not lead to significant changes in response to all tested stresses.

Additional key words: abscisic acid, auxin, *Botrytis cinerea*, callose, cold, nutrient starvation, *Pseudomonas syringae*, ROS, salinity.

Introduction

Plants evolved sophisticated, efficient, and complex responses to both biotic and abiotic stresses. Plasma membrane (PM) serves as a highly exposed platform for responses to stress factors. Receptors responsible for recognition of threats are often present on PM (Ott 2017). Within PM, the crucial role has its compartmentalization to macro, micro, and nanodomains (Sekeres *et al.* 2015). It was shown that membrane microdomains are important for membrane trafficking, signal transduction, and response to pathogen attack (Lefebvre *et al.* 2007, Liu *et al.* 2009, Wang *et al.* 2015, Bucherl *et al.* 2017).

Plant flotillins along with prohibitins (PHB) belong to the stomatin/prohibitin/flotillin/HflK/C (SPFH) domain (also known as Band_7 domain) protein superfamily. Comparative genome analysis of this superfamily reveals deep evolutionary origin and diverse gene functions (Di *et al.* 2010). Flotillins are associated with membrane microdomains and are commonly used as markers of membrane microdomains in both mammalian and plant cells. Flotillins occur not only on the PM but also were

Submitted 10 May 2018, *last revision* 26 June 2018, *accepted* 30 June 2018.
Abbreviations:ABA - abscisic acid, Col-0 - Columbia-0, dpi - days post inoculation, elf18 - acetylated 18-amino acid fragment from N-terminal of elongation factor Tu (acetyl-MSKEKFERTKPHVNVGT), flg22 - 22-amino acid peptide from N-terminal part of flagellin (QRLSTGSRINSAKDDAAGLQIA), FLS2 - flagellin-sensitive 2, FLOT - flotillin, hpi - hours post inoculation, JA - jasmonic acid, MAMP - microbe-associated molecular pattern, MS - Murashige and Skoog, NAA - 1-naphthalene acetic acid, PM - plasma membrane, *Pst* - *Pseudomonas syringae* pv. *tomato* strain DC3000, ROS - reactive oxygen species, SA - salicylic acid, Ws-4 - Wassilievska-4, WT - wild-type.
Acknowledgments: This research was supported by the Czech Science Foundation (grant No. 14-09685S) and by the Ministry of Education, Youth, and Sport of the Czech Republic (MSMT No 21-SVV/2017).
* Author of correspondence; e-mail: martin.janda@vscht.cz

detected in endosomes (Glebov *et al.* 2006, Haney *et al.* 2010, Li *et al.* 2012, Jarsch *et al.* 2014, Yu *et al.* 2017). Three members of flotillin protein family were identified in *A. thaliana*, *At*FLOT1 (At5g25250), *At*FLOT2 (At5g52560), and *At*FLOT3 (At5g64870). It should be noted that in some literature the *At*FLOT1 and *At*FLOT2 are affiliated as *At*FLOT1a and *At*FLOT1b, respectively (Jarsch *et al.* 2014). Yu *et al.* (2017) showed that *At*FLOT1 and *At*FLOT2 share 94 % similarity of amino acid sequence and *At*FLOT1 share 85 % similarity with *At*FLOT3.

Flotillin functions were broadly studied and described in yeasts and mammals; while the proper role of flotillins in plants is still very barely understood. In plants flotillins were shown to play important role in plant-microbe interaction. In *Medicago truncatula,* seven genes encoding flotillin-like proteins were identified (Haney *et al.* 2010). From those *MtFLOT2* and *MtFLOT4* were significantly upregulated during early symbiotic events and play crucial role in establishing the relationship between *M. truncatula* and symbiotic nitrogen-fixing rhizobium *Sinorhizobium meliloti*. Additionally, co-localization of *Mt*FLOT4-mCherry with lysin motif receptor-like kinase 3 (LYK3) was observed in inoculated roots (Haney *et al.* 2010). Yu *et al.* (2017) showed that treatment of plants with flg22 leads to the increased degradation of *At*FLOT1. Moreover, accumulation of callose decreased in *Atflot1* amiRNAi plants in response to flg22 (Yu *et al.* 2017). By contrast, to our best knowledge, no data are available for the role of flotillins in plant responses to abiotic stresses. *In sillico* transcription analysis performed using *Genevestigator*®. It was shown that gene transcription of *AtFLOT*s is increased under various abiotic and biotic stresses (Daněk *et al.* 2016).

The present study was focused on the role of *At*FLOTs in response to following treatments: high salinity, cold, nitrogen and phosphate starvation, abscisic acid (ABA), 1-naphthalene acetic acid (NAA), *Pseudomonas syringae* (*Pst*) and *Botrytis cinerea* infection, and elicitors flg22 or elf18. We analysed transcription of *AtFLOTs* in WT plants together with knock-out T-DNA single mutants of flotillin genes.

Materials and methods

Plants and cultivation: In this study we used *Arabidopsis thaliana* wild type (WT) genotypes: Columbia-0 (Col-0) and Wassilievska-4 (Ws-4) and mutants *Atflot1* (SALK_203966C) and *Atflot3* (SALK_143325C) with Col-0 background, and *Atflot2* (FLAG_352D08) with Ws-4 background.

Surface-sterilized seeds were sown in *Jiffy 7* peat pellets and plants were grown for four weeks in soil, under a 10-h photoperiod, an irradiance of 90 - 120 µmol m^{-2} s^{-1}, a temperature of 22 °C and a 70 % relative humidity. They were watered with distilled water as necessary. Plants grown in these conditions were used for reactive oxygen species (ROS) determination and *Pst* DC3000 and *Botrytis cinerea* treatments.

Further, *A. thaliana* seedlings were grown in liquid Murashige and Skoog (MS) medium or on solid ½ MS medium. The liquid MS medium contained 4.41 g dm^{-3} MS vitamins (*Duchefa*, Haarlem, The Netherlands), 5 g dm^{-3} sucrose, and 5 g dm^{-3} (N-morpholino) ethanesulfonic acid (MES) monohydrate (*Duchefa*). The solid ½ MS medium contained 2.2 g dm^{-3} MS basal salts (*Duchefa*) and 10 g dm^{-3} agar (*Sigma-Aldrich,* St. Louis, USA). Both media were adjusted to pH 5.8 using 1 M KOH. For cultivation in the liquid, surface-sterilized seeds were sown in 24-well plates containing 0.4 cm^3 of liquid MS medium per well and 3 - 5 seeds. Plants were cultivated for 11 d under a 10-h photoperiod, an irradiance of 100 - 130 µmol m^{-2} s^{-1} and a temperature of 22 °C. On the 7th day, the medium in the wells was exchanged for a fresh one. Seedlings from liquid media were used for callose analysis.

For the root length analysis, the seedlings were grown on solid medium in square plates (12 cm side). The plates with seeds were placed to 4 °C for 48 h. Then, the seedlings were grown under a 16-h photoperiod, an irradiance of 100 µmol m^{-2} s^{-1}, and a temperature of 22 °C. At 5th day, seedlings of similar size were transferred to new plates and the length of root was marked. Experiments were designed so that WT seedlings and the particular mutant line were on the same plate. In one biological replicate 20 seedlings for WT and 17 - 20 seedlings for particular mutant line were used. At 7th day after transfer, the root length increase was marked. For the 1-naphthalene acetic acid (NAA) treatment, seedlings of similar size were transferred to new plates at 4th day and at 4th day after transfer, the root length increase was marked. The experiments were performed in three biological repeats.

Transcriptomic analysis: For transcriptomic analysis, seedlings were grown on solid ½ MS media in round plates (6 cm in diameter) lying horizontally in a 16-h photoperiod, an irradiance of 100 µmol m^{-2} s^{-1}, and a temperature of 22 °C. The seedlings (10 - 12 from each plate) were harvested at day 11 and the tissue was stored in liquid nitrogen. For one biological replicate 3 - 4 independent samples were used.

Total RNA was isolated from frozen plant tissue using the *Spectrum Plant Total* RNA kit (*Sigma-Aldrich*) and treated with a DNA-free kit (*Ambion*, Austin, TX, USA). Then 1 µg of RNA was used for reverse transcription to cDNA with *M-MLV RNase H⁻Point Mutant* reverse transcriptase (*Promega*, Fitchburg, WI, USA) and anchored oligo dT21 primer (*Metabion*, Martinsried, Germany). Gene transcription was quantified by q-PCR

using *LightCycler 480 SYBR Green I Master* kit and *LightCycler 480* (*Roche*, Basel, Switzerland). The PCR conditions were: 95 °C for 10 min, followed by 45 cycles of 95 °C for 10 s, 55 °C for 20 s, and 72 °C for 20 s, followed by a melting curve analysis. Relative transcription was calculated with normalization to the housekeeping gene *TIP41-like (At4g34270)*. The list of primers is in Table 1 Suppl.

Abiotic stresses: Under following abiotic stress conditions root length was measured. Seedlings were scanned at day 7 after transfer. Root length was analysed using software *JMicroVision*®. In selected cases transcription of *AtFLOT* genes was analysed as well.

For high salinity, the seedlings were grown on ½ MS solid medium containing 100 mM NaCl. For gene transcription analysis 11-d-old seedlings were flooded with 150 mM NaCl dissolved in liquid ½ MS medium for 3 h. As a control seedlings were flooded with ½ MS liquid medium.

For cold treatment, the seedlings were grown on ½ MS solid medium at 14 °C and control seedlings at 22 °C. For gene transcription analysis, 11-d-old seedlings were treated for 3 h by cultivation at 6 °C in darkness. Control seedlings were put into darkness for 3 h at 22 °C.

For phosphate starvation experiment, the control seedlings were grown on modified half-strength Hoagland's medium (Hoagland *et al.* 1950) with 1 % agar and the treated seedlings were grown on half-strength Hoagland's medium in which $NH_4H_2PO_4$ was replaced with NH_4Cl. The medium was adjusted to pH 6.2 with NaOH.

For nitrogen starvation experiment, the control seedlings were grown on medium containing 1 mM KH_2PO_4, 25 µM H_3BO_3, 2 µM $ZnSO_4$, 2 µM $MnSO_4$, 0.5 mM $MgSO_4$, 20 µM ferric citrate, 0.5 µM $CuSO_4$, 0.5 µM Na_2MoO_4, 1 mM NH_4NO_3, 0.25 mM CaSO4, and 1 % agar and the treated seedlings on the medium without NH_4NO_3.

Biotic stresses: The inoculation with *Pseudomonas syringae* pv. *tomato* DC3000 (*Pst* DC3000) was performed according to Katagiri *et al.* (2002) with slight modifications. In brief, bacteria were cultivated on the Luria-Bertani (LB) solid medium (with 1.2 %, m/v, agar) containing rifampicin (50 g dm^{-3}) overnight. Bacteria were resuspended in 10 mM $MgCl_2$ and a suspension was prepared to absorbance (A_{600}) = 0.001 for infiltration and A_{600} = 0.2 for dipping. For dipping inoculation suspension contained *Silwet Star* (0.02 %, v/v, *AgroBio*, Opava, Czech Republic). Four-week-old plants were infiltrated with needleless syringe or dipped for 30 s in bacterial suspension. Nine discs (6 mm diameter) from three plants were collected as one sample of one genotype at 0 dpi and 3 dpi. The leaf discs were grounded in 10 mM $MgCl_2$ and decimal dilution was performed. The colony forming units were counted. For gene transcription analysis, 4-week-old plants were infiltrated (using needleless syringe) with *Pst* DC3000 for 24 h, control plants were treated with 10 mM $MgCl_2$.

Four-week-old *A. thaliana* plants were treated with a 6-mm^3 drops containing *Botrytis cinerea BMM* spores (5×10^4 spores cm^{-3}) by applying one drop on one leaf, three leaves at similar developmental stage from one plant. The treated plants were transferred into the closed plastic box and were kept at low irradiance of 10 - 20 µmol m^{-2} s^{-1}), a 16-h photoperiod and a temperature of 21 °C for 96 h post inoculation (hpi). For gene transcription analysis, 4-week-old plants were treated with *Botrytis cinerea* BMM spores (5.10^4 spores cm^{-3}) diluted in potato dextrose broth (PDB) liquid medium for 48 h, control plants were treated with a drop of four times diluted PDB liquid medium.

Measurement of H_2O_2 production: H_2O_2 production was determined by the luminol-based assay as described in (Sasek *et al.* 2014). Discs, 3 mm in diameter, were cut from the fully developed leaves (two discs per leaf) of 4-week-old *A. thaliana* plants (three leaves per plant). Discs were incubated in white non-transparent 96-well plate (*NUNC*, *Thermo Fisher Scientific*, Waltham, MA, USA) in 0.15 cm^3 of distilled water for 16 h. Distilled water was replaced by 0.2 cm^3 of reaction solution containing 17 µg cm^{-3} of luminol, 10 µg cm^{-3} of horseradish peroxidase (*Sigma-Aldrich*) and 100 nM flg22 or 100 nM elf18. The measurement was performed immediately after adding the flg22 with a luminometer (*Tecan infinite F200*, Männedorf, Switzerland) for a period of 45 min.

Callose deposition in response to flg22: *A. thaliana* seedlings were treated with 1 µM flg22 for 24 h at day 11, the MS medium was replaced with fresh one with or without flg22. After 24 h the MS medium was replaced with ethanol:glacial acetic acid (3:1, v/v) until the seedlings were decolorized. The seedlings were then rehydrated in successive baths of 70 % ethanol (at least 1 h), 50 % ethanol (at least 1 h), 30 % ethanol (at least 1 h), and water (at least 2 h). Leaves were then incubated in 0.01 % (m/v) aniline blue in 150 mM K_2HPO_4, pH 9.5, for 4 - 6 h. Callose deposition was observed using fluorescence microscope *AxioImager ApoTome2* (*Carl Zeiss*, Oberkochen, Germany) and the number of callose spots per mm^2 were calculated using *Fiji* software (Schindelin *et al.* 2012). For gene transcription analysis, four-week-old *A. thaliana* plants were treated with 100 nM flg22 applied by needleless syringe infiltration for 1 and 4 h. Infiltration with distilled water was used as a control.

Treatments with phytohormones: The seedlings were grown on ½ MS medium containing 2 µM ABA dissolved in EtOH (0.01 %) and 1 % agar, control seedlings grew on ½ MS medium containing only EtOH. Medium was adjusted to pH 5.8 with KOH. Root length was analysed using software *JMicroVision*®. For gene transcription

analysis seedlings at day 11 were flooded with 100 µM ABA in liquid ½ MS medium for 3 h as a control seedlings were flooded with 0.1 % EtOH in liquid ½ MS medium.

The 4-d-old seedlings grown on ½ MS were transferred on ½ MS medium containing 200 nM NAA and length of the root was marked on the plate. The seedlings were scanned at day 4 after transfer and the length of primary root was measured using software *Fiji* (Schindelin *et al.* 2012).

Statistical analysis: If not mentioned otherwise, two-tailed Student's *t*-test was used for statistical evaluation and statistical significance was assigned to difference with *P* values < 0.01.

Results

Transcriptions of all three flotillin genes in 11-d-old *A. thaliana* seedlings exposed to NaCl, cold, ABA, infection, and flg22 treatments were analysed. Flooding seedlings with 150 mM NaCl for 3 h significantly down regulated the transcription of *AtFLOT1* and *AtFLOT2* genes (Fig. 1*A*). Exposure of seedlings to 6 °C for 3 h increased the transcription of *AtFLOT3* gene (Fig. 1*B*). After infiltration of 4-week-old *A. thaliana* with 100 nM flg22, transcriptions of all *AtFLOT* genes increased 1 and 4 h after treatment (Fig. 1*C*) with strongly increased expressions of *AtFLOT1* and *AtFLOT3*. Upregulation of *AtFLOT3* was transient and after 4 h after returned to the basal level. The transcription of *AtFLOT1* and *AtFLOT2* genes further increased at 4 h after flg22 treatment (Fig. 1*C*). Interestingly, bacterial infection of plants with *Pst* DC3000 did not lead to the changes in transcription of *AtFLOT* genes (Fig. 1*D*), whereas infection with fungus *B. cinerea* induced transcription of *AtFLOT1* and *AtFLOT3* (Fig. 1*E*). Treatment with ABA altered the transription of all three *AtFLOTs*, however, the changes were not significant due to high variability of obtained data (Fig. 1*F*). Overall, transcription of at least one *AtFLOT* gene was significantly changed under 4 from 6 tested stress factors which strongly suggests involvement of *AtFLOTs* in response to stresses.

Following transcriptomic analysis, T-DNA knock-out single mutants available from public seeds depositories for each flotillin gene were used for phenotype analysis. These mutants do not transcribe particular *AtFLOT* genes (Fig. 1 Suppl.). We measured root growth of WT and mutant plants exposed to high salinity (100 mM NaCl; Fig. 2*A*), cold (14 °C; Fig. 2*B*), and phosphate (Fig. 2*C*) and nitrogen starvation (Fig. 2*D*). Seedlings were exposed to these stresses for 7 d. In contrast to transcriptomic analysis, comparison of flotillin mutant lines with their background genotype did not reveal any significant changes in root length and other noticeable morphological changes. These results indicate that any of single *AtFLOT* gene does not play particular role in acclimation to all tested abiotic stresses.

Furthermore, we focused on the role of the single flotillin gene in response to biotic stresses. Transcriptional analysis showed changes of *AtFLOT* gene expression in response to flg22 and *B. cinerea* (Fig. 1*C*,*E*). We measured H_2O_2 production upon microbe-associated molecular patterns (MAMP) treatment (Fig. 3*A*) since ROS burst is well described immediate and massive response to MAMPs (Smith *et al.* 2014). For *Atflot1* and *Atflot3* mutants we used flg22 as MAMP. Because *Atflot2* mutant has a genetic background Ws-4 which lacks the flagellin-

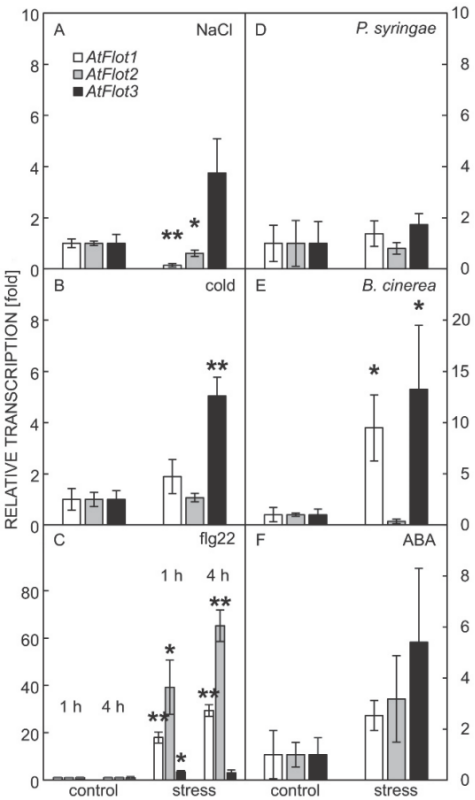

Fig. 1. Transcription analysis of *AtFLOT* genes in response to different stresses. *Arabidopsis thaliana* seedlings were treated at day 11 with 150 mM NaCl for 3 h (*A*), 6 °C for 3 h (*B*), 100 nM flg22 for 1 and 4 h (*C*), infiltration with *Pst* DC3000 for 24 h (*D*), inoculation with *Botrytis cinerea* BMM spores for 48 h (*E*), and 100 µM ABA for 3 h (*F*). Means ± SE, *n* = 3 to 4, *asterisks* indicate statistically significant differences compared to the corresponding control (* - P < 0.05, ** - P < 0.01, Student's *t*-test). Transcription was normalized to a reference gene *TIP41-like*.

sensitive 2 (FLS2) receptor for flg22 (Zipfel *et al.* 2004), we used elf18 (Lu *et al.* 2009). However, none of the mutants had affected ROS production in response to MAMPs (Fig. 3A). Furthermore we tested the resistance of *A. thaliana* WT and mutant plants toward the infection with *Pst* DC3000, which represent model pathosystem in the studies of plant-bacteria interactions (Xin *et al.* 2018).

Here we used two different experimental approaches: infiltration with needleless syringe (Fig. 3*B*) and flooding of plant rosettes in bacterial suspension (Fig. 2 Suppl.). In both setups, no differences in the number of bacteria were found in the mutant line in comparison to the controls. Not surprisingly, the genotypes with Ws-4 background were more susceptible to *Pst* DC3000 compared to Col-0 background genotypes (Figs. 3 and 2 Suppl.). As the *AtFLOT1* and *AtFLOT3* transcription was induced in response to *B. cinerea,* we tested if these mutants would have altered resistance to this necrotrophic fungus. However, we did not see any significant difference between infected mutant and control lines (Fig. 3*C*). Moreover, Ws-4 genotypes were more resistant to the infection in comparison with Col-0 genotypes (Fig. 3*C*).

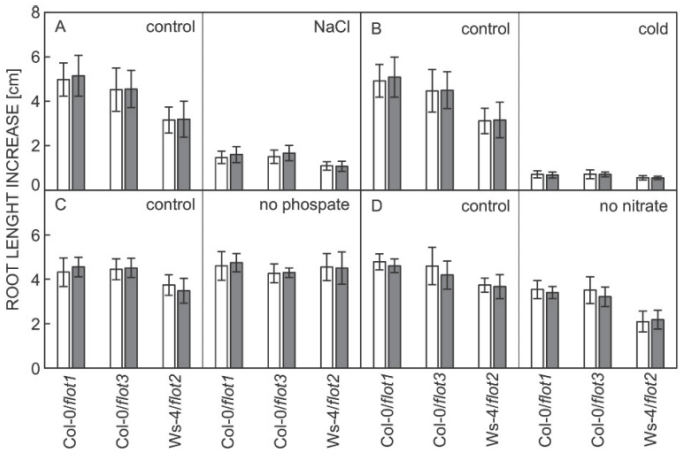

Fig. 2. Response of flotillin T-DNA *A. thaliana* mutants to abiotic stresses. Root growth of 12-d-old seedlings on the medium containing 100 mM NaCl for last 7 d (*A*). Root growth of 12-d-old seedlings 14 °C for last 7 d (*B*). Root growth of 12-d-old seedlings on the medium without phosphate for last 7 d (*C*). Root growth of 12-d-old seedlings medium without nitrogen for last 7 d (*D*). *White bars* represent WT, *grey bars* represent *Atflot* mutant. Means ± SDs, n = 17 to 20 ($P < 0.01$, Student's t-test)

Yu *et al.* (2017) showed decreased callose accumulation in response to flg22 in seedlings of their *Atflot1* knock-down mutant. Therefore, we measured callose accumulation in our *Atflot1* knock-out mutant, but we did not see the difference compared to the control line (Fig. 3*D*). Despite the transcriptional changes in response to biotic stress, we did not reveal the crucial role of particular *AtFLOT* gene under biotic stress conditions tested.

In sillico transcriptomic analysis showed transcriptional changes of *AtFLOT* genes in response to phytohormones ABA and auxin (Daněk *et al.* 2016). Although our transcription analysis after treatment with ABA did not confirm microarray data, we performed the root growth assays with seedlings of all three knock-out mutants where we measured the root growth in presence of 100 µM ABA or 200 nM NAA. The root growth of *Atflot* mutants was similar to control lines (Fig. 4*A*,*B*).

Discussion

In our work we focused on the possible role of flotillins in response to different type of stresses in *A. thaliana*. The available transcriptomic microarray data indicated a possible involvement in response to abiotic and biotic stresses (Daněk *et al*. 2016). In terms of abiotic stress, here we show that transcription of *AtFLOT* genes is altered in early response (after 3 h) to high salinity leading to the inhibition of *AtFLOT1* and *AtFLOT2* (Fig. 1*A*) and exposure to cold leading to the induction of *AtFLOT3* transcription (Fig. 1*B*). In the case of biotic stress, the transcriptional changes were more robust compared to changes under abiotic stresses. In four-week-old *A. thaliana* the transcription of *AtFLOT1* and *AtFLOT2* was increased in response to flg22 (Fig. 1*C*) and transcription of *AtFLOT1* and *AtFLOT3* was increased in response to the infection by *B. cinerea* (Fig. 1*E*). The transcription profile upon *B. cinerea* treatment is interesting because under other tested conditions (high

salinity, cold, flg22), mainly *AtFLOT1* and *AtFLOT2* share similar transcriptional pattern. This is not surprising with respect to the fact that they share 94 % sequence similarity and therefore they may function similarly as well. However, in response to *B. cinerea*, the transcription of *AtFLOT1* and *AtFLOT3* was induced as opposed to the transcription of *AtFLOT2* which remained stable (Fig. 1*E*). Hence, our results imply functional redundancy of *At*FLOT1 and *At*FLOT2 but only in some cases. Results from our transcriptomic analysis do not correspond in all cases with publicly available microarray data. *Pst* DC3000 infection did not affect transcription (Fig. 1*D*) and treatment with ABA did not show significant transcription changes due to very high variability of measurements (Fig. 1*F*). NaCl treatment had the opposite effect than it was revealed with microarray experiments, inhibition of transcription (Fig. 1*A*). However cold stress, flg22 treatment, and *B. cinerea* infection had similar effect on the *AtFLOTs* transcription as was found in database (Daněk *et al.* 2016). These discrepancies may be explained by slightly different conditions used in particular experiments. It must be noted as well that set up of microarray experiments does not allow discrimination between expressions of *AtFLOT1* and *AtFLOT2*.

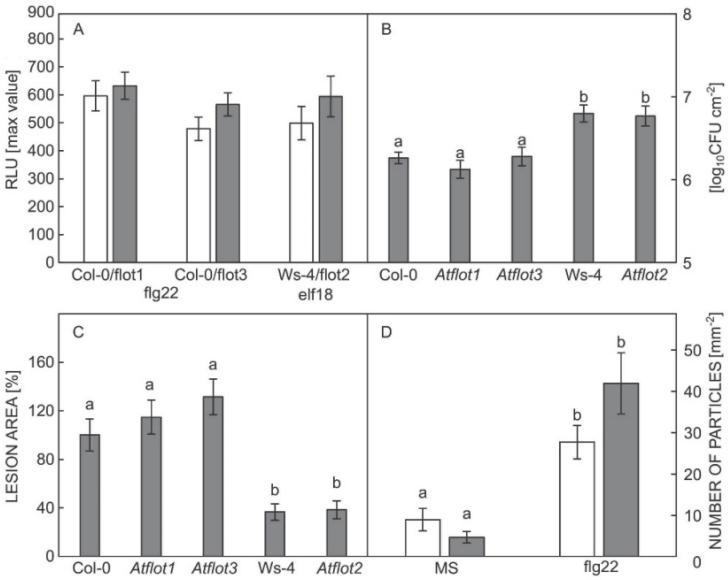

Fig. 3. Response of flotillin T-DNA *A. thaliana* mutants to biotic stresses. *A* - Maximum luminescence induced by 100 nM flg22 for *Atflot1* and *Atflot3* or 100 nM elf18 for *Atflot2* in leaf discs from 4-week-old plants (RLU - relative luminiscence unit). *B* - *Pst* DC3000 was infiltrated into leaves of 4-week-old plants. Values are demonstrated in $\log_{10}$ scale of colony forming units (CFU). *C* - Lesions on 4-week-old *A. thaliana* leaves infected with *Botrytis cinerea BMM* for 96 h. *D* - Callose deposition in 10-d-old seedlings of *A. thaliana* treated with 1 µM flg22 for 24 h (MS - control). In *A* and *D*, white bars represent WT, *grey bars* represent *Atflot* mutant. Means ± SEs, $n = 12$ for *A*,*C* and 6 for *B*,*D*). Different letters indicate significant differences between the samples ($P < 0.01$, Student's *t*-test).

The second goal of the work was to investigate direct involvement of a particular *AtFLOT* gene in response to stresses. For that purpose, we used T-DNA knock-out mutants for every single *AtFLOT* gene. The proper characterisation of the mutants is the critical point. Li *et al.* (2012) showed that some of *AtFLOT1* T-DNA insertion mutant lines had similar *AtFLOT1* expression as WT or even over-expression. Here we used different T-DNA line of *Atflot1* than Li *et al.* (2012) and also T-DNA mutants of *Atflot2* and *Atflot3* (Fig. 1 Suppl.). Obtained T-DNA lines did not show any transcription of particular *AtFLOT* genes (Fig. 1 Suppl.). We used above mentioned mutants for the phenotypic analysis in response to abiotic and biotic stress and for the treatment with phytohormones ABA and NAA.

According to best of our knowledge, no screening study of the involvement of flotillins in abiotic stresses exists until now. *In silico AtFLOTs* transcriptional data, as well as our results, indicated involvement of flotillins in response to abiotic stresses. Moreover, in yeasts and mammals flotillins play a role in endocytosis (Otto *et al.* 2011). Similar role was suggested for *AtFLOT1*. In specific conditions, it was shown that endocytosis of several plasma membrane (PM) proteins such as NADPH/respiratory burst oxidase protein D (RbohD), plasma membrane intrinsic protein 2 (PIP2;1), brassinosteroid insensitive 1 (BRI1) and ammonium transporter 1 (AMT1-3) is mainly dependent on clathrin mediated endocytosis but the role of microdomains and

AtFLOT1 cannot be excluded (Hao *et al.* 2014, Li *et al.* 2012, Liu *et al.* 2009, Wang *et al.* 2013, Yu *et al.* 2017). The role of endocytosis in abiotic stresses was described as well. For example, salt stress increases PM endocytosis (Hamaji *et al.* 2009, Leshem *et al.* 2006) and cold stress inhibits intracellular trafficking (Shibasaki *et al.* 2009). We tested the root growth of mutant and WT plants under high salinity, cold, nitrogen starvation, and phosphate starvation. No differences between mutant and WT root growth under tested abiotic stresses were observed (Fig. 2). One of the possible explanations of this observation is gene redundancy of *A. thaliana* flotillins. This explanation is supported with our results and with results of Li *et al.* (2012) (for details see below) and it is reasonable especially in the case of *AtFLOT1* and *AtFLOT2*. To reveal the role of redundant genes it is necessary to prepare the multiple *Atflot* knock-out mutant lines. CRISPR-Cas9 methodology would be a method of choice because *AtFLOT1* and *AtFLOT2* are in linkage and therefore it is not possible to obtain double mutant by crossing. Also, another experimental design should be considered.

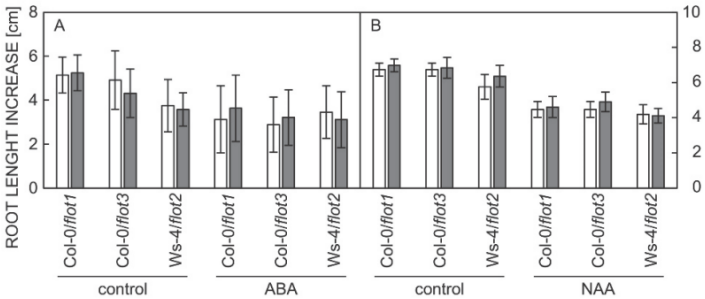

Fig. 4. Response of flotillin T-DNA *A. thaliana* mutants to phytohormones. *A* - The root growth of 12-d-old seedlings on the medium containing 2 µM ABA for last 7 d. *B* - The root growth of 8-d-old seedlings on the media containing 200 nM NAA for last 4 d. *White bars* represent WT, *grey bars* represent *Atflot* mutant. Means ± SD, *n* = 11 to 30.

In contrast to abiotic stresses, data showing the involvement of flotillins in biotic stresses already exist. The critical role of flotillins was shown in *Medicago truncatula* in response to symbiotic rhizobial infection. In *M. truncatula* seven flotillin-genes are recognised. Using silenced mutants in *MtFLOT2* and *MtFLOT4* it was approved that they are required for host derived infection threads and nodule formation (Haney *et al.* 2010). We tested T-DNA *Atflot* lines in response to *Pst* DC3000 and *B. cinerea*. However, we did not observe any difference between WT and T-DNA lines after *Pst* DC3000 and *B. cinerea* infection. The only differences we observed between the background genotypes Col-0 and Ws-4. Plants with Col-0 background were more resistant against *Pst* DC3000 and interestingly, more susceptible to *B. cinerea* in comparison to plants with Ws-4 background (Fig. 3*B*,*C*). However, a molecular background of this phenomenon is not known.

Upregulation of *AtFLOT* gene transcription after flg22 treatment was shown (Daněk *et al.* 2016, Millet *et al.* 2010). In agreement, we observed increased transcription of *AtFLOT* genes after treatment with flg22. It is known that flg22 treatment results in higher ROS production and callose deposition (Denoux *et al.* 2008). We studied transient ROS production in response to treatment with flg22 in our T-DNA mutant lines and we did not observe any difference between flotillin knock-out mutant and WT plants (unpublished results). Also, we studied callose deposition in our T-DNA mutant lines and we did not observe any difference between flotillin knock-out mutant and WT plants. In contrary, Yu *et al.* (2017) showed that knock-down mutant of *Atflot1* has decreased callose deposition in response to flg22. This contradiction may be explained by the downregulation of transcription of both *AtFLOT1* and *AtFLOT2*. Yu *et al.* (2017) used in their study amiRNAi lines. The same lines were used by Li *et al.* (2012). Besides down-regulation of *AtFLOT1,* three from their four amiRNAi lines exhibited also down-regulation of *AtFLOT2* (Li *et al.* 2012). Li *et al.* (2012) also described growth inhibition of *AmiRNAflot1* line, however, we did not observe root growth retardation of our T-DNA *AtFLOT1* line. These indicate that for observed decrease in callose deposition in response to flg22 and also the growth inhibition, both *AtFLOT1* and *AtFLOT2* are responsible.

Phytohormones play indispensable roles in plant growth and development and in response to both biotic and abiotic stresses (Santner *et al.* 2009, Denance *et al.* 2013, Janda and Ruelland 2015). Based on available transcriptomic data we were focused on the role of flotillins in response to ABA and NAA treatments. As for the biotic and abiotic stresses the role of endocytosis and microdomains in ABA and auxin mediated events are demonstrated. For example, auxin transporter PIN1 is present in microdomains (Titapiwatanakun *et al.* 2009) and polar distribution of auxin transporters is dependent on clathrin mediated endocytosis (Kitakura *et al.* 2011). ABA triggers the selective endocytosis of *A. thaliana* potassium

channel KAT1 and its recycling to the PM in epidermal and guard cells (Sutter *et al.* 2007). As for the response to abiotic stress we analysed the effect of ABA and NAA to the root growth of *Atflot* T-DNA mutant lines. However, we did not observe any difference between T-DNA flotillin mutants and WT plants (Fig. 4).

We are aware that interpretation of the data obtained by the application of just one T-DNA mutated allele might be risky. Re-evaluation of function of *abp1-1* mutant could serve as an example of such situation (Dai *et al*. 2015, Enders *et al*. 2015, Michalko *et al*. 2015). Also the recent controversy dealing with commonly used *Syngenta Arabidopsis* insertion lines (SAIL) seeds stock with *qrt1* background serves as highly important warning (Nikoronova *et al.* 2018). However, we believe that our results are not misinterpreted. In our study we did not use seeds from SAIL stock. Moreover, unlike in the above mentioned studies, we do not show an effect of T-DNA insertion into flotillin genes and therefore it is not necessary to consider additional T-DNA insertions.

In conclusion our transcriptomic analyses showed altered transcription of *AtFLOT* genes in response to both biotic and abiotic stresses. We obtained set of T-DNA single mutants which do not transcribe particular *AtFLOT* genes and we used them to screen involvement of single flotillin genes in response to broad spectrum of stresses. Our data showed that single flotillin genes are not the crucial components of *A. thaliana* response reactions to all stress conditions tested. The explanation could be the functional redundancy between *At*FLOTs. Flotillins most probably act through the interaction with other proteins, thus their high sequence similarity may explain their redundancy. Creation of multiple knock-out lines will be necessary for further studies.

References

Bucherl, C. A., Jarsch, I. K., Schudoma, C., Segonzac, C., Mbengue, M., Robatzek, S., MacLean, D., Ott, T., Zipfel, C.: Plant immune and growth receptors share common signalling components but localise to distinct plasma membrane nanodomains. - eLife **6**: e25114, 2017.

Daněk, M., Valentová, O., Martinec, J.: Flotillins, erlins, and hirs: from animal base camp to plant new horizons. - Crit. Rev. Plant Sci. **35**: 191-214, 2016.

Denance, N., Sanchez-Vallet, A., Goffner, D., Molina, A.: Disease resistance or growth: the role of plant hormones in balancing immune responses and fitness costs. - Front. Plant Sci. **4**: 155, 2013.

Denoux, C., Galletti, R., Mammarella, N., Gopalan, S., Werck, D., De Lorenzo, G., Ferrari, S., Ausubel, F. M., Dewdney, J.: Activation of defense response pathways by OGs and Flg22 elicitors in *Arabidopsis* seedlings. - Mol. Plants **1**: 423-445, 2008.

Dai, X., Zhang, Y., Zhang, D., Chen, J., Gao, X., Estelle, M., Zhao, Y.: Embryonic lethality of *Arabidopsis* abp1-1 is caused by deletion of the adjacent *BSM* gene. - Nat. Plants **1**: pii: 15183, 2015.

Di, C., Xu, W., Su, Z., Yuan, J. S.: Comparative genome analysis of *PHB* gene family reveals deep evolutionary origins and diverse gene function. - BMC Bioinformatics **11**(Suppl 6): S22, 2010.

Enders, T. A., Oh, S., Yang, Z. B., Montgomery, B. L., Strader, L. C.: Genome sequencing of *Arabidopsis abp1-5* reveals second-site mutations that may affect phenotypes. - Plant Cell **27**: 1820-1826, 2015.

Glebov, O.O., Bright, N A., Nichols, B.J.: Flotillin-1 defines a clathrin-independent endocytic pathway in mammalian cells. - Nat. Cell Biol **8**: 46-54, 2006.

Hamaji, K., Nagira, M., Yoshida, K., Ohnishi, M., Oda, Y., Uemura, T., Goh, T., Sato, M.H., Morita, M.T., Tasaka, M., Hasezaw, S., Nakano, A., Hara-Nishimura, I., Maeshima, M., Fukaki, H., Mimura, T.: Dynamic aspects of ion accumulation by vesicle traffic under salt stress in *Arabidopsis*. - Plant Cell Physiol. **50**: 2023-2033, 2009.

Haney, C.H., Long, S.R.: Plant flotillins are required for infection by nitrogen-fixing bacteria. - Proc. nat. Acad. Sci. USA **107**: 478-483, 2010.

Hao, H., Fan, L., Chen, T., Li, R., Li, X., He, Q., Botella, M. A., Lin, J.: Clathrin and membrane microdomains cooperatively regulate RbohD dynamics and activity in *Arabidopsis*. - Plant Cell **26**: 1729-1745, 2014.

Hoagland, H., Arnon, D.I.: The water-culture method for growing plants without soil. - Calif. Agr. Exp. Sta **347**: 1-32, 1950.

Janda, M., Ruelland, E.: Magical mystery tour: salicylic acid signalling. - Environ.eExp. Bot. **114**: 117-128, 2015.

Jarsch, I.K., Konrad, S.S., Stratil, T.F., Urbanus, S.L., Szymanski, W., Braun, P., Braun, K.H., Ott, T.: Plasma membranes are subcompartmentalized into a plethora of coexisting and diverse microdomains in *Arabidopsis* and *Nicotiana benthamiana*. - Plant Cell **26**: 1698-1711, 2014.

Katagiri, F., Thilmony, R., He, S.Y.: The *Arabidopsis thaliana* - *Pseudomonas syringae* interaction. - Arabidopsis Book 1: e0039, 2002

Kitakura, S., Vanneste, S., Robert, S., Lofke, C., Teichmann, T., Tanaka, H., Friml, J.: Clathrin mediates endocytosis and polar distribution of PIN auxin transporters in *Arabidopsis*. - Plant Cell **23**: 1920-1931, 2011.

Lefebvre, B., Furt, F., Hartmann, M. A., Michaelson, L. V., Carde, J. P., Sargueil-Boiron, F., Rossignol, M., Napier, J. A., Cullimore, J., Bessoule, J. J., Mongrand, S.: Characterization of lipid rafts from *Medicago truncatula* root plasma membranes: a proteomic study reveals the presence of a raft-associated redox system. - Plant Physio.l **144**: 402-418, 2007.

Leshem, Y., Melamed-Book, N., Cagnac, O., Ronen, G., Nishri, Y., Solomon, M., Cohen, G., Levine, A.: Suppression of *Arabidopsis* vesicle-SNARE expression inhibited fusion of H_2O_2-containing vesicles with tonoplast and increased salt tolerance. – Proc. nat. Acad. Sci. USA **103**: 18008-18013, 2006.

Li, R., Liu, P., Wan, Y., Chen, T., Wang, Q., Mettbach, U., Baluska, F., Samaj, J., Fang, X., Lucas, W. J., Lin, J.: A membrane microdomain-associated protein, *Arabidopsis* Flot1, is involved in a clathrin-independent endocytic pathway and is required for seedling development. - Plant Cell **24**: 2105-2122, 2012.

Liu, P., Li, R. L., Zhang, L., Wang, Q.L., Niehaus, K., Baluska, F., Samaj, J., Lin, J.X.: Lipid microdomain polarization is required for NADPH oxidase-dependent ROS signaling in *Picea meyeri* pollen tube tip growth. - Plant J. **60**: 303-313, 2009.

Lu, X., Tintor, N., Mentzel, T., Kombrink, E., Boller, T., Robatzek, S., Schulze-Lefert, P., Saijo, Y.: Uncoupling of sustained MAMP receptor signaling from early outputs in an *Arabidopsis* endoplasmic reticulum glucosidase II allele. – Proc. natl.Acad. Sci. USA **106**: 22522-22527, 2009.

Michalko, J., Dravecka, M., Bollenbach, T., Friml, J.: Embryo-lethal phenotypes in early *abp1* mutants are due to disruption of the neighboring *BSM* gene. - F1000Res **4**: 1104, 2015.

Millet, Y.A., Danna, C.H., Clay, N.K., Songnuan, W., Simon, M.D., Werck-Reichhart, D., Ausubel, F M.: Innate immune responses activated in *Arabidopsis* roots by microbe-associated molecular patterns. - Plant Cell **22**: 973-990, 2010.

Nikonorova, N., Yue, K., Beeckman, T., De Smet, I.: *Arabidopsis* research requires a critical re-evaluation of genetic tools. - J. exp. Bot. **15**: 3541-3544, 2018.

Ott, T.: Membrane nanodomains and microdomains in plant-microbe interactions. - Curr. Opin. Plant Biol. **40**: 82-88, 2017.

Otto, G.P., Nichols, B.J.: The roles of flotillin microdomains - endocytosis and beyond. - J. cell. Sci. **124**: 3933-3940, 2011.

Santner, A., Estelle, M.: Recent advances and emerging trends in plant hormone signalling. - Nature **459**: 1071-1078, 2009.

Sasek, V., Janda, M., Delage, E., Puyaubert, J., Guivarc'h, A., López Maseda, E., Dobrev, P.I., Caius, J., Bóka, K., Valentová, O., Burketová, L., Zachowski, A., Ruelland, E.: Constitutive salicylic acid accumulation in pi4kIIIbeta1beta2 *Arabidopsis* plants stunts rosette but not root growth. - New Phytol **203**: 805-816, 2014.

Sekeres, J., Pleskot, R., Pejchar, P., Zarsky, V., Potocky, M.: The song of lipids and proteins: dynamic lipid-protein interfaces in the regulation of plant cell polarity at different scales. - J. exp. Bot. **66**: 1587-1598, 2015.

Shibasaki, K., Uemura, M., Tsurumi, S., Rahman, A.: Auxin response in *Arabidopsis* under cold stress: underlying molecular mechanisms. - Plant Cell **21**: 3823-3838, 2009.

Schindelin, J., Arganda-Carreras, I., Frise, E., Kaynig, V., Longair, M., Pietzsch, T., Preibisch, S., Rueden, C., Saalfeld, S., Schmid, B., Tinevez, J.Y., White, D.J., Hartenstein, V., Eliceiri, K., Tomancak, P., Cardona, A.: Fiji: an open-source platform for biological-image analysis. - Nat. Methods **9**: 676-682, 2012.

Smith, J.M., Heese, A.: Rapid bioassay to measure early reactive oxygen species production in *Arabidopsis* leaf tissue in response to living *Pseudomonas syringae*. - Plant Methods **10**: 6, 2014.

Sutter, J. U., Sieben, C., Hartel, A., Eisenach, C., Thiel, G., Blatt, M.R.: Abscisic acid triggers the endocytosis of the *Arabidopsis* KAT1 K+ channel and its recycling to the plasma membrane. - Curr. Biol. **17**: 1396-1402, 2007.

Titapiwatanakun, B., Blakeslee, J.J., Bandyopadhyay, A., Yang, H., Mravec, J., Sauer, M., Cheng, Y., Adamec, J., Nagashima, A., Geisler, M., Sakai, T., Friml, J., Peer ,W.A., Murphy, A.S.: ABCB19/PGP19 stabilises PIN1 in membrane microdomains in *Arabidopsis*. - Plant J. **57**: 27-44, 2009.

Wang, L., Li, H., Lv, X.Q., Chen, T., Li, R.L., Xue, Y.Q., Jiang, J.J., Jin, B., Baluska, F., Samaj, J., Wang, X.L., Lin, J.X.: Spatio-temporal dynamics of the BRI1 receptor and its regulation by membrane microdomains in living *Arabidopsis* cells. - Mol. Plants **8**: 1334-1349, 2015.

Wang, Q., Zhao, Y., Luo, W., Li, R., He, Q., Fang, X., Michele, R. D., Ast, C., Von Wiren, N., Lin, J.: Single-particle analysis reveals shutoff control of the *Arabidopsis* ammonium transporter AMT1;3 by clustering and internalization. – Proc. nat. Acad. Sci. USA **110**: 13204-13209, 2013.

Xin, X.F., Kvitko, B., He, S.Y.: *Pseudomonas syringae*: what it takes to be a pathogen. - Nat. Rev. Microbiol. **16**: 316-328, 2018.

Yu, M., Liu, H., Dong, Z., Xiao, J., Su, B., Fan, L., Komis, G., Samaj, J., Lin, J., Li, R.: The dynamics and endocytosis of Flot1 protein in response to flg22 in *Arabidopsis*. - J. Plant Physio.l **215**: 73-84, 2017.

Zipfel, C., Robatzek, S., Navarro, L., Oakeley, E. J., Jones, J. D., Felix, G., Boller, T.: Bacterial disease resistance in *Arabidopsis* through flagellin perception. - Nature **428**: 764-767, 2004.

Table 1 Suppl. List of primers (LP - left primer, RP - right primer, LB - left border primer, F - forward, R - reverse, RT-qPCR - reverse transcription quantitative PCR).

Targets	Primers (5´→3´)	Experiment	Reference
FLOT1	LP: GGGACAAAGGAGTTTAAGAAGG RP: GTTCCGCACCACGTAGAGTAC	genotyping, RT-PCR	this study
FLOT2	LP: TACCACTCCCACTAGCACCAC RP: TGTTGAAGGTGTTATCGAGGG	genotyping, RT-PCR	this study
FLOT3	LP: TCCCTTCTCCTAGCCTTTGAG RP: TGTAAATAACCGCGTTTCAATG	genotyping	this study
FLOT3	LP: GGTGTTTCCATGGCAGTCTT RP: GCTGATCTTAGGCTGCAGGT	RT-PCR	this study
T-DNA FLAG line	LB: CGTGTGCCAGGTGCCCACGGAATAGT	genotyping	this study
T-DNA SALK lines	LB: ATTTTGCCGATTTCGGAAC	genotyping	this study
Actin2	F: CCGCTCTTTCTTTCCAAGC R: CCGGTACCATTGTCACACAC	RT-PCR	this study
AtFLOT1	F: ATGAACGCTTTGACTCGAAC R: GGCTTGCTTTTGTTTCTCGTA	RT-qPCR	Li *et al*. 2012
AtFLOT2	F: ACTTGCAGCCCAAGATTAGC R: CTCCCACTAGCACCACCAAT	RT-qPCR	this study
AtFLOT3	F: AGTCGCTAAAGCATCGCAGT R: TGCAAGCTTGATGTCTGTGA	RT-qPCR	this study
TIP41	F: GTGAAAACTGTTGGAGAGAAGCAA R: TCAACTGGATACCCTTTCGCA	RT-qPCR	Czechowski *et al.* 2005

Czechowski, T., Stitt, M., Altmann, T., Udvardi, M.K., Scheible, W.R.: Genome-wide identification and testing of superior reference genes for transcript normalization in *Arabidopsis*. - Plant Physiol. **139**: 5-17, 2005.
Li, R., Liu, P., Wan, Y., Chen, T., Wang, Q., Mettbach, U., Baluska, F., Samaj, J., Fang, X., Lucas, W.J., Lin, J.: A membrane microdomain-associated protein, *Arabidopsis* Flot1, is involved in a clathrin-independent endocytic pathway and is required for seedling development. - Plant Cell **24**: 2105-2122, 2012.

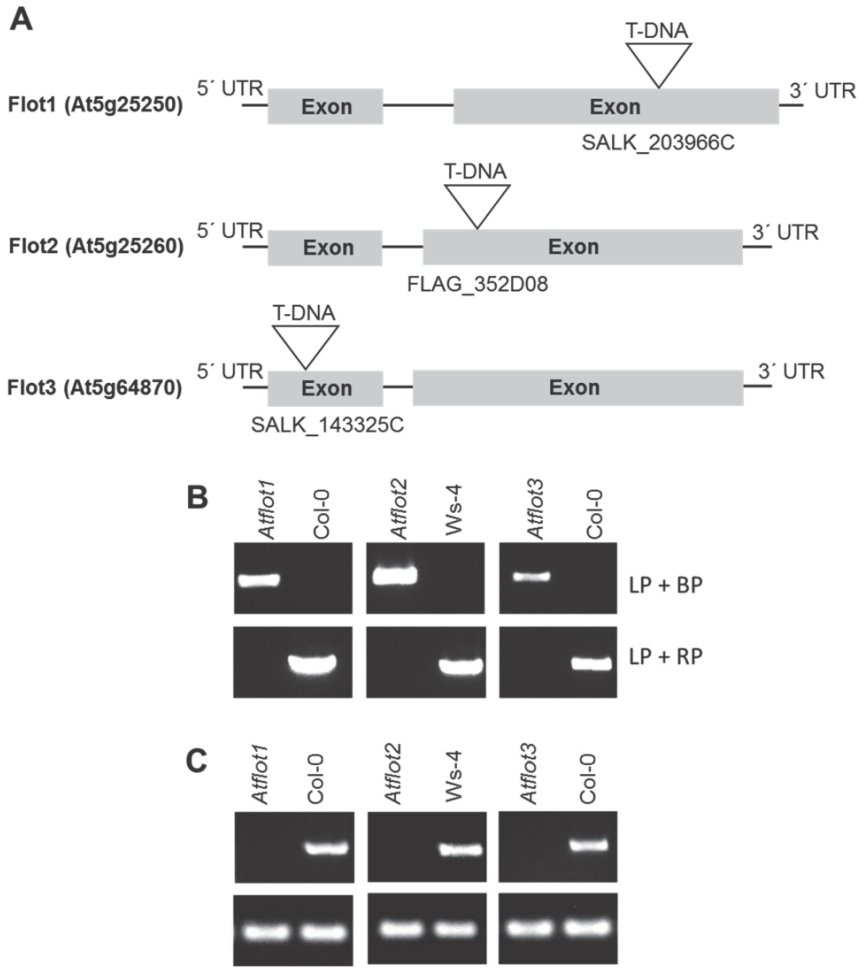

Fig. 1 Suppl. Characterization of T-DNA mutants. *A* - Schematic overview of T-DNA insertion in particular AtFLOT knock-out mutants. *B* - Genomic PCR analysis to confirm the integration of T-DNA in *Atflot1*, *Atflot2*, and *Atflot3* (*upper panels* - PCR products of primers used for amplification of T-DNA insertion allele, *lower panels* - PCR products of primers used for amplification of wild-type allele, LP - left primer, RP - right primer, BP - T-DNA border primer. *C* - RT-PCR analysis of *flot1*, *flot2*, and *flot3* specific transcripts (*upper panels* - RT-PCR with gene specific primers, *lower panels* - *Actin2* used as an internal control).

DNA was isolated from 3-week-old *Atflot1* (SALK_203966), *Atflot2* (FLAG_352D08), and *Atflot3* (SALK_143325C) plants. T-DNA insertion was confirmed by PCR using primers listed in Table 1 Suppl. For RT-PCR analysis the leaf samples were instantly frozen in liquid nitrogen. RNA was isolated using a *Spectrum Plant Total* RNA kit (*Sigma-Aldrich*, St. Louis USA), *Turbo DNA-free* kit (*Applied Biosystems*, Foster City, USA) was used for DNA removal and *Transcriptor High Fidelity* cDNA synthesis kit (*Roche*, Basel, Switzerland) was used for cDNA synthesis. The reverse transcription reaction was primed with anchored-oligo(DT)18 primer. Primers used for RT-PCR analysis are listed in Table 1 Suppl. All PCR reactions were performed using *PPP Master Mix* (*Top-Bio*, Prague, Czech Republic).

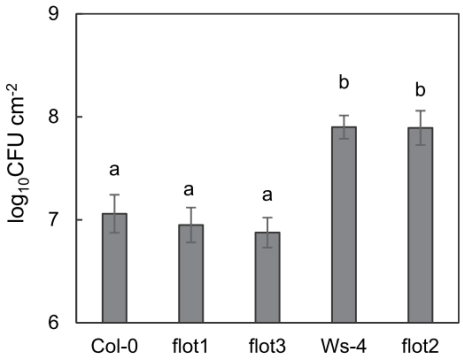

Fig. 2 Suppl. Dipping inoculation with *Pst* DC3000. Four-week-old *A. thaliana* plants were dipped in *Pst* DC3000 suspension. Values are demonstrated in $\log_{10}$ scale of colony forming units (CFU). Means ± SEs, $n = 6$, different letters indicate statistically significant differences between the samples ($P < 0.01$, Student's *t*-test).

Paper # 3

Title: Mapping of Plasma Membrane Proteins Interacting with *Arabidopsis thaliana* Flotillin 2

Authors: Petra Junková, Michal Daněk, Daniela Kocourková, Jitka Brouzdová, Kristýna Kroumanová, Enric Zelazny, Martin Janda, Radovan Hynek, Jan Martinec, Olga Valentová

Summary: Arabidopsis flotillin 2 (At5g25260) belongs to the group of plant flotillins, which are not well characterized. In contrast, metazoan flotillins are well known as plasma membrane proteins associated with membrane microdomains that act as a signaling hub. The similarity of plant and metazoan flotillins, whose functions most likely consist of affecting other proteins via protein–protein interactions, determines the necessity of detecting their interacting partners in plants. Nevertheless, identifying the proteins that form complexes on the plasma membrane is a challenging task due to their low abundance and hydrophobic character. Here we present an approach for mapping *Arabidopsis thaliana* flotillin 2 plasma membrane interactors, based on the immunoaffinity purification of crosslinked and enriched plasma membrane proteins with mass spectrometry detection. Using this approach, 61 proteins were enriched in the *At*Flot-GFP plasma membrane fraction, and 19 of them were proposed to be flotillin 2 interaction partners. Among our proposed partners of Flot2, proteins playing a role in the plant response to various biotic and abiotic stresses were detected. Additionally, the use of the split-ubiquitin yeast system helped us to confirm that plasma-membrane ATPase 1, early-responsive to dehydration stress protein 4, syntaxin-71, harpin-induced protein-like 3, hypersensitive-induced response protein 2 and two aquaporin isoforms interact with flotillin 2 directly. Based on the results of our study and the reported properties of Flot2 interactors, we propose that Flot2 complexes may be involved in plant–pathogen interactions, water transport and intracellular trafficking.

DOI: 10.3389/fpls.2018.00991

Citation: JUNKOVÁ, P., DANĚK, M., KOCOURKOVÁ, D., BROUZDOVÁ, J., KROUMANOVÁ, K., ZELAZNY, E., JANDA, M., HYNEK, R., MARTINEC, J. & VALENTOVÁ, O. 2018. Mapping of Plasma Membrane Proteins Interacting with *Arabidopsis thaliana* Flotillin 2. Frontiers in Plant Science, 9.

My contribution: Shared first authorship with Petra Junková. I took part in the selection of *At*FLOT2-GFP line used for Co-IP/MS. I cloned the constructs used in split-ubiquitin assay and performed the assay. Together with Petra Junková I wrote the majority of the manuscript.

frontiers in Plant Science

ORIGINAL RESEARCH
published: 12 July 2018
doi: 10.3389/fpls.2018.00991

Mapping of Plasma Membrane Proteins Interacting With *Arabidopsis thaliana* Flotillin 2

Petra Junková[1†], Michal Daněk[2,3†], Daniela Kocourková[2], Jitka Brouzdová[2], Kristýna Kroumanová[2], Enric Zelazny[4], Martin Janda[1,2], Radovan Hynek[1], Jan Martinec[2] and Olga Valentová[1]*

[1] Department of Biochemistry and Microbiology, University of Chemistry and Technology Prague, Prague, Czechia, [2] Institute of Experimental Botany of the Czech Academy of Sciences, Prague, Czechia, [3] Department of Experimental Plant Biology, Faculty of Science, Charles University, Prague, Czechia, [4] Institut de Biologie Intégrative de la Cellule (I2BC), CNRS–CEA–Université Paris Sud, Université Paris-Saclay, Gif-sur-Yvette, France

OPEN ACCESS

Edited by:
Ive De Smet,
Flanders Institute for Biotechnology, Belgium

Reviewed by:
Thomas Ott,
Albert-Ludwigs-Universität Freiburg, Germany
Xia Wu,
University of Washington, United States
Jinxing Lin,
Beijing Forestry University, China
Ruili Li,
Beijing Forestry University, China

***Correspondence:**
Petra Junková
Petra.Junkova@vscht.cz;
pjova13@gmail.com

† These authors have contributed equally to this work.

Specialty section:
This article was submitted to Plant Proteomics, a section of the journal Frontiers in Plant Science

Received: 28 February 2018
Accepted: 19 June 2018
Published: 12 July 2018

Citation:
Junková P, Daněk M, Kocourková D, Brouzdová J, Kroumanová K, Zelazny E, Janda M, Hynek R, Martinec J and Valentová O (2018) Mapping of Plasma Membrane Proteins Interacting With Arabidopsis thaliana Flotillin 2. Front. Plant Sci. 9:991. doi: 10.3389/fpls.2018.00991

Arabidopsis flotillin 2 (At5g25260) belongs to the group of plant flotillins, which are not well characterized. In contrast, metazoan flotillins are well known as plasma membrane proteins associated with membrane microdomains that act as a signaling hub. The similarity of plant and metazoan flotillins, whose functions most likely consist of affecting other proteins via protein–protein interactions, determines the necessity of detecting their interacting partners in plants. Nevertheless, identifying the proteins that form complexes on the plasma membrane is a challenging task due to their low abundance and hydrophobic character. Here we present an approach for mapping *Arabidopsis thaliana* flotillin 2 plasma membrane interactors, based on the immunoaffinity purification of crosslinked and enriched plasma membrane proteins with mass spectrometry detection. Using this approach, 61 proteins were enriched in the *AtFlot-GFP* plasma membrane fraction, and 19 of them were proposed to be flotillin 2 interaction partners. Among our proposed partners of Flot2, proteins playing a role in the plant response to various biotic and abiotic stresses were detected. Additionally, the use of the split-ubiquitin yeast system helped us to confirm that plasma-membrane ATPase 1, early-responsive to dehydration stress protein 4, syntaxin-71, harpin-induced protein-like 3, hypersensitive-induced response protein 2 and two aquaporin isoforms interact with flotillin 2 directly. Based on the results of our study and the reported properties of Flot2 interactors, we propose that Flot2 complexes may be involved in plant–pathogen interactions, water transport and intracellular trafficking.

Keywords: Arabidopsis flotillin 2, protein–protein interactions, immunopurification, mass spectrometry, split-ubiquitin yeast system, plant–pathogen interaction, water transport, intracellular trafficking

INTRODUCTION

The SPFH (stomatin/prohibitin/flotillin/HflK/C) domain proteins superfamily consists of membrane proteins which exhibit 40–84% sequence homology (Li et al., 2000; Green and Young, 2008), but are divided into several groups with different functions and localizations (Browman et al., 2007). Flotillins form a group of SPFH domain-containing proteins characterized by their localization in the plasma membrane.

Flotillins were discovered in three independent studies as a human epidermal surface antigen (Schroeder et al., 1994), as proteins induced during optic nerve regeneration in the goldfish retinal ganglion (Schulte et al., 1995) and as proteins of membrane caveolae in a mouse fibroblast tissue culture (Bickel et al., 1997). To this day, the localization and function of metazoan flotillins has been intensively investigated. Metazoan flotillins are predominantly targeted to plasma membrane microdomains, where they are anchored by the SPFH domain (Morrow et al., 2002; Neumann-Giesen et al., 2004; Glebov et al., 2006; Solis et al., 2007; Langhorst et al., 2008). They were found to be involved in the endocytosis of glycophosphatidylinositol (GPI)-anchored proteins as well as caveolae-mediated endocytosis (Volonté et al., 1999; Baumann et al., 2000). Another function of flotillins likely consists of affecting other proteins via protein–protein interactions (Baumann et al., 2000), in which case various tyrosine kinases (Ullrich and Schlessinger, 1990; Neumann-Giesen et al., 2007; Amaddii et al., 2012) or proteins of the cytoskeleton (Baumann et al., 2000; Liu et al., 2005; Langhorst et al., 2008; Peremyslov et al., 2013) are prominent interactors with mammalian flotillins. The interaction with partner proteins as well as homo- and hetero-oligomerization of single metazoan flotillin isoforms is predominantly provided by the C-terminal domain of flotillins, where several coiled-coil stretches are present (Neumann-Giesen et al., 2004; Solis et al., 2007).

The coding regions of flotillin homologs were also identified in various plant genomes (Di et al., 2010). For example, the *A. thaliana* genome contains three homologs of flotillin, Flot1 (At5g25250), Flot2 (At5g25260), and Flot3 (At5g64870) (Gehl et al., 2014; Jarsch et al., 2014) and in this paper these three isoforms are designated Flot1/2/3 unless stated otherwise. Similarly to metazoan homologs, Arabidopsis flotillins are able to form heterooligomers via their C-terminal domain, which was reported for the direct interaction of Flot1 with Flot3 (Yu et al., 2017). However, the role of plant flotillins, as well as of most other proteins with a SPFH domain, has not been fully elucidated. Current findings about the localization and function of plant flotillins in the context of the known role of metazoan flotillins have been recently summarized by Danek et al. (2016). Similarities between the properties of plant and metazoan flotillins lead to the assumption that plant flotillins affect other proteins via protein–protein interactions, as with metazoans.

Arabidopsis thaliana flotillins differ in the localization of their transcription, because Flot1 and Flot2 are predominantly transcribed in leaves and shoots, while Flot3 is mostly transcribed in the flower parts and siliques (Danek et al., 2016). Nevertheless, the subcellular localization is similar for all known flotillins; they are most frequently localized to plasma membrane microdomains (Li et al., 2012; Hao et al., 2014; Jarsch et al., 2014; Ishikawa et al., 2015), which are enriched in sterols, sphingolipids, saturated phospholipids and GPI-anchored proteins, and play a significant role in membrane trafficking and cell signaling (Simons and Ikonen, 1997; Simons and Toomre, 2000; Borner et al., 2005; Jarsch et al., 2014; Cacas et al., 2016).

Although the anchoring of mammalian flotillins is supported by their palmitoylation as well as myristoylation (Morrow et al., 2002; Neumann-Giesen et al., 2004; Langhorst et al., 2008), no sites for palmitoylation or myristoylation were predicted in any of the three *A. thaliana* flotillins. This indicates that the anchoring to the membrane is provided by a different mechanism (Danek et al., 2016). This mechanism could be based on the specific interaction with sterols, since several putative CRAC/CARC motifs providing recognition and interaction with sterols were predicted in the sequence of plant flotillins (Roitbak et al., 2005; Danek et al., 2016). This hypothesis is supported by the finding that the Flot1 diffusion coefficient is decreased in plants treated with methyl-β-cyclodextrin, a sterol-depleting agent (Li et al., 2011, 2012; Hao et al., 2014). Moreover, it was also observed that the knocking-down of *Flot1* affected the internalization of sterol into membranes (Li et al., 2012).

Since proteins involved in vesicular trafficking and endocytosis (e.g., ESCRT proteins, exocyst and SNARE subunits or Rab-GTPase) were proposed to be Flot2 and Flot3 interactors by Associomics, a split-ubiquitin yeast system-based database of direct protein–protein interactions[1] (Jones et al., 2014), this suggests that plant flotillins could play a similar role in membrane transport to mammalian ones. Additionally, plant flotillin microdomains have been shown to be involved in clathrin-independent endocytosis, inducible by various stimuli (Li et al., 2011; Hao et al., 2014; Wang et al., 2015; Yu et al., 2017). The role of flotillins in cell communication and signal transduction is also considered, because several types of kinases were found to co-localize with *Medicago truncatula* Flot4 (Haney et al., 2011) and interact with all three *AtFlot* isoforms (Associomics). The involvement of flotillins in plant–pathogen interactions was demonstrated, as Flot1 lateral mobility in the plasma membrane was altered upon treatment with bacterial elicitor flg22, and reduced or increased flg22-induced callose deposition was observed in plants with *Flot1* knocked-down or overexpressed, respectively (Yu et al., 2017). Arabidopsis amiRNA-Line with reduced *Flot1/Flot2* expression were smaller in size and exhibited structural changes in apical meristems (Li et al., 2012), which points to the involvement of flotillins in plant growth and development. Moreover, functional linkage and co-localization of plant flotillins and the cytoskeleton was observed (Li et al., 2012; Peremyslov et al., 2013).

Protein interactions with other cell components are crucial to maintaining the viability of the whole organism and determining its phenotypic manifestation. Predominantly, protein–protein interactions are nowadays intensively examined by various methods. Among them, immunoprecipitation (IP) or affinity purification (AP) coupled to mass spectrometry (MS) is the method of choice (ten Have et al., 2011; Dunham et al., 2012; Dedecker et al., 2015). However, the investigation of membrane proteins is challenging due to their hydrophobic character and low abundance. Nevertheless, there is a current effort to modify standard procedures in order to facilitate analyses of membrane

[1]https://associomics.dpb.carnegiescience.edu/Associomics/Home.html

protein interactions (Qi and Katagiri, 2009; Smaczniak et al., 2012; Van Leene et al., 2015).

The aim of this study was to perform a screening of Flot2 protein interactors in *A. thaliana* leaves. For this purpose we used IP with a GFP tag followed by the MS of *in vitro* cross-linked membrane proteins. After we confirmed the localization of Flot2 at the plasma membrane, we showed that the enrichment of the plasma membrane prior to the IP-MS is a crucial step for the detection of low–abundance plasma membrane interactors. The direct interaction of Flot2 with several proteins involved in the plant response to biotic as well as abiotic stress was confirmed by an independent method, e.g., by a split-ubiquitin yeast system (SUS) suitable for the analysis of membrane proteins.

MATERIALS AND METHODS

Plant Material

Transgenic *A. thaliana* lines *AtFlot2-GFP* with the p35S::AtFlot2:GFP construct that stably produces the Flot2-GFP protein were prepared as follows: The coding sequence was amplified from cDNA prepared from Col-0 using specific primers 1 and 2 (see Supplementary Table S1) and in-frame introduced in between the EcoRI and BamHI sites of a modified pGreen0029 vector containing the CAMV 35S promoter and 3′-terminal GFP coding sequence by restriction/ligation. Stable transformants were obtained by the *Agrobacterium tumefaciens* floral dip method and selected on kanamycin plates. T3 generation plants were used for microscopy and membrane fractions preparation.

Seeds of the *A. thaliana* wild type (WT, ecotype Col-0) and *AtFlot2-GFP* plants were stratified for 3 days at 4°C, placed on Jiffy 7 peat pellets and cultivated in a growth chamber at 22°C, with a 10-h day (100–130 μmol m^{-2} s^{-1}) and 14-h night cycle at 70% relative humidity for 1 week. One-week-old plantlets were individually replanted to Jiffy 7 peat pellets and placed in a cultivation room with a 16-h day (100–130 μmol m^{-2} s^{-1}) and 8-h night cycle and 40–50% relative humidity. During the cultivation, plants were watered with distilled water. Whole rosettes of 4-week-old plants were frozen in liquid nitrogen to be used as the material for MS analyses.

Confocal Microscopy

For microscopic observations, seeds of *AtFlot2-GFP* plants were surface sterilized and sown onto ½ Murashige-Skoog basal salt (Duchefa) 1% agar plates supplemented with 1% sucrose. The seedlings were grown in a vertical position under 100 μmol m^{-2} s^{-1} in a 16/8 h and 22/20°C (light/dark) cycle. Five-day-old seedlings were observed using a Zeiss 880 laser scanning confocal microscope. Plasmolysis was induced by treatment with 0.8 M mannitol in ½ Murashige-Skoog solution for 30 min. Subsequently, the seedlings were incubated in propidium iodide solution (20 μg/ml in ½ Murashige-Skoog + 0.8 M mannitol) to counterstain the cell walls. GFP fluorescence was collected in the 500–550 nm range using 488 nm laser excitation and a 40× water immersion objective (NA = 1.2).

Preparation of Microsomal and Plasma Membrane Fractions

Membrane fractions were prepared from 30 g of leaves from 4-week-old *A. thaliana* WT and *AtFlot2-GFP* plants. Leaves were ground with a pestle and mortar in liquid nitrogen and further homogenized by sonication for 3 × 35 s (25 W) in 90 ml of extraction buffer (50 mM HEPES pH 7.5, 400 mM sucrose, 85 mM KCl, 100 mM $MgCl_2.6H_2O$, 0.02 mM ascorbic acid) containing cOmplete^{TM} EDTA-free Protease Inhibitor Cocktail according to the manufacturer's instructions (Sigma Aldrich). The homogenate was centrifuged at 5000 × *g* for 20 min at 4°C. The supernatant was filtered through Miracloth (Millipore) and centrifuged at 200,000 × *g* for 1 h at 4°C. The pellet (microsomal membrane fraction) was resuspended in resuspension buffer (20 mM HEPES pH 7.5, 330 mM sucrose, 1 mM EDTA) to a total volume of 6 ml, further homogenized in a Potter-Elvehjem homogenizer and cross-linked by the addition of dithiobis (succinimidyl propionate) (DSP, Thermo Scientific) to a final concentration of 5 mM. The suspension was incubated for 30 min at 4°C with shaking. To quench the reaction, 1 M Tris (pH 7.5) was added to a final concentration of 50 mM, and the suspension was shaken again for 30 min at 4°C. The microsomal fraction with cross-linked proteins was pelleted by centrifugation at 200,000 × *g* for 1 h at 4°C.

To release the protein complexes from the microsomal fraction, the pellet was resuspended in 6 ml of resuspension buffer and homogenized with a Potter-Elvehjem homogenizer, and then 10% (w/v) sodium deoxycholate was added to a final concentration of 0.5% (w/v). The suspension was incubated for 30 min at 4°C. Solubilized proteins were collected in the supernatant obtained by centrifugation at 200,000 × *g* for 30 min at 4°C, and the pellet was resuspended in the same way as before. To further enrich the plasma membrane, the pellet of the cross-linked microsomal fraction was resuspended in 5 mM K/Na-phosphate buffer (pH 7.8) and homogenized with a Potter-Elvehjem homogenizer.

The plasma membrane fraction was prepared from the cross-linked membrane fraction with a PEG/dextran two-phase system (Schindler and Nothwang, 2006; Pleskot et al., 2010). After gentle mixing, the separation was carried out overnight at 4°C, and the tubes were centrifuged at 1500 × *g* for 5 min at 4°C. The upper phase containing the plasma membrane was transferred to the new tubes, mixed with a blank lower phase and centrifuged again. The final upper phase was collected, diluted with three volumes of 5 mM K/Na-phosphate buffer (pH 7.8) and centrifuged again at 200,000 × *g* for 1 h at 4°C. The pellet was resuspended in 600 μl of resuspension buffer, 10% (w/v) sodium deoxycholate was added to a final concentration of 0.5% (w/v), and the suspension was incubated for 30 min at 4°C. The protein content in all isolated fractions was determined by Popov's method (Popov et al., 1975) using bovine serum albumin as the standard. Flow chart of the procedure is depicted on **Figure 2A**.

Western Blotting and Immunodetection

The content of Flot2-GFP in the respective fractions was investigated by western blotting and immunodetection. Proteins

were separated in 10% polyacrylamide SDS-gels at 180 V and electroblotted onto nitrocellulose membranes (BioTrace™ NT Nitrocellulose Transfer Membrane, Pall Corporation) at 50 V. Membranes were rinsed in PBS and blocked in 5% (w/v) non-fat milk powder in PBS with 0.075% (w/v) Tween-20 (PBST-75) overnight. Blocked membranes were washed three times in PBST-75 and incubated with primary antibodies diluted in 5% (w/v) non-fat milk powder in PBST-75 for 1 h. Anti-GFP rabbit polyclonal serum (Thermo Scientific) 1:5000 was used as the primary antibody. Membranes were washed three times in PBST-75 and incubated for 1 h with the secondary antibody, GAR/IgG(H + L)/PO (Nordic-MUbio) 1:5000 diluted in 5% (w/v) non-fat milk powder in PBST-75. Signals were visualized with an AEC staining kit (Sigma Aldrich) or Clarity™ Western ECL Substrate (Bio-rad).

Immunoprecipitation of Microsomal and Plasma Membrane Fractions

The IP procedure was performed with Dynabeads® Protein A microbeads (Thermo Scientific) with bound anti-GFP mouse monoclonal antibody, isotype IgG_{2a} (Thermo Scientific). Fifty microliter of pre-washed beads were mixed with 2 μg of antibodies dissolved in PBS containing 0.05% Tween-20 (PBST-5) and incubated for 1 h in the vertical rotator. Beads with bound antibodies were washed three times with 200 μl of PBST-5 and incubated in 5 mM bis(sulfosuccinimidyl)suberate (BS3, Thermo Scientific) for 30 min to cross-link the bound antibodies to protein A. The reaction was quenched by washing the beads with 200 μl of 1 M Tris/HCl (pH 7.4) three times. The beads were then equilibrated three times with 200 μl of resuspension buffer with 0.5% (w/v) sodium deoxycholate and incubated with 200 μl of the respective membrane fraction for 2 h in a vertical rotator. Protein complexes bound to the beads were washed three times with RIPA buffer (50 mM Tris/HCl pH 7.4, 1 mM EDTA, 50 mM NaCl, 0.5% (w/v) sodium deoxycholate, 1% (w/v) NP-40) and eluted by incubation of the beads with 20 μl of Laemmli buffer 2× for 10 min at 95°C.

Tryptic Digestion of Proteins

Proteins eluted from the microbeads were separated to a distance of 1.5 cm in 10% poly-acrylamide SDS-gels at 180 V. Gels were stained with Imperial™ Protein Stain (Thermo Scientific) and whole line of each elute of was collected. Each lane was further sliced into smaller gel pieces and combined into an Eppendorf tube, washed with water, destained with 0.1 M NH_4HCO_3/acetonitrile 1:1 (v/v) and dried with acetonitrile. To reduce and alkylate the disulphide bonds, the gel pieces were first incubated with a 10 mM solution of dithiothreitol in 0.1 M NH_4HCO_3 for 45 min at 56°C, and then in a 55 mM solution of iodoacetamide in 0.1 M NH_4HCO_3 for 30 min at room temperature. Iodoacetamide solution was discarded and the gel pieces were washed with 0.1 M NH_4HCO_3/acetonitrile 1:1 (v/v) for 10 min and dried with acetonitrile. MS-Grade Trypsin solution at a concentration of 12.5 μg ml^{-1} dissolved in cold 50 mM NH_4HCO_3 was added to the gel pieces in a volume equal to the volume of the pieces, and the mixture was incubated on ice for 30 min. The excess trypsin solution was then discarded; the pieces were covered with 50 mM NH_4HCO_3 and incubated overnight at 37°C. The peptides were extracted from the gel by two consecutive sonications in 35 and 70% solutions of acetonitrile in 0.1% trifluoroacetic acid. Both aliquots were combined and the resulting peptide solution was lyophilized. The lyophilizate was then resuspended in 0.1% trifluoroacetic acid, desalted with ZipTip pipette tips according to the manufacturer's instructions (Millipore) and purified samples were dried in air.

LC-MS/MS Analysis

The mass spectrometric analysis was performed with a UHPLC Dionex Ultimate3000 RSLC nano (Dionex) coupled with an ESI-Q-TOF Maxis Impact (Bruker Daltonics) mass spectrometer. Dried samples were dissolved in a mixture of water:acetonitrile:formic acid (97:3:0.1%) and loaded into the trap column, an Acclaim PepMap 100 C18 (100 μm × 2 cm, particle size 5 μm, Dionex), with a mobile-phase flow rate of 5 μLmin^{-1} of A (0.1% formic acid in water) for 5 min. The peptides were then separated in the analytical column, an Acclaim PepMap RSLC C18 (75 μm × 150 mm, particle size 2 μm, Dionex), and eluted with mobile-phase B (0.1% formic acid in acetonitrile) using the following gradient: 0 min 3% B, 5 min 3% B, 95 min 35% B, 97 min 90% B, 110 min 90% B, 112 min 3% B, and 120 min 3% B. The flow rate during the gradient separation was set to 0.3 μLmin^{-1}. Peptides were eluted directly to the ESI source-captive spray (Bruker Daltonics). Measurements were performed in DDA mode with precursor-ion selection in the range of 400–1400 Da; up to 10 precursor ions were selected for fragmentation from each MS spectrum.

Peak lists were extracted from the raw data with the software Data Analysis 4.1 (Bruker Daltonics). Proteins were identified in the software Proteinscape 3.1 (Bruker Daltonics) using in-house Mascot server 2.4.1 (Matrix Science) with the *A. thaliana* protein database downloaded from[2] (October 2016). The parameters for the database search were set as follows: carbamidomethyl (C) as fixed modification, oxidation (M) and CAMthiopropanoyl (K, N-terminus) as variable modifications, tolerance 10 ppm in MS mode and 0.05 Da in MS/MS mode, enzyme trypsin one miscleavage. In MS intensity-based semiquantitative analysis the relative intensities of unique peptide signals were averaged to express individual protein abundance. Only proteins identified by two or more peptides were taken into account and the intensities of precursor ions with the best mascot score were used. Finally, the relative quantification index (RQI) representing the ratio of the resulting protein abundance between the *AtFlot2-GFP* plant sample and WT sample was calculated for each protein, and the proteins with RQI higher than three were considered to be enriched.

Split-Ubiquitin System

The Flot2 coding sequence was amplified from cDNA prepared from Col-0 using specific primers 3 and 4 (see Supplementary Table S1) and introduced in between the SalI and NotI restriction sites of the pENTR3c Dual Selection vector (Thermo

[2]http://www.uniprot.org

Fisher) in a manner that allowed C-terminal protein fusion by restriction/ligation. LR recombination with the pMetYC-DEST vector encoding the C-terminal split-ubiquitin moiety as well as the LEU2 gene was then performed using Gateway™ LR Clonase™ II Enzyme mix (Thermo Fisher) to obtain the final vector for yeast transformation.

Putative interactor coding sequences were amplified from cDNA prepared from Col-0 using specific primers 5–26 (see Supplementary Table S1) and introduced in between the KpnI and NotI (AtPIP2-6 and AtSYP71) or SalI and NotI (the rest of the sequences) restriction sites of the pENTR3c Dual Selection vector (Thermog Fisher) in a manner that allowed N-terminal protein fusion by restriction/ligation. LR recombination with a pNX35-DEST vector encoding the N-terminal split-ubiquitin moiety as well as the TRP1 gene was then performed using Gateway™ LR Clonase™ II Enzyme mix (Thermo Fisher) to obtain the final vector for yeast transformation.

The THY.AP4 yeast strain was cotransformed (Hachez et al., 2014) with Flot2-pMetYC and X-pNX35 (X = investigated putative interactor of Flot2) vectors by the lithium acetate/single-stranded carrier DNA/PEG method (Grefen et al., 2009; Grefen, 2014) and plated on YNB + CSM (both MP Biomedicals) medium lacking Leu and Trp supplemented with 2% glucose and 50 μM Met. After a 2-day recovery at 30°C, freshly grown colonies were resuspended in milliQ water and diluted to obtain suspensions of optical densities (OD_{600}) equal to 1.0, 0.1, and 0.01. Drops of 10 μl were placed on plates with YNB + CSM selective medium lacking Leu, Trp, Ade, and His, supplemented with 2% glucose and 50, 250, and 500 μM Met. Yeast growth was visually assessed after incubation for 2 days at 30°C.

The non-recombined pNX35 vector encoding for NubG, which was unable to reassemble with Cub co-transformed with Flot2-pMetYC, was used as the negative control, whereas the pNubWT-Xgate vector encoding for the wild-type Nub moiety spontaneously reassembling with Cub cotransformed with Flot2-pMetYC was used as the positive control in the SUS growth assay.

The pMetYC-DEST, pNX35-DEST, and pNubWT-Xgate vectors as well as the THY.AP4 yeast strain were kindly provided by Christopher Grefen, University of Tubingen, Germany. AtPIP2-7-pNX32 was kindly provided by François Chaumont and Timothée Laloux, Université catholique de Louvain, Belgium.

RESULTS

Plasma Membrane Localization of Flot2-GFP

Since the only experimental evidence of the subcellular localization of Flot2 at the plasma membrane was found when YFP-fused *A. thaliana* Flot2 was transiently expressed in *Nicotiana benthamiana* leaf epidermal cells (Jarsch et al., 2014), we investigated the localization of Flot2-GFP directly in the epidermal cells of *A. thaliana* roots and cotyledons (**Figure 1A**). We observed that Flot2-GFP is predominantly localized at the plasma membrane in both of these diverse *A. thaliana* tissues.

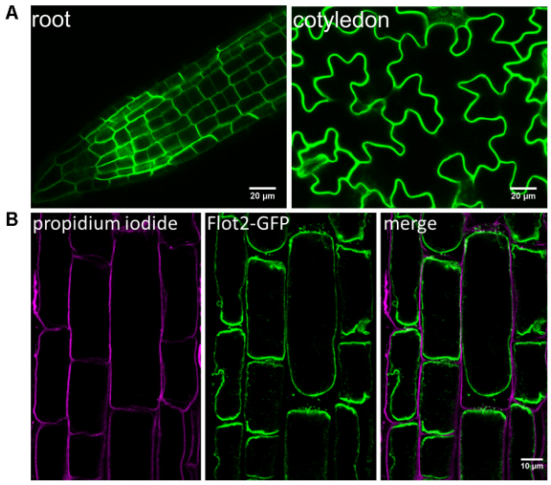

FIGURE 1 | Flot2-GFP localization at plasma membrane. **(A)** Confocal microscopy images showing Flot2-GFP localization at plasma membrane in epidermal cells of roots and cotyledons of Arabidopsis Flot2-GFP plants; **(B)** Confirmation of Flot2-GFP localization at plasma membrane in plasmolyzed root epidermal cells. The Flot2-GFP signal is detected at the plasma membrane of contracted protoplasts. Seedlings were treated with 0.8 M mannitol and subsequently stained with propidium iodide to mark cell walls.

Flot2-GFP localization at plasma membrane was confirmed by subjecting root cells to the plasmolysis induced by mannitol; no Flot2-GFP signal was detected at the cell wall (**Figure 1B**). Therefore, not only the microsomal fraction, but also the enriched plasma membrane fraction was prepared to perform the IP-MS experiment. The lines overexpressing Flot2-GFP did not exhibit any apparent growth differences from Col-0 plants.

Enrichment of Flot2-GFP in Plasma Membrane Fractions

The microsomal fraction was isolated according to Qi and Katagiri (2009). A DSP cross-linker was used to fix the interacting proteins in the microsomal fraction before the dissolution of membranes with 0.5% (w/v) sodium deoxycholate. Due to the plasma membrane localization of Flot2, we also enriched the plasma membrane fraction with an extract from the cross-linked microsomal fraction, because the direct determination of its plasma membrane interactors could better contribute to the characterization of Flot2's function. A flow chart of the procedure is depicted in **Figure 2A**.

During the isolation process, the presence of Flot2-GFP in each obtained fraction was detected by immunoblot analysis using the antibodies against GFP. Significant loss of the Flot2-GFP content caused by additional ultracentrifugation was observed between the native (line M) and cross-linked (line Mx) microsomal fraction (**Figure 2B**). We also analyzed the content of Flot2-GFP in fractions obtained after the dissolution of the cross-linked microsomal fraction by sodium deoxycholate; a higher amount of Flot2-GFP remained in the undissolved

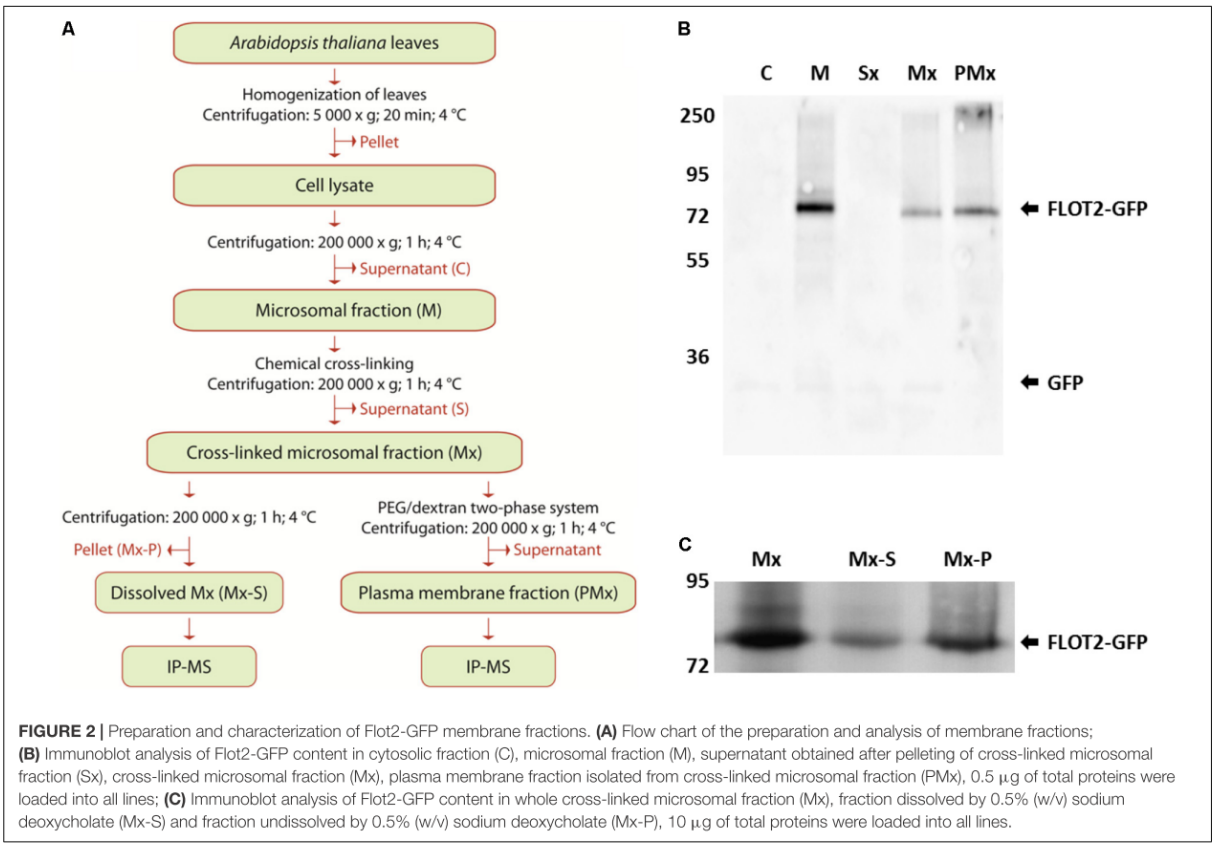

FIGURE 2 | Preparation and characterization of Flot2-GFP membrane fractions. **(A)** Flow chart of the preparation and analysis of membrane fractions; **(B)** Immunoblot analysis of Flot2-GFP content in cytosolic fraction (C), microsomal fraction (M), supernatant obtained after pelleting of cross-linked microsomal fraction (Sx), cross-linked microsomal fraction (Mx), plasma membrane fraction isolated from cross-linked microsomal fraction (PMx), 0.5 μg of total proteins were loaded into all lines; **(C)** Immunoblot analysis of Flot2-GFP content in whole cross-linked microsomal fraction (Mx), fraction dissolved by 0.5% (w/v) sodium deoxycholate (Mx-S) and fraction undissolved by 0.5% (w/v) sodium deoxycholate (Mx-P), 10 μg of total proteins were loaded into all lines.

fraction (**Figure 2C**). Nevertheless, the total protein as well as Flot2-GFP content in the dissolved microsomal fraction was sufficient to perform the IP-MS analysis.

During the isolation of the plasma membrane fraction, a significantly lower yield of total proteins was obtained compared to the yield of proteins in the microsomal fraction. Finally, only approximately 2 μg of total proteins per 1 g of initial material were obtained in the enriched plasma membrane fraction. Nevertheless, the signal of Flot2-GFP in the enriched plasma membrane fraction (PMx line) was more intense than its signal in the cross-linked microsomal fractions (Mx line), which indicates that Flot2-GFP was successfully enriched in the plasma membrane fraction (**Figure 2B**).

Identification of Proteins Interacting With Flot2-GFP

Immunoprecipitation-MS of the microsomal as well as plasma membrane fraction was performed in nine repetitions. Only proteins which were detected at least three times in the immunoprecipitated *AtFlot2-GFP* membrane fractions and were not detected in the WT membrane fractions (control) were considered to be potential interactors of Flot2-GFP (**Table 1**). However, three additional proteins which were also detected in the control samples were included in the list of potential interactors, since they were significantly enriched in the *AtFlot2-GFP* sample according to MS intensity-based semiquantitative analysis. It can be seen in **Table 1** that the IP-MS of the microsomal fraction provided a substantially lower number of potential interactors than the plasma membrane fraction. In total, 16 proteins were detected in this fraction, and only three of those were proposed to be Flot2 interaction partners. The majority of the detected proteins were actually only detected in one or two repetitions (Supplementary Table S2a). On the other hand, 61 proteins were enriched in the *AtFlot-GFP* plasma membrane fraction (Supplementary Table S2b). Of those, 19 proteins were proposed to be Flot2 interaction partners (**Table 1**).

To obtain greater insight into the proteins enriched by IP in both analyzed fractions (see Supplementary Table S2), a cluster analysis of GO annotation terms with respect to their localization and biological significance was performed using the DAVID Bioinformatics Resources annotation tool[3] (Huang et al., 2009; **Figure 3**). Through the analysis of GO Cellular Component terms, it was found that the terms connected with the plasma membrane localization were only enriched when the plasma membrane fraction was used for the purification. This result shows the crucial importance of the appropriate fractioning of membrane proteins prior to their analysis. One of the most

[3]http://david.ncifcrf.gov

TABLE 1 | Potential interactors of Arabidopsis flotillin 2.

F	Protein	Gene name	Locus	Counts		RQI
				AtFlot2-GFP	WT	
M	Flotillin 2	FLOT2	At5g25260	9	–	–
	Ubiquitin-60S ribosomal protein L40-1	RPL40A	At2g36170	5	–	–
	Aquaporin PIP2-1	PIP2-1	At3g53420	5	–	–
	Glyceraldehyde-3-phosphate dehydrogenase	GAPA1	At3g26650	3	–	–
PM	Flotillin 2	FLOT2	At5g25260	9	–	–
	Photosystem I reaction center subunit II-2, chloroplastic	PSAD2	At1g03130	5	–	–
	ATPase 1, plasma membrane-type	AHA1	At2g18960	3	–	–
	Early-responsive to dehydration stress protein	ERD4	At1g30360	3	–	–
	ABC transporter G family member 36	ABCG36	At1g59870	3	–	–
	Ubiquitin-60S ribosomal protein L40-1	RPL40A	At2g36170	3	–	–
	Aquaporin PIP1-2	PIP1-2	At2g45960	3	–	–
	Syntaxin-71	SYP71	At3g09740	3	–	–
	Aquaporin PIP2-2	PIP2-2	At2g37170	3	–	–
	Harpin-induced protein-like	NHL3	At5g06320	3	–	–
	Hypersensitive-induced response protein 2*	HIR2	At3g01290	3	–	–
	Pyrophosphate-energized vacuolar membrane proton pump 1	AVP1	At1g15690	3	–	–
	Tubulin beta-5 chain	TUBB5	At1g20010	3	–	–
	5-methyltetrahydropteroyltri-glutamate-homocysteine methyltransferase 1	MS1	At5g17920	3	–	–
	Probable aquaporin PIP2-6	PIP2-6	At2g39010	3	–	–
	Probable inactive receptor kinase	–	At5g16590	3	–	–
	Aquaporin PIP2-1	PIP2-1	At3g53420	9	5	4.4
	Aquaporin PIP2-7	PIP2-7	At4g35100	8	3	3.5
	Carbonic anhydrase 2, chloroplastic	BCA2	At5g14740	7	1	3.2

*F, fraction; M, microsomal fraction; PM, plasma membrane fraction; Counts, number of IP repetitions (out of nine), in which the protein was detected; RQI, relative intensity index; * At3g01290 is designated as HIR3 in UniProt database (www.uniprot.org).*

frequently occurring annotations of proteins purified from the plasma membrane fraction was localization in chloroplasts. When we mapped the proteins clustered within the chloroplast annotation, we found that half of them are simultaneously annotated to be localized in both, the plasma membrane and chloroplasts. Thus it is clear that the results of GO annotation cluster analysis can be influenced by the multiple annotations that exist for the proteins, and should therefore be carefully inspected.

According to the clustering of the GO Biological Process terms of proteins purified from the plasma membrane fraction, the potential interactors of Flot2 are predominantly involved in the plant response to various stress factors, such as the presence of cadmium ions, abscisic acid, bacteria, salt stress or water deprivation. Additionally, the response to water deprivation is the only process common to the proteins purified from both fractions.

Verification of Flot2 Interactions by Split-Ubiquitin Yeast System

After having determined the potential Flot2 interactors, we applied the yeast SUS to test whether some of the revealed proteins interact directly with Flot2. In the system used, Flot2 was C-terminally fused with the C-terminal moiety of ubiquitin (Cub) and hybrid transcription factor PLV (ProteinA-LexA-VP16), which enables yeast growth on the selection medium. The methionine-repressible vector allows expression tuning in order to avoid false positive results (Grefen et al., 2007). Selected potential interactors of Flot2 were N-terminally fused to the N-terminal moiety of mutated ubiquitin (NubG), which is prevented from spontaneously reassembling with Cub.

Twelve possible interactors from **Table 1** were investigated by SUS, of which seven gave positive results (**Figure 4**). Among the five plasma membrane aquaporins, yeast growth was only observed for PIP1-2 and PIP2-6. Nevertheless, the yeast growth was relatively weak for both PIPs. This suggests a weak or very transient interaction between PIPs and Flot2. The strong yeast growth apparent for plasma membrane ATPase 1 (AHA1), early-responsive to dehydration (ERD) stress protein (ERD4), hypersensitive-induced response protein 2 (HIR2), harpin-induced protein-like (NHL3) and syntaxin-71 (SYP71) demonstrate physical interaction with Flot2. The expression of aquaporins PIP2-1, PIP2-2, and PIP2-7, pyrophosphate-energized vacuolar membrane proton pump 1 (AVP1) and probable inactive receptor kinase (At5g16590) in co-transformed yeasts was confirmed (see Supplementary Figure 1) to rule out the possibility that the lack of yeast growth observed in these cases was caused by a lack of Nub-fused prey proteins. The positive expression of all five putative interactors implies that none of these proteins would directly interact with Flot2.

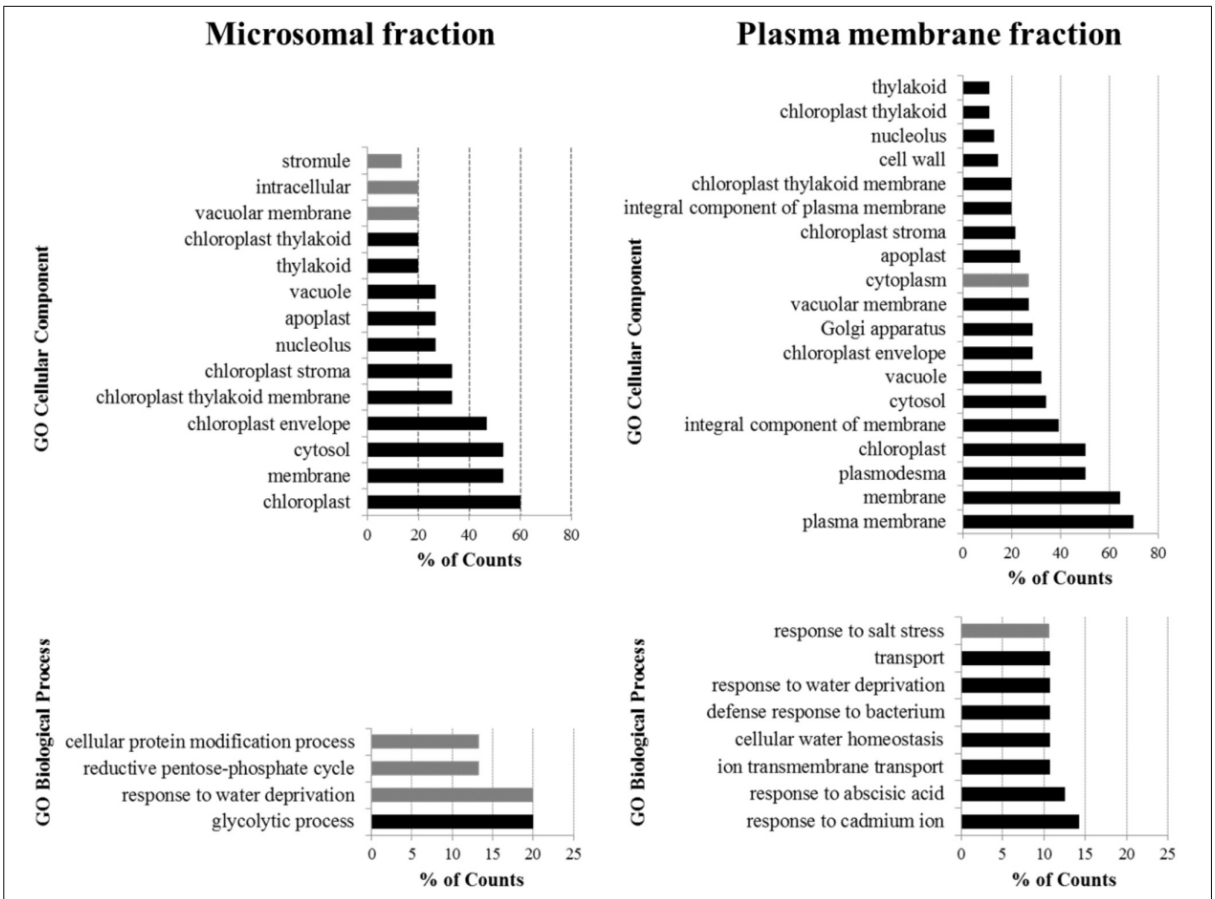

FIGURE 3 | Cluster analysis of GO annotation terms of proteins enriched by IP of microsomal and plasma membrane fraction. The DAVID Bioinformatics Resources functional annotation clustering algorithm was used to cluster the most significant terms in the GO Cellular Component and GO Biological Process annotations. The terms are ordered from least frequent (top) to most frequent (bottom). Black bars indicate terms enriched with $p < 0.01$, gray bars indicate terms enriched with $p \geq 0.01$.

DISCUSSION

Flot2-GFP Cellular Localization

Although metazoan flotillins were found to be most frequently localized to plasma membrane microdomains or endosomes (Baumann et al., 2000; Dermine et al., 2001; Glebov et al., 2006; Neumann-Giesen et al., 2007; Langhorst et al., 2008), they were also rarely detected in the mitochondria or nucleus of human cells (Santamaria et al., 2005; Ogura et al., 2014). In plants, a similar localization was observed in several studies, where the *A. thaliana* Flot1, *Picea meyeri* Flot1, and *Oryza sativa* Flot1 were enriched in the plasma membrane DRM fraction (Triton X-100-insoluble plasma membrane fraction) prepared from *A. thaliana* calli, spruce pollen tubes, and rice cells (Borner et al., 2005; Liu P. et al., 2009; Ishikawa et al., 2015). While Flot1 localization to the plasma membrane was confirmed by the confocal microscopy of *A. thaliana* stably transformed with *GFP-Flot1* (Li et al., 2012; Hao et al., 2014), the localization of Flot2 to the plasma membrane was only observed when YFP-fused Flot2 was transiently expressed in *N. benthamiana* leaf epidermal cells (Jarsch et al., 2014). Therefore, we investigated the localization of Flot2 directly in the epidermal cells of the roots and cotyledons of *A. thaliana* stably transformed with *Flot2-GFP*, and thus we confirmed its predominant localization to the plasma membrane (**Figure 1**).

Enrichment of Flot2-GFP Containing Complexes

Due to the many difficulties associated with the IP/AP-MS of membrane protein complexes, new approaches are being investigated (Qi and Katagiri, 2009; Smaczniak et al., 2012; Huang and Kim, 2013; Dorr et al., 2016). Because of the low abundance of membrane proteins, there is a need to use harsh conditions in order to ensure their efficient solubilization and release from the membrane. To maintain protein interactions under these conditions, chemical cross-linkers providing a covalent

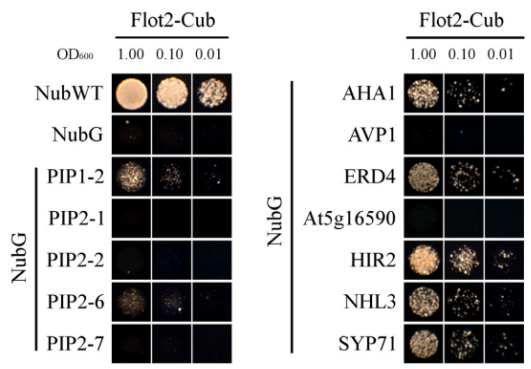

FIGURE 4 | SUS test. Yeast strain THY.AP4 co-expressing Flot2-Cub-PLV and Nub fused with investigated possible interactors were plated in decimal dilution (OD_{600} = 1.00 or 0.10 or 0.01) onto selective media (without Ade, His, Leu, Trp) which was supplemented with 50, 250, or 500 μM Met in order to obtain a different expression level of the bait. Yeast growth rate was gradually repressed with an increasing concentration of Met. Only plates with 500 μM Met are presented. Plates were incubated for 48 h at 28°C. NubWT and NubG as prey were used as positive and negative controls, respectively. Similar growth performance was observed for each interaction with at least three biological replicates.

binding of proteins in complexes could be used. With plant cell suspension cultures or seedlings, *in vivo* cross-linking can be performed using membrane-permeable cross-linkers such as DSP (Jafferali et al., 2014; Kaake et al., 2014). Nevertheless, *in vitro* cross-linking has also been successfully applied, where full-grown plants were used as input material (Qi and Katagiri, 2009; Qi et al., 2011). The chemical cross-linking of protein complexes also enables more stringent conditions to be used during IP/AP to eliminate the non-specific background.

Whole plants or their specific tissues, organs or cell compartments need to be analyzed when the plant development pathways or pathways specific for tissue, cell type or cell compartment are being studied (Ephritikhine et al., 2004; Tan et al., 2008). Nevertheless, the presence of abundant soluble proteins during the purification step can greatly contribute to an increase in false positives and, additionally, could be also problematic in MS-based approaches, where soluble proteins are favored over hydrophobic and low-abundant membrane proteins (Gilmore and Washburn, 2010). Therefore, the isolation of the whole membrane fraction or individual membrane compartments should be performed prior to purification (Speers and Wu, 2007; Qi and Katagiri, 2009; Savas et al., 2011).

In our study, we used both the *in vitro* cross-linking of membrane proteins in close proximity to each other to maintain the interactions in complexes during sample preparation, and the enrichment of Flot2-GFP in microsomes and the plasma membrane fraction prior to IP-MS. Compared to the results obtained by the IP-MS of the microsomal fraction, we were able to capture a substantially higher number of interactors localized to the plasma membrane by IP-MS of the enriched plasma membrane (**Figure 3**). Despite the large amount of initial plant material entering the analysis, due to the low abundance of plasma membrane within plant membranes, together with the substantial loss of plant material during the isolation of the plasma membrane from whole plants, we believe that this direct approach is indispensable for a better description of plasma membrane complexes.

Determination of Flot2 Interactors

We used IP-MS to suggest potential interacting partners of Flot2. IP/AP-MS has become widely used nowadays, mainly thanks to the development of MS instrumentation that enables more efficient data acquisition. On the other hand, unfiltered IP/AP-MS data sets could give a large number of false positive interactions. To deal with this, a high number of repetitions and high number of controls should be analyzed (Pardo and Choudhary, 2012), different tags (Ho et al., 2002) as well as tag combinations (Van Leene et al., 2015) can be used, or some computational or informatics strategies can be applied for the evaluation of specific protein interactors (Collins and Choudhary, 2008; Choi H. et al., 2011; Nesvizhskii, 2012).

To identify specific interactors from the obtained IP-MS data set, some independent techniques such as Förster resonance energy transfer (FRET) or yeast two-hybrid assay can be used. In our study we suggested potential interactors by IP-MS and the specific interactors of Flot2 were then determined by SUS, a variant of yeast two-hybrid assay suitable for detecting a direct interaction between membrane-localized proteins.

Although SUS is far less used than the classical yeast two-hybrid test or bimolecular fluorescence complementation, it has been applied in more than 200 publications in major plant science journals to date (reviewed in Xing et al., 2016). Since SUS is a protein fragment complementation-based assay, there is a possibility of false positive (in comparison with e.g., FRET) as well as false negative results. To assess the possibility of false negative results (i.e., PIP2-1, PIP2-2, PIP2-7, AVP1, and At5g16590 in our study), it is necessary to keep in mind that the proper localization of both split ubiquitin moieties (to enable their reassembling at the cytoplasmatic side of the membrane) is a crucial prerequisite for the successful application of SUS. Therefore, the position of the N- or C-terminus of the investigated proteins (inside versus outside the cytoplasm) has to be considered when deciding, which protein terminus should be tagged with the split-ubiquitin moiety. In our study, all selected putative Flot2 interactors were fused at their N-terminus with NubG. In PIPs, both N- and C-terminal stretches are localized on the cytoplasmic sides of biomembranes (Murata et al., 2000; Luang and Hrmova, 2017), so tagging with NubG at each end is possible.

Nevertheless, proposing a suitable position for NubG fusion is tricky with AVP1 and At5g16590. AVP1 membrane topology prediction in tonoplasts suggests that both ends are localized inside vacuolar lumen (Pizzio et al., 2017). Hence, neither N- nor C-terminal fusion to NubG would be relevant for the interaction with cytoplasm-facing Cub. The structure of the At5g16590 protein is not published, and membrane-protein topology predictors do not provide unambiguous results (e.g., TMpred predicts the N-terminus in the cytoplasm while TMMOD predicts it on the extracellular side). On the other hand, At5g16590 belongs to a leucine-rich repeat kinase family,

the majority of which have their N-terminal domains on the extracellular side of the plasma membrane (Diévart and Clark, 2003). However, several interactors were found for both NubG- and Cub-fused AVP1 and At5g16590 protein in Associomics. Thus, additional SUS assays with AVP1 and At5g16590 fused to NubG at their C-terminus will be necessary to further verify the interaction with Flot2 and potentially rule out the results found in this study as a false negative.

Flot2 Interactors Are Found in Specific Plasma Membrane Subfractions

In our study, Flot2-GFP was found to be enriched in the deoxycholate-insoluble part of the microsomal fraction and the enriched plasma membrane fraction (**Figure 2**). Correspondingly most of the putative interactors found in our screen were already identified in membrane fractions resistant to mild detergents. AHA1, SYP71, NHL3, ERD4, PIP1-2, PIP2-7, and HIR2 as well as other HIR homologs HIR1 and HIR4 were enriched in the plasma membrane DRM fraction obtained from Arabidopsis plants, calli or suspension cells (Shahollari et al., 2004; Borner et al., 2005; Keinath et al., 2010). Moreover, homologs of SYP71, AHA1, and several PIPs were found in the plasma membrane DRM fraction from tobacco leaves (Mongrand et al., 2004). Although Flot2 was not identified in any of those studies, its closest homolog Flot1 (Yu et al., 2017) was reported to be present in similarly prepared plasma membrane fractions (Borner et al., 2005; Ishikawa et al., 2015). Additionally, rice Flot was also enriched when plasma membrane DRM fractions were prepared from rice (Ishikawa et al., 2015). Additionally, AHA1 and HIR2 together with AHA2, HIR1, and HIR4 were identified as major proteins tightly associated with a plasma membrane resistant to NaCl and Na_2CO_3 washing (Marmagne et al., 2007). Such a co-occurrence in specific plasma membrane sub-compartments may suggest a functional linkage in many cellular processes.

Identified Interactors Suggest Putative Functions

Flot2 transcription is highly upregulated upon bacterial, fungal, viral and oomycetal infection (Mohr and Cahill, 2007; Danek et al., 2016). Its transcription together with that of *SYP71*, *HIR2*, *NHL3* and *Flot3*, *HIR1*, *HIR3*, and *HIR4* were increased under viral infection (Ascencio-Ibanez et al., 2008). Increased *HIR2*, *Flot2* as well as *Flot1* transcription in mutants with altered systemic acquired resistance also suggests their involvement in this type of defense mechanism (Mosher et al., 2006). Moreover, the content of direct Flot2 interactors SYP71, AHA1, NHL3, ERD4, HIR2, and the HIR1 and HIR4 content in the plasma membrane DRM fraction was increased after treatment with the bacteria-derived elicitor flg22 (Keinath et al., 2010). Several of these interactors have been reported to be involved in resistance against pathogens.

Flot2 has already been found to directly interact with SYP71, a member of a plant-specific subfamily of Qc SNARE proteins (Sanderfoot et al., 2001). SYP71 transcription is increased under viral infection (Ascencio-Ibanez et al., 2008) and it plays a role in viral protein within the cell (Wei et al., 2013). Wheat and rice SYP71 homologs confer resistance to stripe rust and blast, respectively, and their transcription is upregulated upon infection by the respective pathogens, as well as upon treatment with hydrogen peroxide (Bao et al., 2012; Liu et al., 2016), a hallmark of hypersensitive plant defense (Coll et al., 2011). *Lotus japonicus* SYP71 is important for proper nodulation in *Mesorhizobium loti* symbiosis (Hakoyama et al., 2012). Interestingly, *M. truncatula* Flot2 and Flot4 are involved in nodulation, probably due to an interaction with an activated nodulation factor receptor (Haney and Long, 2010; Haney et al., 2011).

HIR2, another direct interactor of Flot2, belongs to the subfamily of SPFH proteins and is thus related to flotillins (Di et al., 2010). Four Arabidopsis HIRs interact with one another and HIR2 and HIR1 directly interact with the immune receptor RPS2. The interaction participates in effector-triggered resistance against *Pseudomonas syringae* (Qi et al., 2011). HIR homologs in pepper, rice and barley mediate the hypersensitive response to pathogens via an interaction with leucine-rich repeat proteins (Jung and Hwang, 2007; Zhou et al., 2009, 2010; Choi H.W. et al., 2011; Cheng et al., 2017).

NHL3 (NDR1/HIN1-LIKE 3) is another directly interacting protein involved in the plant–pathogen interaction. The transcription of NHL3 is induced by salicylic acid treatment, bacterial infection (Varet et al., 2002; Ditt et al., 2006), hydrogen peroxide treatment (Davletova et al., 2005) and by spermine, a polyamine signaling molecule inducing the expression of pathogenesis-related genes (Zheng et al., 2004). The overexpression of NHL3 leads to increased resistance to *P. syringae*. NHL3 was shown to be tightly associated with the plasma membrane (Varet et al., 2003), where it physically interacts with the oxidation-related zinc finger one protein that is also involved in salicylic acid-mediated defense reactions to bacterial attack (Singh et al., 2018).

The plasma membrane-localized H^+ATPase AHA1 is a major proton pump contributing to stomata opening (Yamauchi et al., 2016), which makes it also closely connected with pathogen resistance reactions. AHA1 activity is altered by methyl jasmonate treatment (Yan et al., 2015) and binding to the bacterial effector AvrB (Zhou et al., 2015) or RIN4, a target of bacterial effectors (Liu J. et al., 2009). AHA1 together with HIR2 and HIR4 co-immunoprecipitated with HIR1 (Lv et al., 2017) and with Bax Inhibitor 1, an ER-localized suppressor of cell death after fungal infection (Weis et al., 2013). Interestingly, the overexpression of Bax Inhibitor 1 in rice cells resulted in the depletion of rice Flot and HIR homologs from DRM (Ishikawa et al., 2015). These findings suggest the involvment of HIRs, Flots and AHA1 in a shared pathway controling cell death and/or the reaction to pathogen attack.

We observed a direct interaction with two (PIP1-2 and PIP2-6) of five PIPs co-immunoprecipitating with Flot2. *PIP1-2*, *PIP2-1*, *PIP2-2*, and *PIP2-7* transcription is significantly decreased under drought stress, whereas *PIP2-6* transcription does not change (Alexandersson et al., 2005). PIP1-2 alone contributes, but due to functional redundancy with other PIPs, it is not essential for plant growth or water transport (Postaire et al., 2010); however, it is important for CO_2 permeability and thus for

the net photosynthesis rate (Heckwolf et al., 2011; Uehlein et al., 2012).

Besides this, the proper cellular trafficking of PIP2-7 and PIP2-2 between endomembranes and the plasma membrane is dependent on direct interaction with SYP121 and SYP61 (Hachez et al., 2014). A similar requirement was reported for maize PIP2-5 (Besserer et al., 2012). SYP121 also directly interacts with PIP2-2 (Besserer et al., 2012) and co-immunoprecipitates with SYP71 as well as some other SYPs, and, moreover, with HIR2 (Fujiwara et al., 2014). In addition, functional aquaporins are formed as tetramers, where the hetero-tetramerization of several single PIP isoforms has been reported (Jozefkowicz et al., 2017). The hetero-oligomerization of PIP1 and PIP2 group aquaporins is necessary for the trafficking of maize PIP1s to the plasma membrane (Zelazny et al., 2007).

PIP2-1 and PIP1-2 interact with several hundred proteins. Physical interaction was confirmed for PIP2-1 and NHL3 (Bellati et al., 2016), and three HIRs were detected to co-immunoprecipitate with at least one of PIP2-1 and PIP1-2. Therefore, a putative indirect linkage between PIP2-1, PIP2-2, PIP2-7, and Flot2 may be realized via PIP2-6 and PIP1-2, via SYP71 and SYP121 (with or without the involvement of HIR2), or via NHL3 or HIR2. Moreover, *PIP2-1* transcription in roots is decreased upon exposure to NaCl (Boursiac et al., 2005) and PIP2-1 was observed to be endocytosed from the plasma membrane upon NaCl treatment via Flot1-mediated endocytosis (Li et al., 2011). A similar involvement of Flot1 in clathrin-independent endocytosis was observed for the ammonium transporter AMT1-3 (Wang et al., 2015). Interestingly AMT1-3 was also found to interact with several Flot2 interactors determined in our study (Bellati et al., 2016). The function of Flot1 endocytosis remains unclear, but based on the very close similarity of both isoforms, it is possible that a Flot2-based complex can be implicated in similar processes.

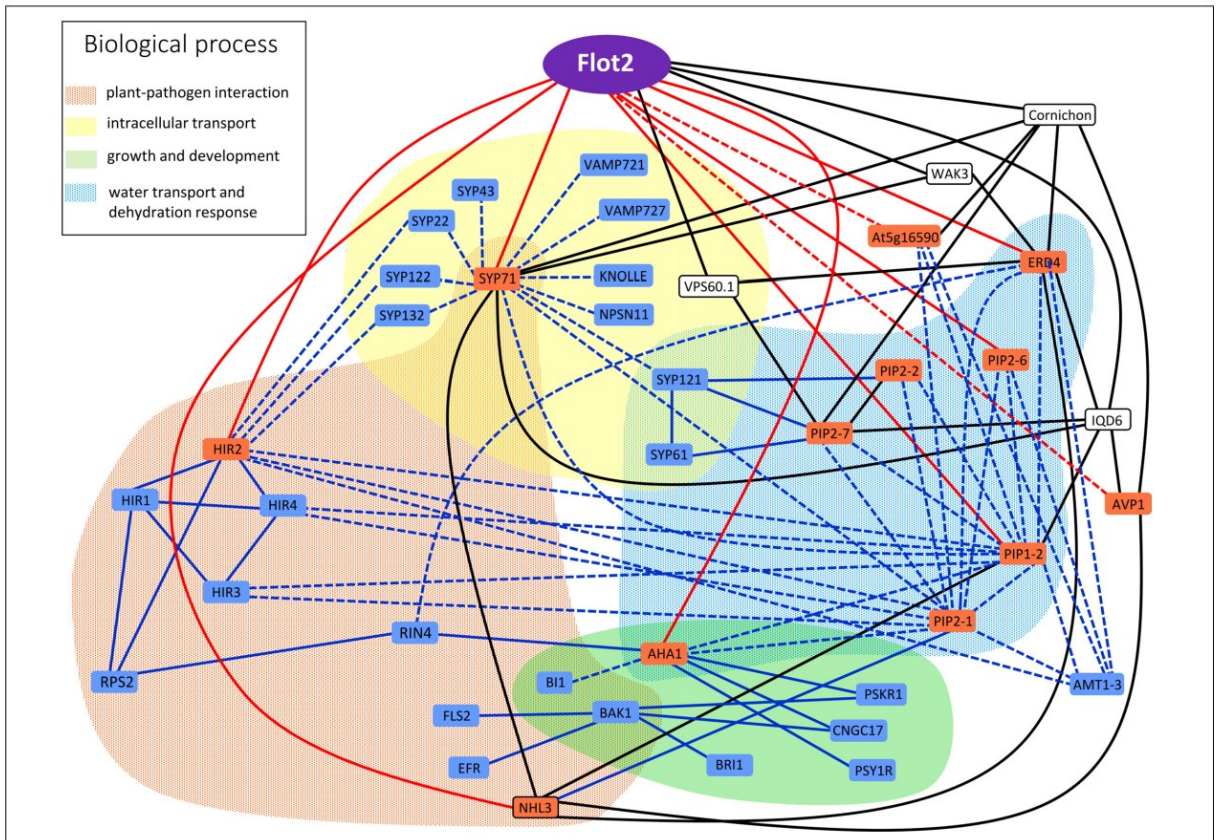

FIGURE 5 | Graphical representation of Flot2 interaction network. Interactors experimentally determined in our study are displayed in red boxes. Solid red lines represent direct binding with Flot2 verified by SUS, while dashed red lines depict putative indirect interactions with Flot2 with negative SUS results. Blue boxes and lines represent direct (solid lines) or indirect (dashed lines) interactions published in literature and mentioned in discussion. Pair–wise interactions confirmed by yeast two hybrid or split ubiquitin assay, bimolecular fluorescence complementation or FRET/FLIM measurement are assumed as direct. Proteins found in co-IP assays and determined by mass spectrometry or revealed in tagged-protein pull-down assays, which were neither tested nor confirmed to be direct (by the methods listed above), were considered putative indirect interactors. Black boxes and lines represent most common direct interactions retrieved from Associomics database, which are common to several proteins detected in our study as well as Flot2. The implication of interactors in important biological processes is distinguished by colored fields.

AHA1 also contributes to water transport by its direct interaction with phytosulfokine receptors PSKR1 and PSKR2 and cyclic nucleotide-gated channel 17, a receptor for cyclic guanosine monophosphate. The application of both signal ligands leads to increased water influx, which is important for the volume growth of plant cells (Ladwig et al., 2015). Similarly, AHA1 is phosphorylated with the activated receptor of the peptide plant regulator PSY1R, which leads to root and hypocotyl elongation (Fuglsang et al., 2014). Proper AHA1 trafficking to the plasma membrane is important for plant growth, as plants with AHA1 accumulated in their endomembranes are smaller in size (Hashimoto-Sugimoto et al., 2013).

The participation of Flot2 in water management is also suggested by the direct interaction between Flot2 and ERD4, a member of the ERD protein family (Kiyosue et al., 1994). Enhanced tolerance to drought and salt stress was observed in Arabidopsis overexpressing maize *ERD4* (Liu Y. et al., 2009).

Although the identification of Flot2 specific interactors can suggest a potential role of Flot2 in *A. thaliana*, further studies are required. Phenotypic analysis of *Flot2* loss-of function mutants could be a valuable approach. We initially tested several abiotic and biotic treatments using a *flot2* T-DNA insertion line but did not observe any major effect different from wild type plants. Since there are three isoforms of flotillins encoded in *A. thaliana*, functional redundancy of these single isoforms may be an explanation for this lack of phenotype. Generation of multiple mutants may thus be necessary.

Flot2 Interactome Forms a Complex Interlinked Network

As has already been pointed out, proteins found to interact with Flot2 in this study may also in many cases interact with each other, and thus it is possible that a given protein may be involved in several cellular functions. The situation gets even more complicated when direct interactors of each protein retrieved from the Associomic database are added to the list (**Figure 5**). Interestingly, it could be seen in Associomics that many of the Flot2 interactors found in this study also interact with other Flot2 interactors listed in Associomics. The most common interactors are NHL3, cornichon and IQD6. Since these proteins have several hundred interactors in Associomics, they could serve as real docking hubs for many proteins in the plasma membrane, and could thus be the crossroads or signposts of many pathways. On the other hand, it is possible that these proteins might be just too prone to giving false positive results. Intriguingly, the direct interactions of Flot2 that we confirmed in our study are not proposed for Flot2 in Associomics. Similarly, the direct interaction of NHL3 with PIP2-1 published in Bellati et al. (2016) is not found in Associomics. This comparison in fact demonstrates the general importance of the IP approach to membrane protein interactome determination.

AUTHOR CONTRIBUTIONS

JB, DK, and MD generated plant material. PJ, MH, RH, and OV contributed to the proteomic analysis and evaluation of results. MD, EZ, and KK prepared and performed SUS assays. PJ, MD, MJ, OV, and JM wrote the manuscript. PJ and MD contributed equally to this article.

FUNDING

This work was supported by the Czech Science Foundation grant no. 14-09685S and by the Program Barrande grant no. 7AMB17FR005 provided by the Czech Ministry of Education, Youth and Sports and by French Ministry for Europe and Foreign Affairs (MEAE), and Ministry of Higher Education, Research and Innovation (MESRI).

ACKNOWLEDGMENTS

The authors would like to thank Christopher Grefen, University of Tuebingen, Germany and François Chaumont and Timothée Laloux, Université catholique de Louvain, Belgium for sharing vectors and the yeast strain used in SUS assay as well as Kateřina Vltavská, Institute of Experimental Botany, Czech Republic, for her excellent technical assistance.

SUPPLEMENTARY MATERIAL

The Supplementary Material for this article can be found online at: https://www.frontiersin.org/articles/10.3389/fpls.2018.00991/full#supplementary-material

REFERENCES

Alexandersson, E., Fraysse, L., Sjovall-Larsen, S., Gustavsson, S., Fellert, M., Karlsson, M., et al. (2005). Whole gene family expression and drought stress regulation of aquaporins. *Plant Mol. Biol.* 59, 469–484. doi: 10.1007/s11103-005-0352-1

Amaddii, M., Meister, M., Banning, A., Tomasovic, A., Mooz, J., Rajalingam, K., et al. (2012). Flotillin-1/reggie-2 protein plays dual role in activation of receptor-tyrosine kinase/mitogen-activated protein kinase signaling. *J. Biol. Chem.* 287, 7265–7278. doi: 10.1074/jbc.M111.287599

Ascencio-Ibanez, J. T., Sozzani, R., Lee, T. J., Chu, T. M., Wolfinger, R. D., Cella, R., et al. (2008). Global analysis of *Arabidopsis* gene expression uncovers a complex array of changes impacting pathogen response and cell cycle during geminivirus infection. *Plant Physiol.* 148, 436–454. doi: 10.1104/pp.108.121038

Bao, Y. M., Sun, S. J., Li, M., Li, L., Cao, W. L., Luo, J., et al. (2012). Overexpression of the Qc-SNARE gene *OsSYP71* enhances tolerance to oxidative stress and resistance to rice blast in rice (*Oryza sativa* L.). *Gene* 504, 238–244. doi: 10.1016/j.gene.2012.05.011

Baumann, C. A., Ribon, V., Kanzaki, M., Thurmond, D. C., Mora, S., Shigematsu, S., et al. (2000). CAP defines a second signalling pathway required for insulin-stimulated glucose transport. *Nature* 407, 202–207. doi: 10.1038/35025089

Bellati, J., Champeyroux, C., Hem, S., Rofidal, V., Krouk, G., Maurel, C., et al. (2016). Novel aquaporin regulatory mechanisms revealed by interactomics. *Mol. Cell. Proteomics* 15, 3473–3487. doi: 10.1074/mcp.M116.060087

Besserer, A., Burnotte, E., Bienert, G. P., Chevalier, A. S., Errachid, A., Grefen, C., et al. (2012). Selective regulation of maize plasma membrane aquaporin

trafficking and activity by the SNARE SYP121. *Plant Cell* 24, 3463–3481. doi: 10.1105/tpc.112.101758

Bickel, P. E., Scherer, P. E., Schnitzer, J. E., Oh, P., Lisanti, M. P., and Lodish, H. F. (1997). Flotillin and epidermal surface antigen define a new family of caveolae-associated integral membrane proteins. *J. Biol. Chem.* 272, 13793–13802. doi: 10.1074/jbc.272.21.13793

Borner, G. H. H., Sherrier, D. J., Weimar, T., Michaelson, L. V., Hawkins, N. D., MacAskill, A., et al. (2005). Analysis of detergent-resistant membranes in *Arabidopsis*. Evidence for plasma membrane lipid rafts. *Plant Physiol.* 137, 104–116. doi: 10.1104/pp.104.053041

Boursiac, Y., Chen, S., Luu, D. T., Sorieul, M., van den Dries, N., and Maurel, C. (2005). Early effects of salinity on water transport in *Arabidopsis* roots. molecular and cellular features of aquaporin expression. *Plant Physiol.* 139, 790–805. doi: 10.1104/pp.105.065029

Browman, D. T., Hoegg, M. B., and Robbins, S. M. (2007). The SPFH domain-containing proteins: more than lipid raft markers. *Trends Cell Biol.* 17, 394–402. doi: 10.1016/j.tcb.2007.06.005

Cacas, J. L., Bure, C., Grosjean, K., Gerbeau-Pissot, P., Lherminier, J., Rombouts, Y., et al. (2016). Revisiting plant plasma membrane lipids in tobacco: a focus on sphingolipids. *Plant Physiol.* 170, 367–384. doi: 10.1104/pp.15.00564

Cheng, W., Xiao, Z. L., Cai, H. Y., Wang, C. Q., Hu, Y., Xiao, Y. P., et al. (2017). A novel leucine-rich repeat protein, CaLRR51, acts as a positive regulator in the response of pepper to *Ralstonia solanacearum* infection. *Mol. Plant Pathol.* 18, 1089–1100. doi: 10.1111/mpp.12462

Choi, H., Larsen, B., Lin, Z. Y., Breitkreutz, A., Mellacheruvu, D., Fermin, D., et al. (2011). SAINT: probabilistic scoring of affinity purification-mass spectrometry data. *Nat. Methods* 8, 70–73. doi: 10.1038/Nmeth.1541

Choi, H. W., Kim, Y. J., and Hwang, B. K. (2011). The Hypersensitive induced reaction and leucine-rich repeat proteins regulate plant cell death associated with disease and plant immunity. *Mol. Plant Microbe Interact.* 24, 68–78. doi: 10.1094/MPMI-02-10-0030

Coll, N. S., Epple, P., and Dangl, J. L. (2011). Programmed cell death in the plant immune system. *Cell Death Differ.* 18, 1247–1256. doi: 10.1038/cdd.2011.37

Collins, M. O., and Choudhary, J. S. (2008). Mapping multiprotein complexes by affinity purification and mass spectrometry. *Curr. Opin. Biotechnol.* 19, 324–330. doi: 10.1016/j.copbio.2008.06.002

Danek, M., Valentova, O., and Martinec, J. (2016). Flotillins, erlins, and hirs: from animal base camp to plant new horizons. *Crit. Rev. Plant Sci.* 35, 191–214. doi: 10.1080/07352689.2016.1249690

Davletova, S., Schlauch, K., Coutu, J., and Mittler, R. (2005). The zinc-finger protein Zat12 plays a central role in reactive oxygen and abiotic stress signaling in *Arabidopsis*. *Plant Physiol.* 139, 847–856. doi: 10.1104/pp.105.068254

Dedecker, M., Van Leene, J., and De Jaeger, G. (2015). Unravelling plant molecular machineries through affinity purification coupled to mass spectrometry. *Curr. Opin. Plant Biol.* 24, 1–9. doi: 10.1016/j.pbi.2015.01.001

Dermine, J. F., Duclos, S., Garin, J., St-Louis, F., Rea, S., Parton, R. G., et al. (2001). Flotillin-1-enriched lipid raft domains accumulate on maturing phagosomes. *J. Biol. Chem.* 276, 18507–18512. doi: 10.1074/jbc.M101113200

Di, C., Xu, W. Y., Su, Z., and Yuan, J. S. (2010). Comparative genome analysis of PHB gene family reveals deep evolutionary origins and diverse gene function. *BMC Bioinformatics* 11(Suppl. 6):S22. doi: 10.1186/1471-2105-11-s6-s22

Diévart, A., and Clark, S. E. (2003). Using mutant alleles to determine the structure and function of leucine-rich repeat receptor-like kinases. *Curr. Opin. Plant Biol.* 6, 507–516. doi: 10.1016/S1369-5266(03)00089-X

Ditt, R. F., Kerr, K. F., de Figueiredo, P., Delrow, J., Comai, L., and Nester, E. W. (2006). The *Arabidopsis thaliana* transcriptome in response to *Agrobacterium tumefaciens*. *Mol. Plant Microbe Interact.* 19, 665–681. doi: 10.1094/MPMI-19-0665

Dorr, J. M., Scheidelaar, S., Koorengevel, M. C., Dominguez, J. J., Schafer, M., van Walree, C. A., et al. (2016). The styrene-maleic acid copolymer: a versatile tool in membrane research. *Eur. Biophys. J.* 45, 3–21. doi: 10.1007/s00249-015-1093-y

Dunham, W. H., Mullin, M., and Gingras, A. C. (2012). Affinity-purification coupled to mass spectrometry: basic principles and strategies. *Proteomics* 12, 1576–1590. doi: 10.1002/pmic.201100523

Ephritikhine, G., Ferro, M., and Rolland, N. (2004). Plant membrane proteomics. *Plant Physiol. Biochem.* 42, 943–962. doi: 10.1016/j.plaphy.2004.11.004

Fuglsang, A. T., Kristensen, A., Cuin, T. A., Schulze, W. X., Persson, J., Thuesen, K. H., et al. (2014). Receptor kinase-mediated control of primary active proton pumping at the plasma membrane. *Plant J.* 80, 951–964. doi: 10.1111/tpj.12680

Fujiwara, M., Uemura, T., Ebine, K., Nishimori, Y., Ueda, T., Nakano, A., et al. (2014). Interactomics of Qa-SNARE in *Arabidopsis thaliana*. *Plant Cell Physiol.* 55, 781–789. doi: 10.1093/pcp/pcu038

Gehl, B., Lee, C. P., Bota, P., Blatt, M. R., and Sweetlove, L. J. (2014). An *Arabidopsis* stomatin-like protein affects mitochondrial respiratory supercomplex organization. *Plant Physiol.* 164, 1389–1400. doi: 10.1104/pp.113.230383

Gilmore, J. M., and Washburn, M. P. (2010). Advances in shotgun proteomics and the analysis of membrane proteomes. *J. Proteomics* 73, 2078–2091. doi: 10.1016/j.jprot.2010.08.005

Glebov, O. O., Bright, N. A., and Nichols, B. J. (2006). Flotillin-1 defines a clathrin-independent endocytic pathway in mammalian cells. *Nat. Cell Biol.* 8, 46–54. doi: 10.1038/ncb1342

Green, J. B., and Young, J. P. W. (2008). Slipins: ancient origin, duplication and diversification of the stomatin protein family. *BMC Evol. Biol.* 8:44. doi: 10.1186/1471-2148-8-44

Grefen, C. (2014). "The split-ubiquitin system for the analysis of three-component interactions," in *Arabidopsis Protocols*, eds J. J. Sanchez-Serrano and J. Salinas (Totowa, NJ: Humana Press), 659–678.

Grefen, C., Lalonde, S., and Obrdlik, P. (2007). Split-ubiquitin system for identifying protein-protein interactions in membrane and full-length proteins. *Curr. Protoc. Neurosci.* 41, 5.27.1–5.27.41. doi: 10.1002/0471142301.ns0527s41

Grefen, C., Obrdlik, P., and Harter, K. (2009). "The determination of protein-protein interactions by the mating-based split-ubiquitin system (mbSUS)," in *Plant Signal Transduction: Methods and Protocols*, ed. T. Pfannschmidt (Totowa, NJ: Humana Press), 217–233.

Hachez, C., Laloux, T., Reinhardt, H., Cavez, D., Degand, H., Grefen, C., et al. (2014). *Arabidopsis* SNAREs SYP61 and SYP121 coordinate the trafficking of plasma membrane aquaporin PIP2;7 to modulate the cell membrane water permeability. *Plant Cell* 26, 3132–3147. doi: 10.1105/tpc.114.127159

Hakoyama, T., Oi, R., Hazuma, K., Suga, E., Adachi, Y., Kobayashi, M., et al. (2012). The SNARE protein SYP71 expressed in vascular tissues is involved in symbiotic nitrogen fixation in *Lotus japonicus* nodules. *Plant Physiol.* 160, 897–905. doi: 10.1104/pp.112.200782

Haney, C. H., and Long, S. R. (2010). Plant flotillins are required for infection by nitrogen-fixing bacteria. *Proc. Natl. Acad. Sci. U.S.A.* 107, 478–483. doi: 10.1073/pnas.0910081107

Haney, C. H., Riely, B. K., Tricoli, D. M., Cook, D. R., Ehrhardt, D. W., and Long, S. R. (2011). Symbiotic rhizobia bacteria trigger a change in localization and dynamics of the *Medicago truncatula* receptor kinase LYK3. *Plant Cell* 23, 2774–2787. doi: 10.1105/tpc.111.086389

Hao, H. Q., Fan, L. S., Chen, T., Li, R. L., Li, X. J., He, Q. H., et al. (2014). Clathrin and membrane microdomains cooperatively regulate rbohd dynamics and activity in *Arabidopsis*. *Plant Cell* 26, 1729–1745. doi: 10.1105/tpc.113.122358

Hashimoto-Sugimoto, M., Higaki, T., Yaeno, T., Nagami, A., Irie, M., Fujimi, M., et al. (2013). A Munc13-like protein in *Arabidopsis* mediates H+-ATPase translocation that is essential for stomatal responses. *Nat. Commun.* 4:2215. doi: 10.1038/ncomms3215

Heckwolf, M., Pater, D., Hanson, D. T., and Kaldenhoff, R. (2011). The *Arabidopsis thaliana* aquaporin AtPIP1;2 is a physiologically relevant CO2 transport facilitator. *Plant J.* 67, 795–804. doi: 10.1111/j.1365-313X.2011.04634.x

Ho, Y., Gruhler, A., Heilbut, A., Bader, G. D., Moore, L., Adams, S. L., et al. (2002). Systematic identification of protein complexes in *Saccharomyces cerevisiae* by mass spectrometry. *Nature* 415, 180–183. doi: 10.1038/415180a

Huang, B. X., and Kim, H. Y. (2013). Effective identification of Akt interacting proteins by two-step chemical crosslinking, co-immunoprecipitation and mass spectrometry. *PLoS One* 8:e61430. doi: 10.1371/journal.pone.0061430

Huang, D. W., Sherman, B. T., and Lempicki, R. A. (2009). Systematic and integrative analysis of large gene lists using DAVID bioinformatics resources. *Nat. Protoc.* 4, 44–57. doi: 10.1038/nprot.2008.211

Ishikawa, T., Aki, T., Yanagisawa, S., Uchimiya, H., and Kawai-Yamada, M. (2015). Overexpression of BAX INHIBITOR-1 links plasma membrane microdomain proteins to stress. *Plant Physiol.* 169, 1333–1343. doi: 10.1104/pp.15.00445

Jafferali, M. H., Vijayaraghavan, B., Figueroa, R. A., Crafoord, E., Gudise, S., Larsson, V. J., et al. (2014). MCLIP, an effective method to detect interactions of transmembrane proteins of the nuclear envelope in live cells. *Biochim. Biophys. Acta* 1838, 2399–2403. doi: 10.1016/j.bbamem.2014.06.008

Jarsch, I. K., Konrad, S. S. A., Stratil, T. F., Urbanus, S. L., Szymanski, W., Braun, P., et al. (2014). Plasma membranes are subcompartmentalized into a plethora of coexisting and diverse microdomains in *Arabidopsis* and *Nicotiana benthamiana*. *Plant Cell* 26, 1698–1711. doi: 10.1105/tpc.114.124446

Jones, A. M., Xuan, Y., Xu, M., Wang, R.-S., Ho, C.-H., Lalonde, S., et al. (2014). Border control-a membrane-linked interactome of *Arabidopsis*. *Science* 344, 711–716. doi: 10.1126/science.1251358

Jozefkowicz, C., Berny, M.C., Chaumont, F., and Alleva, K. (2017). "Heteromerization of plant aquaporins," in *Plant Aquaporins*, eds F. Chaumont and S. D. Tyerman (Berlin: Springer International Publishing), 29–46. doi: 10.1007/978-3-319-49395-4_2

Jung, H. W., and Hwang, B. K. (2007). The leucine-rich repeat (LRR) protein, CaLRR1, interacts with the hypersensitive induced reaction (HIR) protein, CaHIR1, and suppresses cell death induced by the CaHIR1 protein. *Mol. Plant Pathol.* 8, 503–514. doi: 10.1111/j.1364-3703.2007.00410.x

Kaake, R. M., Wang, X. R., Burke, A., Yu, C., Kandur, W., Yang, Y. Y., et al. (2014). A new *in vivo* cross-linking mass spectrometry platform to define protein-protein interactions in living cells. *Mol. Cell. Proteomics* 13, 3533–3543. doi: 10.1074/mcp.M114.042630

Keinath, N. F., Kierszniowska, S., Lorek, J., Bourdais, G., Kessler, S. A., Shimosato-Asano, H., et al. (2010). PAMP (Pathogen-Associated Molecular Pattern)-induced changes in plasma membrane compartmentalization reveal novel components of plant immunity. *J. Biol. Chem.* 285, 39140–39149. doi: 10.1074/jbc.M110.160531

Kiyosue, T., Yamaguchi-Shinozaki, K., and Shinozaki, K. (1994). Cloning of cDNAs for genes that are early-responsive to dehydration stress (ERDs) in *Arabidopsis thaliana* L.: identification of three ERDs as HSP cognate genes. *Plant Mol. Biol.* 25, 791–798. doi: 10.1007/bf00028874

Ladwig, F., Dahlke, R. I., Stuhrwohldt, N., Hartmann, J., Harter, K., and Sauter, M. (2015). Phytosulfokine regulates growth in *Arabidopsis* through a response module at the plasma membrane that includes cyclic nucleotide-gated CHANNEL17, H+-ATPase, and BAK1. *Plant Cell* 27, 1718–1729. doi: 10.1105/tpc.15.00306

Langhorst, M. F., Reuter, A., Jaeger, F. A., Wippich, F. M., Luxenhofer, G., Plattner, H., et al. (2008). Trafficking of the microdomain scaffolding protein reggie-1/flotillin-2. *Eur. J. Cell Biol.* 87, 211–226. doi: 10.1016/j.ejcb.2007.12.001

Li, N., Huang, X., Zhao, Z. L., Chen, G. Y., Zhang, W. P., and Cao, X. T. (2000). Identification and characterization of a novel gene KE04 differentially expressed by activated human dendritic cells. *Biochem. Biophys. Res. Commun.* 279, 487–493. doi: 10.1006/bbrc.2000.3935

Li, R. L., Liu, P., Wan, Y. L., Chen, T., Wang, Q. L., Mettbach, U., et al. (2012). A membrane microdomain-associated protein, *Arabidopsis* Flot1, is involved in a clathrin-independent endocytic pathway and is required for seedling development. *Plant Cell* 24, 2105–2122. doi: 10.1105/tpc.112.095695

Li, X. J., Wang, X. H., Yang, Y., Li, R. L., He, Q. H., Fang, X. H., et al. (2011). Single-molecule analysis of pip2;1 dynamics and partitioning reveals multiple modes of *Arabidopsis* plasma membrane aquaporin regulation. *Plant Cell* 23, 3780–3797. doi: 10.1105/tpc.111.091454

Liu, J., DeYoung, S. M., Zhang, M., Dold, L. H., and Saltiel, A. R. (2005). The stomatin/prohibitin/flotillin/HflK/C domain of flotillin-1 contains distinct sequences that direct plasma membrane localization and protein interactions in 3T3-L1 adipocytes. *J. Biol. Chem.* 280, 16125–16134. doi: 10.1074/jbc.M500940200

Liu, J., Elmore, J. M., Fuglsang, A. T., Palmgren, M. G., Staskawicz, B. J., and Coaker, G. (2009). RIN4 functions with plasma membrane H+-atpases to regulate stomatal apertures during pathogen attack. *PLoS Biol.* 7:e1000139. doi: 10.1371/journal.pbio.1000139

Liu, M. J., Peng, Y., Li, H. Y., Deng, L., Wang, X. J., and Kang, Z. S. (2016). TaSYP71, a Qc-SNARE, contributes to wheat resistance against *Puccinia striiformis* f. sp *tritici*. *Front. Plant Sci.* 7:544. doi: 10.3389/fpls.2016.00544

Liu, P., Li, R. L., Zhang, L., Wang, Q. L., Niehaus, K., Baluska, F., et al. (2009). Lipid microdomain polarization is required for NADPH oxidase-dependent ROS signaling in *Picea meyeri* pollen tube tip growth. *Plant J.* 60, 303–313. doi: 10.1111/j.1365-313X.2009.03955.x

Liu, Y., Li, H., Shi, Y., Song, Y., Wang, T., and Li, Y. (2009). A maize early responsive to dehydration gene, *ZmERD4*, provides enhanced drought and salt tolerance in *Arabidopsis*. *Plant Mol. Biol. Rep.* 27, 542–548. doi: 10.1007/s11105-009-0119-y

Luang, S., and Hrmova, M. (2017). "Structural basis of the permeation function of plant aquaporins," in *Plant Aquaporins*, eds F. Chaumont and S. D. Tyerman (Berlin: Springer International Publishing), 1–28. doi: 10.1007/978-3-319-49395-4_1

Lv, X. Q., Jing, Y. P., Xiao, J. W., Zhang, Y. D., Zhu, Y. F., Julian, R., et al. (2017). Membrane microdomains and the cytoskeleton constrain AtHIR1 dynamics and facilitate the formation of an AtHIR1-associated immune complex. *Plant J.* 90, 3–16. doi: 10.1111/tpj.13480

Marmagne, A., Ferro, M., Meinnel, T., Bruley, C., Kuhn, L., Garin, J., et al. (2007). A high content in lipid-modified peripheral proteins and integral receptor kinases features in the *Arabidopsis* plasma membrane proteome. *Mol. Cell. Proteomics* 6, 1980–1996. doi: 10.1074/mcp.M700099-MCP200

Mohr, P. G., and Cahill, D. M. (2007). Suppression by ABA of salicylic acid and lignin accumulation and the expression of multiple genes, in *Arabidopsis* infected with *Pseudomonas syringae* pv. *tomato*. *Funct. Integr. Genomics* 7, 181–191. doi: 10.1007/s10142-006-0041-4

Mongrand, S., Morel, J., Laroche, J., Claverol, S., Carde, J. P., Hartmann, M. A., et al. (2004). Lipid rafts in higher plant cells – purification and characterization of triton X-100-insoluble microdomains from tobacco plasma membrane. *J. Biol. Chem.* 279, 36277–36286. doi: 10.1074/jbc.M403440200

Morrow, I. C., Rea, S., Martin, S., Prior, I. A., Prohaska, R., Hancock, J. F., et al. (2002). Flotillin-1/Reggie-2 traffics to surface raft domains via a novel Golgi-independent pathway – identification of a novel membrane targeting domain and a role for palmitoylation. *J. Biol. Chem.* 277, 48834–48841. doi: 10.1074/jbc.M209082200

Mosher, R. A., Durrant, W. E., Wang, D., Song, J. Q., and Dong, X. N. (2006). A comprehensive structure-function analysis of *Arabidopsis* SNI1 defines essential regions and transcriptional repressor activity. *Plant Cell* 18, 1750–1765. doi: 10.1105/tpc.105.039677

Murata, K., Mitsuoka, K., Hirai, T., Walz, T., Agre, P., Heymann, J. B., et al. (2000). Structural determinants of water permeation through aquaporin-1. *Nature* 407, 599–605. doi: 10.1038/35036519

Nesvizhskii, A. I. (2012). Computational and informatics strategies for identification of specific protein interaction partners in affinity purification mass spectrometry experiments. *Proteomics* 12, 1639–1655. doi: 10.1002/pmic.201100537

Neumann-Giesen, C., Falkenbach, B., Beicht, P., Claasen, S., Luers, G., Stuermer, C. A. O., et al. (2004). Membrane and raft association of reggie-1/flotillin-2: role of myristoylation, palmitoylation and oligomerization and induction of filopodia by overexpression. *Biochem. J.* 378, 509–518. doi: 10.1042/bj20031100

Neumann-Giesen, C., Fernow, I., Amaddii, M., and Tikkanen, R. (2007). Role of EGF-induced tyrosine phosphorylation of reggie-1/flotillin-2 in cell spreading and signaling to the actin cytoskeleton. *J. Cell Sci.* 120, 395–406. doi: 10.1242/jcs.03336

Ogura, M., Yamaki, J., Homma, M. K., and Homma, Y. (2014). Phosphorylation of flotillin-1 by mitochondrial c-Src is required to prevent the production of reactive oxygen species. *FEBS Lett.* 588, 2837–2843. doi: 10.1016/j.febslet.2014.06.044

Pardo, M., and Choudhary, F. S. (2012). Assignment of protein interactions from affinity purification/mass spectrometry data. *J. Proteome Res.* 11, 1462–1474. doi: 10.1021/pr2011632

Peremyslov, V. V., Morgun, E. A., Kurth, E. G., Makarova, K. S., Koonin, E. V., and Dolja, V. V. (2013). Identification of myosin XI receptors in *Arabidopsis* defines a distinct class of transport vesicles. *Plant Cell* 25, 3022–3038. doi: 10.1105/tpc.113.113704

Pizzio, G. A., Hirschi, K. D., and Gaxiola, R. A. (2017). Conjecture regarding posttranslational modifications to the *Arabidopsis* type I Proton-pumping pyrophosphatase (AVP1). *Front. Plant Sci.* 8:1572. doi: 10.3389/fpls.2017.01572

Pleskot, R., Potocky, M., Pejchar, P., Linek, J., Bezvoda, R., Martinec, J., et al. (2010). Mutual regulation of plant phospholipase D and the actin cytoskeleton. *Plant J.* 62, 494–507. doi: 10.1111/j.1365-313X.2010.04168.x

Popov, N., Schmitt, M., Schulzeck, S., and Matthies, H. (1975). Reliable micromethod for determining protein-content in tissue material. *Acta Biol. Med. Ger.* 34, 1441–1446.

Postaire, O., Tournaire-Roux, C., Grondin, A., Boursiac, Y., Morillon, R., Schaffner, A. R., et al. (2010). A PIP1 aquaporin contributes to hydrostatic pressure-induced water transport in both the root and rosette of *Arabidopsis*. *Plant Physiol.* 152, 1418–1430. doi: 10.1104/pp.109.145326

Qi, Y. P., and Katagiri, F. (2009). Purification of low-abundance *Arabidopsis* plasma-membrane protein complexes and identification of candidate components. *Plant J.* 57, 932–944. doi: 10.1111/j.1365-313X.2008.03736.x

Qi, Y. P., Tsuda, K., Nguyen, L. V., Wang, X., Lin, J. S., Murphy, A. S., et al. (2011). Physical association of *Arabidopsis* hypersensitive induced reaction proteins (HIRs) with the immune receptor RPS2. *J. Biol. Chem.* 286, 31297–31307. doi: 10.1074/jbc.M110.211615

Roitbak, T., Surviladze, Z., Tikkanen, R., and Wandinger-Ness, A. (2005). A polycystin multiprotein complex constitutes a cholesterol-containing signalling microdomain in human kidney epithelia. *Biochem. J.* 392, 29–38. doi: 10.1042/bj20050645

Sanderfoot, A. A., Kovaleva, V., Bassham, D. C., and Raikhel, N. V. (2001). Interactions between syntaxins identify at least five SNARE complexes within the golgi/prevacuolar system of the *Arabidopsis* cell. *Mol. Biol. Cell* 12, 3733–3743. doi: 10.1091/mbc.12.12.3733

Santamaria, A., Castellanos, E., Gomez, V., Benedit, P., Renau-Piqueras, J., Morote, J., et al. (2005). PTOV1 enables the nuclear translocation and mitogenic activity of flotillin-1, a major protein of lipid rafts. *Mol. Cell Biol.* 25, 1900–1911. doi: 10.1128/Mcb.25.5.1900-1911.2005

Savas, J. N., Stein, B. D., Wu, C. C., and Yates, J. R. (2011). Mass spectrometry accelerates membrane protein analysis. *Trends Biochem. Sci.* 36, 388–396. doi: 10.1016/j.tibs.2011.04.005

Shahollari, B., Peskan-Berghöfer, T., and Oelmüller, R. (2004). Receptor kinases with leucine-rich repeats are enriched in Triton X-100 insoluble plasma membrane microdomains from plants. *Physiol. Plant.* 122, 397–403. doi: 10.1111/j.1399-3054.2004.00414.x

Schindler, J., and Nothwang, H. G. (2006). Aqueous polymer two-phase systems: effective tools for plasma membrane proteomics. *Proteomics* 6, 5409–5417. doi: 10.1002/pmic.200600243

Schroeder, W. T., Stewartgaletka, S., Mandavilli, S., Parry, D. A. D., Goldsmith, L., and Duvic, M. (1994). Cloning and characterization of a novel epidermal-cell surface-antigen (Esa). *J. Biol. Chem.* 269, 19983–19991.

Schulte, T., Lottspeich, F., and Stuermer, C. A. O. (1995). Characterization of reggie-1 and isolation of reggie-2, cell surface proteins of the goldfish CNS. *Soc. Neurosci. Abstr.* 21:795.

Simons, K., and Ikonen, E. (1997). Functional rafts in cell membranes. *Nature* 387, 569–572. doi: 10.1038/42408

Simons, K., and Toomre, D. (2000). Lipid rafts and signal transduction. *Nat. Rev. Mol. Cell Biol.* 1, 31–39. doi: 10.1038/35036052

Singh, N., Swain, S., Singh, A., and Nandi, A. K. (2018). AtOZF1 positively regulates defense against bacterial pathogens and NPR1-independent salicylic acid signaling. *Mol. Plant Microbe Interact.* 31, 323–333. doi: 10.1094/MPMI-08-17-0208-R

Smaczniak, C., Li, N., Boeren, S., America, T., van Dongen, W., Goerdayal, S. S., et al. (2012). Proteomics-based identification of low-abundance signaling and regulatory protein complexes in native plant tissues. *Nat. Protoc.* 7, 2144–2158. doi: 10.1038/nprot.2012.129

Solis, G. P., Hoegg, M., Munderloh, C., Schrock, Y., Malaga-Trillo, E., Rivera-Milla, E., et al. (2007). Reggie/flotillin proteins are organized into stable tetramers in membrane microdomains. *Biochem. J.* 403, 313–322. doi: 10.1042/bj20061686

Speers, A. E., and Wu, C. C. (2007). Proteomics of integral membrane proteins-theory and application. *Chem. Rev.* 107, 3687–3714. doi: 10.1021/cr068286z

Tan, S., Tan, H. T., and Chung, M. C. M. (2008). Membrane proteins and membrane proteomics. *Proteomics* 8, 3924–3932. doi: 10.1002/pmic.200800597

ten Have, S., Boulon, S., Ahmad, Y., and Lamond, A. I. (2011). Mass spectrometry-based immuno-precipitation proteomics - The user's guide. *Proteomics* 11, 1153–1159. doi: 10.1002/pmic.201000548

Uehlein, N., Sperling, H., Heckwolf, M., and Kaldenhoff, R. (2012). The *Arabidopsis* aquaporin PIP1;2 rules cellular CO2 uptake. *Plant Cell Environ.* 35, 1077–1083. doi: 10.1111/j.1365-3040.2011.02473.x

Ullrich, A., and Schlessinger, J. (1990). Signal transduction by receptors with tyrosine kinase-activity. *Cell* 61, 203–212. doi: 10.1016/0092-8674(90)90801-K

Van Leene, J., Eeckhout, D., Cannoot, B., De Winne, N., Persiau, G., Van De Slijke, E., et al. (2015). An improved toolbox to unravel the plant cellular machinery by tandem affinity purification of *Arabidopsis* protein complexes. *Nat. Protoc.* 10, 169–187. doi: 10.1038/nprot.2014.199

Varet, A., Hause, B., Hause, G., Scheel, D., and Lee, J. (2003). The Arabidopsis *NHL3* gene encodes a plasma membrane protein and its overexpression correlates with increased resistance to *Pseudomonas syringae* pv. *tomato* DC3000. *Plant Physiol.* 132, 2023–2033. doi: 10.1104/pp.103.020438

Varet, A., Parker, J., Tornero, P., Nass, N., Nürnberger, T., Dangl, J. L., et al. (2002). *NHL25* and *NHL3*, two *NDR1/HIN-like* genes in *Arabidopsis thaliana* with potential role(s) in plant defense. *Mol. Plant Microbe Interact.* 15:608. doi: 10.1094/MPMI.2002.15.6.608

Volonté, D., Galbiati, F., Li, S., Nishiyama, K., Okamoto, T., and Lisanti, M. P. (1999). Flotillins/cavatellins are differentially expressed in cells and tissues and form a hetero-oligomeric complex with caveolins *in vivo*: characterization and epitope-mapping of a novel flotillin-1 monoclonal antibody probe. *J. Biol. Chem.* 274, 12702–12709. doi: 10.1074/jbc.274.18.12702

Wang, L., Li, H., Lv, X. Q., Chen, T., Li, R. L., Xue, Y. Q., et al. (2015). Spatiotemporal dynamics of the bri1 receptor and its regulation by membrane microdomains in living *Arabidopsis* cells. *Mol. Plant* 8, 1334–1349. doi: 10.1016/j.molp.2015.04.005

Wei, T. Y., Zhang, C. W., Hou, X. L., Sanfacon, H., and Wang, A. M. (2013). The SNARE protein SYP71 is essential for turnip mosaic virus infection by mediating fusion of virus-induced vesicles with chloroplasts. *PLoS Pathog.* 9:e1003378. doi: 10.1371/journal.ppat.1003378

Weis, C., Pfeilmeier, S., Glawischnig, E., Isono, E., Pachl, F., Hahne, H., et al. (2013). Co-immunoprecipitation-based identification of putative BAX INHIBITOR-1-interacting proteins involved in cell death regulation and plant-powdery mildew interactions. *Mol. Plant Pathol.* 14, 791–802. doi: 10.1111/mpp.12050

Xing, S., Wallmeroth, N., Berendzen, K. W., and Grefen, C. (2016). Techniques for the analysis of protein-protein interactions in vivo. *Plant Physiol.* 171, 727–758. doi: 10.1104/pp.16.00470

Yamauchi, S., Takemiya, A., Sakamoto, T., Kurata, T., Tsutsumi, T., Kinoshita, T., et al. (2016). The plasma membrane H+-ATPase AHA1 plays a major role in stomatal opening in response to blue light. *Plant Physiol.* 171, 2731–2743. doi: 10.1104/pp.16.01581

Yan, S. L., McLamore, E. S., Dong, S. S., Gao, H. B., Taguchi, M., Wang, N. N., et al. (2015). The role of plasma membrane H+-ATPase in jasmonate-induced ion fluxes and stomatal closure in *Arabidopsis thaliana*. *Plant J.* 83, 638–649. doi: 10.1111/tpj.12915

Yu, M., Liu, H. J., Dong, Z. Y., Xiao, J. W., Su, B. D., Fan, L. S., et al. (2017). The dynamics and endocytosis of Flot1 protein in response to flg22 in *Arabidopsis*. *J. Plant Physiol.* 215, 73–84. doi: 10.1016/j.jplph.2017.05.010

Zelazny, E., Borst, J. W., Muylaert, M., Batoko, H., Hemminga, M. A., and Chaumont, F. (2007). FRET imaging in living maize cells reveals that plasma membrane aquaporins interact to regulate their subcellular localization. *Proc. Natl. Acad. Sci. U.S.A.* 104, 12359–12364. doi: 10.1073/pnas.0701180104

Zheng, M. S., Takahashi, H., Miyazaki, A., Hamamoto, H., Shah, J., Yamaguchi, I., et al. (2004). Up-regulation of *Arabidopsis thaliana NHL10* in the hypersensitive response to *Cucumber mosaic virus* infection and in senescing leaves is controlled by signalling pathways that differ in salicylate involvement. *Planta* 218, 740–750. doi: 10.1007/s00425-003-1169-2

Zhou, L., Cheung, M. Y., Zhang, Q., Lei, C. L., Zhang, S. H., Sun, S. S., et al. (2009). A novel simple extracellular leucine-rich repeat (eLRR) domain protein from rice (OsLRR1) enters the endosomal pathway and interacts with the

hypersensitive-induced reaction protein 1 (OsHIR1). *Plant Cell Environ.* 32, 1804–1820. doi: 10.1111/j.1365-3040.2009.02039.x

Zhou, L. A., Cheung, M. Y., Li, M. W., Fu, Y. P., Sun, Z. X., Sun, S. M., et al. (2010). Rice hypersensitive induced reaction protein 1 (OsHIR1) associates with plasma membrane and triggers hypersensitive cell death. *Bmc Plant Biol.* 10:290. doi: 10.1186/1471-2229-10-290

Zhou, Z. Y., Wu, Y. J., Yang, Y. Q., Du, M. M., Zhang, X. J., Guo, Y., et al. (2015). An *Arabidopsis* plasma membrane proton ATPase modulates ja signaling and is exploited by the *pseudomonas syringae* effector protein avrb for stomatal invasion. *Plant Cell* 27, 2032–2041. doi: 10.1105/tpc.15.00466

Conflict of Interest Statement: The authors declare that the research was conducted in the absence of any commercial or financial relationships that could be construed as a potential conflict of interest.

Supplementary Material

Mapping of Plasma Membrane Proteins Interacting with *Arabidopsis thaliana* Flotillin 2

Petra Junková[1*†], Michal Daněk[2,3†], Daniela Kocourková[2], Jitka Brouzdová[2], Kristýna Kroumanová[2], Enric Zelazny[4], Martin Janda[1,2], Radovan Hynek[1], Jan Martinec[2], Olga Valentová[1]

[1]Department of Biochemistry and Microbiology, University of Chemistry and Technology Prague, Czech Republic

[2]Institute of Experimental Botany of the Czech Academy of Sciences, Prague, Czech Republic

[3]Department of Experimental Plant Biology, Faculty of Science, Charles University, Prague, Czech Republic

[4]Institute for Integrative Biology of the Cell (I2BC), CNRS/CEA/Université Paris Sud, Université Paris-Saclay, Gif-sur-Yvette, France

*** Correspondence:**
Petra Junková, PhD
Petra.Junkova @vscht.cz

† Contributed equally

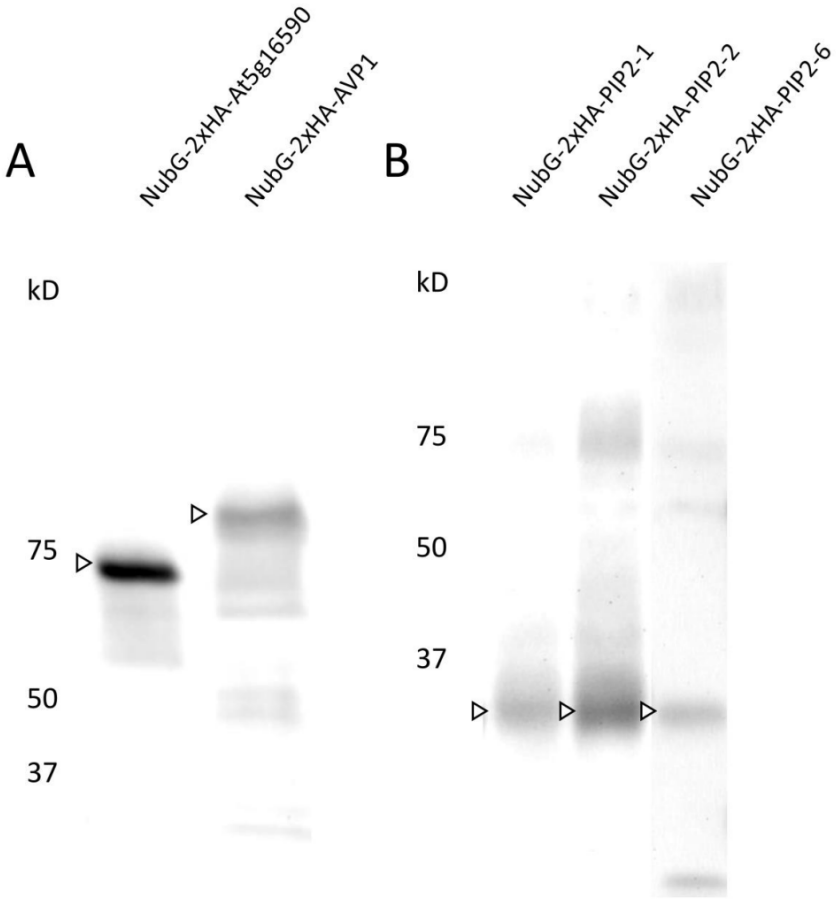

Supplementary Figure 1. Expression of fusion proteins in yeasts. Bands of corresponding molecular weight are marked with arrows. Proteins were separated on SDS-PAGE and blotted onto a nitrocellulose membrane using wet transfer. Membranes were probed with anti-HA primary antibody (Biolegend, cat. no. 901501) (1:2000, 1.5 h) and anti-mouse (1:5000, 1 h) secondary antibody. Panel A - Yeast cells were disrupted in lysis buffer (400 mM sucrose, 50 mM HEPES, 100 mM KCl, 100 mM $MgCl_2$, cOmplete Protease inhibitor Cocktail, 1mM DTT, pH 7.5) and centrifuged for 10 min at 6010 x g. The supernatant was further centrifuged for 1h at 27 460 x g in 4 °C. The pellet was resuspended in 1xPBS containing 5 % glycerol and used for immunoblotting. 15 µg of proteins were loaded into lanes and separated on 4-15 % SDS-PAGE. Panel B - Crude protein extracts were prepared according to (Grefen, 2014) and 10 µl of each sample was separated on 10 % SDS-PAGE.

Manuscript of the Paper # 4

Title: Cell wall contributes to the stability of plasma membrane microdomain organization of *Arabidopsis thaliana* FLOTILLIN2 and HYPERSENSITIVE INDUCED REACTION1 proteins

Authors: Michal Daněk, Jindřiška Angelini, Kateřina Malínská, Jan Andrejch, Zuzana Amlerová, Daniela Kocourková, Jitka Brouzdová, Olga Valentová, Jan Martinec, Jan Petrášek

Summary: Current models of plasma membrane (PM) postulate its organization in various nano- and micro-domains with distinct protein and lipid composition. While metazoan PM microdomains usually display high lateral mobility, the dynamics of plant microdomains is often highly spatially restricted. Here we have focused on the determination of the PM distribution in microdomains for Arabidopsis thaliana flotillin (AtFLOT) and hypersensitive induced reaction proteins (AtHIR), previously showed to be involved in response to extracellular stimuli. Using in vivo laser scanning and spinning disk (SD) confocal microscopy in Arabidopsis thaliana we present here their microdomain localization in various epidermal cell types. Fluorescence recovery after photobleaching (FRAP) and kymographic analysis revealed that PM-associated AtFLOTs contain significantly higher immobile fraction than AtHIRs. In addition, much lower immobile fractions have been shown in tonoplast pool of AtHIR3. Although both groups of proteins were spatially restricted in their PM distribution by corrals co-aligning with microtubules (MTs), pharmacological treatments showed no or very low role of actin and microtubular cytoskeleton for AtFLOT and AtHIR microdomain organization. Finally, pharmacological alteration of cell wall (CW) synthesis and structure resulted in changes in lateral mobility of AtFLOT2 and AtHIR1. Accordingly, partial enzymatic CW removal increased the overall dynamics as well as individual microdomain mobility of these two proteins. Such structural links to CW could play an important role in their correct positioning during PM communication with extracellular environment.

Current state: The manuscript is the revised version of the article. It has been resubmitted in the Plant Journal after original rejection with resubmission encouraged of the previous version of the manuscript. Several items were added in the paper upon request of the reviewers or by the authors themselves in order to increase its quality prior to the resubmission.

My contribution: First and corresponding author. I took part in the selection of *At*FLOT1/2/3-GFP lines. I greatly participated in the microscopic analysis, especially in the original screen of all lines and in final parts involving cell wall alteration. With great help of Jan Petrášek I wrote the manuscript.

Cell wall contributes to the stability of plasma membrane microdomain organization of *Arabidopsis thaliana* FLOTILLIN2 and HYPERSENSITIVE INDUCED REACTION1 proteins

Michal Daněk[1,2,*], Jindřiška Angelini[3], Kateřina Malínská[1], Jan Andrejch[3], Zuzana Amlerová[3], Daniela Kocourková[1], Jitka Brouzdová[1], Olga Valentová[3], Jan Martinec[1], Jan Petrášek[1,2]

[1]Institute of Experimental Botany of the Czech Academy of Sciences, Rozvojová 263, 165 02 Praha 6, Czech Republic

[2]Department of Experimental Plant Biology, Faculty of Science, Charles University, Viničná 5, 128 44 Prague 2, Czech Republic

[3]Department of Biochemistry and Microbiology, University of Chemistry and Technology Prague, Technická 3, 166 28 Prague 6, Czech Republic

* Corresponding author

E-mail of the corresponding author: danek@ueb.cas.cz

Telephone: 00420 225 106 419

SUMMARY

Current models of plasma membrane (PM) postulate its organization in various nano- and micro-domains with distinct protein and lipid composition. While metazoan PM microdomains usually display high lateral mobility, the dynamics of plant microdomains is often highly spatially restricted. Here we have focused on the determination of the PM distribution in microdomains for *Arabidopsis thaliana* flotillin (*At*FLOT) and hypersensitive induced reaction proteins (*At*HIR), previously showed to be involved in response to extracellular stimuli. Using *in vivo* laser scanning and spinning disk (SD) confocal microscopy in *Arabidopsis thaliana* we present here their microdomain localization in various epidermal cell types. Fluorescence recovery after photobleaching (FRAP) and kymographic analysis revealed that PM-associated *At*FLOTs contain significantly higher immobile fraction than *At*HIRs. In addition, much lower immobile fractions have been shown in tonoplast pool of *At*HIR3. Although both groups of proteins were spatially restricted in their PM distribution by corrals co-aligning with microtubules (MTs), pharmacological treatments showed no or very low role of actin and microtubular cytoskeleton for *At*FLOT and *At*HIR microdomain organization. Finally, pharmacological alteration of cell wall (CW) synthesis and structure resulted in changes in lateral mobility of *At*FLOT2 and *At*HIR1. Accordingly, partial enzymatic CW removal increased the overall dynamics as well as individual microdomain mobility of these two proteins. Such structural links to CW could play an important role in their correct positioning during PM communication with extracellular environment.

SIGNIFICANCE STATEMENT

The evidence is provided on higher dynamics of plant-specific hypersensitive induced reaction proteins (*At*HIRs) at the plasma membrane in comparison with closely related flotillins (*At*FLOTs) in *Arabidopsis thaliana*. In addition to the plasma membrane localization, their presence at tonoplast is shown *in vivo* by confocal microscopy and interaction with the cell wall is revealed to be responsible for the stabilization of *At*HIR1 and *At*FLOT2 within the plasma membrane.

INTRODUCTION

Plant PM is an essential cell compartment representing communication and transport interface between cell interior and extracellular environment. PM lipids and proteins are not usually distributed evenly, they are rather clustered, thus forming a variety of membrane multiscale sub-compartments (Mamode Cassim et al., 2019, Gronnier et al., 2018). Various types of membrane proteins are often targeted into specific microdomains (Jarsch et al., 2014, Tapken and Murphy, 2015), which might constitute structural basis for the compartmentalization of PM-associated functions (Konrad and Ott, 2015). The mechanisms ensuring membrane microdomain identity are not fully understood yet, however recent findings show that local PM properties such as fluidity, viscosity, continuity, and protein-protein interactions all affect PM organization (Bernardino de la Serna et al., 2016). PM microdomain lateral mobility may be confined by steric constrains, i.e. by the interaction with cortical cytoskeleton network forming "fences" or with "pickets", transmembrane proteins of small lateral mobility, originally reported in metazoan cells (Ritchie et al., 2003, Kusumi and Sako, 1996). This organization model may be also applicable for plant PM, where an effect of cytoskeleton on protein dynamics and microdomain structure was reported (Szymanski et al., 2015). In addition, another type of spatial hurdles can be represented by interactions of microdomain proteins with extracellular molecules (Bernardino de la Serna et al., 2016), which might be significant also for plant cells surrounded by complex CW (Martiniere et al., 2012, Martiniere and Runions, 2013).

Flotillins and HIRs form subfamilies in a large membrane-localized SPFH (Stomatin/Prohibitin/Flotillin/HflK/C) protein superfamily (Rivera-Milla et al., 2006). Unlike other members of this superfamily, *At*FLOTs and *At*HIRs probably lack transmembrane stretch and are thus peripheral membrane proteins (Daněk et al., 2016).

*At*FLOT1 and *At*FLOT2 as well as *Medicago truncatula* FLOT2 (*Mt*FLOT2) and *Mt*FLOT4 were observed to form membrane microdomains (Jarsch et al., 2014, Li et al., 2012, Haney and Long, 2010), which is reminiscent of their mammalian homologs (Stuermer et al., 2001, Baumann et al., 2000). *Mt*FLOT2 and *Mt*FLOT4 were reported to be involved in nodulation (Haney et al., 2011). The most studied *At*FLOT1 plays a role in callose deposition under bacterial elicitor treatment (Yu et al., 2017) and has been proposed to assist in the endocytosis of *At*PIP2;1 aquaporin, alternative oxidase *At*RbohD or brassinosteroid and flagellin receptors *At*BRI1 and *At*FLS2 upon stress or treatment with their respective ligands (Wang et al., 2015, Hao et al., 2014, Li et al., 2011, Li et al., 2012, Cui et al., 2018). *At*FLOTs seem to be redundant

in function since no apparent phenotype was observed under various stress treatments performed on single isoform loss-of-function mutants (Kroumanová et al., 2019).

HIRs are plant-specific members of the SPFH superfamily (Di et al., 2010). They were reported to be predominantly localized at the PM in several species (Duan et al., 2013, Chen et al., 2007, Choi et al., 2011, Ishikawa et al., 2015, Malakshah et al., 2007, Qi et al., 2011, Li et al., 2019). In pepper, rice and Arabidopsis they were observed to interact with leucine-rich repeat proteins involved in pathogen defence response (Zhou et al., 2009, Qi et al., 2011, Jung and Hwang, 2007) and thus HIRs take part in plant immunity. *At*HIRs form oligomers, all pair-wise combinations of single *At*HIR isoforms were confirmed experimentally (Qi et al., 2011). Direct interaction of *At*FLOT1 and *At*FLOT3 (i.e.heterodi/oligomerization) in which the C-terminal domain (not including the SPFH domain) was found to provide the physical interaction of single isoforms was also reported (Yu et al., 2017). Similar effect was observed in mammalian homologues of flotillins where heterooligomerization is important for endocytosis provided by flotillin microdomains (Neumann-Giesen et al., 2004, Solis et al., 2007, Babuke and Tikkanen, 2007). Recently, we have revealed several PM proteins constituting the interactome of *At*FLOT2 (Junková et al., 2018). In addition, *At*HIRs were found to be a part of PM-associated complexes, which also contained phospholipase Dδ, cytoskeletal proteins, heat-shock proteins, clathrin chain, transporters or kinases (Ho et al., 2009, Qi and Katagiri, 2009).

Within the PM, only some members of the FLOT family were shown to be present in rather immobile microdomains (Jarsch et al 2014), however, the nature of this stability is unknown. As summarized in Martiniere et al. (2012) and Martiniere and Runions (2013), plant PM-associated proteins are usually less dynamic at the PM than in endomembranes, which could be an effect of CW causing steric hindrance for PM-protein mobility.

In this work we have focused on the determination of the character of the distribution in PM microdomains for all isoforms of *At*FLOTs and *At*HIRs. We show that PM-associated *At*FLOTs are significantly more immobile than plant-specific HIR proteins. Much lower immobile fractions have been shown in tonoplast-localized isoform of *At*HIR. Proteins from both subfamilies were spatially restricted in their PM distribution by corrals co-aligning with MTs. We further tested the effect of cytoskeleton depolymerisation, sterol depletion and cell wall disruption on the dynamics of *At*FLOT2 and *At*HIR1 as the representative members of both subfamilies. Out of all tested cues, only cell wall alteration increased the lateral mobility of both isoforms within the PM. Our results thus suggest that PM microdomains of plant FLOT and HIR proteins are structurally linked with the CW. This interconnection may be important

for their appropriate functional positioning during cell communication and transduction of extracellular signals.

RESULTS

*At*FLOTs and *At*HIRs are localized in PM microdomains and/or at the tonoplast of epidermal cells

For the purpose of comparison of the distribution of individual members of *At*FLOT and *At*HIR protein families, *A. thaliana* lines carrying 35S-driven *At*FLOT1-GFP, *At*FLOT2-GFP, *At*FLOT3-GFP, *At*HIR1-YFP, *At*HIR2-YFP, *At*HIR3-YFP and *At*HIR4-YFP were studied *in vivo*. The using of overexpression lines was chosen because of the reported very low to no fluorescence of GFP-tagged *A*tFLOT1 when expressed from its native promoter (Li et al., 2012). All the lines used in our study did not display any growth phenotypes when they were observed (Figure S1). SD confocal microscopy performed in root elongation zone epidermal cells showed that all the *At*FLOT-GFP and *At*HIR-YFP proteins were present in discrete PM microdomains (Figure 1a-f), except for *At*HIR3-YFP, which was exclusively localized at the tonoplast in a form of slightly more diffuse pattern (Figure S2d, e). With the exception of *At*FLOT2-GFP and *At*FLOT3-GFP, all studied proteins were, in addition to PM microdomains, present also at the tonoplast in root epidermal cells (Figure S2). The detailed view of the individual microdomains (Figure 1l-q) revealed that they differ in size and shape as well as in pattern, e.g. interconnected microdomains for *At*HIR1-YFP (Figure 1o) contrasting with rather isolated microdomains defined by *At*FLOT1-GFP (Figure 1l). The average number of PM microdomains in root epidermal cells ranged between 60 and 90 per 25 μm^2, with *At*HIR1-GFP showing the densest pattern (Figure 1r, left panel). The dense pattern of *At*HIR1 microdomains was also shown in three independent Arabidopsis lines transformed with *At*HIR1-GFP (Figure 1r, right panel). To further investigate size difference of microdomains defined by different isoforms we used Airyscan imaging approach which increases the xyz resolution and thus enables more precise assessment of dimensions of smallest objects. The microdomain diameter was estimated as full width at half maximum (FWHM). We observed differential FWHM revealing the largest domains for *At*FLOT2-GFP while the smallest ones were found to be formed by *At*HIR2-YFP (Figure 1s, Figure S3).

PM-associated distribution was observed also in the above ground tissues (with the exception of *At*HIR2-YFP fluorescence of which was not detectable in these tissues), i.e. in the epidermal lobed cells of the first true leaves (Figure 1g-k), as well as in the epidermis of hypocotyls and cotyledon lobed cells (Figure S4). Here again, *At*HIR3-YFP was the only studied protein with predominant tonoplast localization (Figure S4e, k). Altogether, these data

show that members of both *At*FLOT and *At*HIR subfamilies are localized in PM-associated microdomains, but some isoforms are also present at the tonoplast.

_At_FLOTs and _At_HIRs exhibit differential mobility within PM and tonoplast

To characterize the spatiotemporal properties of microdomains containing individual FLOT and HIR proteins, we have applied two independent approaches. Firstly, 120 s time-lapse kymograms (Figure 2a-f,) revealed high temporal stability of *At*FLOT1-GFP, *At*FLOT2-GFP and *At*FLOT3-GFP (Figure 2a-c) microdomains in contrast to more dynamic *At*HIR1-YFP, *At*HIR2-YFP and *At*HIR4-YFP (Figure 2d-f). This difference between *At*FLOTs and *At*HIRs is confirmed by different values of Pearson's correlation coefficients (PCC, Figure S5) calculated for the fluorescence intensity profiles of the first time point (time = 0 s) and the last time point (time = 120 s) of the kymogram (Figure 2g). Secondly, membrane dynamics of single protein isoforms were studied with 80 s FRAP upon their bleaching with laser. Kinetics of FRAP in the rectangular regions of interest applied to the middle of transversal PMs (Figure S6) of elongating root epidermal cells confirmed very low lateral mobility for PM-associated *At*FLOTs and *At*HIRs. The pool of PM-associated immobile fractions was very high reaching more than 90% for *At*FLOTs and around 80% for *At*HIRs (Figure 2h). Importantly, PM-associated *At*FLOTs had significantly higher immobile fraction in comparison with *At*HIRs (Figure 2h). The kinetics of FRAP mobile fraction corresponds to fast, probably diffusion-based, recovery for all studied proteins (Figure 2i, Figure S6). This fast pool of proteins may be in fact the proteins not associated with the PM microdomains but with the areas of PM devoid of microdomains. Therefore we determined coefficient of variation (CV) of fluorescence intensity in linear profile which can be used to assess the fluorescence segregation level (Retzer et al., 2017), i.e. the degree of aggregation of fluorescence in microdomains. Indeed, CV for *At*FLOTs is considerably higher than that for *At*HIRs although the differences among members of each subfamily were also found (Figure S7) indicating lower level of microdomain association of *At*HIRs when compared with *At*FLOTs. Tonoplast-associated *At*HIR3-YFP showed much lower immobile fraction (Figure 2h) with almost 70% recovery during tested period (Figure 2i). Together, analysis of kymograms and FRAP independently demonstrated that PM-associated pool of *At*FLOT or *At*HIR population is quite stable, although *At*HIRs are significantly more mobile. Much higher mobility of tonoplast-localized *At*HIR3-YFP points to the specific interactions taking place at the PM that are responsible for quite low lateral mobility of *At*FLOTs and *At*HIRs.

PM-associated *At*FLOTs and *At*HIRs are restricted by corrals co-aligning with MTs

PM-associated microdomains of all *At*FLOTs and *At*HIRs in root epidermal cells were, to various extent, restricted in their distribution by linear corrals lacking the fluorescence signal (Figure 3a-f, arrows). The orientation of these corrals was preferentially perpendicular to the axis of the cell, but there were also numerous longitudinal corrals in elongating cells. In mature elongated cells of root epidermis, domains with *At*FLOTs were often found to be organized along corrals, forming immobile filamentous clusters of PM-associated domains (Figure 3b, c; Movie S1). Time-lapse imaging also uncovered interesting dynamics of domains with *At*FLOT proteins, which was not so apparent from kymograms or FRAP results in root elongation zone. Although the majority of domains with *At*FLOTs were rather static during 10 minutes of imaging, there were less frequent movements of individual domains. Slightly more frequent were "hopping"-type of movements, oriented perpendicularly to the axis of corrals and longer axis of individual domains. As documented in Movie S2 for *At*FLOT2-GFP, hopping movement was a transient event with speed around 0.2 $\mu m.s^{-1}$. Longer time-lapse imaging allowed to reveal even slower movement of domains in the direction of corrals, perpendicularly to the axis of cells. These movements were much slower, reaching around 0.2 $\mu m.min^{-1}$ for *At*FLOT2-GFP (Movie S3). PM-associated corrals were even more pronounced in epidermal cells of first true leaf (Figure 1g-k), cotyledons (Figure S4a-f) and hypocotyls (Figure S4g-l). The corrals were always better visible in slightly denser pattern of *At*HIRs. Therefore, *At*HIR1-YFP seedlings were transiently co-transformed with MTs-binding domain fused to mRFP (MBD-mRFP, a marker of MTs) and showed co-alignment of corrals with MTs in cotyledon epidermal lobed cells (Figure 3g). Further, we tested another MT-associated protein, *At*IQD6 (Burstenbinder et al., 2017a, Abel et al., 2013) to check whether MT are also present in corral within the pattern of *At*FLOT2-GFP microdomains. To that purpose we agro-infiltrated tobacco leaves with *At*IQD6-mCherry and *At*FLOT2-GFP. Interestingly, we observed similar pattern as with *At*HIR1 and MBD. *At*IQD6-mCherry-labelled MTs often filled linear areas lacking *At*FLOT2-GFP microdomains (Figure 3h). As shown on xz and yz ortogonal projections of z-stacks acquired with Airyscan confocal laser scanning microscopy (CLSM), corrals separating individual microdomains were apparent along whole z stack profile containing PM-associated signal for *At*FLOT2-GFP (Figure 3i) and *At*HIR1-YFP (Figure 3j). Airyscan detection allowed to roughly determine the thickness of domain along z axis, which ranged between 600-900 nm for both proteins. Since MTs were previously reported to limit lateral mobility of *At*HIR1 (Lv et al., 2017b), we applied pharmacological approach to disrupt cytoskeleton dynamics in *At*FLOT2-GFP, *At*FLOT3-GFP and *At*HIR1-YFP seedlings. Surprisingly, there were no

changes observed in the PM-associated pattern as well as in the presence of corrals after 2 h treatments with microtubule drug oryzalin (Ory) (Figure S8a-c), or latrunculin B (LatB) preventing polymerization of actin filaments (Figure S8d-f). Disruption of actin and MT cytoskeleton was verified by the same treatment of FABD-GFP/mCherry-TUA5 double-labelled line expressing markers for both MT and F-actin where depolymerisation was apparent under our experimental conditions (Figure S8g).

Our observations indicate that despite the exclusion of *At*FLOT and *At*HIR microdomains from corrals delimited with MTs, PM-associated microdomain structural identity is not directly dependent on cytoskeleton.

Dynamics of PM-associated *At*FLOT2 and *At*HIR1 microdomains is increased after cell wall disruption

Since the application of cytoskeletal drugs did not change *At*FLOT or *At*HIR localization pattern, possible role of CW was tested by pharmacological approach and in cells with enzymatically removed CW. 2 h treatment with 20 µM isoxaben (ISX), a cellulose synthesis inhibitor, did not generally change the microdomain organization of all tested proteins (Figure 4a-f). Moreover, there was only a very mild increase in their PM lateral dynamics in comparison with mock treatments (0.1% DMSO), as apparent from kymograms (Figure 4g-l, Figure S9).

Interestingly, ISX treatment increased microdomain association (indicated as CV of fluorescence intensities) of *At*FLOT2-GFP whereas there was no difference determined for *At*HIR1-YFP (Figure 4m). Determination of the FRAP immobile fraction for *At*FLOT2-GFP and *At*HIR1-YFP (Figure 4n) showed that ISX treatment significantly decreased the immobile fraction (i.e. increased mobility) in *At*HIR1-YFP. We introduced *At*Lti6b-GFP line as a positive control line for ISX treatment and we observed previously documented decrease of mobility of this protein by ISX (Martiniere et al., 2012). In addition to cellulose synthesis inhibition, we tested the effect of pectin methylesterase inhibitor epigallocatechin gallate (EGCG) affecting the CW structure by the alteration in pectin status (Lewis et al., 2008). We observed slight increase of immobile fraction in *At*FLOT2-GFP (Figure 4o), however, no apparent changes were to be seen in localization pattern (Figure S10a, b) or kymograms and PCC (Figure S10c-e). Similarly to ISX treatment, EGCG caused increase of CV, i.e. more pronounced association of *At*FLOT2-GFP with microdomains (Figure S10f).

Although the application of 20 µM ISX for 1 h triggers fast changes in cellulose biosynthesis, the identity of microdomains might be still preserved by existing CW structure. Therefore, we first tested the effect of PM detachment from the CW by performing plasmolysis. This treatment

induced prominent change of localization of both proteins tested but they were of different nature. While *At*FLOT2-GFP mostly remained at PM where it formed less dense but more aggregated clusters (Figure 5a, b, e) only a small fraction of *At*HIR1-YFP signal was still present at the PM (Figure 5c, d) the most of the protein was rather translocated into cell interior where it accumulated in endomembrane compartments (Figure 5f). Surprisingly, immobile fraction of both *At*FLOT2-GFP and *At*HIR1-YFP in plasmolysed PM was even higher than that of control treated seedlings (Figure 5g).

Then we further followed the dynamics of microdomains after enzymatic removal of CW. First we performed partial CW digestion in roots (Feraru et al., 2011) of *At*FLOT2-GFP and *At*HIR1-YFP lines. We used lower mannitol concentration (0.2 M) in the enzyme solution to avoid excessive osmotic challenging of cells. We observed distinct PM areas under the combination of mild plasmolysis and CW digestion (Figure 5h): PM partially detached from CW (DPM), PM that was partially released from the CW-delimited space (RPM) as well as PM still anchored to CW (APM). We determined immobile fractions of both proteins in these PM areas. In both proteins, even 0.2 M mannitol still induced slight increase of immobility (Figure 5i, j), however *At*FLOT2-GFP immobile fraction gradually decreased from APM to DPM and RPM (Figure 5i). The effect was even more pronounced for *At*HIR1-YFP where enzymatic CW digestion decreased immobile fraction not only in DPM and RPM but also in APM (Figure 5j). As the effect of partial CW digestion was low in *At*FLOT2-GFP we further investigated the impact of CW removal in protoplasts prepared from leaves of *At*FLOT2-GFP line. After the isolation, protoplasts were immediately imaged with SD confocal microscopy. The mobility of individual microdomains shown at kymograms was substantially higher in protoplasts where fluctuation is apparent (Figure 6b) than in leaf cells (Figure 6a) during 120 s observation period (Movie S4). This is also demonstrated on merge of images acquired at time 0 and 120 s and on corresponding co-localization scatter-plots (Figure 6c, d).

Interestingly, PM corrals restricting the microdomains with *At*FLOT2-GFP remained to be visible in released protoplasts (arrows in Figure 6e), which suggest that CW is not necessary for their constitution. Further analysis of the mobility of *At*FLOT2-GFP showed that CW removal induced not only higher lateral microdomain dynamics, but also more frequent appearance and disappearance of single microdomains within the single SD confocal plane of the PM (Movie S5), suggesting faster dynamics in z axis. Therefore, trajectories of individual microdomains were tracked during 120 s (Figure 6f, g). This analysis showed that *At*FLOT2-GFP microdomains in intact epidermal cells were less mobile and remained for a longer period in the observed focal plane. This is demonstrated as longer track duration (pseudo colour

coded), i.e. longer continuous period when a given microdomain (mobile or stable) was detectable in the focal plane (Figure 6f). In contrast, microdomains in protoplasts remained for a shorter period within the focal plane (shown in pseudocolors as short track duration) but even in this shorter timespan they were of longer trajectories (Figure 6g).

Altogether these findings suggest that CW represent important structural component necessary for the stabilization of PM-associated HIR and FLOT-containing microdomains in plant cells.

DISCUSSION

PM proteins often exhibit aggregated distribution, i.e. they are localized in PM-associated microdomains. This has been described for many plant PM proteins with various cellular functions, such as water transporters, ion channels, auxin carriers, remorins, alternative oxidase, various receptor kinases and phospholipases (Martiniere and Runions, 2013, Angelini et al., 2018, Tapken and Murphy, 2015, Jarsch et al., 2014, Konrad and Ott, 2015, Hao et al., 2014, Li et al., 2012). In this work, we demonstrate that microdomain localization is also shared among isoforms of *At*FLOTs and *At*HIRs. They display low lateral PM dynamics and high level of immobile fractions as revealed by FRAP experiments. However, our detailed study revealed significant differences in the mobility of *At*FLOTs and plant-specific *At*HIRs associated with the PM, with *At*HIRs being significantly more dynamic. Since all *At*HIRs and none of *At*FLOTs have been recently experimentally found to be palmitoylated (Hemsley et al., 2013) or myristoylated (Majeran et al., 2018), the observed difference may be attributed to a different PM association characteristics for *At*FLOTs and *At*HIRs. Myristoylation, an irreversible modification, was reported to be important for plant endomembrane localization whereas additional, potentially reversible, palmitoylation determines PM localization of thioredoxins (Traverso et al., 2013). It is thus possible that *At*HIR may be differentially fatty-acylated when located at the PM. In contrast to metazoan flotillins, no myristoylation or palmitoylation motif was predicted for *AtFLOT* sequences (Daněk et al., 2016) suggesting other way of interaction with PM. Using a BH search tool (Brzeska et al., 2010) we noticed a presence of a putative membrane binding site in N-termini of several plant FLOTs which was present also in all three *At*FLOTs but was not detected in *At*HIRs (Figure S11a). Similar motifs have been reported to bind acidic phospholipids and thus mediate the association with PM or other membranes (Barbosa et al., 2016). Moreover, a short conserved sequence enriched in basic and hydrophobic amino acids corresponding with the putative membrane binding sites was detected in all plant FLOTs tested but not in *At*HIRs (Figure S11b).

Importantly, a previous study showed that the mobility of *At*FLOT1 fluorescence foci was higher than those of *At*HIR1 (Lv et al., 2017b), contrasting with our results. However, this difference might be attributed to the position of fluorescence tag. All isoforms used in our study were tagged at their C-terminus, i.e. both *At*FLOTs (this study) or *At*HIRs (Qi et al., 2011), whereas in (Li et al., 2012) and (Lv et al., 2017b), authors used *At*FLOT1 tagged at N-terminus and *At*HIR1 tagged at C-terminus. Since N-terminal SPFH domain is *bona fide* responsible for the localization and interaction with PM as reported for metazoan flotillins (Morrow et al.,

2002, Langhorst et al., 2008, Neumann-Giesen et al., 2004) we assume that N-terminal tagging may affect the protein-membrane interactions and this inconsistency might thus result in different properties of *At*FLOT1 observed in our study and mentioned previous studies. The difference in lateral mobility of N- vs C-tagged *At*PIP1;2 and *At*PIP2;1 aquaporins was reported (Luu et al., 2012).

In this study, we provide direct live imaging microscopy evidence that members of FLOT/HIR protein family are localized besides PM also at the tonoplast in epidermal cells of various organs. Numerous proteome-based studies with manual and automatic predictions reported tonoplast and PM signatures for both FLOT and HIR homologs from several plant species as indicated e.g. in SUBA3 localisation database (Tanz et al., 2013). Tonoplast localization is shown in our study to be more frequent for *At*HIR proteins, with *At*HIR3-YFP being present only at the tonoplast. Accordingly, *At*HIR1/2/4 were reported to be enriched in PM fraction in contrast to *At*HIR3 that was found more abundant in the endomembrane fractions (Majeran et al., 2018).

We have been interested in the definition of factors affecting high stability of *At*FLOT and *At*HIR microdomains at the PM and their spatial distribution. Distinct linear corrals, void of fluorescence and co-aligning with MTs, were observed in the microdomain localization pattern for all *At*FLOTs and *At*HIRs except *At*HIR3. PM-associated corrals were reported previously for the distribution of formin1 (Martiniere et al., 2011) and they are also obvious on images of *At*FLOT1 and *At*FLOT2 in Jarsch et al. (2014), although not explicitly termed as "corrals". According to associomics.org protein interaction database (Jones et al., 2014), all three *At*FLOT isoforms interact with *At*IQD6, a putative calmodulin-binding protein binding MTs (Burstenbinder et al., 2017b), which we demonstrated to colocalize with corrals within *At*FLOT2-GFP microdomain pattern. PM-MT corrals might then restrict mobility of PM-associated proteins, as shown for *At*HIR1 microdomains being confined in their mobility by cortical MTs (Lv et al., 2017b).

We have further focused on the understanding the significance of intact cytoskeleton for the PM-associated stable microdomain structural identity and showed that neither MTs, nor actin filament disruption had an effect on the PM-association and patterning of microdomains with *At*FLOTs and *At*HIRs. Our results are thus partially in line with the ones obtained for a remorin where the microdomain identity was conserved under MT. On the other hand, the lack of effect of actin depolymerization found in our work is in contrast with the important impact on remorin, clustering of which was abolished or enhanced under actin filament depolymerization or hyperstabilization respectively (Szymanski et al., 2015). Single particle mobility of *At*PIP2;1

aquaporin was enhanced under actin depolymerization while no effect was observed for MT disruption (Hosy et al., 2014). This suggest that specific proteins might be differentially affected by interaction with either microtubules or actin filaments which is consistent with the opposite effects observed previously for *At*FLOT1, where both Ory and LatB treatments lowered the mobility of individual *At*FLOT1 puncta (Li et al., 2012) while dynamics of *At*HIR1 was increased by Ory and LatB (Lv et al., 2017b). Influence of cytoskeleton components thus seems to be specific for a given protein which was also documented for *M. truncatula* remorin where actin depolymerisation decreased the number of microdomains while microtubule disruption had not any effect (Liang et al., 2018).

An opposite effect of sterol depletion was reported for *At*FLOT1 and *At*HIR1 puncta where either a decrease or an increase of diffusion coefficient was observed under the treatment with sterol depletion agent methyl-ß-cyclodextrin (Li et al., 2012, Lv et al., 2017b). Interestingly, we have not observed any effect of such a treatment on localization pattern or microdomain mobility shown at kymograms for any of the tested isoforms (Figure S12a-x)). Moreover, immobile fractions of *At*FLOT2-GDP and *At*HIR1-YFP were not affected by sterol depletion (Figure S12y). However, different methods of mobility determination were carried out in the cited publications and in our work which could be the reason for different results obtained.

Low lateral mobility and high immobile fraction of *At*FLOTs is in sharp contrast to very high mobility of human flotillin2 (Langhorst et al., 2007) and the same difference could be found among metazoan aquaporins and their plant homologs (Martiniere and Runions, 2013). This was already shown for tonoplast-localized isoform of aquaporin, which exhibited higher mobility than the one residing at the PM (Luu et al., 2012) and there was also a large difference in single particle mobility between tonoplast and PM localized isoforms of aquaporins with much higher values reached by tonoplast isoform (Hosy et al., 2014). Even the same membrane protein mobility can differ depending on its localization, which was demonstrated for a PM intrinsic protein retained at the ER membrane, that was able to recover with substantially higher rate than the form properly localized at the PM (Sorieul et al., 2011). Finally *At*HIR1 mobility has been recently shown to be higher at the tonoplast than at the PM (Lv et al., 2017a).

Exceptionally high immobility measured by FRAP of *At*FLOTs is apparent when compared with the values obtained by the same method for other PM microdomain proteins such as remorins exhibiting mobile fractions > 23 % (McKenna et al., 2014) or even > 60 % (Jarsch et al., 2014). Phototropin1 localized in PM microdomains recovered by about 50% within 120 s (Xue et al., 2018). Very low recovery rate presented here for inner leaflet peripheral *At*FLOTs and *At*HIRs thus do not seem to be a general feature of plant PM microdomain proteins. They

are rather comparable with mobile fractions of 10-20% measured for proteins such as *At*FLS2, *At*FH1, *At*PIN2 or *At*PIP2;1 (McKenna et al., 2014), i.e. transmembrane proteins or even proteins with extracellular domain.

Differential mobility of homologs localized at the tonoplast or PM points to the specific interaction at the PM, which could potentially be relevant also for PM-CW continuum (Liu et al., 2015). In this work, we tested fast response to high concentration of ISX, an inhibitor of cellulose synthesis through *At*CESA3 and *At*CESA6 (Scheible et al., 2001, Desprez et al., 2002) known for the disruption of cell wall structure. ISX had only small effects on lateral dynamics of *At*FLOT2-GFP and increased significantly only *At*HIR1-YFP mobility. On the contrary, EGCG treatment interfering with pectin status decreased only the mobility of *At*FLOT2-GFP. It thus seems that different PM proteins might be linked to specific CW components. Cellulose synthesis inhibition or pectin methylation alteration was demonstrated to promote the mobility of *At*PIN2, *At*PIN3 and *At*FLS2 whereas there was no effect or even decrease in diffusion rate of *At*Lti6b (Martiniere et al., 2012, McKenna et al., 2019, Feraru et al., 2011).

Despite the reports that PM protein mobility is increased under plasmolysis (Feraru et al., 2011, Martiniere et al., 2012, Hosy et al., 2014) we observed rather an opposite effect. Plasmolysis induce dramatic changes in several cellular processes including reduced movement of endoplasmic reticulum structures (Cheng et al., 2017) or decreased actin dynamics (Tolmie et al., 2017) and polymerization (Yu et al., 2018). It is thus possible that reported increase in mobility may not be a direct effect of PM detachment but rather a result of complex changes induced by plasmolysis in a cell which probably involve also cytoskeleton dynamics alteration that were in many cases also documented to affect PM protein mobility (see the Discussion above). In our work, mild osmotic treatment combined with enzymatic CW degradation resulted in an increase in *At*FLOT2-GFP and *At*HIR1-YFP mobility. Similar increase after protoplast release was observed for GFP fused with glycophosphatidylinositol (GPI) (Martiniere et al., 2012). However, GPI always faces the extracellular side of PM, i.e. it can directly interact with the cell wall. This cannot be the case of any *At*FLOTs or *At*HIRs since they are supposed to be peripheral membrane proteins facing the cytoplasmic side of the PM.

Protein-protein interaction can confine a single protein mobility, which was reported for human flotillins where decreased recovery was observed when two flotillin isoforms were co-expressed when compared with single isoform expression (Affentranger et al., 2011). In Arabidopsis, direct interaction of *At*FLOT1 and *At*FLOT3 was found (Yu et al., 2017) and heterooligomerization of single isoforms of *At*HIRs can be realized (Qi et al., 2011). This could lower the potential of *At*HIR3 protein-protein interaction when compared with other isoforms.

Such differences might be responsible for distinct *At*HIR3-YFP traits observed in this work. In remorins, trimerization is an indispensable prerequisite for PM microdomain formation (Konrad et al., 2014, Martinez et al., 2018). Similarly, metazoan flotillins needs to hetero-oligomerize to form PM microdomains (Solis et al., 2007). Our lines expressed only a single isoform, however there is still a possibility of interaction of expressed tagged proteins with endogenous protein partners.

The interaction of *At*FLOTs (or possibly also *At*HIRs) with the CW constituents is probably indirect, i.e. via other proteins, supposedly with the ones containing extracellular domains. In our previous study, we found several transmembrane proteins, such as receptor-like kinases, aquaporins, ATPases or other transporters in the interactome of *At*FLOT2 (Junková et al., 2018). *At*FLOT2 and *At*FLOT3 also interact with *At*TBL36 (associomics.org), a homolog of transmembrane trichome birefringence protein which is necessary for proper cellulose composition of the CW (Bischoff et al., 2010). Furthermore, *Mt*FLOT4 was found to co-localize with *Mt*LYK3, a lysine motif receptor-like kinase (Haney et al., 2011). This is mediated by *a* remorin which forms microdomain upon interaction with pre-existing *Mt*FLOT4 microdomains (Liang et al., 2018). Possibility of the interaction of *At*FLOTs and *At*HIRs with lysine motif receptor kinases recognizing chitin was discussed also in *A. thaliana* (Faulkner, 2013). *At*HIR1 and *At*HIR2 directly interact with *At*RPS2, a PM-associated resistance protein (Qi et al., 2011) and were found as parts of *At*RPS2-formed protein complex containing transmembrane proteins such as aquaporins, receptor-like kinases or metal transporters (Qi and Katagiri, 2009). These transmembrane proteins can also serve as "pickets" (Ritchie et al., 2003) limiting the lateral movement of *At*FLOT or *At*HIR microdomains and on the other hand, FLOT and HIR-defined microdomains may take part in proper functioning of these proteins.

Besides direct protein-protein interaction, an interconnection between both PM leaflets via long acyl chains of locally enriched specific lipids was reported in metazoan cells. Together with proteins interacting on both sides of the membrane or with cytoskeleton in the cell interior they form clusters of reduced mobility (Raghupathy et al., 2015). This so called interdigitation was proposed also in plants with reported involvement of sphingolipids (Cacas et al., 2016). It is thus tempting to speculate of such a process induced by similar protein local enrichment or immobilization caused by interacting with the CW which could enhance the formation of this extra-to-intracellular linkage leading to changes in *At*FLOT or *At*HIR dynamics.

EXPERIMENTAL PROCEDURES

Chemicals

Unless stated otherwise, all chemicals were supplied by Sigma Aldrich (St Louis, MO, USA).

Plant material and cloning

Col-0 *A. thaliana* lines carrying 35S::*At*HIR1:YFP, 35S::*At*HIR2:YFP, 35S::*At*HIR3:YFP, 35S::*At*HIR4:YFP were described previously (Qi et al., 2011). *At*PIP2;1-GFP (Boursiac et al., 2005), *At*VAMP711-GFP (Geldner et al., 2009), *At*Lti6b-GFP (Grebe et al., 2003) and FABD:GFP/mCherry:TUA5 (Sampathkumar et al., 2011) lines were obtained from Doan-Trung Luu, Markus Grebe, Niko Geldner and Staffan Persson respectively. *At*FLOT1 (At5g25250), *At*FLOT2 (At5g25260), *At*FLOT3 (At5g64870), *At*HIR1 (At1g69840) and *At*IQD6 (At2g26180) coding sequences were amplified from *A. thaliana* cDNA prepared as described elsewhere (Krckova et al., 2018) using PCR with specific primers (*At*FLOT1 FP: CGCGGATCCATGTTCA AAGTTGCAAGAGCG; *At*FLOT1 RP: CGGAATTCGCTGCGAGTCACTTGC; *At*FLOT2 FP: TTAGGATCCATGTTCAAGGTTGCAAGAG; *At*FLOT2 RP: TTAGAATTCCTTGC TTAGAGTACCGATCC; *At*FLOT3 FP: TTAGGATCCATGAGTTACAGAGTCGC TAAAGCA; *At*FLOT3 RP: TTAGAATTCACCTCTGTGTTGTTGAGCATG; *At*HIR1 FP: TTAGGATCCATGGGTCAAGCTTTGGGTTG; *At*HIR1 RP: TTAGAATTCCTCAGCA GCAGAGTTACCCTG; *At*IQD6 FP: GCGGGATCCATGGGTGCTTCAGGGAAATG and *At*IQD6 RP: CCGAATTCACCTCTCGGCTTCTCGAATC). Obtained amplicons were digested using EcoRI and BamHI (both Thermo Fisher Scientific, Waltham, MA, USA) and in frame directly introduced in between corresponding restriction sites of modified pGreen0029 plasmid (Hellens et al., 2000) containing CaMV 35S promoter and C-terminal mCherry (*At*IQD6) or eGFP sequence (the rest of amplicons). Stable transformants were obtained by floral dip method (Clough and Bent, 1998) and selected on half-strength MS medium (Duchefa, Haarlem, The Netherlands) with 1% sucrose, 1% plant tissue culture agar and kanamycin (50 $\mu g \cdot ml^{-1}$).

Growth conditions and transient transformation

Seeds were surface-sterilised with diluted commercial bleach for 10 minutes and sown on plates with half strength MS (Duchefa, Haarlem, The Netherlands) medium solidified with 1%

agar and supplemented with 1% sucrose. Seedlings were grown in vertical position in 16/8 h light (100 µmol $m^{-2}\cdot s^{-1}$)/dark cycle. 6-day-old or 10-day-old plants were used for the analysis of roots, cotyledons and hypocotyls and first true leaves, respectively.

Seedling expressing *At*HIR1-YFP were transformed with FAST/AGROBEST method using *Agrobacterium tumefaciens* strain C58C1 carrying MBD-mRFP gene construct (Angelini et al., 2018) according to (Li et al., 2009). Briefly, 4-day-old seedlings were co-cultivated with Agrobacterium suspensions of OD_{600} = 0.1, 0.06, and 0.04 in quarter strength liquid MS medium supplemented with 100 µM acetosyringon for 48 hours in darkness and subsequently rinsed twice with quarter strength MS medium supplemented with cefotaxime (600 $\mu g\cdot ml^{-1}$ for 10 min and 200 $\mu g\cdot ml^{-1}$ for 1-2 hours). Transformed seedlings were observed after 24-96 h.

Nicotiana benthamiana leaves (3-4 week old) were transformed (Batoko et al., 2000) by infiltration of suspension (OD_{600} = 0.1 for each construct) of *A. tumefaciens* strain C58C1 carrying *At*FLOT2-GFP/pGreen0029 or *At*IQD6-mCherry/pGreen0029 vector. Epidermal leaf cells were observed 36 – 48 h after the transformation

Pharmacological treatments and cell wall digestion

Stock solutions of LatB (2.53 mM), Ory (57.7 mM), ISX (20 mM) and EGCG (50 mM; Santa Cruz Biotechnology, TX, USA) in DMSO were added to 1 ml aliquots of half strength MS medium with 1% sucrose in a multi-well plastic plate to reach final concentrations 1 µM LatB, 20 µM Ory, 20 µM ISX and 50 µM EGCG. mßCD was dissolved directly in half strength MS medium with 1% sucrose to obtain 10 mM working solution. Seedlings were transferred from agar plates into the multi-well plate and incubated for desired time. Appropriate amount of DMSO was added to controls.

Partial cell wall digestion by macerozyme R10 and cellulose Onozuka R10 (both Yakult Pharmaceutical, Tokyo, Japan) was performed as described in Feraru et al., 2011 with this modification: 0.2 M mannitol was used instead of 0.4 M mentioned in the cited paper. The treatment was performed by mounting the seedling in the enzyme solution on slides. The slides were then incubated for 30 min at room temperature in 100 % air humidity to prevent drying of the samples.

Protoplasts from Arabidopsis leaves were prepared according to (Wu et al., 2009) from 5-week-old plants. Briefly, the peeled leaves were incubated in enzyme solution (1% cellulase Onozuka R10, 0.25% macerozyme R10 (both Yakult Pharmaceutical, Tokyo, Japan), 0.1% BSA, 0.4 M mannitol, 10 mM $CaCl_2$, 20 mM KCl, 20 mM 2-morpholinoethanesulfonic acid (MES), pH 5.7 for 1 hour under gentle shaking (40 rpm). Protoplasts were centrifuged at 100 g

for 3 min. The pellet was twice resuspended and subsequently centrifuged in 25 ml modified W5 solution (154 mM NaCl, 125 mM $CaCl_2$, 5 mM glucose, 5 mM KCl, 2 mM MES, pH 5.7) to rinse.

Confocal microscopy

For confocal imaging of non-treated plants and time-lapse imaging, rectangular piece of agar medium with seedling was placed into Lab-Tek chambered Borosilicate cover glass (Nunc, Rochester, NY, USA). Drug-treated seedlings were imaged after their transfer from the liquid medium into the drop of medium in the chamber and covered with coverslip.

SD confocal microscopy was performed using a Nikon Eclipse Ti inverted microscope (Nikon, Tokyo, Japan) equipped with a spinning disk unit CSU-X1 (Yokogawa, Tokyo, Japan) and oil plan apochromatic objective 100x (NA 1.45). Fluorescence signals were excited with diode lasers (488 nm or 561 nm; Agilent, Santa Clara, CA, USA). For majority of imaging, the fluorescence emission was recorded with an Andor Zyla sCMOS camera with 2560x2160 pixel resolution (Andor Technology, Belfast, Northern Ireland, UK) using Semrock Brightline single-pass filters (Semrock, Rochester, NY, USA) for GFP/YFP (488 nm/525-030 or RFP (561 nm/607-036).

CLSM was performed with Zeiss LSM 880 confocal setup on Axio Observer Z1 inverted microscope (Carl Zeiss, Jena, Germany), using 63x oil immersion objective (NA=1.40) for FRAP experiments and 100x oil immersion objective (NA=1.46) for imaging using Airyscan detector. GFP fluorescence was excited with Argon laser (488 nm) and detected using GaAsP detector between 505 and 550 nm. For super-resolution imaging in xyz, the array of 32 GaAsP detectors was used for detection of signal and images processed with SR processing function using Zen Black software (Carl Zeiss, Jena, Germany), reaching near diffraction spatial resolution (170 nm).

FRAP analysis

FRAP analysis was performed according to (Lankova et al., 2016) with modifications. Region of interest (ROI) for bleaching and FRAP was interactively applied at the transversal PMs, non-bleached control ROI at lateral PM and background ROI outside of the root (see Figure S6). Bleaching with maximal laser intensity was followed by tracking fluorescence recovery for 60 s. Data recorded using Zeiss Zen Black software were processed in Microsoft Excel. Since the photobleaching during the FRAP period was negligible, it was not necessary

to correct data for this effect. Fluorescence intensity data were normalized using following equation:

$$I_n = (I_t - I_{min})/(I_{max} - I_{min}),$$

where I_n is the normalized intensity, I_t is the intensity in specific time, I_{min} is the intensity after the photobleach and I_{max} is the intensity before bleaching. Sets of normalized values were transferred to Sigma Plot 12.5 software (Systat Software, San Jose, CA, USA) and fitted with single exponential fit with two parameters, according to following equation:

$$y = a \cdot (1 - \exp(-b \cdot x),$$

where y is normalized intensity, a represents mobile fraction and b reflects the recovery speed, from which recovery halftimes were calculated using $t_{1/2} = -\ln \cdot (0.5)/b$ equation.

Image processing and analysis

Determination of microdomain density from SD images was performed in the square ROI (5x5 µm) applied interactively at the maximum intensity projections from z-stacks (step size 200 nm) covering cell surface of elongated root epidermal cells. Number of microdomains within the sampling squares were determined using Find Maxima tool in ImageJ/Fiji software (Schindelin et al., 2012). Six or seven plants of each line were sampled and four to seven sampling squares per image were analysed (at least 30 overall sampling squares for each line). Kruskal-Wallis test followed with multiple comparison Dunn test were performed to assess differences between individual lines.

Microdomain size was assessed from images obtained by using Airyscan as a diameter estimated as FWHM determined from Gaussian function fitted on the fluorescence intensity profile linearly transecting an individual microdomain fluorescent spot and its adjacent background. In case of asymmetric microdomains (e.g. elongated in one direction), the shorter diameter was concerned. FWHM determination was performed in ImageJ using a macro developed by Soon Yew John Lim, Skin Research Institute of Singapore, A*STAR.

Kymograms were constructed from time-lapse acquisitions (1 fps) with intensities equalized in time in NIS Elements software (Laboratory Imaging, Prague, Czech Republic). PCC of the fluorescence intensity profiles in the first (t = 0 s) and last (t = 60 s or 120 s) time points of a given kymogram was calculated in Microsoft Excel according to the equation:

$$PCC = \frac{\sum_{i=0}^{n}(x_i - x_{mean})\cdot(y_i - y_{mean})}{\sqrt{\sum_{i=0}^{n}(x_i - x_{mean})^2}\cdot\sqrt{\sum_{i=0}^{n}(y_i - y_{mean})^2}}$$

where x_i and y_i are the measured intensities in the first and last time point for a given pixel and x_{mean} and y_{mean} are average intensities in the first and last time point for the whole kymogram. Colocalization scatter-plot was generated using Colocalization Threshold in ImageJ.

CV of the fluorescence intensity profiles was calculated in Microsoft Excel according to the equation:

$$CV = \frac{sd\ (I)}{mean\ (I)}$$

where *sd (I)* is standard deviation and *mean (I)* is mean of fluorescence intensities obtained for each pixel of a given intensity profile.

Microdomain trajectory tracking was performed in ImageJ using TrackMate plugin (Tinevez et al., 2017) as follows. LoG detector was used with estimated blob diameter set to 0.45 µm, median filter and auto threshold on the quality feature was applied to detect individual spots which were subsequently traced using simple LAP tracer with the following parameters: linking max distance = 0.5 µm, gap-closing max distance = 0.6 µm and gap-closing max frame gap = 2.

ACKNOWLEDGEMENTS

Authors would like to thank Dr. Fumiaki Katagiri for kindly providing Arabidopsis lines 35S::*At*HIR1:YFP, 35S::*At*HIR2:YFP, 35S::*At*HIR3:YFP and 35S::*At*HIR4:YFP and to Dr. Doan-Trung Luu, Dr. Markus Grebe, Dr. Niko Geldner and Dr. Staffan Persson for providing the marker lines. The work was supported by Czech Science Foundation project n. 14-09685S and by the Ministry of Education, Youth and Sports of CR from European Regional Development Fund-Project "Centre for Experimental Plant Biology": No. 209 CZ.02.1.01/0.0/0.0/16_019/0000738. Institute of Experimental Botany Imaging Facility is supported by operational program Prague – competitiveness CZ.2.16/3.1.00/21519 and Ministry of Education, Youth and Sports project LM2015062 (Czech-BioImaging).

SUPPORTING INFORMATION

Figure S1. *Arabidopsis thaliana* lines overexpressing *At*FLOTs do not exhibit any apparent phenotype.

Figure S2. Tonoplast and plasma membrane localization of *At*FLOTs and *At*HIRs in the root epidermal cells.

Figure S3. Distribution of *At*FLOT and *At*HIR individual PM-associated microdomain size in root epidermal cells.

Figure S4. *At*FLOTs and *At*HIRs are localized in PM microdomains in cotyledon and hypocotyl epidermal cells.

Figure S5. Determination of correlation coefficient as a way to analyse a kymogram.

Figure S6. FRAP experiment description.

Figure S7. *At*FLOT and *At*HIR differ in the degree of fluorescence signal association with PM.

Figure S8. *At*FLOT and *At*HIR microdomain localization pattern does not depend on the integrity of microtubules and actin filaments.

Figure S9. Control treatment (0.1% DMSO) for ISX experiments presented in Figure 4a-l.

Figure S10. EGCG treatment of *At*FLOT2-GFP epidermal root cells.

Figure S11. *At*FLOTs but not *At*HIRs may interact with PM by their putative N-terminal membrane binding site.

Figure S12. Sterol depletion does not affect mobility of PM-associated *At*FLOTs and *At*HIRs.

Movie S1. Time-lapse imaging of *At*FLOT3-GFP in elongated epidermal root cell.

Movie S2. Time-lapse imaging of *At*FLOT2-GFP in elongating cells showing lateral hopping movement of some domains.

Movie S3. Time-lapse imaging of *At*FLOT2-GFP in elongating cells showing slower movement of whole domain in the direction of corrals.

Movie S4. Comparison of *At*FLOT2-GFP microdomain mobility in PM of a protoplast and intact leaf epidermal cell.

Movie S5. Close-up view of *At*FLOT2-GFP microdomain in PM of a protoplast and intact leaf epidermal cell used for trajectory tracking in Figure 6f, g.

REFERENCES

ABEL, S., BURSTENBINDER, K. & MULLER, J. 2013. The emerging function of IQD proteins as scaffolds in cellular signaling and trafficking. *Plant Signal Behav,* 8**,** e24369.

AFFENTRANGER, S., MARTINELLI, S., HAHN, J., ROSSY, J. & NIGGLI, V. 2011. Dynamic reorganization of flotillins in chemokine-stimulated human T-lymphocytes. *BMC Cell Biol,* 12**,** 28.

ANGELINI, J., VOSOLSOBĚ, S., SKŮPA, P., HO, A. Y. Y., BELLINVIA, E., VALENTOVÁ, O. & MARC, J. 2018. Phospholipase Dδ assists to cortical microtubule recovery after salt stress. *Protoplasma,* 255**,** 1195-1204.

BABUKE, T. & TIKKANEN, R. 2007. Dissecting the molecular function of reggie/flotillin proteins. *European Journal of Cell Biology,* 86**,** 525-532.

BARBOSA, I. C. R., SHIKATA, H., ZOURELIDOU, M., HEILMANN, M., HEILMANN, I. & SCHWECHHEIMER, C. 2016. Phospholipid composition and a polybasic motif determine D6 PROTEIN KINASE polar association with the plasma membrane and tropic responses. *Development,* 143**,** 4687-4700.

BATOKO, H., ZHENG, H.-Q., HAWES, C. & MOORE, I. 2000. A Rab1 GTPase Is Required for Transport between the Endoplasmic Reticulum and Golgi Apparatus and for Normal Golgi Movement in Plants. *The Plant Cell,* 12**,** 2201-2217.

BAUMANN, C. A., RIBON, V., KANZAKI, M., THURMOND, D. C., MORA, S., SHIGEMATSU, S., BICKEL, P. E., PESSIN, J. E. & SALTIEL, A. R. 2000. CAP defines a second signalling pathway required for insulin-stimulated glucose transport. *Nature,* 407**,** 202-207.

BERNARDINO DE LA SERNA, J., SCHÜTZ, G. J., EGGELING, C. & CEBECAUER, M. 2016. There Is No Simple Model of the Plasma Membrane Organization. *Frontiers in Cell and Developmental Biology,* 4.

BISCHOFF, V., NITA, S., NEUMETZLER, L., SCHINDELASCH, D., URBAIN, A., ESHED, R., PERSSON, S., DELMER, D. & SCHEIBLE, W.-R. 2010. TRICHOME BIREFRINGENCE and Its Homolog AT5G01360 Encode Plant-Specific DUF231 Proteins Required for Cellulose Biosynthesis in Arabidopsis. *Plant Physiology,* 153**,** 590-602.

BOURSIAC, Y., CHEN, S., LUU, D. T., SORIEUL, M., VAN DEN DRIES, N. & MAUREL, C. 2005. Early effects of salinity on water transport in Arabidopsis roots. Molecular and cellular features of aquaporin expression. *Plant Physiol,* 139**,** 790-805.

BRZESKA, H., GUAG, J., REMMERT, K., CHACKO, S. & KORN, E. D. 2010. An experimentally based computer search identifies unstructured membrane-binding sites in proteins: application to class I myosins, PAKS, and CARMIL. *J Biol Chem,* 285**,** 5738-47.

BURSTENBINDER, K., MITRA, D. & QUEGWER, J. 2017a. Functions of IQD proteins as hubs in cellular calcium and auxin signaling: A toolbox for shape formation and tissue-specification in plants? *Plant Signal Behav,* 12**,** e1331198.

BURSTENBINDER, K., MOLLER, B., PLOTNER, R., STAMM, G., HAUSE, G., MITRA, D. & ABEL, S. 2017b. The IQD Family of Calmodulin-Binding Proteins Links Calcium Signaling to Microtubules, Membrane Subdomains, and the Nucleus. *Plant Physiol,* 173**,** 1692-1708.

CACAS, J. L., BURE, C., GROSJEAN, K., GERBEAU-PISSOT, P., LHERMINIER, J., ROMBOUTS, Y., MAES, E., BOSSARD, C., GRONNIER, J., FURT, F., FOUILLEN, L., GERMAIN, V., BAYER, E., CLUZET, S., ROBERT, F., SCHMITTER, J. M., DELEU, M., LINS, L., SIMON-PLAS, F. & MONGRAND, S. 2016. Revisiting Plant Plasma Membrane Lipids in Tobacco: A Focus on Sphingolipids. *Plant Physiology,* 170**,** 367-384.

CLOUGH, S. J. & BENT, A. F. 1998. Floral dip: a simplified method for Agrobacterium-mediated transformation of Arabidopsis thaliana. *Plant J,* 16**,** 735-43.

CUI, Y., LI, X., YU, M., LI, R., FAN, L., ZHU, Y. & LIN, J. 2018. Sterols regulate endocytic pathways during flg22-induced defense responses in Arabidopsis. *Development,* 145.

DANĚK, M., VALENTOVÁ, O. & MARTINEC, J. 2016. Flotillins, Erlins, and HIRs: From Animal Base Camp to Plant New Horizons. *Critical Reviews in Plant Sciences,* 35**,** 191-214.

DESPREZ, T., VERNHETTES, S., FAGARD, M., REFRÉGIER, G., DESNOS, T., ALETTI, E., PY, N., PELLETIER, S. & HÖFTE, H. 2002. Resistance against Herbicide Isoxaben and Cellulose Deficiency Caused by Distinct Mutations in Same Cellulose Synthase Isoform CESA6. *Plant Physiology,* 128**,** 482-490.

DI, C., XU, W. Y., SU, Z. & YUAN, J. S. 2010. Comparative genome analysis of PHB gene family reveals deep evolutionary origins and diverse gene function. *Bmc Bioinformatics,* 11.

DUAN, Y. H., GUO, J., SHI, X. X., GUAN, X. N., LIU, F. R., BAI, P. F., HUANG, L. L. & KANG, Z. S. 2013. Wheat hypersensitive-induced reaction genes TaHIR1 and TaHIR3 are involved in response to stripe rust fungus infection and abiotic stresses. *Plant Cell Reports,* 32**,** 273-283.

FAULKNER, C. 2013. Receptor-mediated signaling at plasmodesnnata. *Frontiers in Plant Science,* 4.

FERARU, E., FERARU, M. I., KLEINE-VEHN, J., MARTINIERE, A., MOUILLE, G., VANNESTE, S., VERNHETTES, S., RUNIONS, J. & FRIML, J. 2011. PIN polarity maintenance by the cell wall in Arabidopsis. *Curr Biol,* 21**,** 338-43.

GELDNER, N., DENERVAUD-TENDON, V., HYMAN, D. L., MAYER, U., STIERHOF, Y. D. & CHORY, J. 2009. Rapid, combinatorial analysis of membrane compartments in intact plants with a multicolor marker set. *Plant Journal,* 59**,** 169-178.

GREBE, M., XU, J., MOBIUS, W., UEDA, T., NAKANO, A., GEUZE, H. J., ROOK, M. B. & SCHERES, B. 2003. Arabidopsis sterol endocytosis involves actin-mediated trafficking via ARA6-positive early endosomes. *Curr Biol,* 13**,** 1378-87.

GRONNIER, J., GERBEAU-PISSOT, P., GERMAIN, V., MONGRAND, S. & SIMON-PLAS, F. 2018. Divide and Rule: Plant Plasma Membrane Organization. *Trends in Plant Science,* 23**,** 899-917.

HANEY, C. H. & LONG, S. R. 2010. Plant flotillins are required for infection by nitrogen-fixing bacteria. *Proceedings of the National Academy of Sciences of the United States of America,* 107**,** 478-483.

HANEY, C. H., RIELY, B. K., TRICOLI, D. M., COOK, D. R., EHRHARDT, D. W. & LONG, S. R. 2011. Symbiotic *Rhizobia* bacteria trigger a change in localization and dynamics of the *Medicago truncatula* Receptor Kinase LYK3. *Plant Cell,* 23**,** 2774-2787.

HAO, H. Q., FAN, L. S., CHEN, T., LI, R. L., LI, X. J., HE, Q. H., BOTELLA, M. A. & LIN, J. X. 2014. Clathrin and membrane microdomains cooperatively regulate RbohD dynamics and activity in *Arabidopsis*. *Plant Cell,* 26**,** 1729-1745.

HELLENS, R. P., EDWARDS, E. A., LEYLAND, N. R., BEAN, S. & MULLINEAUX, P. M. 2000. pGreen: a versatile and flexible binary Ti vector for Agrobacterium-mediated plant transformation. *Plant Molecular Biology,* 42**,** 819-832.

HEMSLEY, P. A., WEIMAR, T., LILLEY, K. S., DUPREE, P. & GRIERSON, C. S. 2013. A proteomic approach identifies many novel palmitoylated proteins in Arabidopsis. *New Phytol,* 197**,** 805-14.

HO, A. Y. Y., DAY, D. A., BROWN, M. H. & MARC, J. 2009. *Arabidopsis* phospholipase D delta as an initiator of cytoskeleton-mediated signalling to fundamental cellular processes. *Functional Plant Biology,* 36**,** 190-198.

HOSY, E., MARTINIERE, A., CHOQUET, D., MAUREL, C. & LUU, D. T. 2014. Super-resolved and dynamic imaging of membrane proteins in plant cells reveal contrasting kinetic profiles and multiple confinement mechanisms. *Mol Plant*.

CHEN, F., YUAN, Y. X., LI, Q. & HE, Z. H. 2007. Proteomic analysis of rice plasma membrane reveals proteins involved in early defense response to bacterial blight. *Proteomics,* 7**,** 1529-1539.

CHENG, X., LANG, I., ADENIJI, O. S. & GRIFFING, L. 2017. Plasmolysis-deplasmolysis causes changes in endoplasmic reticulum form, movement, flow, and cytoskeletal association. *Journal of Experimental Botany,* 68**,** 4075-4087.

CHOI, H. W., KIM, Y. J. & HWANG, B. K. 2011. The hypersensitive induced reaction and leucine-rich repeat proteins regulate plant cell death associated with disease and plant immunity. *Molecular Plant-Microbe Interactions,* 24**,** 68-78.

ISHIKAWA, T., AKI, T., YANAGISAWA, S., UCHIMIYA, H. & KAWAI-YAMADA, M. 2015. Overexpression of BAX INHIBITOR-1 Links Plasma Membrane Microdomain Proteins to Stress. *Plant Physiology,* 169**,** 1333-1343.

JARSCH, I. K., KONRAD, S. S. A., STRATIL, T. F., URBANUS, S. L., SZYMANSKI, W., BRAUN, P., BRAUN, K. H. & OTT, T. 2014. Plasma membranes are subcompartmentalized into a plethora of coexisting and diverse microdomains in *Arabidopsis* and *Nicotiana benthamiana*. *Plant Cell,* 26**,** 1698-1711.

JONES, A. M., XUAN, Y., XU, M., WANG, R.-S., HO, C.-H., LALONDE, S., YOU, C. H., SARDI, M. I., PARSA, S. A., SMITH-VALLE, E., SU, T., FRAZER, K. A., PILOT, G., PRATELLI, R., GROSSMANN, G., ACHARYA, B. R., HU, H.-C., ENGINEER, C., VILLIERS, F., JU, C., TAKEDA, K., SU, Z., DONG, Q., ASSMANN, S. M., CHEN, J., KWAK, J. M., SCHROEDER, J. I., ALBERT, R., RHEE, S. Y. & FROMMER, W. B. 2014. Border Control-A Membrane-Linked Interactome of Arabidopsis. *Science,* 344**,** 711-716.

JUNG, H. W. & HWANG, B. K. 2007. The leucine-rich repeat (LRR) protein, CaLRR1, interacts with the hypersensitive induced reaction (HIR) protein, CaHIR1, and suppresses cell death induced by the CaHIR1 protein. *Molecular Plant Pathology,* 8**,** 503-514.

JUNKOVÁ, P., DANĚK, M., KOCOURKOVÁ, D., BROUZDOVÁ, J., KROUMANOVÁ, K., ZELAZNY, E., JANDA, M., HYNEK, R., MARTINEC, J. & VALENTOVÁ, O. 2018. Mapping of Plasma Membrane Proteins Interacting With Arabidopsis thaliana Flotillin 2. *Frontiers in Plant Science,* 9.

KONRAD, S. S., POPP, C., STRATIL, T. F., JARSCH, I. K., THALLMAIR, V., FOLGMANN, J., MARIN, M. & OTT, T. 2014. S-acylation anchors remorin proteins to the plasma membrane but does not primarily determine their localization in membrane microdomains. *New Phytol,* 203**,** 758-69.

KONRAD, S. S. A. & OTT, T. 2015. Molecular principles of membrane microdomain targeting in plants. *Trends in Plant Science,* 20**,** 351-361.

KRCKOVA, Z., KOCOURKOVA, D., DANEK, M., BROUZDOVA, J., PEJCHAR, P., JANDA, M., POKOTYLO, I., OTT, P. G., VALENTOVA, O. & MARTINEC, J. 2018. The Arabidopsis thaliana non-specific phospholipase C2 is involved in the response to Pseudomonas syringae attack. *Ann Bot,* 121**,** 297-310.

KROUMANOVÁ, K., KOCOURKOVÁ, D., DANĚK, M., LAMPAROVÁ, L., POSPÍCHALOVÁ, R., MALÍNSKÁ, K., KRČKOVÁ, Z., BURKETOVÁ, L., VALENTOVÁ, O., MARTINEC, J. & JANDA, M. 2019. Characterisation of Arabidopsis flotillins in response to stresses. *Biologia plantarum,* 63**,** 144-152.

KUSUMI, A. & SAKO, Y. 1996. Cell surface organization by the membrane skeleton. *Current Opinion in Cell Biology,* 8**,** 566-574.

LANGHORST, M. F., REUTER, A., JAEGER, F. A., WIPPICH, F. M., LUXENHOFER, G., PLATTNER, H. & STUERMER, C. A. O. 2008. Trafficking of the microdomain scaffolding protein reggie-1/flotillin-2. *European Journal of Cell Biology,* 87**,** 211-226.

LANGHORST, M. F., SOLIS, G. P., HANNBECK, S., PLATTNER, H. & STUERMER, C. A. O. 2007. Linking membrane microdomains to the cytoskeleton: Regulation of the lateral mobility of reggie-1/flotillin-2 by interaction with actin. *Febs Letters,* 581**,** 4697-4703.

LANKOVA, M., HUMPOLICKOVA, J., VOSOLSOBE, S., CIT, Z., LACEK, J., COVAN, M., COVANOVA, M., HOF, M. & PETRASEK, J. 2016. Determination of Dynamics of Plant Plasma Membrane Proteins with Fluorescence Recovery and Raster Image Correlation Spectroscopy. *Microsc Microanal,* 22**,** 290-9.

LEWIS, K. C., SELZER, T., SHAHAR, C., UDI, Y., TWOROWSKI, D. & SAGI, I. 2008. Inhibition of pectin methyl esterase activity by green tea catechins. *Phytochemistry,* 69**,** 2586-92.

LI, J. F., PARK, E., VON ARNIM, A. G. & NEBENFUHR, A. 2009. The FAST technique: a simplified Agrobacterium-based transformation method for transient gene expression analysis in seedlings of Arabidopsis and other plant species. *Plant Methods,* 5.

LI, R. L., LIU, P., WAN, Y. L., CHEN, T., WANG, Q. L., METTBACH, U., BALUSKA, F., SAMAJ, J., FANG, X. H., LUCAS, W. J. & LIN, J. X. 2012. A membrane microdomain-associated protein, *Arabidopsis*

Flot1, is involved in a clathrin-independent endocytic pathway and is required for seedling development. *Plant Cell,* 24**,** 2105-2122.

LI, S., ZHAO, J., ZHAI, Y., YUAN, Q., ZHANG, H., WU, X., LU, Y., PENG, J., SUN, Z., LIN, L., ZHENG, H., CHEN, J. & YAN, F. 2019. The hypersensitive induced reaction 3 (HIR3) gene contributes to plant basal resistance via an EDS1 and salicylic acid-dependent pathway. *Plant J*.

LI, X. J., WANG, X. H., YANG, Y., LI, R. L., HE, Q. H., FANG, X. H., LUU, D. T., MAUREL, C. & LIN, J. X. 2011. Single-molecule analysis of PIP2;1 dynamics and partitioning reveals multiple modes of *Arabidopsis* plasma membrane aquaporin regulation. *Plant Cell,* 23**,** 3780-3797.

LIANG, P., STRATIL, T. F., POPP, C., MARÍN, M., FOLGMANN, J., MYSORE, K. S., WEN, J. & OTT, T. 2018. Symbiotic root infections in *Medicago truncatula* require remorin-mediated receptor stabilization in membrane nanodomains. *Proceedings of the National Academy of Sciences*.

LIU, Z., PERSSON, S. & SANCHEZ-RODRIGUEZ, C. 2015. At the border: the plasma membrane-cell wall continuum. *J Exp Bot,* 66**,** 1553-63.

LUU, D. T., MARTINIERE, A., SORIEUL, M., RUNIONS, J. & MAUREL, C. 2012. Fluorescence recovery after photobleaching reveals high cycling dynamics of plasma membrane aquaporins in Arabidopsis roots under salt stress. *Plant Journal,* 69**,** 894-905.

LV, X., JING, Y., WU, H. & LIN, J. 2017a. Tracking Tonoplast Protein Behaviors in Intact Vacuoles Isolated from Arabidopsis Leaves. *Molecular Plant,* 10**,** 349-352.

LV, X., JING, Y., XIAO, J., ZHANG, Y., ZHU, Y., JULIAN, R. & LIN, J. 2017b. Membrane microdomains and the cytoskeleton constrain AtHIR1 dynamics and facilitate the formation of an AtHIR1-associated immune complex. *The Plant Journal,* 90**,** 3-16.

MAJERAN, W., LE CAER, J.-P., PONNALA, L., MEINNEL, T. & GIGLIONE, C. 2018. Targeted profiling of A. thaliana sub-proteomes illuminates new co- and post-translationally N-terminal Myristoylated proteins. *The Plant Cell*.

MALAKSHAH, S. N., REZAEI, M. H., HEIDARI, M. & SALEKDEH, G. H. 2007. Proteomics reveals new salt responsive proteins associated with rice plasma membrane. *Bioscience Biotechnology and Biochemistry,* 71**,** 2144-2154.

MAMODE CASSIM, A., GOUGUET, P., GRONNIER, J., LAURENT, N., GERMAIN, V., GRISON, M., BOUTTE, Y., GERBEAU-PISSOT, P., SIMON-PLAS, F. & MONGRAND, S. 2019. Plant lipids: Key players of plasma membrane organization and function. *Prog Lipid Res,* 73**,** 1-27.

MARTINEZ, D., LEGRAND, A., GRONNIER, J., DECOSSAS, M., GOUGUET, P., LAMBERT, O., BERBON, M., VERRON, L., GRÉLARD, A., GERMAIN, V., LOQUET, A., MONGRAND, S. & HABENSTEIN, B. 2018. Coiled-coil oligomerization controls localization of the plasma membrane REMORINs. *Journal of Structural Biology*.

MARTINIERE, A., GAYRAL, P., HAWES, C. & RUNIONS, J. 2011. Building bridges: formin1 of Arabidopsis forms a connection between the cell wall and the actin cytoskeleton. *Plant J,* 66**,** 354-65.

MARTINIERE, A., LAVAGI, I., NAGESWARAN, G., ROLFE, D. J., MANETA-PEYRET, L., LUU, D. T., BOTCHWAY, S. W., WEBB, S. E., MONGRAND, S., MAUREL, C., MARTIN-FERNANDEZ, M. L., KLEINE-VEHN, J., FRIML, J., MOREAU, P. & RUNIONS, J. 2012. Cell wall constrains lateral diffusion of plant plasma-membrane proteins. *Proc Natl Acad Sci U S A,* 109**,** 12805-10.

MARTINIERE, A. & RUNIONS, J. 2013. Protein diffusion in plant cell plasma membranes: the cell-wall corral. *Front Plant Sci,* 4**,** 515.

MCKENNA, J. F., ROLFE, D. J., WEBB, S. E. D., TOLMIE, A. F., BOTCHWAY, S. W., MARTIN-FERNANDEZ, M. L., HAWES, C. & RUNIONS, J. 2019. The cell wall regulates dynamics and size of plasma-membrane nanodomains in Arabidopsis. *Proceedings of the National Academy of Sciences***,** 201819077.

MCKENNA, J. F., TOLMIE, A. F. & RUNIONS, J. 2014. Across the great divide: the plant cell surface continuum. *Curr Opin Plant Biol,* 22**,** 132-140.

MORROW, I. C., REA, S., MARTIN, S., PRIOR, I. A., PROHASKA, R., HANCOCK, J. F., JAMES, D. E. & PARTON, R. G. 2002. Flotillin-1/Reggie-2 traffics to surface raft domains via a novel Golgi-independent pathway - Identification of a novel membrane targeting domain and a role for palmitoylation. *Journal of Biological Chemistry,* 277**,** 48834-48841.

NEUMANN-GIESEN, C., FALKENBACH, B., BEICHT, P., CLAASEN, S., LUERS, G., STUERMER, C. A. O., HERZOG, V. & TIKKANEN, R. 2004. Membrane and raft association of reggie-1/flotillin-2: role of myristoylation, palmitoylation and oligomerization and induction of filopodia by overexpression. *Biochemical Journal,* 378**,** 509-518.

QI, Y. P. & KATAGIRI, F. 2009. Purification of low-abundance *Arabidopsis* plasma-membrane protein complexes and identification of candidate components. *Plant Journal,* 57**,** 932-944.

QI, Y. P., TSUDA, K., NGUYEN, L. V., WANG, X., LIN, J. S., MURPHY, A. S., GLAZEBROOK, J., THORDAL-CHRISTENSEN, H. & KATAGIRI, F. 2011. Physical asssociation of *Arabidopsis* hypersensitive induced reaction proteins (HIRs) with the immune receptor RPS2. *Journal of Biological Chemistry,* 286**,** 31297-31307.

RAGHUPATHY, R., ANILKUMAR, A. A., POLLEY, A., SINGH, P. P., YADAV, M., JOHNSON, C., SURYAWANSHI, S., SAIKAM, V., SAWANT, S. D., PANDA, A., GUO, Z., VISHWAKARMA, R. A., RAO, M. & MAYOR, S. 2015. Transbilayer lipid interactions mediate nanoclustering of lipid-anchored proteins. *Cell,* 161**,** 581-594.

RETZER, K., LACEK, J., SKOKAN, R., DEL GENIO, C. I., VOSOLSOBĚ, S., LAŇKOVÁ, M., MALÍNSKÁ, K., KONSTANTINOVA, N., ZAŽÍMALOVÁ, E., NAPIER, R. M., PETRÁŠEK, J. & LUSCHNIG, C. 2017. Evolutionary Conserved Cysteines Function as cis-Acting Regulators of Arabidopsis PIN-FORMED 2 Distribution. *International Journal of Molecular Sciences,* 18**,** 2274.

RITCHIE, K., IINO, R., FUJIWARA, T., MURASE, K. & KUSUMI, A. 2003. The fence and picket structure of the plasma membrane of live cells as revealed by single molecule techniques (Review). *Molecular Membrane Biology,* 20**,** 13-18.

RIVERA-MILLA, E., STUERMER, C. A. O. & MALAGA-TRILLO, E. 2006. Ancient origin of reggie (flotillin), reggie-like, and other lipid-raft proteins: convergent evolution of the SPFH domain. *Cellular and Molecular Life Sciences,* 63**,** 343-357.

SAMPATHKUMAR, A., LINDEBOOM, J. J., DEBOLT, S., GUTIERREZ, R., EHRHARDT, D. W., KETELAAR, T. & PERSSON, S. 2011. Live cell imaging reveals structural associations between the actin and microtubule cytoskeleton in Arabidopsis. *Plant Cell,* 23**,** 2302-13.

SCHEIBLE, W.-R., ESHED, R., RICHMOND, T., DELMER, D. & SOMERVILLE, C. 2001. Modifications of cellulose synthase confer resistance to isoxaben and thiazolidinone herbicides in Arabidopsis Ixr1 mutants. *Proceedings of the National Academy of Sciences,* 98**,** 10079-10084.

SCHINDELIN, J., ARGANDA-CARRERAS, I., FRISE, E., KAYNIG, V., LONGAIR, M., PIETZSCH, T., PREIBISCH, S., RUEDEN, C., SAALFELD, S., SCHMID, B., TINEVEZ, J.-Y., WHITE, D. J., HARTENSTEIN, V., ELICEIRI, K., TOMANCAK, P. & CARDONA, A. 2012. Fiji: an open-source platform for biological-image analysis. *Nature Methods,* 9**,** 676.

SOLIS, G. P., HOEGG, M., MUNDERLOH, C., SCHROCK, Y., MALAGA-TRILLO, E., RIVERA-MILLA, E. & STUERIVIER, C. A. O. 2007. Reggie/flotillin proteins are organized into stable tetramers in membrane microdomains. *Biochemical Journal,* 403**,** 313-322.

SORIEUL, M., SANTONI, V., MAUREL, C. & LUU, D. T. 2011. Mechanisms and effects of retention of over-expressed aquaporin AtPIP2;1 in the endoplasmic reticulum. *Traffic,* 12**,** 473-82.

STUERMER, C. A. O., LANG, D. M., KIRSCH, F., WIECHERS, M., DEININGER, S. O. & PLATTNER, H. 2001. Glycosylphosphatidyl inositol-anchored proteins and fyn kinase assemble in noncaveolar plasma membrane microdomains defined by reggie-1 and-2. *Molecular Biology of the Cell,* 12**,** 3031-3045.

SZYMANSKI, W. G., ZAUBER, H., ERBAN, A., GORKA, M., WU, X. N. & SCHULZE, W. X. 2015. Cytoskeletal Components Define Protein Location to Membrane Microdomains. *Molecular & Cellular Proteomics,* 14**,** 2493-2509.

TANZ, S. K., CASTLEDEN, I., HOOPER, C. M., VACHER, M., SMALL, I. & MILLAR, H. A. 2013. SUBA3: a database for integrating experimentation and prediction to define the SUBcellular location of proteins in Arabidopsis. *Nucleic Acids Research,* 41**,** D1185-D1191.

TAPKEN, W. & MURPHY, A. S. 2015. Membrane nanodomains in plants: capturing form, function, and movement. *Journal of Experimental Botany,* 66**,** 1573-1586.

TINEVEZ, J.-Y., PERRY, N., SCHINDELIN, J., HOOPES, G. M., REYNOLDS, G. D., LAPLANTINE, E., BEDNAREK, S. Y., SHORTE, S. L. & ELICEIRI, K. W. 2017. TrackMate: An open and extensible platform for single-particle tracking. *Methods,* 115**,** 80-90.

TOLMIE, F., POULET, A., MCKENNA, J., SASSMANN, S., GRAUMANN, K., DEEKS, M. & RUNIONS, J. 2017. The cell wall of Arabidopsis thaliana influences actin network dynamics. *J Exp Bot,* 68**,** 4517-4527.

TRAVERSO, J. A., MICALELLA, C., MARTINEZ, A., BROWN, S. C., SATIAT-JEUNEMAÎTRE, B., MEINNEL, T. & GIGLIONE, C. 2013. Roles of N-Terminal Fatty Acid Acylations in Membrane Compartment Partitioning: Arabidopsis h-Type Thioredoxins as a Case Study. *The Plant Cell,* 25**,** 1056-1077.

WANG, X. H., LI, X. J., DENG, X., LUU, D. T., MAUREL, C. & LIN, J. X. 2015. Single-molecule fluorescence imaging to quantify membrane protein dynamics and oligomerization in living plant cells. *Nature Protocols,* 10**,** 2054-2063.

WU, F. H., SHEN, S. C., LEE, L. Y., LEE, S. H., CHAN, M. T. & LIN, C. S. 2009. Tape-Arabidopsis Sandwich - a simpler Arabidopsis protoplast isolation method. *Plant Methods,* 5**,** 16.

XUE, Y., XING, J., WAN, Y., LV, X., FAN, L., ZHANG, Y., SONG, K., WANG, L., WANG, X., DENG, X., BALUSKA, F., CHRISTIE, J. M. & LIN, J. 2018. Arabidopsis Blue Light Receptor Phototropin 1 Undergoes Blue Light-Induced Activation in Membrane Microdomains. *Mol Plant,* 11**,** 846-859.

YU, M., LIU, H., DONG, Z., XIAO, J., SU, B., FAN, L., KOMIS, G., ŠAMAJ, J., LIN, J. & LI, R. 2017. The dynamics and endocytosis of Flot1 protein in response to flg22 in Arabidopsis. *Journal of Plant Physiology,* 215**,** 73-84.

YU, Q., REN, J. J., KONG, L. J. & WANG, X. L. 2018. Actin filaments regulate the adhesion between the plasma membrane and the cell wall of tobacco guard cells. *Protoplasma,* 255**,** 235-245.

ZHOU, L., CHEUNG, M. Y., ZHANG, Q., LEI, C. L., ZHANG, S. H., SUN, S. S. & LAM, H. M. 2009. A novel simple extracellular leucine-rich repeat (eLRR) domain protein from rice (OsLRR1) enters the endosomal pathway and interacts with the hypersensitive-induced reaction protein 1 (OsHIR1). *Plant Cell Environ,* 32**,** 1804-20.

FIGURE LEGENDS

Figure 1. *At*FLOTs and *At*HIRs are localized in PM microdomains in root and leaf epidermal cells. (a-f) Elongating root epidermal cells in 5-day-old seedlings, (g-k) epidermal lobed cells of the first true leaf in 10-day-old seedlings. SD confocal surface sections showing PM-associated microdomains for *At*FLOT1-GFP (a, g), *At*FLOT2-GFP (b, h), *At*FLOT3-GFP (c, i), *At*HIR1-YFP (d, j), *At*HIR2-YFP (e) and *At*HIR4-YFP (f, k). Scale bars 5 µm. (l-q) Airyscan images of PM surface focusing in detail on single PM-associated microdomains of *At*FLOT1-GFP (l), *At*FLOT2-GFP (m), *At*FLOT3-GFP (n), *At*HIR1-YFP (o), *At*HIR2-YFP (p) and *At*HIR4-YFP (q) in root epidermal cells of 5-day-old seedlings. Scale bars 500 nm. (r) Densities of PM-associated microdomains in root elongated epidermal cells of 5-day old seedling showing the highest density for *At*HIR1-YFP line (left panel), which is supported by comparison with three independent *At*HIR1-GFP lines (right panel). Letters indicate the groups of different distribution according to Kruskal-Wallis test followed by post hoc Dunn multiple comparison test ($p < 0.05$, $n = 30$ to 33 for each individual line). (s) Size of individual microdomains determined as FWHM from Airyscan imaging. Letters indicate the groups of different distribution according to Kruskal-Wallis test followed by post hoc Dunn multiple comparison test ($p < 0.05$, $n = 1415$ to 2595 measured in 35 to 56 cells from 10 to 11 plants for each individual line). Whiskers in boxplots (r, s) represent 10th and 90th percentile. In (s), the values exceeding whiskers are dot displayed. FWHM - full width at half maximum.

Figure 2. Differential mobility of *At*FLOTs and *At*HIRs within PM. (a-f) Kymograms for *At*FLOT1 (a), *At*FLOT2-GFP (b), *At*FLOT3-GFP (c), *At*HIR1-YFP (d), *At*HIR2-YFP (e) and *At*HIR4-YFP (f) obtained from 120 s time-lapse SD confocal time-lapse acquisition in elongating root epidermal cells of 5-day-old seedlings. Scale bar 5 µm. (g) Distribution of PCC values calculated from fluorescence intensity profiles of the first ($t = 0$ s) and last ($t = 120$ s) time point of kymograms. Letters indicate the groups of different distribution according to Kruskal-Wallis test followed by post hoc Dunn multiple comparison test ($p < 0.01$, $n = 83$ to 156 (2 to 3 kymograms constructed for each epidermal root cell) from 9 to 13 plants for each individual line). Note higher immobility of *At*FLOTs in contrast to *At*HIRs. (h) Quantification of FRAP immobile fractions obtained by CLSM showing significantly different mobility for PM-associated *At*FLOTs and *At*HIRs and for tonoplast-localized *At*HIR3-YFP and all other PM-associated proteins (one-way ANOVA, $p < 0.001$). (i) Single exponential fits applied on normalized FRAP data for *At*FLOT1-GFP ($\tau_{1/2} = 8.3$ s; $R^2 = 0.89$, $n = 27$), *At*FLOT2-GFP ($\tau_{1/2}$

= 28.3 s; R^2 = 0.81, n = 9), *At*FLOT3-GFP ($\tau_{1/2}$ = 8.5 s; R^2 = 0.65, n = 9), *At*HIR1-YFP ($\tau_{1/2}$ = 12.3 s; R^2 = 0.86, n = 13), *At*HIR2-YFP ($\tau_{1/2}$ = 16.2 s; R^2 = 0.85, n = 11), *At*HIR3-YFP ($\tau_{1/2}$ = 12.8 s; R^2 = 0.97, n = 26) and *At*HIR4-YFP ($\tau_{1/2}$ = 12.9 s; R^2 = 0.82, n = 17). Whiskers in boxplots (g, h) represent 10th and 90th percentile. PCC - Pearson's correlation coefficient.

Figure 3. *At*FLOTs and *At*HIRs are localized along PM corrals co-aligning with microtubules. (a-f) PM-associated corrals restricting the localization of *At*FLOT1-GFP (a), *At*FLOT2-GFP (b), *At*FLOT3-GFP (c), *At*HIR1-YFP (d), *At*HIR2-YFP (e) and *At*HIR4-YFP (f) domains in elongating root epidermal cells of 5-day-old seedlings. Confocal SD microscopy. Note negative corrals (arrows) and aligning of domains in filamentous-like pattern (arrowheads). Scale bars 5 µm. (g) *At*HIR1-YFP line co-transformed transiently with microtubular marker MBD-mRFP, epidermal cells of cotyledons. Scale bars 10 µm. (h) *At*FLOT2-GFP coexpressed with *At*IQD6-mCherry bound to microtubules transiently in tobacco epidermal leaf cells. Scale bars 10 µm. (i, j) *At*FLOT2-GFP (i) and *At*HIR1-YFP (j) orthogonal CLSM projections obtained with Airyscan detector in cotyledon epidermal cells. xz, yz projections and xy section through the middle of the PM region. Arrows point to the position of corrals. Scale bars 2 µm. MBD – microtubule-binding domain, IQD6 – IQ67 DOMAIN6.

Figure 4. Cellulose biosynthesis or pectin status interference with ISX or EGCG differentially affects the mobility of *At*FLOT2 and *At*HIR1. (a-f) Microdomain organization of *At*FLOT1-GFP (a), *At*FLOT2-GFP (b), *At*FLOT3-GFP (c), *At*HIR1-YFP (d), *At*HIR2-YFP (e) and *At*HIR4-YFP (f) after 1 h in 20 µM ISX. Confocal SD microscopy. Note generally unchanged patterns. (g-l) Kymograms of *At*FLOT1-GFP (g), *At*FLOT2-GFP (h), *At*FLOT3-GFP (i), *At*HIR1-YFP (j), *At*HIR2-YFP (k) and *At*HIR4-YFP (l) obtained from 120 s time-lapse acquisition on root elongating epidermal cells upon treatment with ISX. Scale bars 5 µm. (m) The quantification of CV of fluorescence intensities from 15 µm linear transect within the PM sufrace indicating higher segregation of fluorescence in *At*FLOT2-GFP under ISX treatment. (n) The quantification of FRAP immobile fractions obtained by CLSM showing significantly increased mobility for *At*HIR1-YFP after 1 h in 20 µM ISX in comparison with control in 0.1% DMSO. No significant difference was observed for *At*FLOT2-GFP. *At*Lti6b-GFP line was used as a positive control for ISX treatment. (o) The quantification of FRAP immobile fractions obtained by CLSM showing a decrease in mobility of *At*FLOT2-GFP when treated with 50 µM EGCG for 1 hour while no difference observed for *At*HIR1-YFP. (m-o) Asterisks indicate p-value of Wilcoxon rank-sum test: * $p < 0.05$, *** $p < 0.001$, n = 15 – 65 from 7 – 16 seedlings

for each individual line. Whiskers in boxplots (m-o) represent 10th and 90th percentile. ISX – isoxaben, CV – coefficient of variation, EGCG – epigallocatechin gallate.

Figure 5. Cell wall removal increases the mobility of *At*FLOT2 and *At*HIR1. (a, d) SD confocal surface section of *At*FLOT2-GFP (a, b) and *At*HIR1-YFP (c, d) showing different localization pattern under plasmolysis (0.5 M mannitol, 30 min, b, d,) when compared with control (half strength MS liquid medium supplemented with 1% sucrose, a, c). (e, f) Maximum intensity projection from Z-stack acquisitions (total Z-range = 4 µm) in grayscale (left panels) and depth-coded (right panels, fire look-up table, dark blue represents the objects closest to the surface while white is most distant from the surface) showing different effect of plasmolysis on relocalization of *At*FLOT2-GFP and *At*HIR1-YFP. (g) The quantification of FRAP immobile fractions obtained by CLSM showing the decrease of *At*FLOT2-GFP and *At*HIR1-YFP mobility in response to strong plasmolysis (0.8 M mannitol, 30 min) when compared with control (half strength MS liquid medium supplemented with 1% sucrose). Wilcoxon rank-sum test: *** $p < 0.001$, n = 15 – 40 from 7-9 seedlings for each individual line. (h) Cartoon depicting the events and further analysed structures occurring under partial CW digestion. (i, j) The quantification of FRAP immobile fractions obtained by CLSM showing increase of mobility of *At*FLOT2-GFP (i) and *At*HIR1-YFP (j) at the PM under partial CW digestion when compared with seedling treated with liquid half strength MS or with 0.2 M mannitol-based buffer without enzymes. Letters indicate the groups of different distribution according to Kruskal-Wallis test followed by post hoc Dunn multiple comparison test ($p < 0.05$, n = 15 to 55 from 9 to 19 plants for each individual line, treatment or measured structure). Whiskers in boxplots (g, i, j) represent 10th and 90th percentile. Scale bars 5 µm (a-d), 10 µm (e, f). man. – mannitol, APM – anchored plasma membrane, DPM – detached plasma membrane, RPM – released plasma membrane.

Figure 6. *At*FLOT2 individual microdomain mobility is increased in protoplast. (a,b) Kymograms for *At*FLOT2-GFP obtained from 120 s time-lapse SD confocal acquisition of intact leaf epidermal cell (a) or protoplast (b) prepared from leaf showing higher dynamics of *At*FLOT2-GFP microdomains in protoplast. (c, d) Merge of images corresponding to 0 s (red) and 120 s (green) of a time-lapse SD confocal acquisition of intact leaf epidermal cell (c) or protoplast (d) prepared from leaf showing much higher level of co-localization (scatter-plot shape with higher PCC values) in intact leaf epidermal cell (c) compared to protoplast (d). (e) Maximum intensity projection from 44 SD confocal sections (step size 200 nm) showing PM-

associated microdomains in protoplast including corrals (arrows). Trajectories of individual microdomains within 120 s time-lapse acquisition and pseudocolor-coded microdomain track duration in intact leaf epidermal cell (f) and released protoplast (g). Note longer duration and shorter trajectories for microdomains in leaf cell (f) and shorter duration and longer trajectories in protoplast (g). Scale bars 5 µm (a-e), 1 µm (f, g). PCC - Pearson's correlation coefficient.

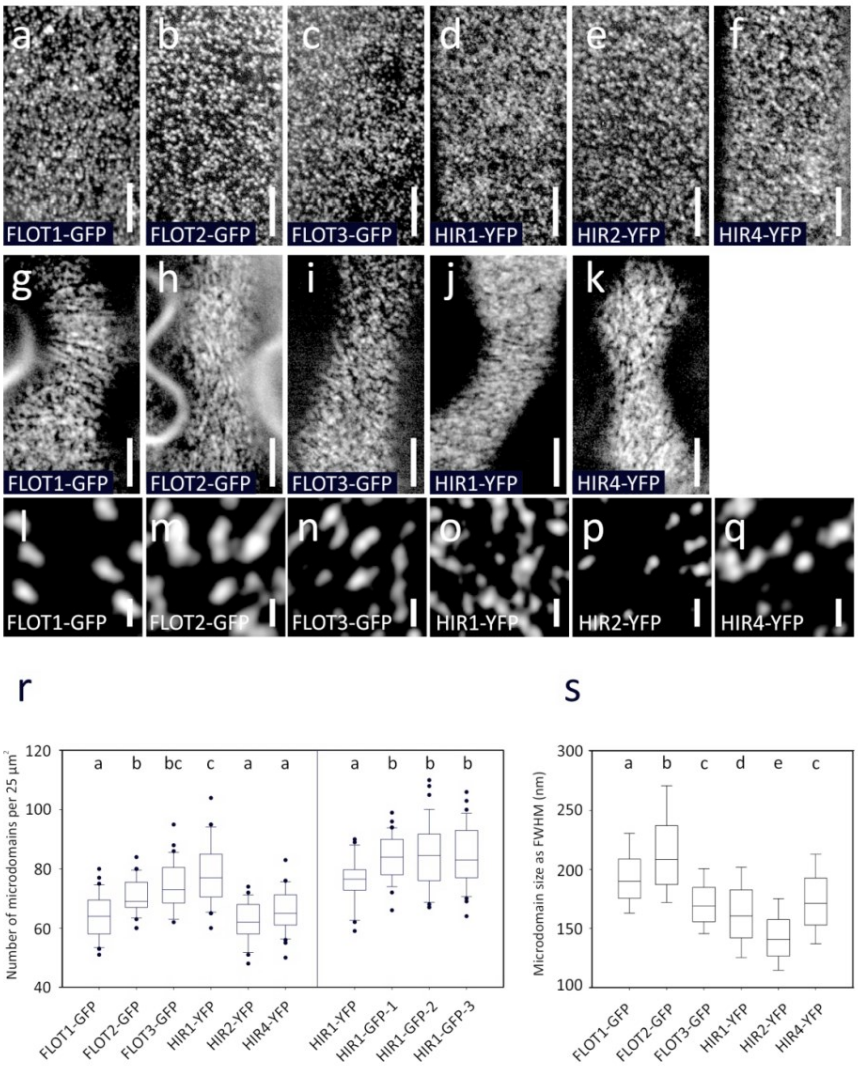

Figure 1. *At*FLOTs and *At*HIRs are localized in PM microdomains in root and leaf epidermal cells. (a-f) Elongating root epidermal cells in 5-day-old seedlings, (g-k) epidermal lobed cells of the first true leaf in 10-day-old seedlings. SD confocal surface sections showing PM-associated microdomains for *At*FLOT1-GFP (a, g), *At*FLOT2-GFP (b, h), *At*FLOT3-GFP (c, i), *At*HIR1-YFP (d, j), *At*HIR2-YFP (e) and *At*HIR4-YFP (f, k). Scale bars 5 µm. (l-q) Airyscan images of PM surface focusing in detail on single PM-associated microdomains of *At*FLOT1-GFP (l), *At*FLOT2-GFP (m), *At*FLOT3-GFP (n), *At*HIR1-YFP (o), *At*HIR2-YFP (p) and *At*HIR4-YFP (q) in root epidermal cells of 5-day-old seedlings. Scale bars 500 nm. (r) Densities of PM-associated microdomains in root elongated epidermal cells of 5-day old seedling showing the highest density for *At*HIR1-YFP line (left panel), which is supported by comparison with three independent *At*HIR1-GFP lines (right panel). Letters indicate the groups of different distribution according to Kruskal-Wallis test followed by post hoc Dunn multiple comparison test ($p < 0.05$, n = 30 to 33 for each individual line). (s) Size of individual microdomains determined as FWHM from Airyscan imaging. Letters indicate the groups of different distribution according to Kruskal-Wallis test followed by post hoc Dunn multiple comparison test ($p < 0.05$, n = 1415 to 2595 measured in 35 to 56 cells from 10 to 11 plants for each individual line). Whiskers in

boxplots (r, s) represent 10th and 90th percentile. In (s), the values exceeding whiskers are dot displayed. FWHM - full width at half maximum.

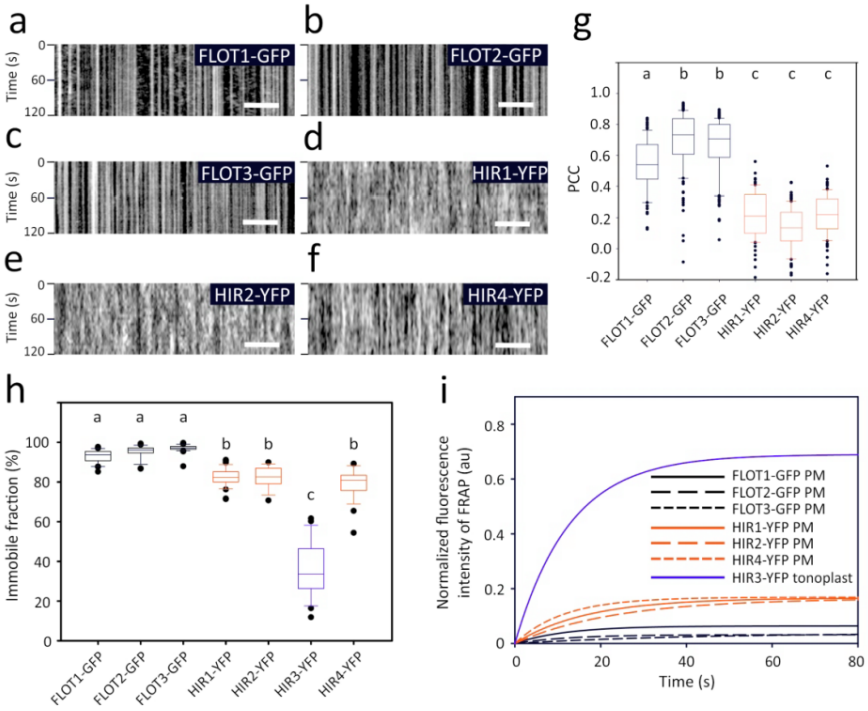

Figure 2. Differential mobility of *At*FLOTs and *At*HIRs within PM. (a-f) Kymograms for *At*FLOT1 (a), *At*FLOT2-GFP (b), *At*FLOT3-GFP (c), *At*HIR1-YFP (d), *At*HIR2-YFP (e) and *At*HIR4-YFP (f) obtained from 120 s time-lapse SD confocal time-lapse acquisition in elongating root epidermal cells of 5-day-old seedlings. Scale bar 5 µm. (g) Distribution of PCC values calculated from fluorescence intensity profiles of the first (t = 0 s) and last (t = 120 s) time point of kymograms. Letters indicate the groups of different distribution according to Kruskal-Wallis test followed by post hoc Dunn multiple comparison test ($p < 0.01$, n = 83 to 156 (2 to 3 kymograms constructed for each epidermal root cell) from 9 to 13 plants for each individual line). Note higher immobility of *At*FLOTs in contrast to *At*HIRs. (h) Quantification of FRAP immobile fractions obtained by CLSM showing significantly different mobility for PM-associated *At*FLOTs and *At*HIRs and for tonoplast-localized *At*HIR3-YFP and all other PM-associated proteins (one-way ANOVA, $p < 0.001$). (i) Single exponential fits applied on normalized FRAP data for *At*FLOT1-GFP ($\tau 1/2$ = 8.3 s; R2 = 0.89, n = 27), *At*FLOT2-GFP ($\tau 1/2$ = 28.3 s; R2 = 0.81, n = 9), *At*FLOT3-GFP ($\tau 1/2$ = 8.5 s; R2 = 0.65, n = 9), *At*HIR1-YFP ($\tau 1/2$ = 12.3 s; R2 = 0.86, n = 13), *At*HIR2-YFP ($\tau 1/2$ = 16.2 s; R2 = 0.85, n = 11), *At*HIR3-YFP ($\tau 1/2$ = 12.8 s; R2 = 0.97, n = 26) and *At*HIR4-YFP ($\tau 1/2$ = 12.9 s; R2 = 0.82, n = 17). Whiskers in boxplots (g, h) represent 10th and 90th percentile. PCC - Pearson's correlation coefficient.

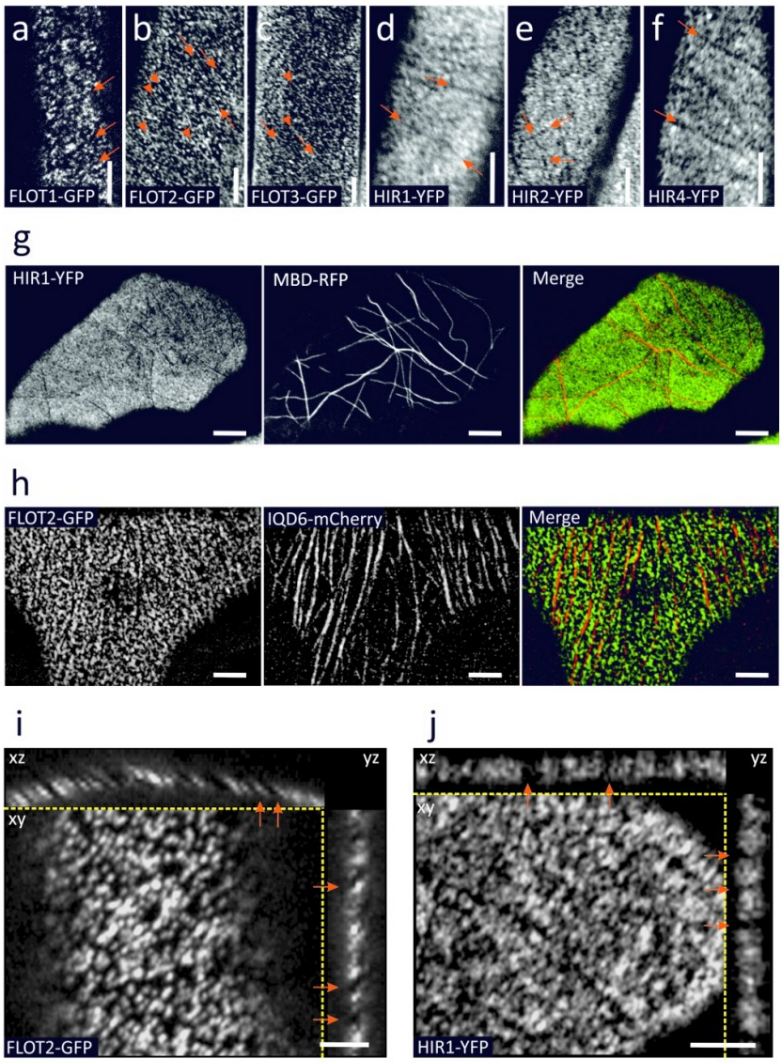

Figure 3. *At*FLOTs and *At*HIRs are localized along PM corrals co-aligning with microtubules. (a-f) PM-associated corrals restricting the localization of *At*FLOT1-GFP (a), *At*FLOT2-GFP (b), *At*FLOT3-GFP (c), *At*HIR1-YFP (d), *At*HIR2-YFP (e) and *At*HIR4-YFP (f) domains in elongating root epidermal cells of 5-day-old seedlings. Confocal SD microscopy. Note negative corrals (arrows) and aligning of domains in filamentous-like pattern (arrowheads). Scale bars 5 µm. (g) *At*HIR1-YFP line co-transformed transiently with microtubular marker MBD-mRFP, epidermal cells of cotyledons. Scale bars 10 µm. (h) *At*FLOT2-GFP coexpressed with *At*IQD6-mCherry bound to microtubules transiently in tobacco epidermal leaf cells. Scale bars 10 µm. (i, j) *At*FLOT2-GFP (i) and *At*HIR1-YFP (j) orthogonal CLSM projections obtained with Airyscan detector in cotyledon epidermal cells. xz, yz projections and xy section through the middle of the PM region. Arrows point to the position of corrals. Scale bars 2 µm. MBD – microtubule-binding domain, IQD6 – IQ67 DOMAIN6.

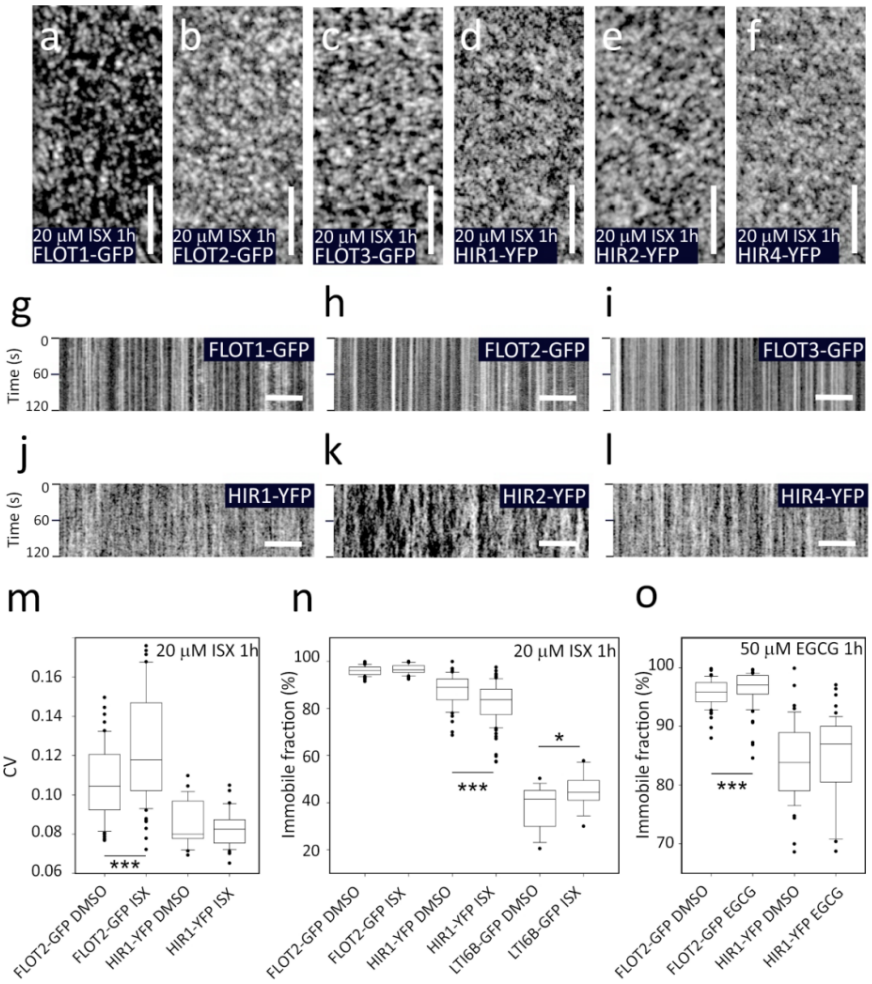

Figure 4. Cellulose biosynthesis or pectin status interference with ISX or EGCG differentially affects the mobility of *At*FLOT2 and *At*HIR1. (a-f) Microdomain organization of *At*FLOT1-GFP (a), *At*FLOT2-GFP (b), *At*FLOT3-GFP (c), *At*HIR1-YFP (d), *At*HIR2-YFP (e) and *At*HIR4-YFP (f) after 1 h in 20 µM ISX. Confocal SD microscopy. Note generally unchanged patterns. (g-l) Kymograms of *At*FLOT1-GFP (g), *At*FLOT2-GFP (h), *At*FLOT3-GFP (i), *At*HIR1-YFP (j), *At*HIR2-YFP (k) and *At*HIR4-YFP (l) obtained from 120 s time-lapse acquisition on root elongating epidermal cells upon treatment with ISX. Scale bars 5 µm. (m) The quantification of CV of fluorescence intensities from 15 µm linear transect within the PM sufrace indicating higher segregation of fluorescence in *At*FLOT2-GFP under ISX treatment. (n) The quantification of FRAP immobile fractions obtained by CLSM showing significantly increased mobility for *At*HIR1-YFP after 1 h in 20 µM ISX in comparison with control in 0.1% DMSO. No significant difference was observed for *At*FLOT2-GFP. *At*Lti6b-GFP line was used as a positive control for ISX treatment. (o) The quantification of FRAP immobile fractions obtained by CLSM showing a decrease in mobility of *At*FLOT2-GFP when treated with 50 µM EGCG for 1 hour while no difference observed for *At*HIR1-YFP. (m-o) Asterisks indicate p-value of Wilcoxon rank-sum test: * $p < 0.05$, *** $p < 0.001$, n = 15 – 65 from 7 – 16 seedlings for each individual line. Whiskers in boxplots (m-o) represent 10th and 90th percentile. ISX – isoxaben, CV – coefficient of variation, EGCG – epigallocatechin gallate.

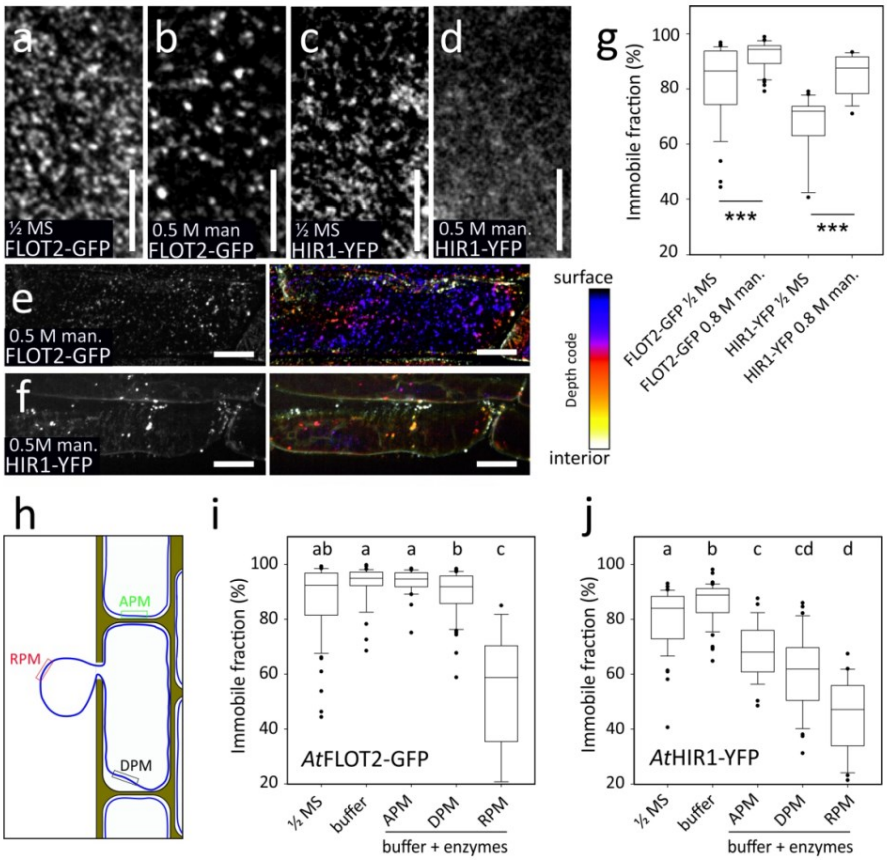

Figure 5. Cell wall removal increases the mobility of *At*FLOT2 and *At*HIR1. (a, d) SD confocal surface section of *At*FLOT2-GFP (a, b) and *At*HIR1-YFP (c, d) showing different localization pattern under plasmolysis (0.5 M mannitol, 30 min, b, d,) when compared with control (half strength MS liquid medium supplemented with 1% sucrose, a, c). (e, f) Maximum intensity projection from Z-stack acquisitions (total Z-range = 4 µm) in grayscale (left panels) and depth-coded (right panels, fire look-up table, dark blue represents the objects closest to the surface while white is most distant from the surface) showing different effect of plasmolysis on relocalization of *At*FLOT2-GFP and *At*HIR1-YFP. (g) The quantification of FRAP immobile fractions obtained by CLSM showing the decrease of *At*FLOT2-GFP and *At*HIR1-YFP mobility in response to strong plasmolysis (0.8 M mannitol, 30 min) when compared with control (half strength MS liquid medium supplemented with 1% sucrose). Wilcoxon rank-sum test: *** $p < 0.001$, n = 15 – 40 from 7-9 seedlings for each individual line. (h) Cartoon depicting the events and further analysed structures occurring under partial CW digestion. (i, j) The quantification of FRAP immobile fractions obtained by CLSM showing increase of mobility of *At*FLOT2-GFP (i) and *At*HIR1-YFP (j) at the PM under partial CW digestion when compared with seedling treated with liquid half strength MS or with 0.2 M mannitol-based buffer without enzymes. Letters indicate the groups of different distribution according to Kruskal-Wallis test followed by post hoc Dunn multiple comparison test ($p < 0.05$, n = 15 to 55 from 9 to 19 plants for each individual line, treatment or measured structure). Whiskers in boxplots (g, i, j) represent 10th and 90th percentile. Scale bars 5 µm (a-d), 10 µm (e, f). man. – mannitol, APM – anchored plasma membrane, DPM – detached plasma membrane, RPM – released plasma membrane.

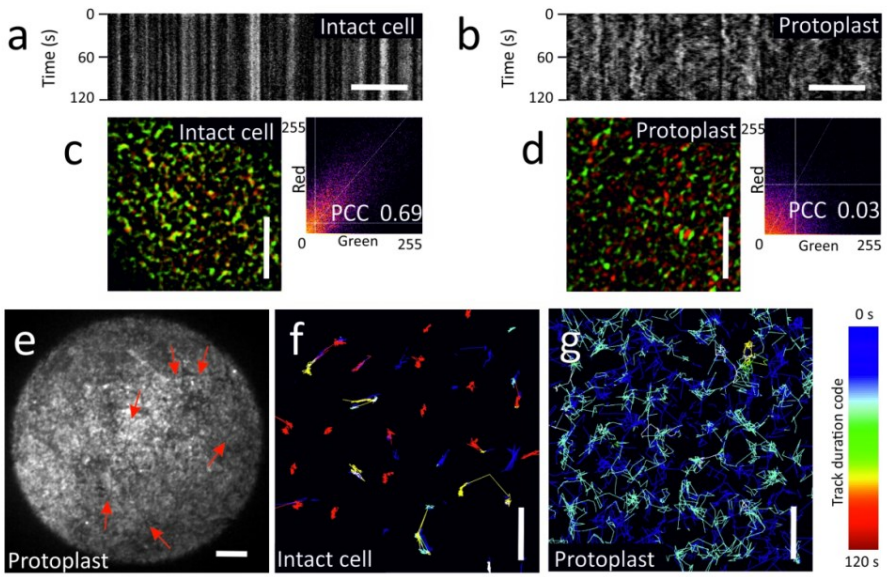

Figure 6. *At*FLOT2 individual microdomain mobility is increased in protoplast. (a,b) Kymograms for *At*FLOT2-GFP obtained from 120 s time-lapse SD confocal acquisition of intact leaf epidermal cell (a) or protoplast (b) prepared from leaf showing higher dynamics of *At*FLOT2-GFP microdomains in protoplast. (c, d) Merge of images corresponding to 0 s (red) and 120 s (green) of a time-lapse SD confocal acquisition of intact leaf epidermal cell (c) or protoplast (d) prepared from leaf showing much higher level of co-localization (scatter-plot shape with higher PCC values) in intact leaf epidermal cell (c) compared to protoplast (d). (e) Maximum intensity projection from 44 SD confocal sections (step size 200 nm) showing PM-associated microdomains in protoplast including corrals (arrows). Trajectories of individual microdomains within 120 s time-lapse acquisition and pseudocolor-coded microdomain track duration in intact leaf epidermal cell (f) and released protoplast (g). Note longer duration and shorter trajectories for microdomains in leaf cell (f) and shorter duration and longer trajectories in protoplast (g). Scale bars 5 μm (a-e), 1 μm (f, g). PCC - Pearson's correlation coefficient.

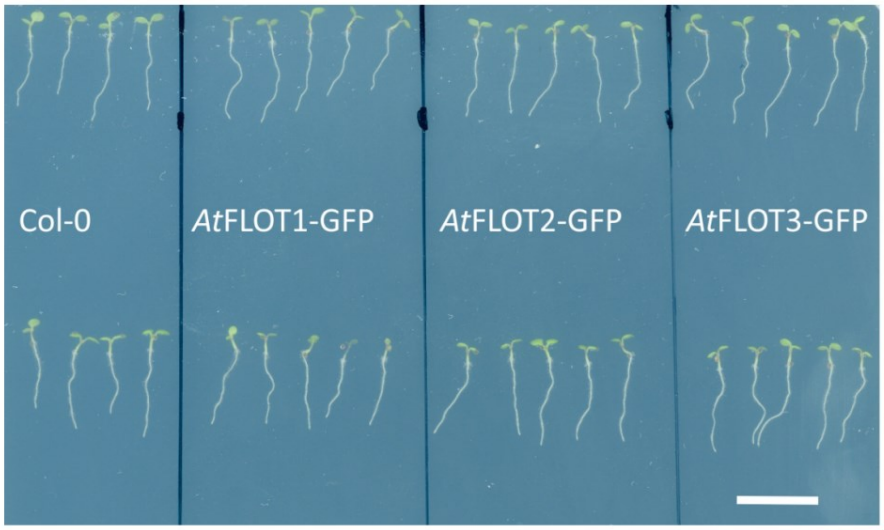

Figure S1. Arabidopsis thaliana lines overexpressing AtFLOTs do not exhibit any apparent phenotype. Col-0, *At*FLOT1-GFP, *At*FLOT2-GFP and *At*FLOT3-GFP lines were sown onto vertical agar plates and grown for six days. Scale bar 1 cm.

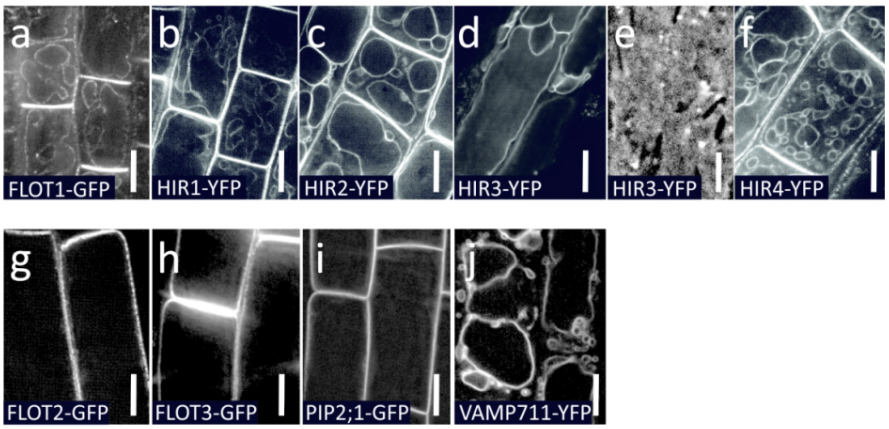

Figure S2. Tonoplast and plasma membrane localization of *At*FLOTs and *At*HIRs in the root epidermal cells. 5-day-old seedlings, confocal SD cross sections for *At*FLOT1-GFP (a), *At*HIR1-YFP (b), *At*HIR2-YFP (c), and *At*HIR4-YFP (f) showing concomitant localisation in both plasma membrane and tonoplast while *At*HIR3-YFP (d) is present exclusively in tonoplast and *At*FLOT2-GFP (g) and *At*FLOT3-GFP (h) only in plasma membrane. Confocal SD section of tonoplast surface for *At*HIR3-YFP (e). *At*PIP2;1-GFP (i) or *At*VAMP711-YFP (j) were used as marker lines for plasma membrane or tonoplast localization, respectively. Scale bars 10 µm (a-d, f-j) or 5 µm (e).

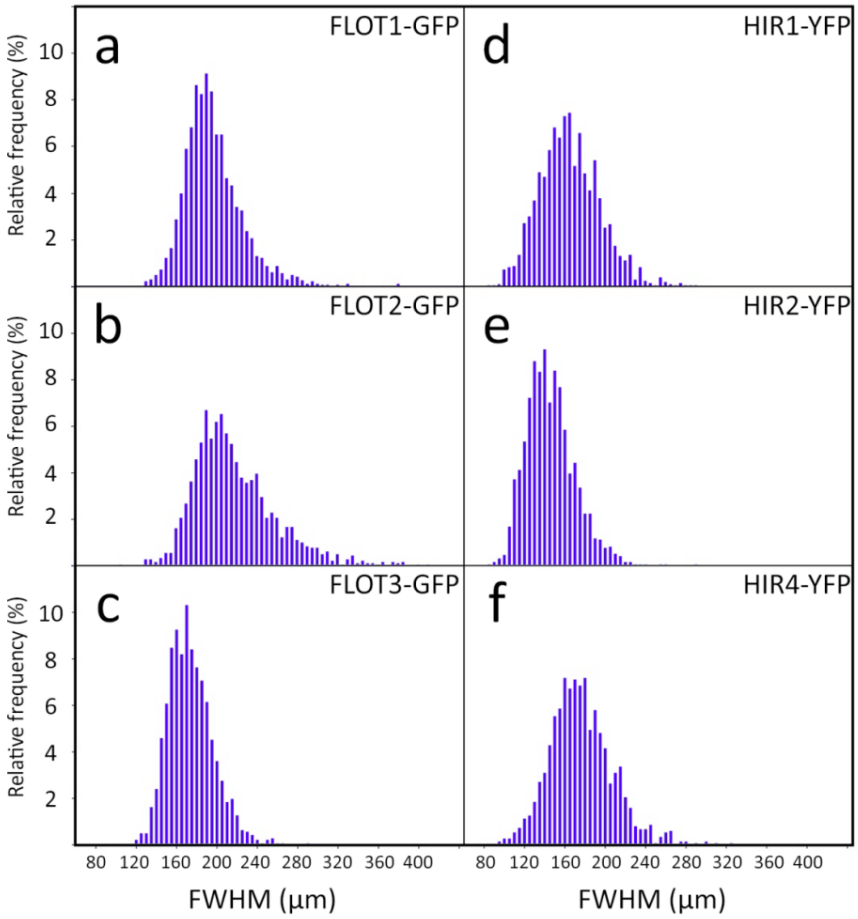

Figure S3. Distribution of *At*FLOT and *At*HIR individual PM-associated microdomain size in root epidermal cells. Histograms of individual microdomain diameters determined as FWHM for *At*FLOT1-GFP (a), *At*FLOT2-GFP (b), *At*FLOT3-GFP (c), *At*HIR1-YFP (d), *At*HIR2-YFP (e) and *At*HIR4-YFP (f). Airyscan confocal microscopy. FWHM – full width at half maximum.

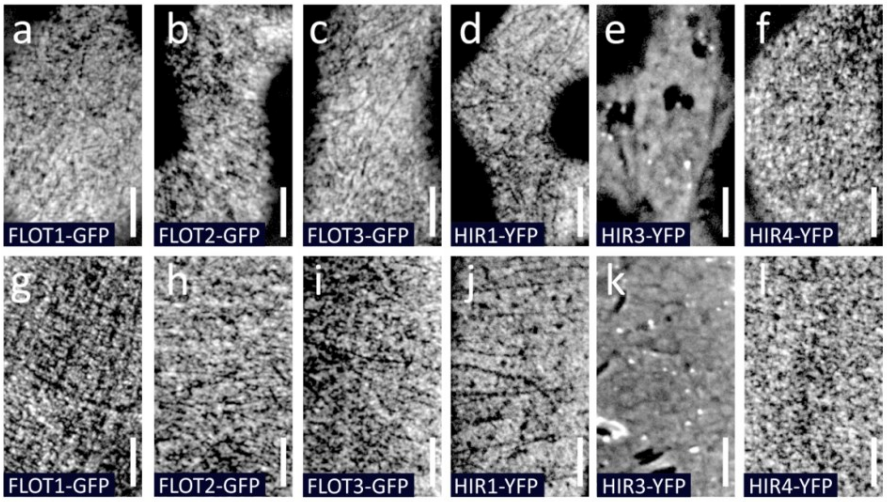

Figure S4. *At*FLOTs and *At*HIRs are localized in PM microdomains in cotyledon and hypocotyl epidermal cells. (a-f) Epidermal lobed cells of cotyledons, (g-l) hypocotyl epidermal cells. 5-day-old seedlings, SD confocal cell surface sections showing PM-associated microdomains for *At*FLOT1-GFP (a, g), *At*FLOT2-GFP (b, h), *At*FLOT3-GFP (c, i), *At*HIR1-YFP (d, j), *At*HIR3-YFP (e, k) and *At*HIR4-YFP (f, l). SD confocal microscopy. Scale bars 5 µm. Note: *At*HIR2-YFP fluorescence was not detected in aerial tissues.

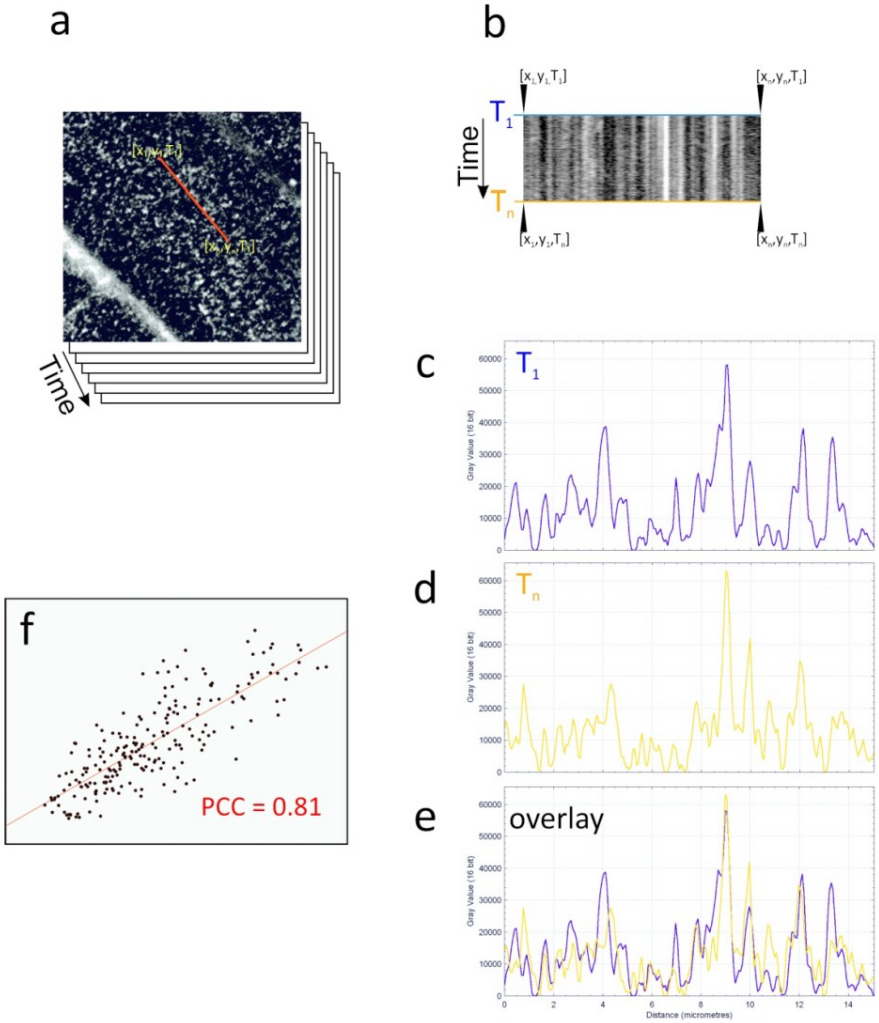

Figure S5. Determination of correlation coefficient as a way to analyse a kymogram. (a) A time-lapse series is acquired. For each pixel of such an acquisition three variables are to be read out – x and y radial coordinate corresponding to the position at the sample with regards to the camera or another acquisition device, and time (T) value corresponding with the time layer in the stack of images acquired. At the first time point (first layer in the time stack) a linear region of interest (red line) is created representing a sequence of pixels (with radial coordinates from x1, y1 to xn, yn). These lines are then stacked one onto another by the time points of acquisition and a kymogram is thus produced (b). We used the sequence of fluorescence intensities from the first (c) and last (d) time point and plotted them against each other (e). Finally, PCC was calculated for these sequence of intensities (f).

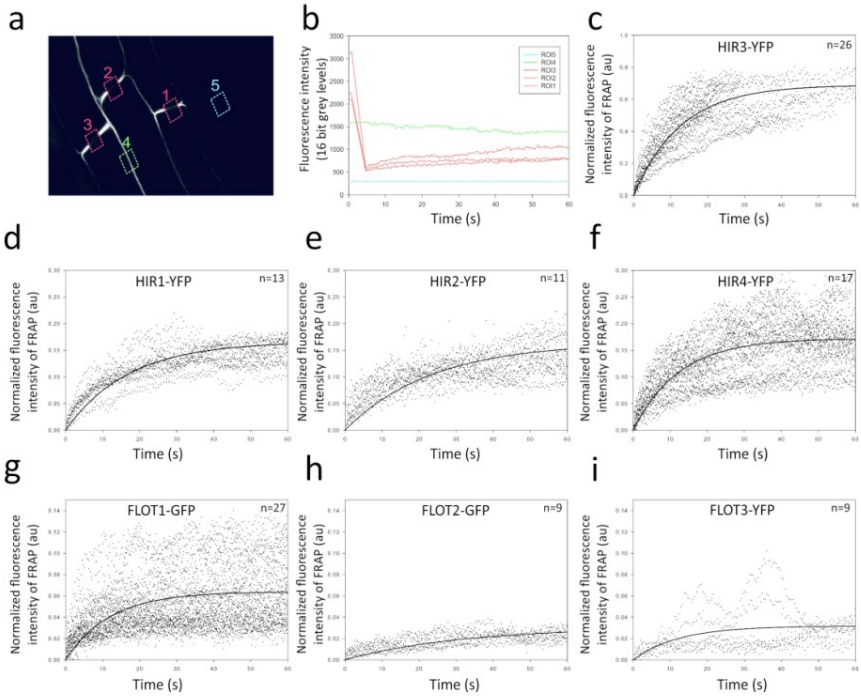

Figure S6. FRAP experiment description. (a) ROIs for bleaching (1, 2, 3), non-bleached control (4) and background control (5) in root epidermal cells of 5-day-old seedlings. (b) Fluorescence intensity values during pre-bleach, post bleach and FRAP period. (c-i) Normalized fluorescence intensity of FRAP with single exponential fits for tonoplast-localized *At*HIR3-YFP (c) and PM-associated *At*HIR1-YFP (d), *At*HIR2-YFP (e), *At*HIR4-YFP (f), *At*FLOT1 (g), *At*FLOT2-GFP (h) and *At*FLOT3-GFP (i).

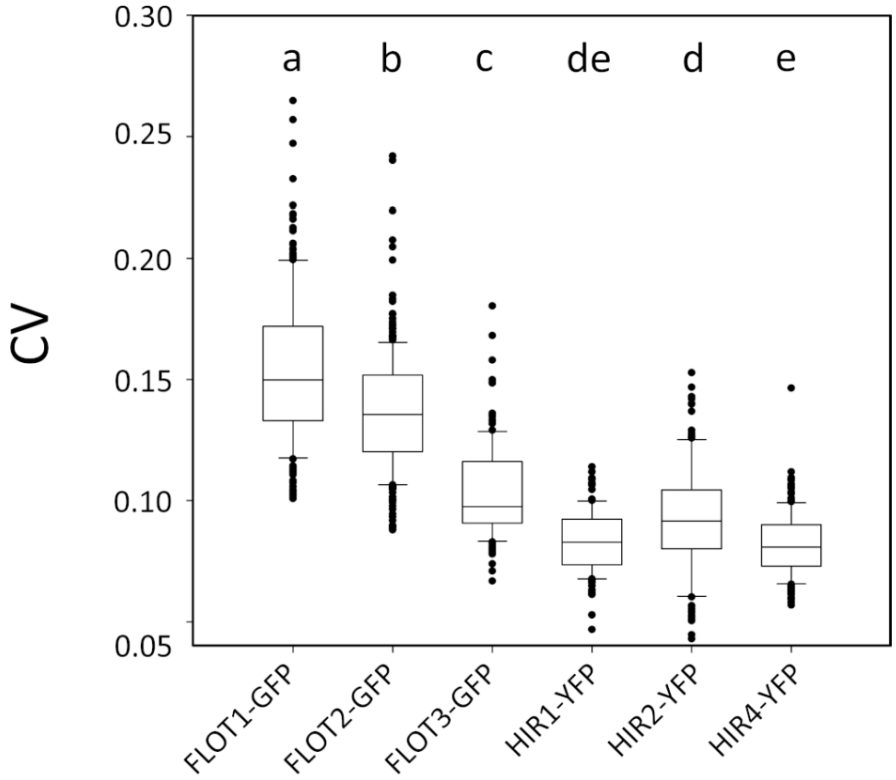

Figure S7. *At*FLOT and *At*HIR differ in the degree of fluorescence signal association with PM. The quantification of CV of fluorescence intensities from 15 µm linear transect within the PM surface indicating higher segregation of fluorescence in *At*FLOTs and lower in *At*HIRs. Letters indicate the groups of different distribution according to Kruskal-Wallis test followed by post hoc Dunn multiple comparison test ($p < 0.01$, n = 124 to 268 (2 – 3 intensity profiles per cell) from 9 to 11 plants for each individual line). Whiskers in boxplots represent 10th and 90th percentile. CV – coefficient of variation.

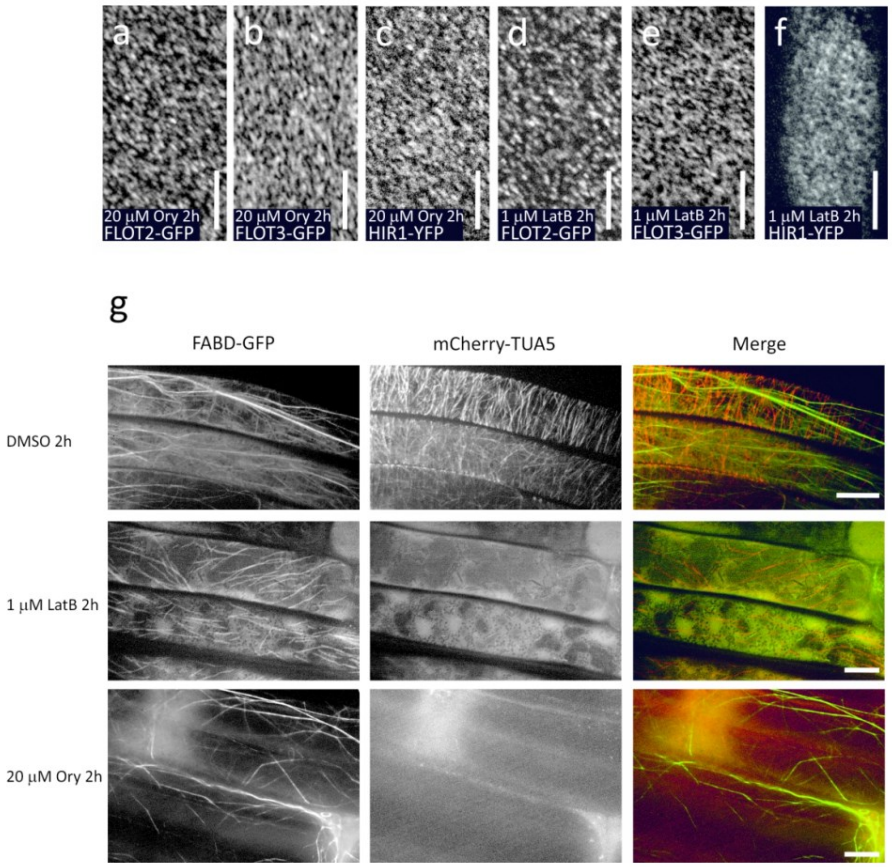

Figure S8. *At*FLOT and *At*HIR microdomain localization pattern does not depend on the integrity of microtubules and actin filaments. 5-day-old seedlings, root epidermal cells in elongation zone, confocal SD surface sections for *At*FLOT2-GFP (a, d), *At*FLOT3-GFP (b, e) and *At*HIR1-YFP (c, f), FABD-GFP/mCherry-TUA5 (g) treated for 2 h with 20 µM Ory (a-c, g lower row) or 1 µM LatB (d-f, g middle row). Scale bars 5 µm (a-f), 10µm (g). Ory, oryzalin, LatB, latrunculin B.

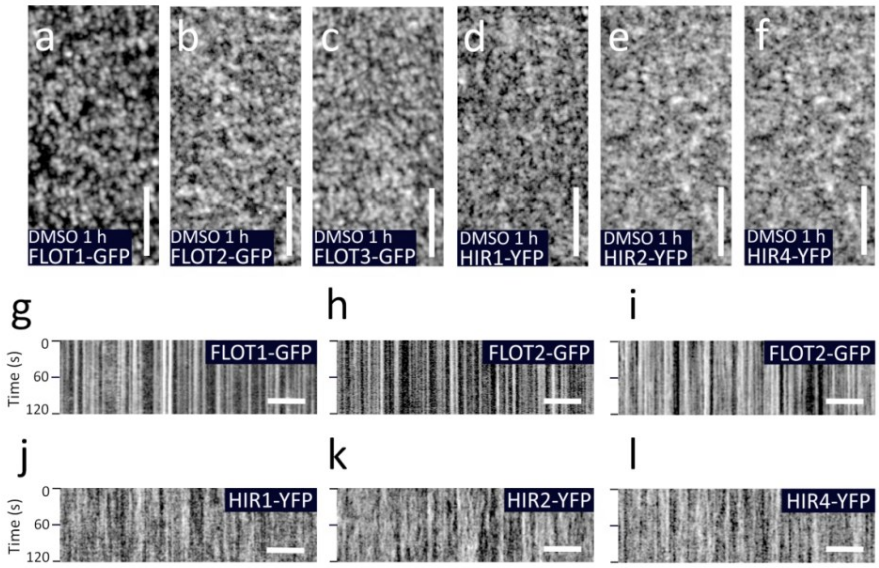

Figure S9. Control treatment (0.1% DMSO) for ISX experiments presented in Figure 4a-l. Confocal SD surface sections and representative kymograms obtained from 120 s time-lapse acquisition in root elongating epidermal cells for *At*FLOT1-GFP (a, g), *At*FLOT2-GFP (b, h), *At*FLOT3-GFP (c, i), *At*HIR1-YFP (d, j), *At*HIR2-YFP (e, k) and *At*HIR4-YFP (f, l). Scale bars 5 µm.

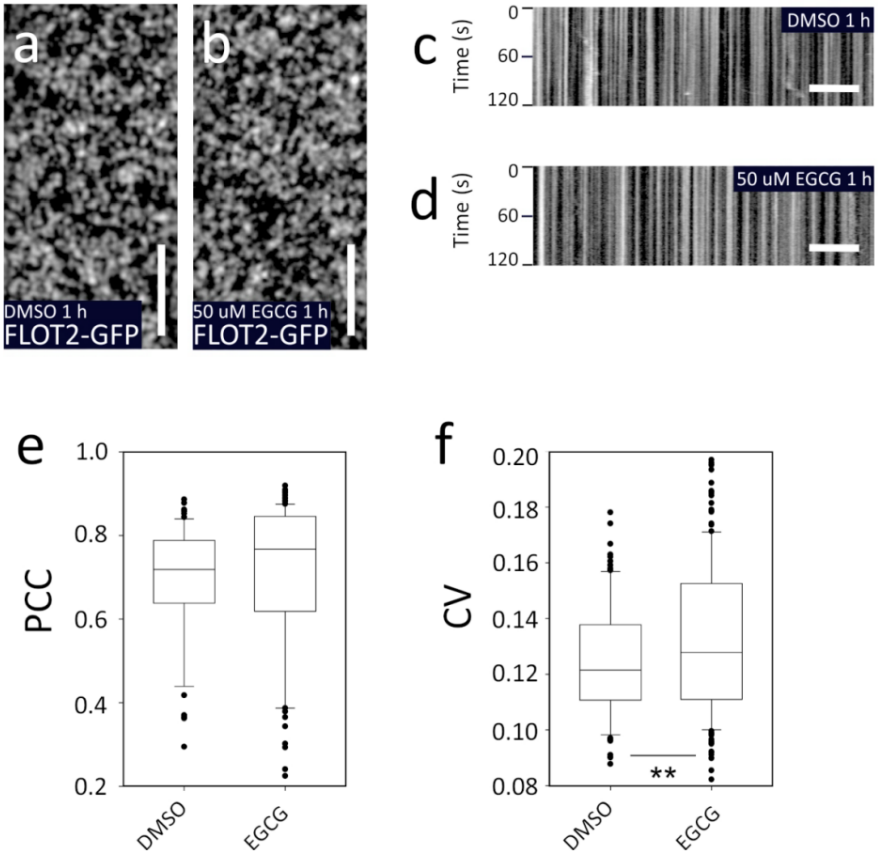

Figure S10. EGCG treatment of *At*FLOT2-GFP epidermal root cells. Localization pattern (a, b) and kymograms (c, d) remain without apparent changes upon 1 h treatment with 50 μM EGCG (b, d) when compared with control 0.1 % DMSO treatment (a, c). (e) Distribution of PCC values calculated from fluorescence intensity profiles of the first (t = 0 s) and last (t = 120 s) time point of kymograms. No difference detected ($p > 0.05$, n = 60 and 101 (2 to 3 kymographs constructed for each epidermal root cell) from 6 and 10 plants for DMSO or EGCG respectively). (f) Distribution of CV values of fluorescence intensities from 15 μm linear transect within the PM surface showing higher segregation of fluorescence under 1 h treatment with 50 μM EGCG when compared with control 0.1 % DMSO treatment (**$p < 0.01$, n = 107 and 216 (2 – 3 intensity profiles per cell) from 12 and 16 plants for DMSO or EGCG respectively). Whiskers in boxplots (e, f) represent 10th and 90th percentile Scale bars 5 μm. EGCG – epigallocatechin gallate, PCC – Pearsons' correlation coefficient, CV – coefficient of variation.

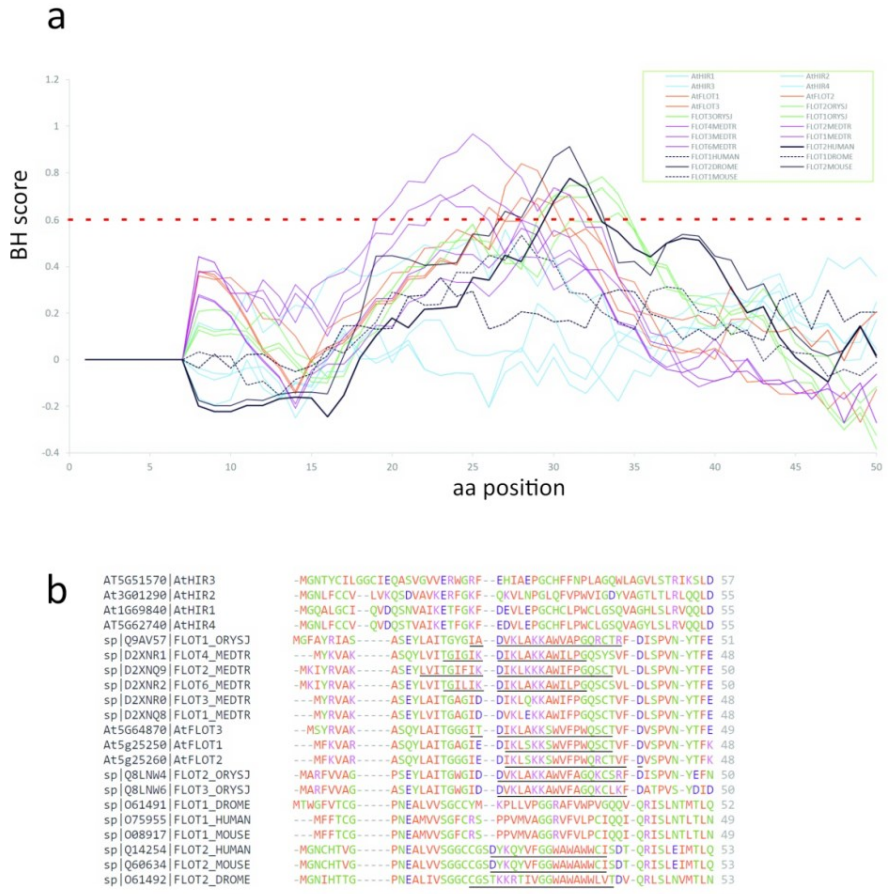

Figure S11. *At*FLOTs but not *At*HIRs may interact with PM by their putative N-terminal membrane binding site. (a) Stretches of high BH score (> 0.6, considered as putative membrane-binding sites, dashed horizontal line) were identified in FLOT aa sequences from *Arabidopsis thaliana* (red lines), *Medicago truncatula* (purple lines), *Oryza sativa* (green lines) and FLOT1s (black dashed lines) and FLOT2s (black solid lines) from *Mus musculus*, *Drosophila melanogaster* and *Homo sapiens*. It was not found in AtHIR sequences (blue lines). The sequences were obtained from UniProt (https://www.uniprot.org) and the search was carried out using BH search tool (https://hpcwebapps.cit.nih.gov/bhsearch/) with window size set to 15. Values for first 50 residues are shown, no additional peak of values exceeding BH-score 0.6 were found throughout all the sequences. (b) Alignment of the sequences showing conserved motif rich in basic and hydrophobic aa residues shared among plant FLOTs which was not found in Arabidopsis HIRs. Underlined residues contribute to BH score > 0.6 of the sequences. Alignment was performed in Clustal Omega (https://www.ebi.ac.uk/Tools/msa/clustalo/) with default settings. Note: during the BH search, 7 residues surrounding in both directions a given position of a residue were considered for counting the BH score at the given position (when the window was set to 15, i.e. 7+1+7). For this reason, there are BH-score = 0 for the first aa positions (a). However, as depicted in the alignment, an additional short motif rich in basic and hydrophobic residues is conserved among plant FLOT sequences at their very N-termini. This one is also not present in *At*HIR sequences (b).

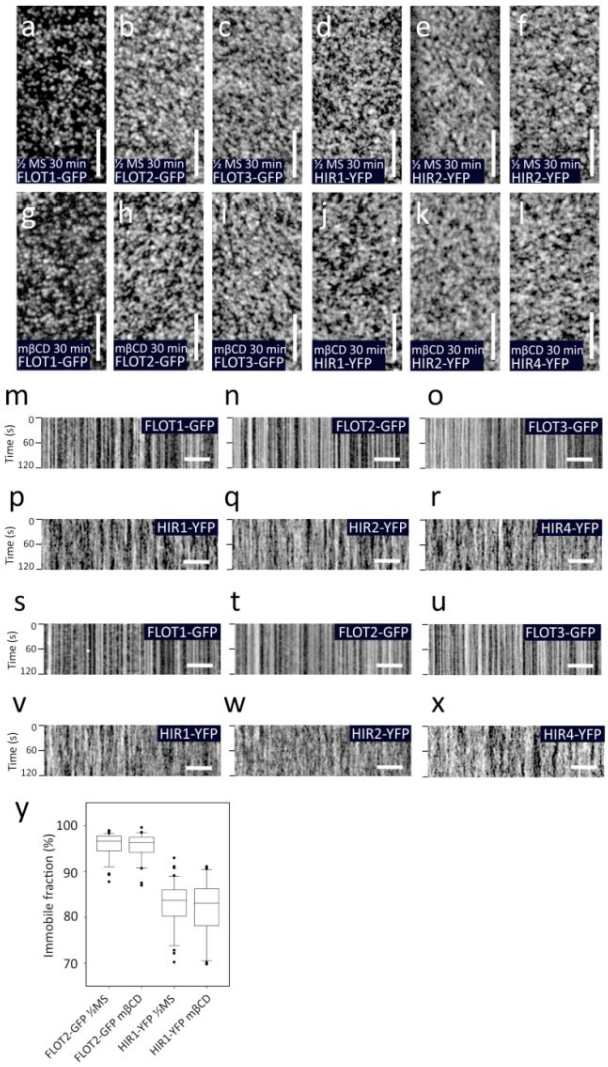

Figure S12. Sterol depletion does not affect mobility of PM-associated *At*FLOTs and *At*HIRs. Localization pattern (a, l) and kymograms (m-x) of *At*FLOT1-GFP (a, g, m, s), *At*FLOT2-GFP (b, h, n, t), *At*FLOT3-GFP (c, i, o, u), *At*HIR1-YFP (d, j, p, v), *At*HIR2-YFP (e, k, q, w) and *At*HIR4-YFP (f, l, r, x) remain without apparent changes upon 30 min treatment with 10 mM mßCD (g-l, p-r, v-x) when compared with control (a-f, m-o, s-u; half strength liquid MS medium supplemented with 1 % sucrose). Quantification of FRAP immobile fractions (y) showing no change of mobility of *At*FLOT2-GFP and *At*HIR1-YFP between control and mßCD-treated seedlings (Wilcox rank-sum test, $p > 0.05$, n = 27 to 9 seedlings for each line and treatment). 6-day old seedling were used. Whiskers in boxplots (y) represent 10th and 90th percentile Scale bars 5 µm. mßCD – methyl-ß-cyclodextrin.

Discussion and perspectives

In the presented papers we showed (i) that transcription of *AtFLOT*s is changed under several stimuli, however no apparent phenotype was observed in single isoform loss-of-function mutants under the treatments tested. (ii) We revealed several membrane proteins to interact with *At*FLOT2, many of these interactions are direct. Among them, important parts of the identified proteins are involved in transport (especially water transport) and response to biotic and abiotic stress. (iii) We observed differences in the localization of single isoforms of *At*FLOTs and *At*HIRs – some of them were found only at PM while others shared PM and tonoplast localization. One *At*HIR isoform was localized exclusively at the tonoplast. We observed differences in single isoform dynamics at PM, when *At*FLOTs were generally more stable than *At*HIRs, however overall mobility of the proteins from the both groups were very low. We observed the effect of CW on the mobility of the proteins from both groups.

Lack of phenotype in single loss-of-function mutants of *At*FLOTs

To find out the possible functions of *At*FLOTs we decided to apply reverse genetics approach. We focused on *At*FLOTs since only low knowledge has been gained so far on them while *At*HIRs have been already documented to play an important role in induction and control of hypersensitive response intensity under pathogen attack by the mechanism of interaction with resistance proteins (Qi et al., 2011, Qi and Katagiri, 2009). Similar function and mechanism was reported for HIRs from other plants such as pepper (Choi et al., 2013, Jung and Hwang, 2007, Jung et al., 2008), rice (Zhou et al., 2010, Zhou et al., 2009), barley (Rostoks et al., 2003), wheat (Zhang et al., 2011, Zhang et al., 2009, Yu et al., 2013, Yu et al., 2008, Liu et al., 2013, Chen et al., 2012, Duan et al., 2013), tobacco (Choi et al., 2011, Li et al., 2019) or soy (Xiang et al., 2015).

Before the beginning of the phenotyping screen we selected the treatments based on expression data obtained from Genevestigator (Daněk et al., 2016). As Genevestigator ATH1 chip recognizes both *AtFLOT1* and *AtFLOT2* transcripts by the same probe and it is thus impossible to discern whether the two closely related isoform respond in the same way to a given cue we measured the transcription level of *AtFLOT*s under some of the treatments using quantitative real-time PCR. We decided to test biotic, abiotic and phytohormone cues and performed performance tests under cold, salt, nitrogen and phosphate starvation, abscisic acid (ABA), naphthaleneacetic acid (NAA) *Botrytis cinerea* BMM (BMM), *Pseudomonas syringae* pv. tomato DC3000 (Pst) and bacterial elicitor flg22. For the treatment of *AtFLOT2* mutant,

another bacterial elicitor elf18 was used as *AtFLOT2* mutant was in the background of Wassilewskija ecotype which is deficient in functional *AtFLS2* that encodes flagellin receptor (Gomez-Gomez et al., 1999).

We observed some differences between our measurements and Genevestigator data where all of the selected treatments induced an increase in the transcription. The most pronounced difference was in case of Pst and ABA, where we did not detect any difference in transcription of all three *AtFLOT*s. In case of ABA, the observed lack of a change may be caused by the great variability in our transcription data after ABA treatment. Salt treatment downregulated *AtFLOT1* and *AtFLOT2* instead of an increase. Cold treatment enhanced the transcription only in *AtFLOT3* while the other two isoforms remained unaffected. On the other hand, bacterial elicitor flg22 and BMM induced the expected increase in transcription. In case of salt, flg22 and BMM treatment more than one isoform of *AtFLOT*s responded in the same direction (usually *AtFLOT1* and *AtFLOT2* shared the same pattern) which suggests redundant involvement of *At*FLOTs in the related biological processes.

The functional redundancy of single isoforms is a probable explanation for the absence of any phenotype in the tested single loss-of-function mutants. Especially the functional linkage between *At*FLOT1 and *At*FLOT2 seems probable as these two are tandem duplicates (Di et al., 2010) and their transcription responded similarly in our screen. Moreover, a growth phenotype as well as reduction of flg22-induced callose deposition is described in amiRNA knock-down line with simultaneously decreased *AtFLOT1* and *AtFLOT2* expression (Li et al., 2012, Yu et al., 2017). We did not observe any such effect in single mutants for neither of the two isoforms and we also did not detect any differences in hydrogen peroxide production upon flg22 treatment in none of *At*FLOT single mutants when compared with wild type. Interestingly, the involvement of FLOTs in plant-microbe interaction was reported in *M. truncatula*, where several *Mt*FLOTs are important for nodulation by the means of functional linkage with receptor kinase *Mt*LYK3 recognizing rhizobacterial signalling molecule Nod factor. This resembles the situation in *A. thaliana* where receptor kinase *At*FLS2 upon activation by its ligand flg22 increases its colocalization with *At*FLOT1 (Cui et al., 2018) which is then endocytosed and degraded with an increased intensity (Yu et al., 2017).

We did not observe any phenotype in nitrogen starvation experiments although cellular dynamics of ammonium transporter *At*AMT1;3 was described to be altered in *AtFLOT1*/*AtFLOT2* double knock-down mutant (Wang et al., 2013).

Based on our observation of no phenotype in single mutants it is necessary to produce multiple mutants of *AtFLOT*s. Given that *AtFLOT1* and *AtFLOT2* loci are adjacent one to each other at the same chromosome, there is no way to obtain double mutants in these genes by crossing individual single mutants. One possibility to generate double mutant the usage of RNAi-based approach (as in Li et al. 2012) where both loci can be targeted by single interfering RNA

with a high probability due to close sequence similarity of both genes. Another method is CRISPR/Cas9 editing which enables multiple targeting and thus to delete all three *AtFLOT*s in one go. Attempts have been made in out lab without satisfying results yet. RNAi-produced knock-down mutants might be in fact more valuable in case that total ablation of multiple isoforms had a severe impact on plant performance.

Interactome of *At*FLOT2

Mammalian homologs of FLOTs were reported to form functional complexes with a number of proteins among which cytoskeleton related proteins (Baumann et al., 2000, Liu et al., 2005, Langhorst et al., 2008) and tyrosine kinases (Ullrich and Schlessinger, 1990, Neumann-Giesen et al., 2007, Amaddii et al., 2012) are the most frequent. The interaction with protein partners is realized by coiled coil motifs in C-terminus of FLOT sequences (Neumann-Giesen et al., 2004, Solis et al., 2007) that were also predicted in *At*FLOTs (Daněk et al., 2016).

Determination of PM-bound protein complexes by co-immunoprecipitation and subsequent mass spectrometry (Co-IP/MS) can be tricky due to low fraction of PM proteins and relatively drastic conditions that are required to solubilize the complexes from PM. Therefore we applied modified protocol involving covalent cross-linking of the members of putative complexes (Qi and Katagiri, 2009, Qi et al., 2011) which allows the usage of such conditions. In order to minimize the false positive results originating from cross-linking of *At*FLOT2 e.g. with abundant cytoplasmic proteins we isolated and purified microsomal fraction prior to cross-linking.

*At*FLOT2 was substantially enriched in both microsomal and PM fraction. Intriguingly only few proteins were repeatedly identified from microsomal fraction while much more were found to bind *At*FLOT2 when PM fraction was used. This effect is due to low portion of PM in microsomal membrane and associated low amount of PM-associated proteins which are thus more diluted in total membrane proteins. Our microscopic observation indeed detected *At*FLOT2 only in PM and thus working with PM-enriched membrane fraction in Co-IP/MS analysis is a reasonable approach to obtain valid results in this case.

The determined interactors were mostly involved in cell transport (*At*AHA1, *At*ABCG36, *At*PIP1;2, *At*PIP2;1, *At*PIP2;2, *At*PIP2;6, *At*PIP2;7, *At*SYP71), plant immunity (*At*AHA1, *At*HIR2, *At*ABCG39, *At*NHL3, *At*SYP71) or water stress (*At*PIPs, *At*ERD4). Interestingly the interaction of *At*FLOT2 with *At*HIR2 was detected and subsequently verified as direct, while none of the two other *At*FLOT isoforms were found. We suppose that this can be due to generally lower level of *At*FLOT proteins in leaf cell when compared with *At*HIRs among which *At*HIR2 is the most expressed one (Daněk et al., 2016). Among the detected interactors many of them such as *At*AHA1, *At*PIP1;2, *At*PIP2;7, *At*SYP71, *At*NHL3, *At*ERD4, *At*HIR2 were in previous

studies detected in DRM (Borner et al., 2005, Shahollari et al., 2004, Keinath et al., 2010) which is also the case of *At*FLOT2 homologs (Borner et al., 2005, Ishikawa et al., 2015) which suggests that these proteins preferentially localize in similar PM sub-areas where they can interact which could be important for their proper functioning.

Some of the revealed interactions were proven direct using split-ubiquitin system. Interestingly *At*PIP1;2 and *At*PIP2;6 directly bound *At*FLOT2 while the rest of the tested *At*PIP isoforms did not. Indirect interaction with other isoforms may be realized by binding *At*PIP1;2 and *At*PIP2;6 subunits of tetramers composed of different *At*PIP isoforms (Jozefkowicz et al., 2017). Moreover, interactome of *At*PIPs comprises several hundreds of proteins (Bellati et al., 2016) some of which can potentially indirectly interact with *At*FLOT2.

In addition, *At*FLOT1 was found to bind *A*tFLOT3 (Yu et al., 2017) so the interaction with *At*FLOT2 seems also probable. *At*FLOT1 was found to colocalize (but the interaction *per se* was not investigated) with *At*AMT1;3 (Wang et al., 2013), *At*BRI1 (Wang et al., 2015), *At*PIP2;1 (Li et al., 2011), *At*RbohD (Liu et al., 2015) and *At*FLS2 (Cui et al., 2018) where it was important for the clathrin-independent endocytosis of these proteins. *At*FLOT1 was also found in early and late endosome where it colocalized with the markers of these structures – *At*VHA-a1 and *At*RabG3f (Yu et al., 2017). Moreover it was shown to colocalize with myosin-binding protein *At*MyoB1 (Peremyslov et al., 2013) which indicates that the vesicular transport of *At*FLOT1 might be provided by its functional linking with actin cytoskeleton. *At*FLOT2 may be involved in similar processes as we identified *At*SYP71, a Qc SNARE protein important for vesicular transport (Sanderfoot et al., 2001) as its direct interactor.

Interestingly, we did not find any of the putative interactors which are available in Associomics interaction database (Jones et al., 2014) for *At*FLOT2 (Daněk et al., 2016) in our study. Associomics interactions were determined in a screen using split-ubiquitin system and revealed thus direct interactions (Jones et al., 2014). We suppose that these distinct approaches in initial screen could contribute to different proteins determined.

The found interaction of *At*FLOT2 should be in next steps verified *in planta* using e.g. FRET or FLIM or cross-correlation spectroscopy techniques which would allow dynamic study of the interaction *in vivo*.

Differences between AtFLOT and AtHIR behaviour at the plasma membrane

In our microscopic study we were using stable transformants of *A. thaliana* expressing single isoforms of *At*FLOT or *At*HIR fused to GFP or YFP respectively under the control of CaMV 35S promoter as there was very low fluorescence of *At*FLOT1-GFP reported when the expression was driven by endogenous promoter (Li et al., 2012).

Although both subgroups of proteins were found at PM where they formed microdomains, in all *At*HIRs we observed minor pool of the proteins to concomitantly localize at the tonoplast. This tendency was most prominent in *At*HIR3 which was present only at the tonoplast. Intriguingly, *At*FLOT1 was also localized at the tonoplast and probably also at other endomembranes which is in line with the published results obtained using electron microscopy (Li et al., 2012) as well as with its involvement in endocytosis of several membrane proteins (Hao et al., 2014, Li et al., 2011, Cui et al., 2018, Wang et al., 2015).

Both subgroups significantly differed in lateral mobility at PM, where *At*FLOTs were generally more stable than *At*HIRs. This was apparent at the kymographs which allows to display the mobility of the whole fluorescent foci over time. Here it is visible that the majority of *At*FLOT-defined microdomains remains at the same position throughout the entire 120 s observation period whereas *At*HIR microdomains were more fluctuating. Corresponding results were achieved by application of FRAP. Mobility of *At*HIR3 at the tonoplast was however the far highest of all isoforms from both groups. Similar difference was observed in case of aquaporins where tonoplast localized isoform exhibited strikingly higher mobility than PM-localized one (Hosy et al., 2014, Luu et al., 2012). Moreover, the same pattern was present in *At*PIP2;1 where PM pool was more immobile than the protein localized at endomembranes (Sorieul et al., 2011). The higher mobility at the tonoplast than at PM has been recently also presented for *At*HIR1 (Lv et al., 2017a). In our case we can hypothesize that concomitant presence at the tonoplast promotes the mobility of PM pool of the same protein. In addition to *At*HIR1/2/4 this is also slightly apparent for *At*FLOT1 which is in minor pool present at the tonoplast and which was in our study the least immobile of three *At*FLOTs, however the difference was not significant. This higher mobility may be caused by faster exchange between endomembranes and PM or by the different way of interaction with PM.

The second possibility seems plausible to take place in our case as *At*HIRs unlike *At*FLOTs harbour putative lipidation sites in their sequences (Daněk et al., 2016). Accordingly *At*HIRs were experimentally found to be myristoylated and palmitoylated while *At*FLOTs were not (Hemsley et al., 2013, Majeran et al., 2018). Both modifications were described to differentially influence PM and endomembrane localization (Traverso et al., 2013). Moreover,

we found a putative membrane-binding motif containing enrichment in basic and hydrophobic aa residues (so called polybasic motif) in the very N-termini of all *At*FLOTs and in several FLOTs of other plant species. This motif seems relatively conserved in plant isoforms and it is not present in *At*HIRs suggesting that *At*HIR and *At*FLOT interaction with PM and/or other membranes is indeed of a different mechanism. PM protein mobility was shown to be affected by lipid composition. Plant PM is specifically rich in phosphatidylinositol 4-phosphate (PI4P) which makes it highly negatively charged and acidic (Simon et al., 2016). The putative polybasic motif of *At*FLOTs is prone to interact with the negatively charged PM by electrostatic interactions. Reduction in PI4P content lowered the clustering of *St*REM1.3 into microdomains within PM probably due to the impeded interaction between the protein and the lipid (Gronnier et al., 2017). Interestingly, we observed a lower degree of clustering in *At*HIRS than in *At*FLOTs. We speculate that the presence versus absence of the polybasic motif in the both groups may be a possible explanation. Experimental verification of the contribution of the described motif (e.g. by generation of truncated versions of the proteins lacking the respective motifs or by mutation of the basic aa within the motifs) or the investigation of the effect of PI4P level on *At*FLOTs and *At*HIR localization (e.g. by using inhibitors of synthesis of PI4P such as wortmannin and phenylarsine oxide or genetically encoded PI4P phosphatase SAC1 (Simon et al., 2016)) however remains to be carried out.

Interestingly, the observed difference in mobility of the subgroups is in contrast with the published data, where N-terminally tagged *At*FLOT1 was more mobile than *At*HIR1 tagged at its C-terminus (Lv et al., 2017b). We think that the position of the tag can greatly contribute to the difference as it was shown for *At*PIP2;1 and *At*PIP1;2 where C–terminal fusion of the fluorophore exhibited higher mobile fraction, the increase was about 50 % in one of the isoform (Luu et al., 2012). As both *At*FLOTs and *At*HIRs are supposed to interact with the membranes by its N-terminal SPFH domain and the lipidation sites of *At*HIRs as well as the putative membrane-binding motifs of *At*FLOT are localized at the very N-termini we conclude that C-terminal fusion is more safe with regards to a possibility of steric interference of the fluorophore with the interaction between the protein and the membrane which could alter the natural behaviour of a the proteins within the membrane. We assume that proteins with putative similar topology should be tagged at the same manner (i. e. at C- or N-terminus) if they are to be compared.

Cytoskeleton roles in AtFLOT and AtHIR localization and dynamics

In addition to the prominent microdomain localization we observed another larger scale pattern present in all isoforms localized at PM. Linear corrals lacking fluorescence signal were to a various extend present in all tissues tested. In *At*FLOT2 and *At*HIR1 we demonstrate the colocalization of such corrals with MTs or rather with MT bundles. Similar observation was made

with more detailed focus where individual fluorescent foci were reported to be restricted in movement by fine cytoskeleton network (Lv et al., 2017b).

We did not detect any apparent changes in localization pattern after the disruption of actin of MT cytoskeleton in *At*FLOT2, *At*FLOT3 or *At*HIR1, however a slight change in microdomain density was reported in the literature after actin or MT depolymerisation due to reduced endocytosis when measured using VAEM/TIRF imaging (Lv et al., 2017b). We suppose that our confocal imaging may not be sensitive enough to reveal such smaller differences.

In *Mt*SYMREM1 microdomains actin depolymerisation caused a decrease in density while MT disruption had no effect (Liang et al., 2018) while in *At*REM1.2 microdomain pattern was "dissolved" under actin depolymerisation and a decrease in density was observed under disruption of MTs (Szymanski et al., 2015). The effect of the cytoskeleton proteins is thus different even on related proteins and the intensity of such an impact can also be quite variable.

Low mobility of plasma membrane proteins

When compared with metazoan homologs plant isoforms of related proteins often exhibit much lower mobility (Martiniere and Runions, 2013). This is also the case of FLOTs as *Hs*FLOT2 fluorescence recovery was rapid and reached approx. 80 % (Langhorst et al., 2007) which is in great contrast with more than 90 % of immobile fractions measured in our study for *At*FLOTs.

The values of FRAP reached for *At*FLOTs and *At*HIRs are in fact far high even when compared with other plant PM proteins. The published values of mobile fractions reach roughly from 10 % to 90 % (McKenna et al., 2014). The latter value is achieved for *At*LTI6b, a PM protein with far highest lateral mobility to be found in the literature (at least to my knowledge). Interestingly the *At*PIP2;1 and *At*REM1.3 expressed transiently in tobacco reached much higher recovery than in stable Arabidopsis transformants (McKenna et al., 2014, Jarsch et al., 2014). *At*FLOTs and *At*HIRs are substantially more immobile than other peripheral PM proteins remorins (McKenna et al., 2014, Jarsch et al., 2014) their FRAP values are rather similar to proteins such as *At*PIPs, *At*FLS2, *At*PIN2 or GFP fused to GPI anchor (McKenna et al., 2014, Luu et al., 2012, Martiniere et al., 2012), i.e. transmembrane proteins or a protein localizes at the apoplastic side of PM. The mere PM localization or even transmembrane stretch does not qualify a protein to be immobilized since lipidated GFP (anchored to inner PM leaflet) or *At*LTI6b (having transmembrane stretch) exhibit much quicker lateral mobility and higher recovery rates (Martiniere et al., 2012).

Sterols were reported to be involved in PM protein mobility. Lower sterol amount in PM resulted in decrease mobility of *At*PIP2;1 (Li et al., 2011), *At*RbohD (Hao et al., 2014), *At*FLS2 (Cui et al., 2018) as well as *At*FLOT1 (Li et al., 2012) and *Hs*FLOT2 (Langhorst et al., 2007). On

the contrary *At*HIR1 was more mobile under alteration of sterol synthesis and the mobility was not changed under sterol depletion (Lv et al., 2017b). In our study we did not see any striking changes in localization pattern in neither isoform of *At*FLOT or *At*HIR, nor a change in mobility of *At*FLOT2 and *At*HIR1 under sterol depletion. Due to very high immobility of *At*FLOT2 in control conditions (immobile fraction > 95 %) it is possible that a relative increase of immobile fraction would be too low to be detected.

Cell wall interaction with *At*FLOT2 and *At*HIR1

CW impact on PM dynamics is intuitive and deductible from the observed differences between plant and metazoan isoforms of PM proteins or from the discrepancies in the mobility of the same protein localized at PM and endomembranes (see above). In the presented work we investigated the alteration in lateral mobility under CW disruption in *At*FLOT2 and *At*HIR1.

Isoxaben (ISX), a cellulose synthesis inhibitor (Scheible et al., 2003) induced a small increase in mobility only in *At*HIR1 while epigallocatechin gallate (EGCG), a pectin methyl esterase inhibitor (Lewis et al., 2008) induced a small decrease of mobility in *At*FLOT2. This opposite effect points to the possibility that proteins may be functionally lined to different components of CW. EGCG treatment has been recently reported to increase the mobility and microdomain size of *At*FLS2 and *At*PIN3 and the same effect was described for, 2,6-dichlorobenzonitrile (DCB) another drug disrupting cellulose deposition to CW (McKenna et al., 2019). Similarly, ISX treatment increased the mobility of *At*PIN2 (Feraru et al., 2011). Interestingly, DCB and ISX affected the mobility of the same protein *At*LTI6b in the opposite way, the former induced an increase (McKenna et al., 2019) while the latter provoked a decrease which was also observed in our study (Martiniere et al., 2012). Given that DCB impairs the cellulose deposition by a different way than ISX (Tateno et al., 2016) it seems that it is not only overall amount of cellulose in CW which is important for a given protein features but also putative changes in CW microarchitecture (probably different under different inhibitors) may cause substantial alterations.

Unlike in *At*PIN2 (Feraru et al., 2011) and *At*PIP2;1 (Hosy et al., 2014) where an increase of mobility was described under plasmolysis, i.e. the physical separation of PM from CW we observed an opposite effect in both isoforms tested under strong osmotic challenging. However, when mild osmotic treatment combined with partial CW digestion was applied we observed an increase of mobility in subareas of PM detached to a various extend from CW which is in line with the observation made in *At*PIN2 (Feraru et al., 2011). Similar effect was induced by complete

CW removal in protoplasts of *At*FLOT2 reminiscent to the increase of mobility of GPI-anchored GFP in protoplast (Martiniere et al., 2012).

It is important to take into account that all the reported proteins affected by CW disruption mentioned in this section are PM transmembrane proteins some of which also possess a prominent extracellular domain. This is not the case of *At*FLOTs nor *At*HIRs which cannot directly interact with CW as they are localized at the opposite side of PM. The interaction thus must be indirect. Interactors of *At*FLOT2, many of which are transmembrane proteins, have been described above in this text. In addition to them, *At*TBL36 is proposed as an interactor of *At*FLOT2 and *At*FLOT3 in Associomics (Jones et al., 2014, Daněk et al., 2016). The protein is a homolog of a protein important for cellulose deposition to CW (Bischoff et al., 2010). *At*HIRs were reported to constitute a PM-localized complex containing several transmembrane proteins (Qi and Katagiri, 2009, Qi et al., 2011).

Another possibility is the connection through PM leaflets by interdigitation of long acyl chains of lipids from the extracellular side where GPI-proteins (sterically interacting with CW) stabilize these interconnected PM subregions within cytoplasmic side of which peripheral proteins (such as *At*FLOTs or *At*HIRs) can be anchored. However, such a system has been so far described only in metazoan cells (Raghupathy et al., 2015).

Finally, CW disruption induces a variety of physiological responses as it produces a number of molecular patterns which can act as elicitors and also activates mechanosensing pathways (Engelsdorf et al., 2018). As *At*FLOT1 mobility is enhanced by flg22 elicitor (Lv et al., 2017b) and *At*HIRs were found to bind lipoglycan elicitor (Vilakazi et al., 2017) it is possible that CW alteration not only removes physical barriers for *At*FLOT2 and *At*HIR1 movement but also release signalling agents that can contribute to the increase of mobility. To discern these two possible effects, protein mobility could be tested under the treatment with CW-derived elicitors or damage-associated molecular patterns such as oligogalacturonides (Bacete et al., 2018) or by application of specific peptides described to impede metazoan cell adhesion which are in plants reported to decrease the attachment of PM to CW (Gouget et al., 2006).

Conclusions

In our study we find out that transcription of *AtFLOT*s is upregulated in response to *Botrytis cinerea*, flagellin or cold and decreased under salt treatment. Interestingly, more than one isoform reacts to a given stimulus which suggest possible redundancy of *AtFLOT*s in response to such cues. This redundancy can also explain the lack of phenotype in single loss-of-function mutants of *AtFLOT*s in our screen comprising salt treatment, phosphorus and nitrogen starvation, infection with *Pseudomonas syringae* and *Botrytis cinerea*, treatment with bacterial elicitors or auxin and abscisic acid. By Co-IP/MS analysis we revealed proteins interacting with *At*FLOT2 that are mainly involved in transport, water stress response and pathogen interactions which to a certain extend correspond with the transcription changes induced by such treatments in our phenotype screen. Finally, we focused on the localization pattern of *At*FLOTs and *At*HIRs using confocal microscopy. We observed PM microdomain localization of all the isoforms except *At*HIR3 which was present only at the tonoplost. Minor tonoplast localization in addition to predominant PM localization was however revealed to be shared in *At*HIRs and *At*FLOT1. Proteins at PM from both groups were very stable, however *At*HIRs were generally slightly more dynamic than *At*FLOTs as determined by FRAP approach and analysis of kymograms. We suppose that these differences between the two groups in localization and dynamics may be attributed to their putative distinct ways of association with PM. PM microdomain defined by proteins from both groups are excluded from the linear corrals in PM surface. These corrals colocalize with MTs, however MT or actin destabilization does not affect localization pattern of *At*FLOTs and *At*HIRs. Increase in mobility of *At*HIR1 and *At*FLOT2 was observed under pharmacological or alteration or enzymatic digestion of CW. CW thus affect the mobility of PM associated proteins that are not in direct contact with it as both *At*FLOTs and *At*HIRs are inner leaflet peripheral proteins. Proteins from both groups can be therefore involved in processes taking place at the CW/PM interface. As CW alteration can be perceived as stimulus to a certain level resembling a pathogen attack and with respect to observed transcriptional changes under pathogen or elicitor treatments as well as to the determined protein interactors of *At*FLOT2 involved in plant-pathogen interactions it is possible that the effect of CW disruption on *At*FLOT2 and *At*HIR1 mobility at PM may be a manifestation of their role in such processes.

References

AMADDII, M., MEISTER, M., BANNING, A., TOMASOVIC, A., MOOZ, J., RAJALINGAM, K. & TIKKANEN, R. 2012. Flotillin-1/Reggie-2 protein plays dual role in activation of receptor-tyrosine kinase/mitogen-activated protein kinase signaling. *Journal of Biological Chemistry,* 287**,** 7265-7278.

AMARO, M., REINA, F., HOF, M., EGGELING, C. & SEZGIN, E. 2017. Laurdan and Di-4-ANEPPDHQ probe different properties of the membrane. *Journal of physics D: Applied physics,* 50**,** 134004-134004.

BABUKE, T., RUONALA, M., MEISTER, M., AMADDII, M., GENZLER, C., ESPOSITO, A. & TIKKANEN, R. 2009. Hetero-oligomerization of reggie-1/flotillin-2 and reggie-2/flotillin-1 is required for their endocytosis. *Cellular Signalling,* 21**,** 1287-1297.

BACETE, L., MÉLIDA, H., MIEDES, E. & MOLINA, A. 2018. Plant cell wall-mediated immunity: cell wall changes trigger disease resistance responses. *The Plant Journal,* 93**,** 614-636.

BASHLINE, L., LI, S. D., ZHU, X. Y. & GU, Y. 2015. The TWD40-2 protein and the AP2 complex cooperate in the clathrin-mediated endocytosis of cellulose synthase to regulate cellulose biosynthesis. *Proceedings of the National Academy of Sciences of the United States of America,* 112**,** 12870-12875.

BAUMANN, C. A., RIBON, V., KANZAKI, M., THURMOND, D. C., MORA, S., SHIGEMATSU, S., BICKEL, P. E., PESSIN, J. E. & SALTIEL, A. R. 2000. CAP defines a second signalling pathway required for insulin-stimulated glucose transport. *Nature,* 407**,** 202-207.

BELLATI, J., CHAMPEYROUX, C., HEM, S., ROFIDAL, V., KROUK, G., MAUREL, C. & SANTONI, V. 2016. Novel Aquaporin Regulatory Mechanisms Revealed by Interactomics. *Mol Cell Proteomics,* 15**,** 3473-3487.

BISCHOFF, V., NITA, S., NEUMETZLER, L., SCHINDELASCH, D., URBAIN, A., ESHED, R., PERSSON, S., DELMER, D. & SCHEIBLE, W.-R. 2010. TRICHOME BIREFRINGENCE and its homolog AT5G01360 encode plant-specific DUF231 proteins required for cellulose biosynthesis in Arabidopsis. *Plant physiology,* 153**,** 590-602.

BONNEAU, L., GERBEAU-PISSOT, P., THOMAS, D., DER, C., LHERMINIER, J., BOURQUE, S., ROCHE, Y. & SIMON-PLAS, F. 2010. Plasma membrane sterol complexation, generated by filipin, triggers signaling responses in tobacco cells. *Biochim Biophys Acta,* 1798**,** 2150-9.

BORNER, G. H. H., SHERRIER, D. J., WEIMAR, T., MICHAELSON, L. V., HAWKINS, N. D., MACASKILL, A., NAPIER, J. A., BEALE, M. H., LILLEY, K. S. & DUPREE, P. 2005. Analysis of detergent-resistant membranes in *Arabidopsis*. Evidence for plasma membrane lipid rafts. *Plant Physiology,* 137**,** 104-116.

BÜCHERL, C. A., JARSCH, I. K., SCHUDOMA, C., SEGONZAC, C., MBENGUE, M., ROBATZEK, S., MACLEAN, D., OTT, T. & ZIPFEL, C. 2017. Plant immune and growth receptors share common signalling components but localise to distinct plasma membrane nanodomains. *eLife,* 6**,** e25114.

CACAS, J. L., BURE, C., GROSJEAN, K., GERBEAU-PISSOT, P., LHERMINIER, J., ROMBOUTS, Y., MAES, E., BOSSARD, C., GRONNIER, J., FURT, F., FOUILLEN, L., GERMAIN, V., BAYER, E., CLUZET, S., ROBERT, F., SCHMITTER, J. M., DELEU, M., LINS, L., SIMON-PLAS, F. & MONGRAND, S. 2016. Revisiting Plant Plasma Membrane Lipids in Tobacco: A Focus on Sphingolipids. *Plant Physiology,* 170**,** 367-384.

CUI, Y., LI, X., YU, M., LI, R., FAN, L., ZHU, Y. & LIN, J. 2018. Sterols regulate endocytic pathways during flg22-induced defense responses in Arabidopsis. *Development,* 145.

DANĚK, M., VALENTOVÁ, O. & MARTINEC, J. 2016. Flotillins, Erlins, and HIRs: From Animal Base Camp to Plant New Horizons. *Critical Reviews in Plant Sciences,* 35**,** 191-214.

DEMIR, F. 2010. *Lipid Rafts in Arabidopsis thaliana leaves.* Julius-von-Sachs Institute for Biosciences.

DEMIR, F., HORNTRICH, C., BLACHUTZIK, J. O., SCHERZER, S., REINDERS, Y., KIERSZNIOWSKA, S., SCHULZE, W. X., HARMS, G. S., HEDRICH, R., GEIGER, D. & KREUZER, I. 2013. Arabidopsis nanodomain-

delimited ABA signaling pathway regulates the anion channel SLAH3. *Proceedings of the National Academy of Sciences of the United States of America,* 110**,** 8296-8301.

DI, C., XU, W. Y., SU, Z. & YUAN, J. S. 2010. Comparative genome analysis of PHB gene family reveals deep evolutionary origins and diverse gene function. *Bmc Bioinformatics,* 11.

DUAN, Y. H., GUO, J., SHI, X. X., GUAN, X. N., LIU, F. R., BAI, P. F., HUANG, L. L. & KANG, Z. S. 2013. Wheat hypersensitive-induced reaction genes TaHIR1 and TaHIR3 are involved in response to stripe rust fungus infection and abiotic stresses. *Plant Cell Reports,* 32**,** 273-283.

ENGELSDORF, T., GIGLI-BISCEGLIA, N., VEERABAGU, M., MCKENNA, J. F., VAAHTERA, L., AUGSTEIN, F., VAN DER DOES, D., ZIPFEL, C. & HAMANN, T. 2018. The plant cell wall integrity maintenance and immune signaling systems cooperate to control stress responses in *Arabidopsis thaliana*. *Science Signaling,* 11**,** eaao3070.

FERARU, E., FERARU, M. I., KLEINE-VEHN, J., MARTINIERE, A., MOUILLE, G., VANNESTE, S., VERNHETTES, S., RUNIONS, J. & FRIML, J. 2011. PIN polarity maintenance by the cell wall in Arabidopsis. *Curr Biol,* 21**,** 338-43.

FUJIWARA, T., RITCHIE, K., MURAKOSHI, H., JACOBSON, K. & KUSUMI, A. 2002. Phospholipids undergo hop diffusion in compartmentalized cell membrane. *The Journal of Cell Biology,* 157**,** 1071-1082.

FURT, F., KÖNIG, S., BESSOULE, J.-J., SARGUEIL, F., ZALLOT, R., STANISLAS, T., NOIROT, E., LHERMINIER, J., SIMON-PLAS, F., HEILMANN, I. & MONGRAND, S. 2010. Polyphosphoinositides are enriched in plant membrane rafts and form microdomains in the plasma membrane. *Plant physiology,* 152**,** 2173-2187.

GEHL, B. & SWEETLOVE, L. J. 2014. Mitochondrial Band-7 family proteins: scaffolds for respiratory chain assembly? *Frontiers in Plant Science,* 5.

GERBEAU-PISSOT, P., DER, C., THOMAS, D., ANCA, I.-A., GROSJEAN, K., ROCHE, Y., PERRIER-CORNET, J.-M., MONGRAND, S. & SIMON-PLAS, F. 2014. Modification of plasma membrane organization in tobacco cells elicited by cryptogein. *Plant physiology,* 164**,** 273-286.

GOMEZ-GOMEZ, L., FELIX, G. & BOLLER, T. 1999. A single locus determines sensitivity to bacterial flagellin in Arabidopsis thaliana. *Plant J,* 18**,** 277-84.

GOUGET, A., SENCHOU, V., GOVERS, F., SANSON, A., BARRE, A., ROUGÉ, P., PONT-LEZICA, R. & CANUT, H. 2006. Lectin receptor kinases participate in protein-protein interactions to mediate plasma membrane-cell wall adhesions in Arabidopsis. *Plant physiology,* 140**,** 81-90.

GRONNIER, J., CROWET, J. M., HABENSTEIN, B., NASIR, M. N., BAYLE, V., HOSY, E., PLATRE, M. P., GOUGUET, P., RAFFAELE, S., MARTINEZ, D., GRELARD, A., LOQUET, A., SIMON-PLAS, F., GERBEAU-PISSOT, P., DER, C., BAYER, E. M., JAILLAIS, Y., DELEU, M., GERMAIN, V., LINS, L. & MONGRAND, S. 2017. Structural basis for plant plasma membrane protein dynamics and organization into functional nanodomains. *Elife,* 6.

GROSJEAN, K., DER, C., ROBERT, F., THOMAS, D., MONGRAND, S., SIMON-PLAS, F. & GERBEAU-PISSOT, P. 2018. Interactions between lipids and proteins are critical for organization of plasma membrane-ordered domains in tobacco BY-2 cells. *J Exp Bot,* 69**,** 3545-3557.

GROSJEAN, K., MONGRAND, S., BENEY, L., SIMON-PLAS, F. & GERBEAU-PISSOT, P. 2015. Differential effect of plant lipids on membrane organization: specificities of phytosphingolipids and phytosterols. *The Journal of biological chemistry,* 290**,** 5810-5825.

GUILLIER, C., CACAS, J. L., RECORBET, G., DEPRETRE, N., MOUNIER, A., MONGRAND, S., SIMON-PLAS, F., WIPF, D. & DUMAS-GAUDOT, E. 2014. Direct purification of detergent-insoluble membranes from *Medicago truncatula* root microsomes: comparison between floatation and sedimentation. *BMC Plant Biol,* 14**,** 255.

HANEY, C. H., RIELY, B. K., TRICOLI, D. M., COOK, D. R., EHRHARDT, D. W. & LONG, S. R. 2011. Symbiotic *Rhizobia* bacteria trigger a change in localization and dynamics of the *Medicago truncatula* Receptor Kinase LYK3. *Plant Cell,* 23**,** 2774-2787.

HAO, H. Q., FAN, L. S., CHEN, T., LI, R. L., LI, X. J., HE, Q. H., BOTELLA, M. A. & LIN, J. X. 2014. Clathrin and membrane microdomains cooperatively regulate RbohD dynamics and activity in *Arabidopsis*. *Plant Cell,* 26**,** 1729-1745.

HEMSLEY, P. A., WEIMAR, T., LILLEY, K. S., DUPREE, P. & GRIERSON, C. S. 2013. A proteomic approach identifies many novel palmitoylated proteins in Arabidopsis. *New Phytologist,* 197**,** 805-814.

HOSY, E., MARTINIERE, A., CHOQUET, D., MAUREL, C. & LUU, D. T. 2014. Super-resolved and dynamic imaging of membrane proteins in plant cells reveal contrasting kinetic profiles and multiple confinement mechanisms. *Mol Plant*.

CHEN, J. P., YU, X. M., ZHAO, W. Q., LI, X., MENG, T., LIU, F., YANG, W. X., ZHANG, T. & LIU, D. Q. 2012. Temporal and tissue-specific expression of wheat TaHIR2 gene and resistant role of recombinant protein during interactions between wheat and leaf rust pathogen. *Physiological and Molecular Plant Pathology,* 79**,** 64-70.

CHEN, K.-Q., ZHAO, X.-Y., AN, X.-H., TIAN, Y., LIU, D.-D., YOU, C.-X. & HAO, Y.-J. 2017. MdHIR proteins repress anthocyanin accumulation by interacting with the MdJAZ2 protein to inhibit its degradation in apples. *Scientific Reports,* 7**,** 44484.

CHOI, H. W., KIM, D. S., KIM, N. H., JUNG, H. W., HAM, J. H. & HWANG, B. K. 2013. *Xanthomonas* filamentous hemagglutinin-like protein Fha1 interacts with pepper hypersensitive-induced reaction protein CaHIR1 and functions as a virulence factor in host plants. *Molecular Plant-Microbe Interactions,* 26**,** 1441-1454.

CHOI, H. W., KIM, Y. J. & HWANG, B. K. 2011. The hypersensitive induced reaction and leucine-rich repeat proteins regulate plant cell death associated with disease and plant immunity. *Molecular Plant-Microbe Interactions,* 24**,** 68-78.

ISHIKAWA, T., AKI, T., YANAGISAWA, S., UCHIMIYA, H. & KAWAI-YAMADA, M. 2015. Overexpression of BAX INHIBITOR-1 Links Plasma Membrane Microdomain Proteins to Stress. *Plant Physiology,* 169**,** 1333-1343.

JARSCH, I. K., KONRAD, S. S. A., STRATIL, T. F., URBANUS, S. L., SZYMANSKI, W., BRAUN, P., BRAUN, K. H. & OTT, T. 2014. Plasma membranes are subcompartmentalized into a plethora of coexisting and diverse microdomains in *Arabidopsis* and *Nicotiana benthamiana*. *Plant Cell,* 26**,** 1698-1711.

JONES, A. M., XUAN, Y., XU, M., WANG, R.-S., HO, C.-H., LALONDE, S., YOU, C. H., SARDI, M. I., PARSA, S. A., SMITH-VALLE, E., SU, T., FRAZER, K. A., PILOT, G., PRATELLI, R., GROSSMANN, G., ACHARYA, B. R., HU, H.-C., ENGINEER, C., VILLIERS, F., JU, C., TAKEDA, K., SU, Z., DONG, Q., ASSMANN, S. M., CHEN, J., KWAK, J. M., SCHROEDER, J. I., ALBERT, R., RHEE, S. Y. & FROMMER, W. B. 2014. Border Control-A Membrane-Linked Interactome of Arabidopsis. *Science,* 344**,** 711-716.

JOZEFKOWICZ, C., BERNY, M. C., CHAUMONT, F. & ALLEVA, K. 2017. Heteromerization of plant aquaporins. *In:* CHAUMONT, F. & TYERMAN, S. D. (eds.) *Plant Aquaporins From Transport to Signaling.* New York: Springer.

JUNG, H. W. & HWANG, B. K. 2007. The leucine-rich repeat (LRR) protein, CaLRR1, interacts with the hypersensitive induced reaction (HIR) protein, CaHIR1, and suppresses cell death induced by the CaHIR1 protein. *Molecular Plant Pathology,* 8**,** 503-514.

JUNG, H. W., LIM, C. W., LEE, S. C., CHOI, H. W., HWANG, C. H. & HWANG, B. K. 2008. Distinct roles of the pepper hypersensitive induced reaction protein gene CaHIR1 in disease and osmotic stress, as determined by comparative transcriptome and proteome analyses. *Planta,* 227**,** 409-425.

KAISER, H.-J., LINGWOOD, D., LEVENTAL, I., SAMPAIO, J. L., KALVODOVA, L., RAJENDRAN, L. & SIMONS, K. 2009. Order of lipid phases in model and plasma membranes. *Proceedings of the National Academy of Sciences of the United States of America,* 106**,** 16645-16650.

KEINATH, N. F., KIERSZNIOWSKA, S., LOREK, J., BOURDAIS, G., KESSLER, S. A., SHIMOSATO-ASANO, H., GROSSNIKLAUS, U., SCHULZE, W. X., ROBATZEK, S. & PANSTRUGA, R. 2010. PAMP (Pathogen-associated Molecular Pattern)-induced Changes in Plasma Membrane Compartmentalization Reveal Novel Components of Plant Immunity. *Journal of Biological Chemistry,* 285**,** 39140-39149.

KONOPKA, C. A., BACKUES, S. K. & BEDNAREK, S. Y. 2008. Dynamics of Arabidopsis Dynamin-Related Protein 1C and a Clathrin Light Chain at the Plasma Membrane. *The Plant Cell,* 20**,** 1363-1380.

KONOPKA, C. A. & BEDNAREK, S. Y. 2008. Comparison of the Dynamics and Functional Redundancy of the Arabidopsis Dynamin-Related Isoforms DRP1A and DRP1C during Plant Development. *Plant Physiology,* 147**,** 1590-1602.

KRÜGEL, U., VEENHOFF, L. M., LANGBEIN, J., WIEDERHOLD, E., LIESCHE, J., FRIEDRICH, T., GRIMM, B., MARTINOIA, E., POOLMAN, B. & KÜHN, C. 2008. Transport and Sorting of the *Solanum tuberosum* Sucrose Transporter SUT1 Is Affected by Posttranslational Modification. *The Plant Cell,* 20**,** 2497-2513.

KUSUMI, A. & SAKO, Y. 1996. Cell surface organization by the membrane skeleton. *Current Opinion in Cell Biology,* 8**,** 566-574.

LANGHORST, M. F., REUTER, A., JAEGER, F. A., WIPPICH, F. M., LUXENHOFER, G., PLATTNER, H. & STUERMER, C. A. O. 2008. Trafficking of the microdomain scaffolding protein reggie-1/flotillin-2. *European Journal of Cell Biology,* 87**,** 211-226.

LANGHORST, M. F., SOLIS, G. P., HANNBECK, S., PLATTNER, H. & STUERMER, C. A. O. 2007. Linking membrane microdomains to the cytoskeleton: Regulation of the lateral mobility of reggie-1/flotillin-2 by interaction with actin. *Febs Letters,* 581**,** 4697-4703.

LEWIS, K. C., SELZER, T., SHAHAR, C., UDI, Y., TWOROWSKI, D. & SAGI, I. 2008. Inhibition of pectin methyl esterase activity by green tea catechins. *Phytochemistry,* 69**,** 2586-92.

LI, R. L., LIU, P., WAN, Y. L., CHEN, T., WANG, Q. L., METTBACH, U., BALUSKA, F., SAMAJ, J., FANG, X. H., LUCAS, W. J. & LIN, J. X. 2012. A membrane microdomain-associated protein, *Arabidopsis* Flot1, is involved in a clathrin-independent endocytic pathway and is required for seedling development. *Plant Cell,* 24**,** 2105-2122.

LI, S., ZHAO, J., ZHAI, Y., YUAN, Q., ZHANG, H., WU, X., LU, Y., PENG, J., SUN, Z., LIN, L., ZHENG, H., CHEN, J. & YAN, F. 2019. The hypersensitive induced reaction 3 (HIR3) gene contributes to plant basal resistance via an EDS1 and salicylic acid-dependent pathway. *The Plant Journal,* 98**,** 783-797.

LI, X. J., WANG, X. H., YANG, Y., LI, R. L., HE, Q. H., FANG, X. H., LUU, D. T., MAUREL, C. & LIN, J. X. 2011. Single-molecule analysis of PIP2;1 dynamics and partitioning reveals multiple modes of *Arabidopsis* plasma membrane aquaporin regulation. *Plant Cell,* 23**,** 3780-3797.

LIANG, P., STRATIL, T. F., POPP, C., MARÍN, M., FOLGMANN, J., MYSORE, K. S., WEN, J. & OTT, T. 2018. Symbiotic root infections in *Medicago truncatula* require remorin-mediated receptor stabilization in membrane nanodomains. *Proceedings of the National Academy of Sciences*.

LIU, F., YU, X. M., ZHAO, W. Q., CHEN, J. P., GOYER, C., YANG, W. X. & LIU, D. Q. 2013. Effects of the leaf rust pathogen on expression of TaHIR4 at the gene and protein levels in wheat. *Journal of Plant Interactions,* 8**,** 304-311.

LIU, H., WANG, X., ZHANG, Y., DONG, J., MA, C. & CHEN, W. 2015. NADPH oxidase RBOHD contributes to autophagy and hypersensitive cell death during the plant defense response in *Arabidopsis thaliana*. *Biologia Plantarum,* 59**,** 570-580.

LIU, J., DEYOUNG, S. M., ZHANG, M., DOLD, L. H. & SALTIEL, A. R. 2005. The stomatin/prohibitin/flotillin/HflK/C domain of flotillin-1 contains distinct sequences that direct plasma membrane localization and protein interactions in 3T3-L1 adipocytes. *Journal of Biological Chemistry,* 280**,** 16125-16134.

LIU, P., LI, R. L., ZHANG, L., WANG, Q. L., NIEHAUS, K., BALUSKA, F., SAMAJ, J. & LIN, J. X. 2009. Lipid microdomain polarization is required for NADPH oxidase-dependent ROS signaling in Picea meyeri pollen tube tip growth. *Plant Journal,* 60**,** 303-313.

LUU, D.-T., MARTINIÈRE, A., SORIEUL, M., RUNIONS, J. & MAUREL, C. 2012. Fluorescence recovery after photobleaching reveals high cycling dynamics of plasma membrane aquaporins in Arabidopsis roots under salt stress. *The Plant Journal,* 69**,** 894-905.

LV, X., JING, Y., WU, H. & LIN, J. 2017a. Tracking Tonoplast Protein Behaviors in Intact Vacuoles Isolated from Arabidopsis Leaves. *Molecular Plant,* 10**,** 349-352.

LV, X., JING, Y., XIAO, J., ZHANG, Y., ZHU, Y., JULIAN, R. & LIN, J. 2017b. Membrane microdomains and the cytoskeleton constrain AtHIR1 dynamics and facilitate the formation of an AtHIR1-associated immune complex. *The Plant Journal,* 90**,** 3-16.

MAJERAN, W., LE CAER, J.-P., PONNALA, L., MEINNEL, T. & GIGLIONE, C. 2018. Targeted profiling of A. thaliana sub-proteomes illuminates new co- and post-translationally N-terminal Myristoylated proteins. *The Plant Cell*.

MARTINIERE, A., LAVAGI, I., NAGESWARAN, G., ROLFE, D. J., MANETA-PEYRET, L., LUU, D. T., BOTCHWAY, S. W., WEBB, S. E., MONGRAND, S., MAUREL, C., MARTIN-FERNANDEZ, M. L., KLEINE-VEHN, J., FRIML, J., MOREAU, P. & RUNIONS, J. 2012. Cell wall constrains lateral diffusion of plant plasma-membrane proteins. *Proc Natl Acad Sci U S A,* 109**,** 12805-10.

MARTINIERE, A. & RUNIONS, J. 2013. Protein diffusion in plant cell plasma membranes: the cell-wall corral. *Front Plant Sci,* 4**,** 515.

MCKENNA, J. F., ROLFE, D. J., WEBB, S. E. D., TOLMIE, A. F., BOTCHWAY, S. W., MARTIN-FERNANDEZ, M. L., HAWES, C. & RUNIONS, J. 2019. The cell wall regulates dynamics and size of plasma-membrane nanodomains in Arabidopsis. *Proceedings of the National Academy of Sciences***,** 201819077.

MCKENNA, J. F., TOLMIE, A. F. & RUNIONS, J. 2014. Across the great divide: the plant cell surface continuum. *Curr Opin Plant Biol,* 22**,** 132-140.

MONGRAND, S., MOREL, J., LAROCHE, J., CLAVEROL, S., CARDE, J. P., HARTMANN, M. A., BONNEU, M., SIMON-PLAS, F., LESSIRE, R. & BESSOULE, J. J. 2004. Lipid rafts in higher plant cells - Purification

and characterization of triton X-100-insoluble microdomains from tobacco plasma membrane. *Journal of Biological Chemistry,* 279**,** 36277-36286.

NAGANO, M., ISHIKAWA, T., FUJIWARA, M., FUKAO, Y., KAWANO, Y., KAWAI-YAMADA, M. & SHIMAMOTO, K. 2016. Plasma Membrane Microdomains Are Essential for Rac1-RbohB/H-Mediated Immunity in Rice. *Plant Cell,* 28**,** 1966-83.

NEUMANN-GIESEN, C., FALKENBACH, B., BEICHT, P., CLAASEN, S., LUERS, G., STUERMER, C. A. O., HERZOG, V. & TIKKANEN, R. 2004. Membrane and raft association of reggie-1/flotillin-2: role of myristoylation, palmitoylation and oligomerization and induction of filopodia by overexpression. *Biochemical Journal,* 378**,** 509-518.

NEUMANN-GIESEN, C., FERNOW, I., AMADDII, M. & TIKKANEN, R. 2007. Role of EGF-induced tyrosine phosphorylation of reggie-1/flotillin-2 in cell spreading and signaling to the actin cytoskeleton. *Journal of Cell Science,* 120**,** 395-406.

PEREMYSLOV, V. V., MORGUN, E. A., KURTH, E. G., MAKAROVA, K. S., KOONIN, E. V. & DOLJA, V. V. 2013. Identification of myosin XI receptors in *Arabidopsis* defines a distinct class of transport vesicles. *Plant Cell,* 25**,** 3022-3038.

PLATRE, M. P., BAYLE, V., ARMENGOT, L., BAREILLE, J., MARQUÈS-BUENO, M. D. M., CREFF, A., MANETA-PEYRET, L., FICHE, J.-B., NOLLMANN, M., MIÈGE, C., MOREAU, P., MARTINIÈRE, A. & JAILLAIS, Y. 2019. Developmental control of plant Rho GTPase nano-organization by the lipid phosphatidylserine. *Science,* 364**,** 57-62.

QI, Y. P. & KATAGIRI, F. 2009. Purification of low-abundance *Arabidopsis* plasma-membrane protein complexes and identification of candidate components. *Plant Journal,* 57**,** 932-944.

QI, Y. P., TSUDA, K., NGUYEN, L. V., WANG, X., LIN, J. S., MURPHY, A. S., GLAZEBROOK, J., THORDAL-CHRISTENSEN, H. & KATAGIRI, F. 2011. Physical asssociation of *Arabidopsis* hypersensitive induced reaction proteins (HIRs) with the immune receptor RPS2. *Journal of Biological Chemistry,* 286**,** 31297-31307.

RAFFAELE, S., BAYER, E., LAFARGE, D., CLUZET, S., GERMAN RETANA, S., BOUBEKEUR, T., LEBORGNE-CASTEL, N., CARDE, J.-P., LHERMINIER, J., NOIROT, E., SATIAT-JEUNEMAÎTRE, B., LAROCHE-TRAINEAU, J., MOREAU, P., OTT, T., MAULE, A. J., REYMOND, P., SIMON-PLAS, F., FARMER, E. E., BESSOULE, J.-J. & MONGRAND, S. 2009. Remorin, a Solanaceae Protein Resident in Membrane Rafts and Plasmodesmata, Impairs Potato virus X Movement. *The Plant Cell,* 21**,** 1541-1555.

RAGHUPATHY, R., ANILKUMAR, A. A., POLLEY, A., SINGH, P. P., YADAV, M., JOHNSON, C., SURYAWANSHI, S., SAIKAM, V., SAWANT, S. D., PANDA, A., GUO, Z., VISHWAKARMA, R. A., RAO, M. & MAYOR, S. 2015. Transbilayer lipid interactions mediate nanoclustering of lipid-anchored proteins. *Cell,* 161**,** 581-594.

RETZER, K., LACEK, J., SKOKAN, R., DEL GENIO, C. I., VOSOLSOBĚ, S., LAŇKOVÁ, M., MALÍNSKÁ, K., KONSTANTINOVA, N., ZAŽÍMALOVÁ, E., NAPIER, R. M., PETRÁŠEK, J. & LUSCHNIG, C. 2017. Evolutionary Conserved Cysteines Function as cis-Acting Regulators of Arabidopsis PIN-FORMED 2 Distribution. *International Journal of Molecular Sciences,* 18**,** 2274.

RIENTO, K., ZHANG, Q., CLARK, J., BEGUM, F., STEPHENS, E., WAKELAM, M. J. & NICHOLS, B. J. 2018. Flotillin proteins recruit sphingosine to membranes and maintain cellular sphingosine-1-phosphate levels. *PLoS One,* 13**,** e0197401.

RITCHIE, K., IINO, R., FUJIWARA, T., MURASE, K. & KUSUMI, A. 2003. The fence and picket structure of the plasma membrane of live cells as revealed by single molecule techniques (Review). *Molecular Membrane Biology,* 20**,** 13-18.

RIVERA-MILLA, E., STUERMER, C. A. O. & MALAGA-TRILLO, E. 2006. Ancient origin of reggie (flotillin), reggie-like, and other lipid-raft proteins: convergent evolution of the SPFH domain. *Cellular and Molecular Life Sciences,* 63**,** 343-357.

ROITBAK, T., SURVILADZE, Z., TIKKANEN, R. & WANDINGER-NESS, A. 2005. A polycystin multiprotein complex constitutes a cholesterol-containing signalling microdomain in human kidney epithelia. *Biochemical Journal,* 392**,** 29-38.

ROSE, S. L., FULTON, J. M., BROWN, C. M., NATALE, F., VAN MOOY, B. A. S. & BIDLE, K. D. 2014. Isolation and characterization of lipid rafts in *Emiliania huxleyi*: a role for membrane microdomains in host-virus interactions. *Environmental Microbiology,* 16**,** 1150-1166.

ROSTOKS, N., SCHMIERER, D., KUDRNA, D. & KLEINHOFS, A. 2003. Barley putative hypersensitive induced reaction genes: genetic mapping, sequence analyses and differential expression in disease lesion mimic mutants. *Theoretical and Applied Genetics,* 107**,** 1094-1101.

SANDERFOOT, A. A., KOVALEVA, V., BASSHAM, D. C. & RAIKHEL, N. V. 2001. Interactions between syntaxins identify at least five SNARE complexes within the golgi/prevacuolar system of the arabidopsis cell. *Molecular Biology of the Cell,* 12**,** 3733-3743.

SHAHOLLARI, B., PESKAN-BERGHÖFER, T. & OELMÜLLER, R. 2004. Receptor kinases with leucine-rich repeats are enriched in Triton X-100 insoluble plasma membrane microdomains from plants. *Physiologia Plantarum,* 122**,** 397-403.

SHI, Q., ARAIE, H., BAKKU, R. K., FUKAO, Y., RAKWAL, R., SUZUKI, I. & SHIRAIWA, Y. 2015. Proteomic analysis of lipid body from the alkenone-producing marine haptophyte alga Tisochrysis lutea. *Proteomics,* 15**,** 4145-4158.

SCHEIBLE, W. R., FRY, B., KOCHEVENKO, A., SCHINDELASCH, D., ZIMMERLI, L., SOMERVILLE, S., LORIA, R. & SOMERVILLE, C. R. 2003. An *Arabidopsis* mutant resistant to thaxtomin A, a cellulose synthesis inhibitor from *Streptomyces* species. *Plant Cell,* 15**,** 1781-1794.

SIMON, M. L., PLATRE, M. P., MARQUES-BUENO, M. M., ARMENGOT, L., STANISLAS, T., BAYLE, V., CAILLAUD, M. C. & JAILLAIS, Y. 2016. A PtdIns(4)P-driven electrostatic field controls cell membrane identity and signalling in plants. *Nat Plants,* 2**,** 16089.

SIMONS, K. & IKONEN, E. 1997. Functional rafts in cell membranes. *Nature,* 387**,** 569-572.

SINGER, S. J. & NICOLSON, G. L. 1972. The Fluid Mosaic Model of the Structure of Cell Membranes. *Science,* 175**,** 720-731.

SOLIS, G. P., HOEGG, M., MUNDERLOH, C., SCHROCK, Y., MALAGA-TRILLO, E., RIVERA-MILLA, E. & STUERIVIER, C. A. O. 2007. Reggie/flotillin proteins are organized into stable tetramers in membrane microdomains. *Biochemical Journal,* 403**,** 313-322.

SOLIS, G. P., SCHROCK, Y., HULSBUSCH, N., WIECHERS, M., PLATTNER, H. & STUERMER, C. A. O. 2012. Reggies/flotillins regulate E-cadherin-mediated cell contact formation by affecting EGFR trafficking. *Molecular Biology of the Cell,* 23**,** 1812-1825.

SOREK, N., PORATY, L., STERNBERG, H., BURIAKOVSKY, E., BAR, E., LEWINSOHN, E. & YALOVSKY, S. 2017. Corrected and Republished from: Activation Status-Coupled Transient S-Acylation Determines Membrane Partitioning of a Plant Rho-Related GTPase. *Molecular and cellular biology,* 37**,** e00333-17.

SORIEUL, M., SANTONI, V., MAUREL, C. & LUU, D. T. 2011. Mechanisms and effects of retention of over-expressed aquaporin AtPIP2;1 in the endoplasmic reticulum. *Traffic,* 12**,** 473-82.

SZYMANSKI, W. G., ZAUBER, H., ERBAN, A., GORKA, M., WU, X. N. & SCHULZE, W. X. 2015. Cytoskeletal Components Define Protein Location to Membrane Microdomains. *Molecular & Cellular Proteomics,* 14**,** 2493-2509.

TAN, S., ZHANG, P., XIAO, W., FENG, B., CHEN, L. Y., LI, S., LI, P., ZHAO, W. Z., QI, X. T. & YIN, L. P. 2018. TMD1 domain and CRAC motif determine the association and disassociation of MxIRT1 with detergent-resistant membranes. *Traffic,* 19**,** 122-137.

TATENO, M., BRABHAM, C. & DEBOLT, S. 2016. Cellulose biosynthesis inhibitors - a multifunctional toolbox. *J Exp Bot,* 67**,** 533-42.

TJELLSTROM, H., HELLGREN, L. I., WIESLANDER, A. & SANDELIUS, A. S. 2010. Lipid asymmetry in plant plasma membranes: phosphate deficiency-induced phospholipid replacement is restricted to the cytosolic leaflet. *Faseb j,* 24**,** 1128-38.

TOLMIE, F., POULET, A., MCKENNA, J., SASSMANN, S., GRAUMANN, K., DEEKS, M. & RUNIONS, J. 2017. The cell wall of Arabidopsis thaliana influences actin network dynamics. *J Exp Bot,* 68**,** 4517-4527.

TRAVERSO, J. A., MICALELLA, C., MARTINEZ, A., BROWN, S. C., SATIAT-JEUNEMAÎTRE, B., MEINNEL, T. & GIGLIONE, C. 2013. Roles of N-Terminal Fatty Acid Acylations in Membrane Compartment Partitioning: Arabidopsis h-Type Thioredoxins as a Case Study. *The Plant Cell,* 25**,** 1056-1077.

ULLRICH, A. & SCHLESSINGER, J. 1990. Signal transduction by receptors with tyrosine kinase-activity. *Cell,* 61**,** 203-212.

VEATCH, S. L. & KELLER, S. L. 2003. Separation of liquid phases in giant vesicles of ternary mixtures of phospholipids and cholesterol. *Biophysical journal,* 85**,** 3074-3083.

VILAKAZI, C. S., DUBERY, I. A. & PIATER, L. A. 2017. Identification of lipopolysaccharide-interacting plasma membrane-type proteins in Arabidopsis thaliana. *Plant Physiol Biochem,* 111**,** 155-165.

WANG, L., LI, H., LV, X. Q., CHEN, T., LI, R. L., XUE, Y. Q., JIANG, J. J., JIN, B., BALUSKA, F., SAMAJ, J., WANG, X. L. & LIN, J. X. 2015. Spatiotemporal Dynamics of the BRI1 Receptor and its Regulation by Membrane Microdomains in Living Arabidopsis Cells. *Molecular Plant,* 8**,** 1334-1349.

WANG, Q. L., ZHAO, Y. Y., LUO, W. X., LI, R. L., HE, Q. H., FANG, X. H., DE MICHELE, R., AST, C., VON WIREN, N. & LIN, J. X. 2013. Single-particle analysis reveals shutoff control of the Arabidopsis ammonium

transporter AMT1;3 by clustering and internalization. *Proceedings of the National Academy of Sciences of the United States of America,* 110**,** 13204-13209.

WORDEN, N., WILKOP, T. E., ESTEVE, V. E., JEANNOTTE, R., LATHE, R., VERNHETTES, S., WEIMER, B., HICKS, G., ALONSO, J., LABAVITCH, J., PERSSON, S., EHRHARDT, D. & DRAKAKAKI, G. 2015. CESA TRAFFICKING INHIBITOR Inhibits Cellulose Deposition and Interferes with the Trafficking of Cellulose Synthase Complexes and Their Associated Proteins KORRIGAN1 and POM2/CELLULOSE SYNTHASE INTERACTIVE PROTEIN1. *Plant Physiology,* 167**,** 381-393.

XIANG, Y., SONG, M., ZHANG, M. Q., CAO, S. F. & HAN, H. S. 2015. Molecular characterization of three hypersensitive-induced reaction genes that respond to *Phytophthora sojae* infection in *Glycine max* L. Merr. *Legume Research,* 38**,** 313-320.

XUE, Y., XING, J., WAN, Y., LV, X., FAN, L., ZHANG, Y., SONG, K., WANG, L., WANG, X., DENG, X., BALUSKA, F., CHRISTIE, J. M. & LIN, J. 2018. Arabidopsis Blue Light Receptor Phototropin 1 Undergoes Blue Light-Induced Activation in Membrane Microdomains. *Mol Plant,* 11**,** 846-859.

YU, M., LIU, H., DONG, Z., XIAO, J., SU, B., FAN, L., KOMIS, G., ŠAMAJ, J., LIN, J. & LI, R. 2017. The dynamics and endocytosis of Flot1 protein in response to flg22 in Arabidopsis. *Journal of Plant Physiology,* 215**,** 73-84.

YU, Q., REN, J. J., KONG, L. J. & WANG, X. L. 2018. Actin filaments regulate the adhesion between the plasma membrane and the cell wall of tobacco guard cells. *Protoplasma,* 255**,** 235-245.

YU, X. M., YU, X. D., QU, Z. P., HUANG, X. J., GUO, J., HAN, Q. M., ZHAO, J., HUANG, L. L. & KANG, Z. S. 2008. Cloning of a putative hypersensitive induced reaction gene from wheat infected by stripe rust fungus. *Gene,* 407**,** 193-198.

YU, X. M., ZHAO, W. Q., YANG, W. X., LIU, F., CHEN, J. P., GOYER, C. & LIU, D. Q. 2013. Characterization of a hypersensitive response-induced gene TaHIR3 from wheat leaves infected with leaf rust. *Plant Molecular Biology Reporter,* 31**,** 314-322.

ZHANG, G., DONG, Y. L., ZHANG, Y., LI, Y. M., WANG, X. J., HAN, Q. M., GUO, J., HUANG, L. L. & KANG, Z. S. 2009. Cloning and characterization of a novel hypersensitive-induced reaction gene from wheat infected by stripe rust pathogen. *Journal of Phytopathology,* 157**,** 722-728.

ZHANG, G., LI, Y. M., SUN, Y. F., WANG, J. M., LIU, B., ZHAO, J., GUO, J., HUANG, L. L., CHEN, X. M. & KANG, Z. S. 2011. Molecular characterization of a gene induced during wheat hypersensitive reaction to stripe rust. *Biologia Plantarum,* 55**,** 696-702.

ZHAO, X. Y., LI, R. L., LU, C. F., BALUSKA, F. & WAN, Y. L. 2015. Di-4-ANEPPDHQ, a fluorescent probe for the visualisation of membrane microdomains in living Arabidopsis thaliana cells. *Plant Physiology and Biochemistry,* 87**,** 53-60.

ZHOU, L., CHEUNG, M. Y., ZHANG, Q., LEI, C. L., ZHANG, S. H., SUN, S. S. & LAM, H. M. 2009. A novel simple extracellular leucine-rich repeat (eLRR) domain protein from rice (OsLRR1) enters the endosomal pathway and interacts with the hypersensitive-induced reaction protein 1 (OsHIR1). *Plant Cell Environ,* 32**,** 1804-20.

ZHOU, L. A., CHEUNG, M. Y., LI, M. W., FU, Y. P., SUN, Z. X., SUN, S. M. & LAM, H. M. 2010. Rice hypersensitive induced reaction protein 1 (OsHIR1) associates with plasma membrane and triggers hypersensitive cell death. *Bmc Plant Biology,* 10.